

https://dspace.org/

A review of the geology, mineralisation, and structural controls on the emplacement of the Bikita LCT pegmatites, Masvingo Greenstone Belt, Zimbabwe Craton

Gogodo, Arthur Samuel

2021
https://hdl.handle.net/10539/33054

Downloaded from a DSpace repository. https://dspace.org/

A REVIEW OF THE GEOLOGY, MINERALISATION, AND STRUCTURAL CONTROLS ON THE EMPLACEMENT OF THE BIKITA LCT PEGMATITES, MASVINGO GREENSTONE BELT, ZIMBABWE CRATON



WITS
UNIVERSITY

Submitted by

Arthur Samuel Gogodo

1784967

A research report submitted to the Faculty of Science, University of the Witwatersrand, Johannesburg, in partial fulfilment of the requirements for the degree of Master of Science.

Year 2021

Supervisor: Prof. Paul Nex

Co-Supervisor: Prof. Judith Kinnaird

Declaration

I declare that this dissertation is my own, unaided work. It is being submitted for the Degree of Master in Science by Coursework and Research Report to the University of the Witwatersrand, Johannesburg, South Africa. It has not been submitted before for any degree or examination in any other University.



Signature of candidate

Date: 06 October 2021

Abstract

The world-class Meso-Neoarchaean Bikita pegmatites which host Li, Cs, Ta, Be and Sn mineralisation are enclosed by the elongate shaped Masvingo Greenstone Belt which is situated within the southern part of the Zimbabwe Craton. There are 15 denoted pegmatites within the Bikita mining lease and from these the main pegmatite is the most extensively worked and has been the backbone of the mine since its discovery around 1911 when mining started. These pegmatites have intruded the greenstone-epidiorite country rocks presumed to be metamorphosed basic volcanic rocks with interbedded metamorphosed sediments comprising calcareous and semipelitic schist, siliceous granulite and banded ferruginous quartzite. The Bikita pegmatites are heterogeneous with a complex mineralogical composition containing lithium-bearing minerals (amblygonite, bikitaite, eucryptite, lepidolite, petalite, hectorite, and spodumene). The geology of the Bikita Tinfield was extensively studied prior to its initial mapping by Martin (1964) and most of the interpretations in use have been based on this work. Considering the fact that mining has been ongoing since then, there has been a gap in terms of updating of the geology for these pegmatites which this research work intends to fill. The main purpose of this study is to advance the technical knowledge pertainining to these pegmatites using modern techniques, with particular focus on the geology and mineralisation of the Bikita pegmatites.

The possible structural controls on the emplacement of the pegmatites was investigated through satellite imagery and geophysical data. Structural analysis suggests that the NE–SW trending Gono fault and the N-S trending Popoteke fault are the major features on a regional scale understood to have played a vital role in the emplacement mechanism of the pegmatites. These fault zones can provide conduits and with reactivation focus migrating pegmatite melts. On a local structural scale, fractures and shears are the most dominant structures mapped in the study area. Field evidence suggests that most of the structures within the mining lease are on the same strike as that of the pegmatites (NE, N to S, NNE and ENE) therefore cutting across the fabric of the country rock which has an E-W orientation. Some of these structures have been subsequently filled by pegmatitic material proving that they were part of the locus along which the pegmatite intruded.

The whole-rock geochemical dataset consists of 1143 samples analysed with AAS for 7 major element oxides in percentages (%) and a dataset of 441 samples analysed by XRF with 6 minor and trace elements (Ta, Nb, Sn, Fe, Rb and Sr) reported in parts per million (ppm). The highest lithium concentration found from the analysed samples is within the Dam Site pit, the highest caesium concentration is at Victor's pit, the highest tantalum concentration is at Bikita quarry and the highest tin concentration is at the West pegmatite body. The Li_2O average abundance across all the pegmatites studied is 2.08 wt %. Results from the Bikita quarry locality have shown the best behaved dataset from which the typical mineral compositions have helped to ascertain mineral deportment and the main definable trends are a high K trend governed by micas i.e. lepidolite and a low K trend which appears to be illustrating the control by petalite. The other Li-Al minerals (spodumene, amblygonite, eucryptite) associate with this low K trend. Essentially all samples show mineralogical control by muscovite and mainly lepidolite (correcting for the build up of radiogenic Sr) exerting a strong influence on Rb contents of extremely differentiated melts containing practically no original Sr. Generally, the Bikita pegmatites are highly fractionated as indicated by their high Rb values (36 700 to 44 283 ppm) from McMurdon pit and Dam Site pit respectively.

Spatial data processing, analysis and integration using Remote Sensing, geophysics, geochemistry and GIS applications were useful in understanding the geology, mineralisation and structural controls on emplacement of the Bikita pegmatites. Geochemical work applied in this report work has proved that the Bikita pegmatites are richly endowed in lithium ore minerals with lepidolite and petalite being the most dominant.

Acknowledgements

I would like to thank Bikita Minerals (Pvt) Ltd directors for giving me the opportunity to do my Master's Degree and for providing me with the necessary resources during my research. The Bikita Minerals geology team is especially thanked for their immense contribution towards the successful completion of this work. I also would like to thank the Bikita Minerals assay laboratory staff for ensuring the research samples were analysed with utmost precision and accuracy.

I thank my supervisors Prof Paul Nex and Prof Judith Kinnaird from the University of the Witwatersrand for all their supervision, support and time they dedicated to help and guide me throughout this research journey. Furthermore, I would like to thank the University of Witwatersrand in general, and the School of Geosciences in particular for the opportunity offered to me to study at this wonderful university.

I am also deeply grateful and indebted to my family, friends and everyone who supported me in any way during this research journey for without your contributions I would not have easily accomplished this journey. To my wife Elina, your unconditional love, support, motivation, understanding, consideration and encouragement has been phenomenal and I cannot adequately express my appreciation for it.

Above all, I thank the Almighty for the strength and blessings bestowed upon me as well as his wisdom and grace that enabled me to complete this research report.

Table of contents

Declaration i

Abstract ii

Acknowledgements iii

List of Figures vii

List of Tables x

List of Abbreviations ..... **xi**

List of Mineral Formulae xii

CHAPTER 1: 1

INTRODUCTION 1

1.1 Research background 1

1.2 Historical background of the Bikita Tinfield 1

1.3 Location of the project area 2

1.4 Scope and research problem statements 4

1.5 Research general aims and objectives 5

1.6 General overview of the Zimbabwean Craton geology 5

1.7 Archaean stratigraphy and general overview of the Zimbabwean Craton greenstone belts 7

1.7.1 General overview of the Masvingo Greenstone Belt geology 7

1.7.2 Tectonostratigraphic framework of the Masvingo Greenstone Belt 8

1.8 The regional geological setting of the Bikita pegmatites 9

CHAPTER 2: **11**

RESEARCH METHODOLOGY **11**

2.1 Research methods background 11

2.2 Whole-rock geochemical sampling 11

2.3 Sample selection 14

2.4 Geochemical sampling and logging 15

2.4.1 Whole-rock channel chip/grab sampling and logging 15

2.4.2 Whole-rock drill chip sampling and logging 16

2.4.3 Whole-rock diamond drill core sampling and logging 17

2.4.4 Laboratory work and techniques 19

2.4.5 Sample geochemical analysis 19

2.5 Geological mapping 19

2.5.1 Map generation 19

2.5.2 Structural field investigations 19

2.5.3 Designing the ground magnetic and radiometric geophysical survey 20
2.5.4 Remote sensing satellite image data collection 21
2.5.5 Section generation 22
CHAPTER 3: 23
LOCAL GEOLOGICAL SETTING AND FIELD RELATIONSHIPS 23
3.1 Introduction 23
3.2 The geological setting of the Bikita pegmatites 23
3.2.1 Internal structure of the pegmatites 26
3.3 Mineralisation of the Bikita pegmatites 26
3.4 The Bikita Main pegmatite (1) 27
3.4.1 The Bikita quarry 27
3.5 Detailed internal zoning within the Bikita quarry 28
3.5.1 Border Zones 28
3.5.2 Wall Zones 29
3.5.3 Upper Intermediate Zones 30
3.5.4 Core Zone 32
3.5.5 Lower Intermediate Zones 33
3.6 The Al Hayat pit 35
3.6.1 Zoning within the Al Hayat pit 35
3.7 The McMurdon pit 37
3.8 The Spodumene pegmatite (2) 38
3.8.1 Zoning of the Spodumene pegmatite 40
3.9 The Boomerang pegmatite (3) 41
3.10 The East pegmatite (4) 41
3.10.1 Zoning of the East pegmatite 42
3.11 The Shaft pegmatite (5) 43
3.12 The West pegmatite (6) 44
3.13 The Giant pegmatites (7) 44
3.14 The Mauve Kop pegmatites (8-10) 44
3.15 The Dam Site pegmatite (11) 45
3.16 The Nigel pegmatites (12 &13) 47
3.17 The Ranga pegmatite (14) 47
3.18 The Cemetery pegmatite (15) 47
3.19 Alteration in the Bikita pegmatites and relationship with the country wall-rocks 48
3.20 Age of the Bikita pegmatites 50

3.21 Geological summary of the Bikita pegmatites 50
CHAPTER 4: 52
GEOCHEMISTRY OF THE PEGMATITES 52
4.1 Introduction 52
4.2 Whole-rock geochemical data 522
4.2.1 Major element geochemistry 52
4.2.2 Trace element geochemistry 70
CHAPTER 5: 82
GEOPHYSICAL STUDY AND REMOTE SENSING 82
5.1 Introduction 82
5.2 Ground magnetics survey results 82
5.3 Radiometric survey results 85
5.4 Combination of radiometrics and magnetics data 86
5.5 Landsat 7 ETM+ Image processing 88
5.5.1 Landsat True colour composite (RGB) 321 89
5.5.2 Landsat False colour composite (RGB) 432 89
CHAPTER 6: 93
DATA INTERPRETATION AND DISCUSSION 93
6.1 Introduction 93
6.2 Geochemical data 93
6.3 Geophysical and Remote Sensing data interpretations 97
6.4 Structural controls 99
6.4.1 Regional structural controls 99
6.4.2 Local structural controls 102
6.5 Possible mechanisms regarding the genesis and emplacement of the Bikita pegmatites 102
CHAPTER 7: 105
CONCLUSION AND RECOMMENDATION 105
7.1 Conclusion 105
7.2 Recommendation 107
References 108
Appendices 111

List of Figures

Figure 1.1: Simplified map showing the location of the Bikita Mine lease area (red star) east of Masvingo.....3
Figure 1.2: Topographic map showing the location of the mine lease area on the farms Glen Clova and Glen Shee together with the individual historical and current pits.....4
Figure 1.3: Simplified geological map showing the geological architecture of the Zimbabwe Craton. Modified after Wilson (1981); Campbell and Pitfield (1994). 6
Figure 1.4: Regional geological map of the Masvingo Greenstone Belt and surrounding granite-gneiss terrains.....8
Figure 1.5: Extract from 1:100,000 geological map showing the regional geological setting of the Bikita pegmatites. Adapted from Wilson (1964). Green represents the greenstones, Yellow represents the older sediments in the synformal core of the MGB and the pink-brown colour represents the granites and gneisses. 10
Figure 2.1: Google Earth image of the Bikita Mine area showing individual open-cast pits and channel chip/grab sample locations 12
Figure 2.2: Google Earth image of the Bikita Mine area showing individual open cast pits and various drill hole localities which were drilled in McMurdon, Bikita, Al Hayat, Victor's, Nigel's, Shaft, Ledingham, West and Mauve Kop sectors.....13
Figure 2.3: Photograph of a typical sample chip tray and its labelling 16
Figure 2.4: Preliminary diamond drill core photo from the Shaft pegmatite body showing how the different lithological boundaries were marked. Black lines show core orientantion markings and black numbers represent the metre markings and red letters are abbreviations for the different lithologies. 17
Figure 2.5: Preliminary lithostratigraphic diamond drill profile for VB-DDH-008. L represents lepidolite, AF represents albite feldspar, MZ represents mixed zone, Pt represents petalite and SQI represents spodumene. ..18
Figure 2.6: Planning diagram showing the layout of the Bikita ground magnetic and radiometric survey. Current pits are shown in purple. 21
Figure 3.1: A local geological map of the Bikita Tinfield showing the distribution of the pegmatites and the associated rocks. Also depicted are section lines, mine pits, dips/strikes and shear zones (Modified after Martin, 1962). The numbers 1-15 represent the depicted pegmatite names.....24
Figure 3.2: Photograph showing disseminated cassiterite crystals (black) within a matrix of muscovite, quartz and albite feldspar. 27
Figure 3.3: Photograph showing the Border Zone mineralisation on the sharp greenstone and pegmatite marginal contact 29
Figure 3.4: Photograph showing the typical "spotted dog" (matrix of albite, quartz and muscovite) with petalite being altered to hectorite (pink).....30
Figure 3.5: Photograph showing the association of albite, SQI and quartz within the Upper Intermediate Zone of the Bikita sector 31
Figure 3.6: Photograph showing typical All Mixed Zone showing association of various mineral species within the Bikita sector.....32
Figure 3.7: Photograph showing the association of tantalite mineralisation with albite and quartz within the Core Zone of the Bikita sector 33
Figure 3.8: Typical Cobbled Zone which consists of a matrix of albite feldspar partly replaced by lepidolite forming spherical masses of various sizes within the Bikita Sector 34
Figure 3.9: Photograph of the typical Lower Intermediate Zone showing feldspathic lepidolite within the footwall of Bikita North pit.....35
Figure 3.10: Typical footwall spotted dog albite zone in the Al Hayat pit showing rhythmic banding 36
Figure 3.11: Schematic cross section through the Al Hayat sector from north to south 37

Figure 3.12: Photograph showing the association of mangano-tantalite and fractured quartz within the McMurdon Sector 38
Figure 3.13: Borehole layout plan of the Ledingham area showing the location of SQI_DDH44.....39
Figure 3.14: Core sample from the Spodumene pegmatite showing massive SQI indicated by the pink colour with distictive elongated accicular crystals of spodumene 40
Figure 3.15: Schematic cross section through the Spodumene pegmatite. The location of section line A-B is shown in Figure 3.1.....41
Figure 3.16: Overview picture of the Nigel pit (view to south west) showing typical mineral zoning 42
Figure 3.17: Schematic cross section through the East pegmatite showing the different lithologies. The Quartz Core is depicted in yellow.....43
Figure 3.18: Schematic cross section through the Shaft pegmatite showing the diferent lithologies.....44
Figure 3.19: Lepidolite varieties. (a) Photograph showing the beautiful deep mauve lepidolite (b) Photograph showing the radial morphology on lepidolite embedded in quartz and albite 45
Figure 3.20: Photograph showing the outline of the Damsite pegmatite with a view to the north 46
Figure 3.21: Schematic cross section through the Dam Site pegmatite showing the associated lithologies.....47
Figure 3.1: Photograph showing an undulating contact between the greenstone and the pegmatite in Al Hayat pit with a view to the south east.....48
Figure 3.2: Metamorphic selvedge of tourmaline in the Bikita quarry (marginal contact)..... 49
Figure 3.3: Photograph showing typical wall-rock alteration within the Victor's pit showing carbonatisation, oxidation, silicification and chloritisation with disseminated suphidation.....49
Figure 3.4: Photograph showing a greenstone xenolith embedded within the spotted dog albite on the haulage ramp on the Al Hayat pit with a view to the West..... 50
Figure 4.5: Major element bivariate x-y diagram for the McMurdom pit pegmatite body.....53
Figure 4.2: Li_2O vs K_2O major element bivariate x-y diagram for the Bikita quarry pegmatite body.....54
Figure 4.3: Li_2O vs Na_2O major element bivariate x-y diagram for the Bikita quarry pegmatite body.....55
Figure 4.4: Li_2O vs Al_2O_3 major element bivariate x-y diagram for the Bikita quarry pegmatite body.....56
Figure 4.5: Major element bivariate x-y diagram for the Al Hayat pit pegmatite body.....57
Figure 4.6: Major element bivariate x-y diagram for the Ledingham sector pegmatite body.....58
Figure 4.7: Major element bivariate x-y diagram for the Victor's pit pegmatite body.....59
Figure 4.8: Major element bivariate x-y diagram for the Nigel's pit pegmatite body.....60
Figure 4.9: Major element bivariate x-y diagram for the Shaft sector pegmatite body.....61
Figure 4.10: Major element bivariate x-y diagram for the West sector pegmatite body.....62
Figure 4.11: Major element bivariate x-y diagram for the Giant East sector pegmatite body.....63
Figure 4.12: Major element bivariate x-y diagram for the Mauve Kop sector pegmatite body.....64
Figure 4.13: Major element bivariate x-y diagram for the Dam Site pit pegmatite body.....65
Figure 4.14: Major element bivariate x-y diagram for the Cemetary sector pegmatite body.....66
Figure 4.15: Major element bivariate x-y diagram for all the pegmatite bodies combined.....67
Figure 4.16: Major element oxides chemostratigraphy variation plot for borehole SQIDDH44.....69
Figure 4.17: Major element oxides chemostratigraphy variation plot for borehole AHHDDH002.....70
Figure 4.18: Trace element bivariate x-y diagram for the McMurdorn pit pegmatite body.....71
Figure 4.19: Trace element bivariate x-y diagram for the Bikita quarry pegmatite body.....72
Figure 4.20: Trace element bivariate x-y diagram for the Al Hayat pit pegmatite body.....73
Figure 4.21: Trace element bivariate x-y diagram for the Ledingham sector pegmatite body.....74
Figure 4.22: Trace element bivariate x-y diagram for the Victor's pit pegmatite body.....75

Figure 4.23: Trace element bivariate x-y diagram for the Nigel's pit pegmatite body……76
Figure 4.24: Trace element bivariate x-y diagram for the Shaft sector pegmatite body……77
Figure 4.25: Trace element bivariate x-y diagram for the West sector pegmatite body……78
Figure 4.26: Trace element bivariate x-y diagram for the Mauve Kop sector pegmatite body……79
Figure 4.27: Trace element bivariate x-y diagram for the Dam Site pit pegmatite body……80
Figure 4.28: Plot of Sr versus Rb for analysed samples from the Bikita quarry locality……81
Figure 5.6: Total field magnetics showing clear, mainly NE-trending, structures with a strong WNW-trending anomaly in the north and another, similar one in the south……83
Figure 5.7: First vertical derivative of the Bikita ground magnetics data with interpreted NE shears and dolerite dykes overlaid in dark green……84
Figure 5.8: NW horizontal gradient of the Bikita ground magnetics data, perpendicular to strike. Interpreted NE shears, dolerite dykes, EW and ENE brittle fractures, and form lines overlaid……85
Figure 5.9: Potassium (K) percentage with interpreted pegmatites (in purple) overlaid……86
Figure 5.10: Ternary radiometrics image showing the different lithologies within the project area. In this RGB, Red represents K, Green represents Th and Blue represents U ……87
Figure 5.11: Analytical signal of the ground magnetics of the project area……88
Figure 5.12: A Landsat map covering the Masvingo Greenstone Belt produced from true colour composite image of bands 321 showing the main features within the study area……89
Figure 5.13: A Landsat map covering the Masvingo Greenstone Belt produced from false-colour composite image of bands 432 showing the main geological formations and signatures……90
Figure 5.14: A Landsat map covering the Masvingo Greenstone Belt showing correlations between the geology produced from unsupervised classification. The white outline shows the trend of the MGB……91
Figure 5.15: A Landsat map covering the Masvingo Greenstone Belt in white outline produced from principle component transformation showing the delineation of structural lineaments shown in black lines……92
Figure 6.16: Geological map of the Bikita Tinfield showing pegmatite mineralisation distribution patterns. Numbers 1-15 in circles are pegmatite names and those around the pits are dip angles……96
Figure 6.17: A map of the Bikita Tinfield showing a ground magnetic broad-scale local structural lineament interpretation……98
Figure 6.18: Interpreted pegmatites (from K %) in black outline, overlaid on mapped pegmatites in red……99
Figure 6.19: Comparison images of satellite, regional geophysics……100
Figure 6.20: Final interpretation map showing the Masvingo Greenstone Belt and combined regional structural lineaments……101
Figure 6.21: Field evidence for possible local emplacement along lineaments of the pegmatites……102
Figure 7.22: Final interpretation geological map of the Bikita Tinfield showing the updated structures and section lines……106

List of Tables

Table 2.1: Geochemical dataset summary. 15
Table 2.2: Preliminary channel chip log sheet. 16
Table 3.1: Table of the denoted Bikita Pegmatites with the associated pits showing their economic mineralisation after (Martin, 1964) 25
Table 3.2: Table showing the zones of the pegmatite within the Bikita sector 28
Table 4.1: Whole-rock geochemical dataset summary showing the total numbers of samples analysed by the different methods. 52
Table 4.2: Combined major element variations for the various pegmatite bodies 68
Table 6.1: Highest major element abundances for each pegmatite body 94
Table 6.2: Highest trace element abundances for each pegmatite body 95

List of Abbreviations

Amb	Amblygonite
AAS	Atomic Absorption Spectrometry
Ab	Albite Feldspar
Be	Beryl
Bt	Biotite Mica
Cst	Cassiterite
Cs	Caesium
D	Dolerite
DDH	Diamond Drill Hole
Eucr	Eucryptite
FW	Footwall
GIS	Geographic Information Systems
GPS	Global Position System
Gst	Greenstone
Hect	Hectorite
HW	Hangingwall
Lpd	Lepidolite
Landsat (ETM+)	Landsat Enhanced Thematic mapper plus
Landsat (TM)	Thematic Mapper
LCT	Lithium Caesium Tantalum
Li	Lithium
Ms	Muscovite
Mc	Microcline Feldspar
MGB	Masvingo Greenstone Belt
NYF	Niobium Yttrium Fluorine
OB	Overburden
PD	Percussion Drilling
Poll	Pollucite
Pet	Petalite
Qtz	Quartz
RC	Reverse Circulation
RS	Remote Sensing
Srp	Serpentinite
Sn	Tin
SQI	Spodumene Quartz Intergrowth
Ta	Tantalite
UTM	Universal Transverse Mercator
XRF	X-Ray Fluorescent

List of Mineral Formulae

Amblygonite	$LiAl(PO_4)(F,OH)$
Albite Feldspar	$NaAlSi_3O_8$
Beryl	$Be_3Al_2(SiO_3)_6$
Bikitaite	$Li_2[Al_2Si_4O_{12}]•2(H_2O)$
Biotite Mica	$K(Mg,Fe)_3AlSi_3O_{10}(F,OH)_2$
Cassiterite	SnO_2
Eucryptite	$LiAlSiO_4$
Hectorite	$Na_{0.3}(Mg,Li)_3Si_4O_{10}(OH)_2$
Lepidolite	$K(Li,Al)_3(Si,Al)_4O_{10}(F,OH)_2$
Microcline Feldspar	$KAlSi_3O_8$
Muscovite	$KAl_2(Si_3Al)O_{10}(OH,F)_2$
Petalite	$LiAl(Si_4O_{10})$
Pollucite	$Cs(Si_2Al)O_6.nH_2O$
Quartz	SiO_2
Spodumene Quartz Intergrowth	$LiAl(SiO_3)_2$
Tantalite	$(Mn,Fe)(Ta,Nb)2O_6$

CHAPTER 1:

INTRODUCTION

1.1 Research background

The demand for lithium from pegmatites has increased as a result of innovations in the electric car industry which is trying to reduce the emission of gases from motor vehicles. Due to this demand, the motor industry requires battery-grade lithium. The Bikita lithium-caesium-tantalum (LCT) pegmatites have provided a steady source of income to the Zimbabwean economy mostly in the ceramics industry for over a century since the discovery of cassiterite on the Bikita Tinfield in 1911. These world-class pegmatites are frequently ranked number three in the world after Greenbushes (Australia) and Tanco (Canada) and are most probably the largest lithium producer in Africa. Currently the Bikita pegmatites are being exploited for lithium from petalite, lepidolite, eucryptite and spodumene-quartz-intergrowths (SQI), caesium (from pollucite) and tantalum ores. The growing demand for lithium use in lithium-ion batteries has led to lithium minerals becoming a focus of attention for exploration and mining. According to Tyndale Biscoe (1951), Martin (1964) and Cooper (1964), the geology of the Bikita pegmatites was extensively studied prior to its initial mining in 1911. With advances in exploration technologies, this report reviews and updates our knowledge on the emplacement of the pegmatites as well as investigating the possible structures that may have controlled their emplacement. It is essential to understand how these pegmatites originate in different geologic terranes and environments. The present work combines understanding the geologic environment, mineralisation and the structural framework that was responsible for controlling the emplacement process of the large pegmatite dykes.

1.2 Historical background of the Bikita Tinfield

The Bikita Tinfield that is host to the Li-bearing pegmatites was discovered in 1909 by the German Koestlich brothers Henry and Justice, whose original discovery was on the old Squenula claims, now the Nigel Tin claims (Martin, 1964). The first mineral to be discovered in these pegmatites was cassiterite (Symons, 1959) hence the geological name for the area “the Bikita Tinfield”. The discovery of tin led to the first claims being pegged over and around the sites of the present Bikita and Al Hayat quarries by the Koestlich brothers in 1911. The initial mining started with the extraction of eluvial deposits manually by gathering in all the boulders and lumps that were small enough to be picked up by hands (Martin, 1964). This proved to be profitable and the rest becomes the story of the Tinfield.

Beryl mining operations involving handpicking were profitable in the early years (1950-1951). At this point in time the real wealth of the Bikita Tinfield was yet to be realised and Americans were the first to enquire about lithium and suddenly Bikita became important to the western world. The first lithium minerals were produced in 1950 in relatively small quantities. Amblygonite was the first lithium mineral to be recovered, followed by lepidolite and petalite. R. Tyndale-Biscoe and D. G. Cooper were the first geologists to be involved in the investigations carried out on the pegmatites between 1951 and 1952 (Symons, 1961). Ownership and operations on the Tinfield was then divided into two with Herbet Nolan the father and then George Nolan the son operating from the northern side (Al Hayat group of claims) of the Tinfield whilst Douglas Lawrie was operating from the southern side (Bikita group of claims) of the Tinfield. In June 1952, the Bikita Company involving Douglas Lawrie and Selection Trust Limited was incorporated (Symons, 1961).

By November 1953 prospecting work had proved the existence of a large orebody of high-grade lepidolite. Orders for lepidolite and petalite were received and started with the primitive pick-shovel-wheelbarrow mining which then led to jackhammers, compressed air, explosives, mechanical shovels and ore carrying trucks. Production resumed using Douglas Lawrie's temporary crushing and picking plant realising serious revenue for the mine. It took Selection Trust Limited three years to develop and bring the mine to full production and by the end of 1956, a permanent crushing and picking plant was in full operation with 153 000 tonnes of lepidolite having been produced to prove the viability of the mine. Early in 1955, the company through E. C. Whaton –Tigar secured a five year contract with the US government to supply lepidolite and by the end of this contract in 1959, Bikita had produced 370 000 tonnes of lepidolite, 63 000 tonnes of petalite, 14 000 tonnes of spodumene, 4 200 tonnes of amblygonite and 383 tonnes of beryl (Symons, 1961).

In October 1959, an option on Nolan's claims was obtained by Bikita Minerals and this option was exercised in December 1959, thus bringing the entire lithium and beryl deposits in the area under the company's ownership to give yet another new lease of life to Bikita. Soon after acquiring George Nolan's claims, the reserves of lithium minerals were almost doubled and petalite became the sought after lithium minerals as it was required for the glass and ceramic industries in the USA. Between the period of 1960 and 1968, Bikita's production prospered as they produced 270 000 tonnes of petalite, 120 000 tonnes of lepidolite, 37 000 tonnes of spodumene, 10 000 tonnes of eucryptite and 3 000 tonnes of lepidolite concentrates which were produced from a pilot floatation plant that was built in 1966. The mine was the largest lithium producer and the 6th largest beryllium producer in the world during the 1960s and 1970s (Symons, 1959). Active mining has been carried out for the past century for tin, tantalum, beryllium, caesium, and lithium. Currently Bikita Minerals uses conventional opencast mining on all its pits.

1.3 Location of the project area

Bikita Minerals mine is a privately owned mine situated about 325 kilometres southeast of the capital Harare, 67 kilometres east of Masvingo town and 2 kilometres to the north of the main Masvingo to Mutare highway (Figure 1.1). The mining lease area which was the first in Zimbabwe (ML-No.1. 31st August 1963) is situated on the farms Glen Clova and Glen Shee covering an area of about 1.539 Hectares (15.4 square kilometres) and consists of several old and current mine workings (Figure 1.2). The old workings include Mdara mine which used to produce tantalite, together with Ranga and Nigel mines which used to produce tin. The current workings include the Al Hayat pit which produces mainly petalite with spodumene, lepidolite, and eucryptite as by-products, Victor's pit which produces mainly petalite with spodumene, lepidolite, and eucryptite as by-products and Bikita pit which produces pollucite, petalite, lepidolite, amblygonite, tantalite, and spodumene.

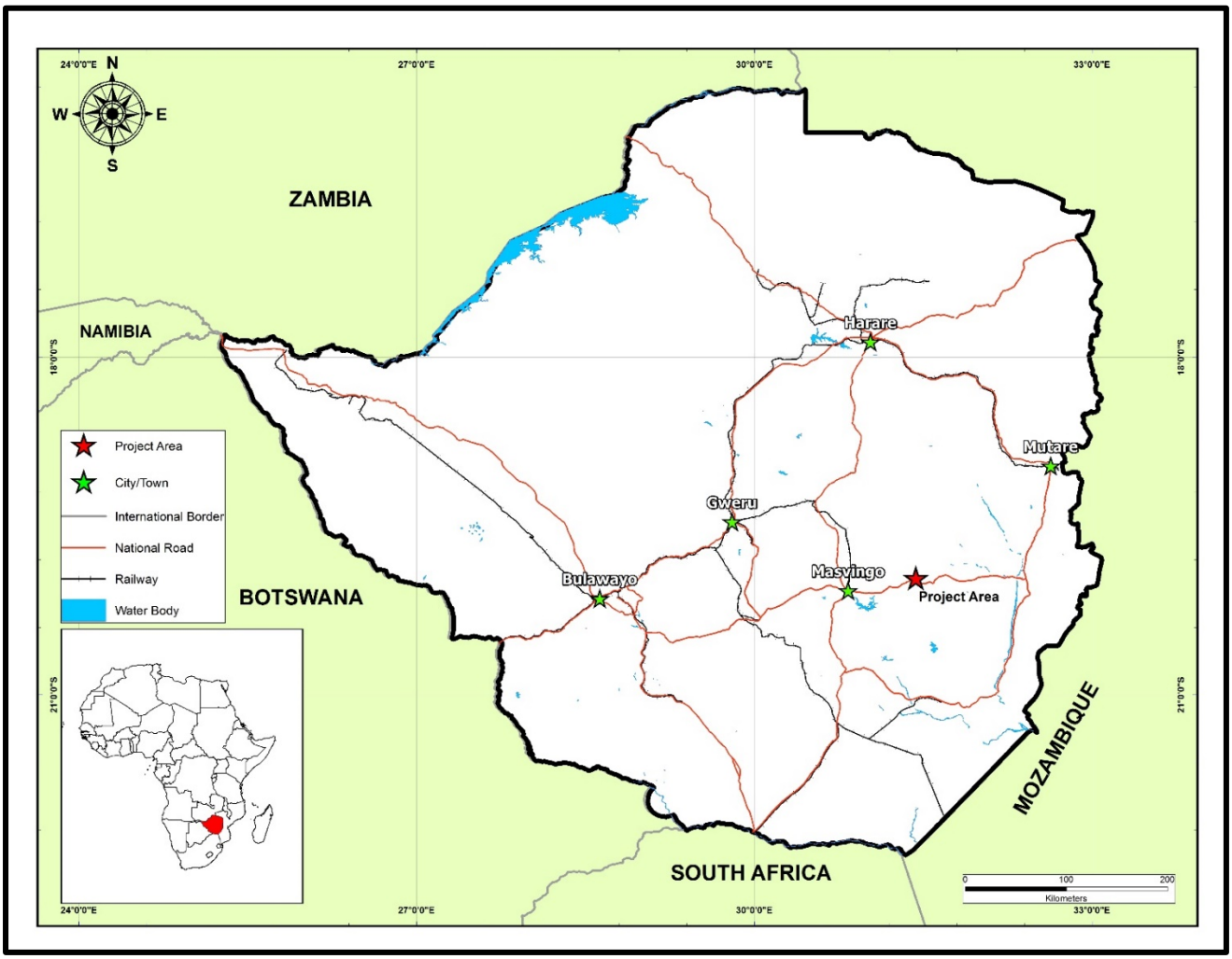

Figure 1.1*: Simplified map showing the location of the Bikita Mine lease area (red star) east of Masvingo.*

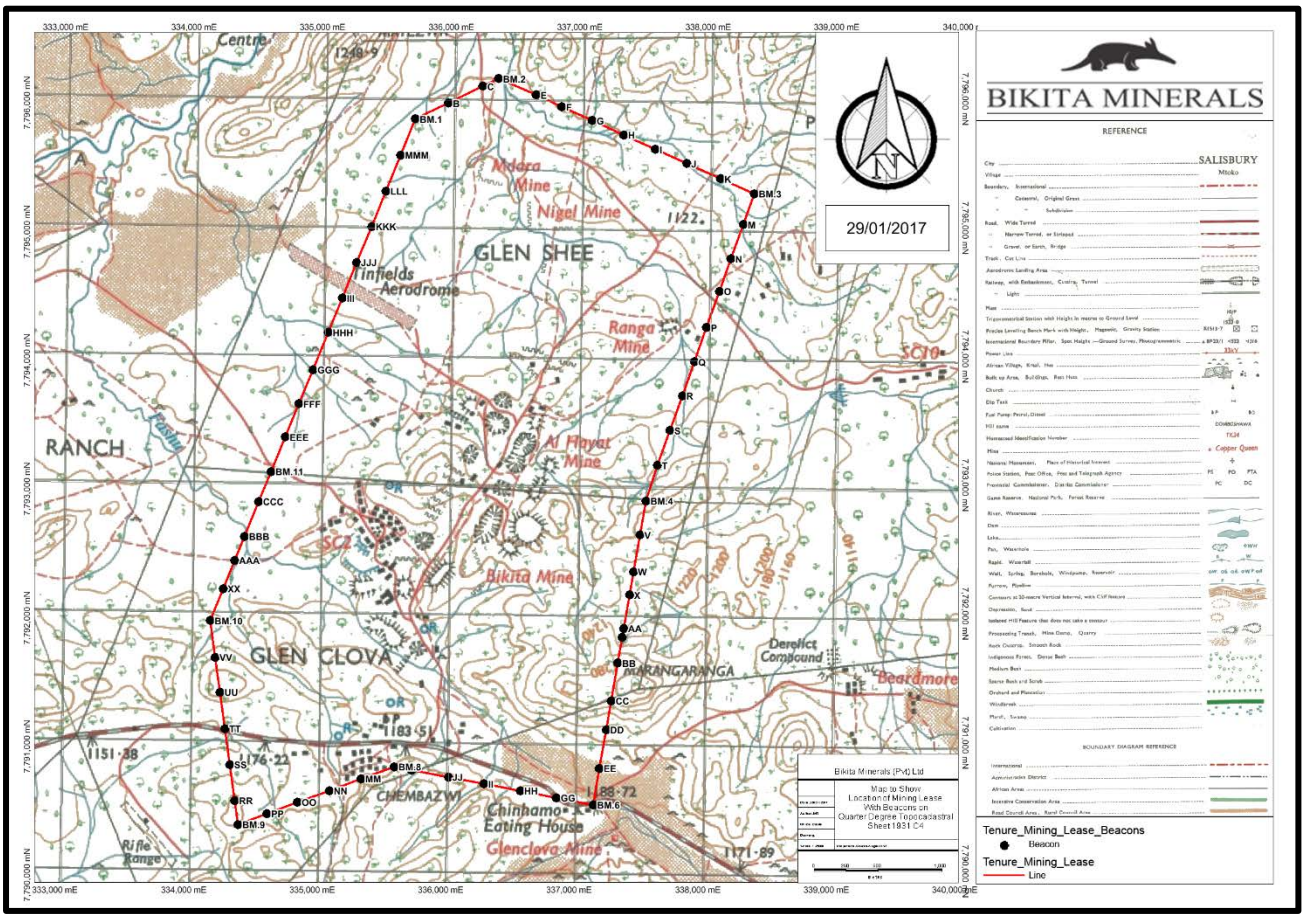

Figure 1.2*: Topographic map showing the location of the mine lease area on the farms Glen Clova and Glen Shee together with the individual historical and current pits.* The mine lease area is outlined in red.

1.4 Scope and research problem statements

The thesis is focused firstly on examining the previous work done on the pegmatites then evaluates the detailed geological settings of the pegmatites so that maps and sections can be updated based on the new lithological data obtained from drilling through the individual pegmatites. Secondly, the thesis will then focus on understanding the deformation, metamorphism and structural framework of the Masvingo Greenstone Belt (MGB). Thirdly the thesis focuses on understanding the mineralogical distribution associated with these various pegmatite dykes in order to know where to extract the economic constituents of the main ore minerals. Finally, the data obtained from the study will be interpreted and integrated in order to formulate conclusions and recommendations.

In order to accomplish these goals, the local 1:10 000 geological map by Martin (1964) was digitised and updated based on the drilling done on the individual pegmatites. Since some of the pegmatites do not outcrop on the surface, radiometric geophysics was used to map these concealed pegmatites throughout the mining lease area. Diamond drill core, reverse circulation and percussion drill chips were also used to understand the distribution of different mineral commodities found within these pegmatites in order to determine their economic potential and viability. Wherever possible, rock chip samples were collected from the different pits to understand the mineral assemblages of the pegmatites. Sections representing some of the pegmatites drilled are shown under their respective pegmatite names. A Landsat 7 ETM+ image together with geophysical surveys were used to help in mapping and interpreting the regional geology and structures of the area. Structural measurements for visible

local structures were recorded and interpreted but the majority of the interpretations were based on ground magnetics data that was available for the area.

The Bikita Minerals mining lease contains several pegmatite bodies which were discovered as a result of follow up investigation of old workings exploited by local people early in the 19th century. Currently the Main pegmatite (1) is the most active one but it is almost exhausted due to a long period of exploitation. The other pegmatite bodies like the Ranga, Nigel (East and North), Dam Site, and Mauve Kop were small and have probably been mined out as well. Other orebodies include the Spodumene pegmatite, the Boomerang pegmatite, the East pegmatite, on which Victor's and Nigel's pits are located, the Shaft pegmatite, the West pegmatite, the Giant pegmatites (east and west) and the Cemetery pegmatite. History has it that exploration of new potential locations for mineral development commonly takes place in and around areas where mineral deposits have already been found (van Roij, 2006). For this reason, and considering the area covered by the Bikita Minerals mining lease, there is great potential to discover new deposits and shift attention away from the Main pegmatite. Modern exploration techniques and new tools like Remote Sensing and GIS that have not been used to integrate the diverse geological datasets to predict mineral potential map for the Bikita mining lease area.

1.5 Research general aims and objectives

Having considered the relevance of understanding the geology, mineralisation and structural controls on the emplacement of the Bikita pegmatites, the aims and objectives of this study are:

i) To give a reviewed comprehensive account on the geological and lithological characteristics for both mineralised and barren pegmatites in selected bodies within the mining lease using whole-rock geochemistry data.
ii) To apply remote sensing Landsat ETM+ and geophysical data to delineate the possible structures (regional and local) that controlled the pegmatite emplacement.
iii) To give a general overview of the characteristics and economic potential of different pegmatites found within the Bikita mining lease area as well as the different mineral commodities they host in order to give exploration guidelines on the best possible areas that host potential mineralisation that can help increase the resource base of the mine.
iv) To determine if the geological map and sections of the Bikita Tinfield pegmatites can be updated by combining the old data and current field observations data and then integrating the datasets into Arc GIS.

1.6 General overview of the Zimbabwean Craton geology

The Archaean Zimbabwean Craton, which covers an area of about 650 kilometres by 350 kilometres is characterised by granite-greenstone terranes in which granitic rocks constitute 85% (Figure 1.3) and the greenstone belt remnants constitute approximately 15% of the craton (Anhaeusser, 1976). The area underlain by this oval-shaped craton is approximately 300 000 square kilometres in total area (Bliss and Stidolph, 1969). The granitic-gneissic portion of the craton consists of tonalitic-granodioritic gneissic basement rocks, which in one case clearly predate the greenstone supracrustals (Bickle et al., 1975), and widespread granitoids which clearly post-date all these supracrustals and are therefore termed Late Archean granitoids. These late granitoids include the ca.2.6 Ga Chilimanzi Suite which is a potash-rich, adamellitic, largely post-tectonic sill-like monzogranites emplaced

as the last major Archaean igneous event in Zimbabwe, heralding final cratonisation and the ca2.7 Ga tonalitic Sesombi Suite (Wilson, 1990).

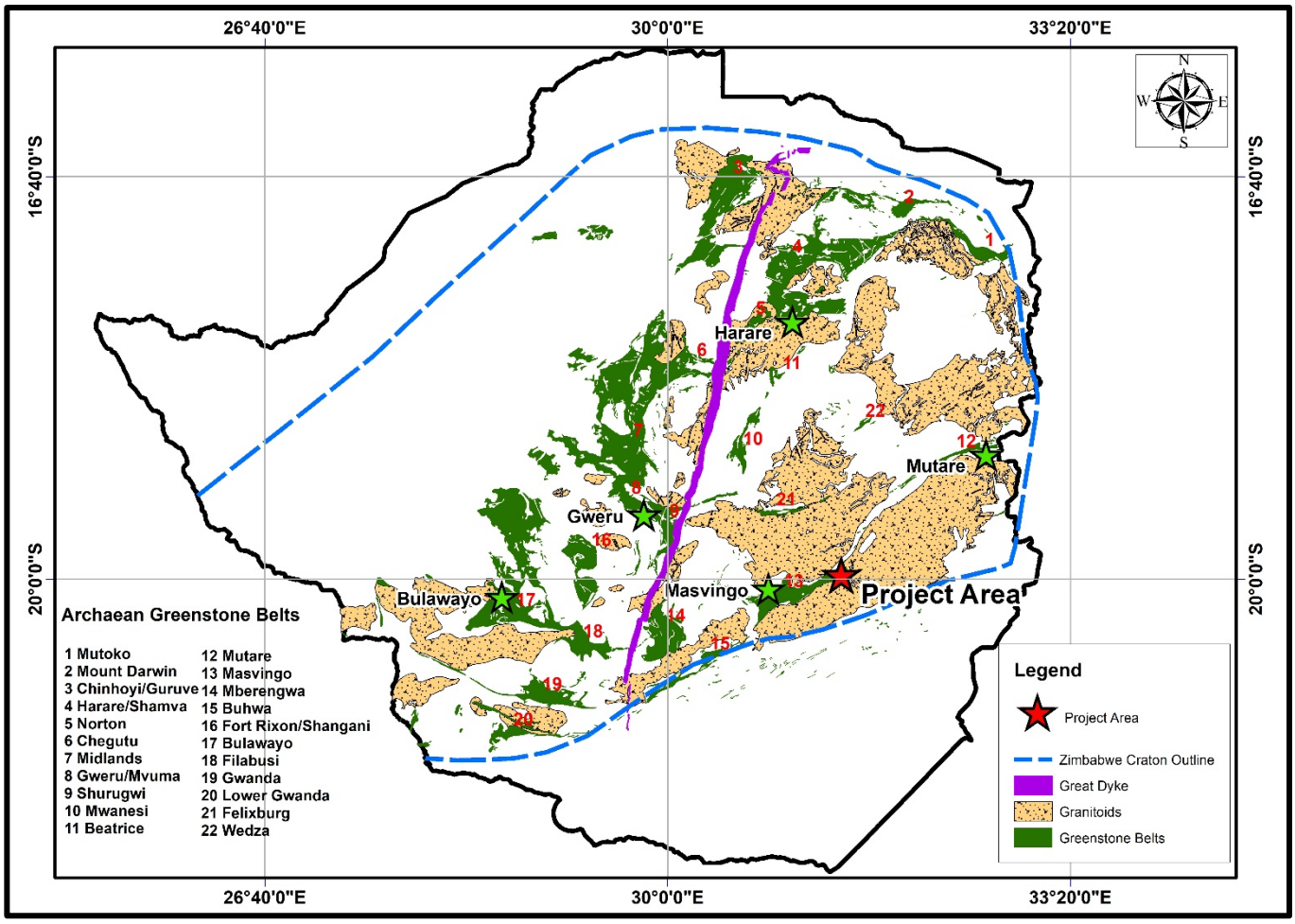

Figure 1.3*: Simplified geological map showing the geological architecture of the Zimbabwe Craton. Modified after Wilson (1981), and Campbell and Pitfield (1994).*

The Zimbabwe craton is surrounded by three orogenic belts: the Limpopo Belt (2.0–2.6 Ga) to the south, the Magondi Mobile Belt (1.8–2.0 Ga) to the north and west, and the Zambezi Mobile Belt to the northeast (0.5–0.7Ga) (Blenkinsop et al., 1997). The greenstone belts are surrounded by the granitic-gneissic rocks of the craton and cut across by the Great Dyke. This craton is dominated by a suite of predominantly NNE trending fractures, for instance, one which was occupied by the Great Dyke whilst the others are occupied by the Umvimeela and East satellite dikes (Wilson et al., 1987) and a number of sinistral wrench faults further to the east (Figure 1.3). The same fracture trend is noticeable in some of the major greenstone belts and older gneisses of the craton (Figure 1.3) which are believed to be indicative of tectonically unstable conditions during the Archaean, i.e. prior to the Great Dyke emplacement event (Murahwi, 1995). It was noted that by 2 500 Ma, the Zimbabwe Craton had finally stabilised with the emplacement of the late Archaean granites (i.e Chilimanzi Granite Suite) and had become sufficiently brittle to produce major fractures that allowed the intrusion of the Great Dyke magmatic event (Murahwi, 1995). The structural evolution of the Zimbabwe Craton was controlled by the relative southwestward movement of the Zimbabwe Craton against the Kaapvaal Craton during the Limpopo orogenesis. Numerous granites and quartz monzonites of the Chilimanzi suite were intruded between 2.55-2.6 Ga

(Hickman, 1978). Metamorphic grades and deformation intensities vary within the craton. There are amphibolite facies and generally strong deformation towards the craton margins and there are greenschist facies with only locally intense deformation towards the craton centre (Wilson, 1990).

1.7 Archaean stratigraphy and general overview of the Zimbabwean Craton greenstone belts

The granite-greenstone belt stratigraphy is divided into remnants of the volcano-sedimentary strata which are now represented by synformally-folded schist belts that fall into three distinct stratigraphic groups. From oldest to youngest, these are (i) the Sebakwian (3.5 Ga), (ii) the lower Bulawayan (2.9 Ga) and the upper Bulawayan (2.7 Ga) (iii) the locally developed Shamvaian (Wilson, 1979; Wilson, 1981). The rocks are named after the areas in which they were first studied or are most extensively developed. These rocks together with masses of granite and gneiss constitute the Basement Complex of the Zimbabwe Craton.

There are more than twenty greenstone belts (Figure 1.3) that are enclosed and spatially distributed within the Archean craton and these comprise mainly mafic, ultramafic and felsic volcanics, volcaniclastics, epiclastics, BIF and intrusions (Campbell and Pitfield, 1994). According to Wilson (1990), the main greenstone belts (ca.2.7-ca.2.9 Ga) were laid down on a granitic crust containing the remnants of earlier greenstone belts and correlations of the major stratigraphic units of the 2.7 Ga Upper Greenstones across the craton indicate the remnants actually were part of a much more continuous cover. The greenstone belts of the craton are characterised by steeply dipping sequences and regional-scale folding, and the granite-gneiss terranes show variable deformation. Early models of crustal development involved mainly vertical tectonics (e.g. Macgregor, 1951), but more recent work (e.g. Wilson, 1990; Treloar and Blenkinsop, 1995; Blenkinsop and Frei, 1997; Dirks and Jelsma, 1998) has emphasised the role of wrench and/or accretionary tectonics. The metamorphic grades and intensity of deformation within the craton varies from amphibolite facies grades (higher within the Limpopo Belt) and deformation tends to be stronger towards the margin of the craton (most notably in the SW), to lower greenschist facies with only locally intense deformation nearer the centre of the craton, for example, the Midlands Greenstone Belt (Campbell and Pitfield, 1994).

The greenstones have an asymmetrical distribution across the craton as they are concentrated in the west and particularly south-west of the Great Dyke (McCourt and Vearncombe, 1992). The structural grain of the craton is quite complex and Macgregor (1951) noted that as a result of this complexity, the craton reflects polyphase deformation and diapiric plutonism. The major period of greenstone belt formation, granitic plutonism, metamorphism and deformation within the craton is believed to have occurred between 2.6-2.7 Ga. This is the period in which the Bulawayan and Shamvaian Groups were formed, the intrusion of mafic dykes and the Mashava complex as well as the emplacement of various tonalitic plutons.

1.7.1 General overview of the Masvingo Greenstone Belt geology

According to Tyndale-Biscoe (1951), the Masvingo Greenstone Belt forms the host rocks to the Bikita Tinfield pegmatites which are located near the eastern tip of this belt (Figure 1.4). The 100 kilometres long by 22 kilometres wide elongate Masvingo Greenstone Belt lies in the southeastern part of the Zimbabwean craton (Figure 1.3) and contains rocks that are mostly foliated with an east-northeast trend. The belt is dominated by Upper Bulawayan Greenstones, basic and ultrabasic volcanic and minor interbedded sediments overlain by coarse-clastic Shamvaian-type sediments (Wilson, 1964). Most of the rock units within the Masvingo Greenstone Belt have been folded and metamorphosed to different grades with the exception of basaltic lavas which are relatively undeformed and show

existing pillow structures in some places (Wilson, 1964). Coward and James (1974) linked the deformation to the events in the adjacent Limpopo orogenic belt with pluton emplacement. As a result of this deformation, the belt exhibits a synformal structure. The Jenya Fault System and the Popoteke Fault Systems (Figure 1.4) are the major regional structures that transact the belt (Wilson, 1990).

1.7.2 Tectonostratigraphic framework of the Masvingo Greenstone Belt

There are several tectonic events that can be noted and recorded in the Masvingo Greenstone Belt rocks and the surrounding plutons. It is one of the many Basement Complex relict masses of sedimentary rocks in Zimbabwe. The Masvingo Greenstone Belt contains all the stratigraphic rock sequences of the Zimbabwean Craton (Sebakwean, Bulawayan, and Shamvaian) and these rock sequences were intruded by ultramafic rocks, granites, pegmatites and various generations of felsic dykes and quartz veins. Rocks of the Sebakwian Group are mostly granitic gneisses which tend to be rare within the belt and only occur along the northern and western margin of the greenstone belt and include gneisses of various ages from 3 500–2 700 Ma (Gwavava and Ranganai, 2009) that surround the Masvingo Greenstone Belt. The majority of the rocks within the belt are of the Lower and Upper Bulawayan Group constituting quartz-mica schist, pelitic metasedimentary rocks with intercalated bands or lenses of banded ironstone, banded quartzite or limestone and these are found in the westernmost portion of the Masvingo Greenstone Belt and within the northern part of the Bikita pegmatite field.

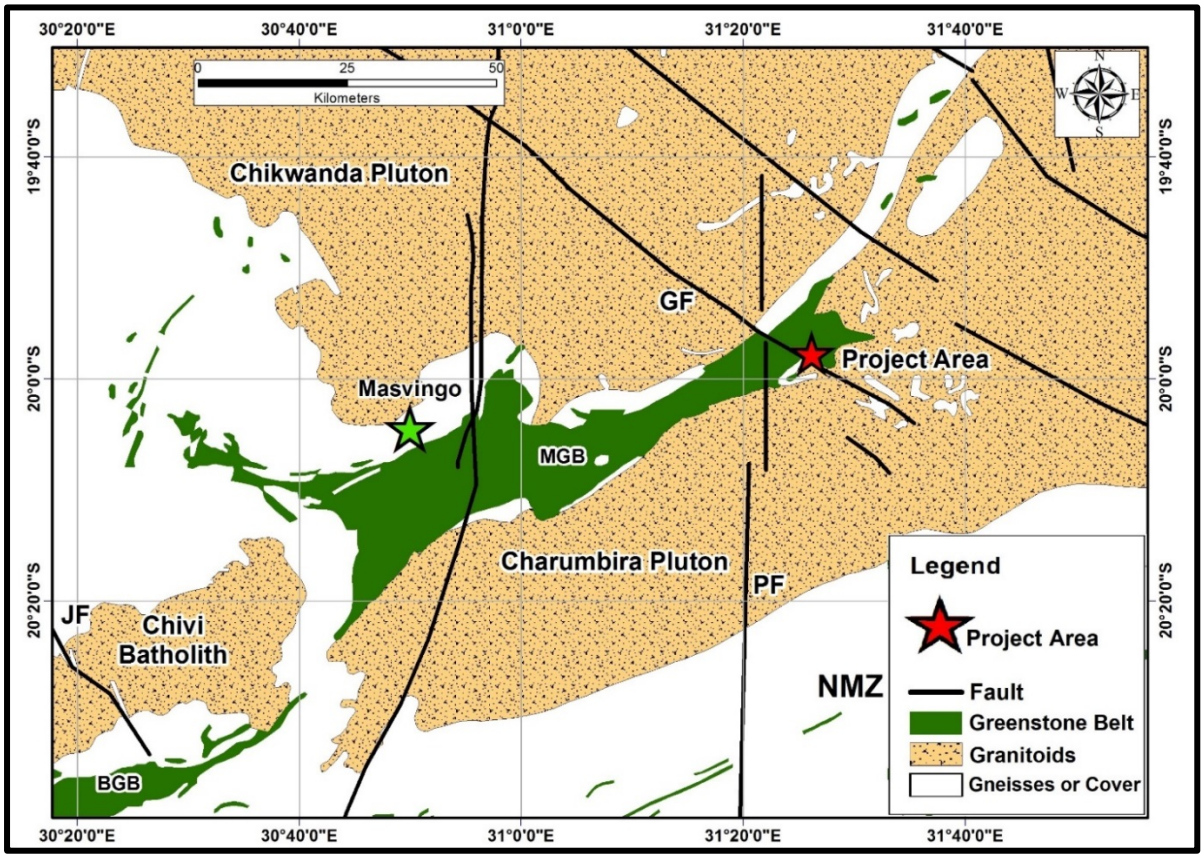

Figure 1.4*: Regional geological map of the Masvingo Greenstone Belt and surrounding granite-gneiss terrains.*BGB Buhwa Greenstone Belt; MGB Masvingo Greenstone Belt; PF Popoteke Fault; GF Gono Fault; JF Jenya Fault; NMZ northern Marginal Zone of the Limpopo Belt. (Modified and redrawn after Wilson, 1990).

The mafic rocks belonging to the Upper Bulawayan Group are predominant within the Greenstone Belt. These comprise metabasalts, chlorite, or hornblende-schist and metadiorites and these are the rocks into which the Bikita pegmatites were emplaced. This rock unit succession was overlain unconformably by clastic metasedimentary rocks of the Shamvaian Group (e.g., conglomerate, phyllite, banded ironstone) and was metamorphosed and tightly folded to a synclinal structure under a compressional tectonic setting (Coward and James, 1974) during the NW directed thrusting of the Limpopo belt onto the Zimbabwe Craton at 2 700 Ma. The subsequent extension is attributed to have started at 2 670 Ma and is concomitant with the emplacement of the Chilimanzi Suite granitoids (Hamilton, 1977). Within the area of the Masvingo Greenstone Belt, this magmatic suite is expressed by the surrounding Chivi batholith to the west, the Chikwanda pluton to the north and Charumbira pluton to the south (Figure 1.4). The relationship between the Masvingo Greenstone Belt and different intrusions was unravelled by the geophysical work of Gwavava and Ranganai (2009).

According to the geophysical interpretations of Gwavava and Ranganai (2009), the area south of the Masvingo Greenstone Belt is a zone of crustal weakness in which the intrusions of the Charumbira pluton were emplaced as part of the Chilimanzi Suite. The intrusion-related extension within the rocks is responsible for the formation of the NW-SE striking Gono fault and the N-S striking Popoteke fault within the Masvingo Greenstone Belt (Figure 1.4). Late-stage intrusions within the belt have resulted in a contact metamorphic overprint of the lithologies expressed by the formation of tremolite-actinolite schists, or talc and talc-carbonate schists at the western margin of the greenstone belt, as well as the formation of numerous lensoid serpentinite bodies throughout the greenstone belt. The serpentinite bodies are mainly confined to the north of the Gono fault. These events were interpreted by Dittrich (2017) to be related to the extensive tectonic regime during the emplacement of the pegmatites and associated fluid flow and thus probably represent ultrabasic intrusions in the greenstones. The other significant event within the rocks of the Masvingo Greenstone Belt is the formation of various generations of quartz veins that display multiple orientations and are believed to have formed along pre-existing faults or structures at the boundary of the greenstone belt to the granite or the Popoteke and Gono faults (Figure 1.4), as well as along structures formed during later events (Dittrich, 2017).

According to Tyndale-Biscoe (1951), the granitoids surrounding the Masvingo Greenstone Belt are probably the source of the materials which formed the greisenised pegmatites and ore-bearing skarn lode veins of the district such as the Beardmore scheelite mine which is located close to the granodiorite contact southeast of the Bikita tin-field close to the margins of the Masvingo Greenstone Belt where epidote and garnet are dominant. The last recognisable episode in the geological history of the area is the intrusion of basic magma to form dolerite dikes which penetrate the greisenised pegmatite bodies and has added considerably to the difficulties of mining.

1.8 The regional geological setting of the Bikita pegmatites

The Bikita pegmatite field also known as the Bikita Tinfield is hosted within the easternmost portion of the elongate shaped Masvingo Greenstone Belt (Figure 1.5) which is invariably foliated with an ENE trend. The pegmatites within the field are intrusive into the Chilimanzi granitic rocks on the southern and eastern margins of the belt and extend into the metavolcanic and metasedimentary rocks of the Upper Bulawayan Group. Within the fields, three pegmatite districts are recognised and in order of economic importance these are Bikita, Rurgwe, and Chikwanda (Figure 1.5). The Bikita district comprises two distinct pegmatite fields, a northern N–S trending pegmatite field, and a southern E-W trending pegmatite field. Individual pegmatites are hosted within predominantly greenstone

belt lithologies (i.e., metabasalt, metadiorite) of the Upper Bulawayan Group and only minor occurrences are within pelitic rocks of the Lower Bulawayan Group (Wilson, 1964).

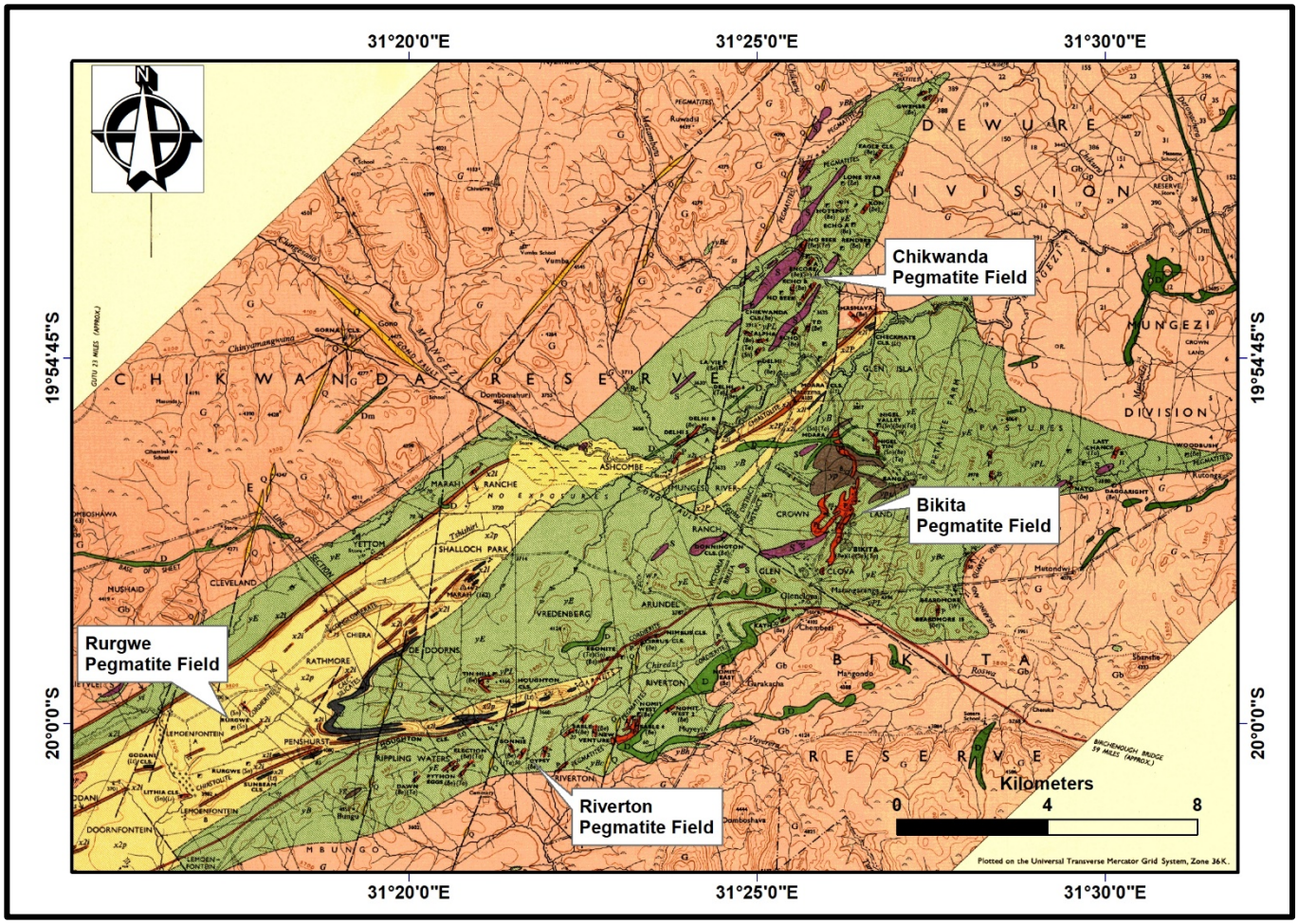

Figure 1.5: *Extract from 1:100,000 geological map showing the regional geological setting of the Bikita pegmatites. Adapted from Wilson (1964).* Green represents the greenstones, Yellow represents the older sediments in the synformal core of the MGB and the pink-brown colour represents the granites and gneisses.

The greenstone belts are rimmed by older granitic gneisses probably belonging to the >3 300 Ma Sebakwaian Group and two granite plutons of Archean granitoid rocks (2 600 Ma) of the Chilimanzi Suite (Tyndale-Biscoe 1951, Martin 1964). These are the Chikwanda pluton to the north and the Charumbira pluton along the southern margin of the Masvingo Greenstone Belt. These pegmatites are predominantly confined to upper greenschist and amphibolite-facies metabasalts of the Mesoarchean Bulawayan Group (Dittrich, 2017).

CHAPTER 2:

RESEARCH METHODOLOGY

2.1 Research methods background

In order to achieve the project objectives, the methodology adopted for this research work consisted of a field study, whole-rock geochemical laboratory analyses, data integration into GIS formats with the main focus on the historic and current work done within the Bikita pegmatite field. For the purposes of understanding the pegmatites, a literature survey was done on granitic rare-element-hosted pegmatite mineralisation with a particular review of the LCT pegmatites. The local geology map of the Bikita pegmatites was digitised in order to filter in the new data sets collected from the field with the main objective of updating this map and its sections. The Bikita Minerals laboratory was used for the geochemical analysis. Whole-rock major and trace element geochemical sampling from reverse circulation and percussion chips, core from diamond drilling as well as channel chip/grab sampling on pit faces was conducted to determine the variations in mineralisation of the pegmatite bodies. Logging and sampling were done on selected key exploration boreholes which have intersected the major pegmatite mineralisation of significance (Li, Be, Ta, Sn, Cs) and those that make a meaningful contribution based on their geochemical composition. In areas where drilling data is not obtainable, chip/grab sampling was used in order to understand the distribution of different mineral commodities found within the various pegmatites within the mining lease. Drill hole profiles (strata) and sections were produced in order to understand mineral zoning.

The analysis involved whole-rock geochemical analysis using a portable Innov XRF gun and a Pinnacle 900 AAS machine for both major and trace elements. Structural analysis and interpretation of the data were done in order to understand the distribution trends of the structural patterns and their possible role in controlling the pegmatite emplacement. This was done using remotely sensed satellite Landsat ETM+ image together with the integration of ground magnetic survey in order to map the geology and identify the local structural zones of weakness (brittle/ductile) such as faults and shear zones. For ground truthing, the local and regional geological maps of the Bikita Tinfield were used. Field measurements were collected on structures that were mapped. The different data sets from these geochemical and structural studies were then integrated into a GIS database format for analysis, evaluation, and interpretation. QGis and Arc Map were used for the main tasks of the project.

2.2 Whole-rock geochemical sampling

This section describes the sampling that was undertaken to represent mineralisation potential as well as mineralisation distribution trends. The geochemical data is useful in determining the chemical composition of these individual samples. The geochemical sampling methods employed in the research involved in-situ whole-rock channel chip/grab, drill chip and drill core intersections that were intercepted by drilling. The localities of the channel chip/grab samples and drill holes are shown in Figures 2.1 and 2.2 respectively. The localities where samples were collected have been divided into quarry, pits and sectors i.e (Bikita quarry), (McMurdon, Al Hayat, Victor's, Nigel's and Dam Site pits) and (Ledingham, Shaft, West, Giant East, Mauve Kop and Cemetery sectors)

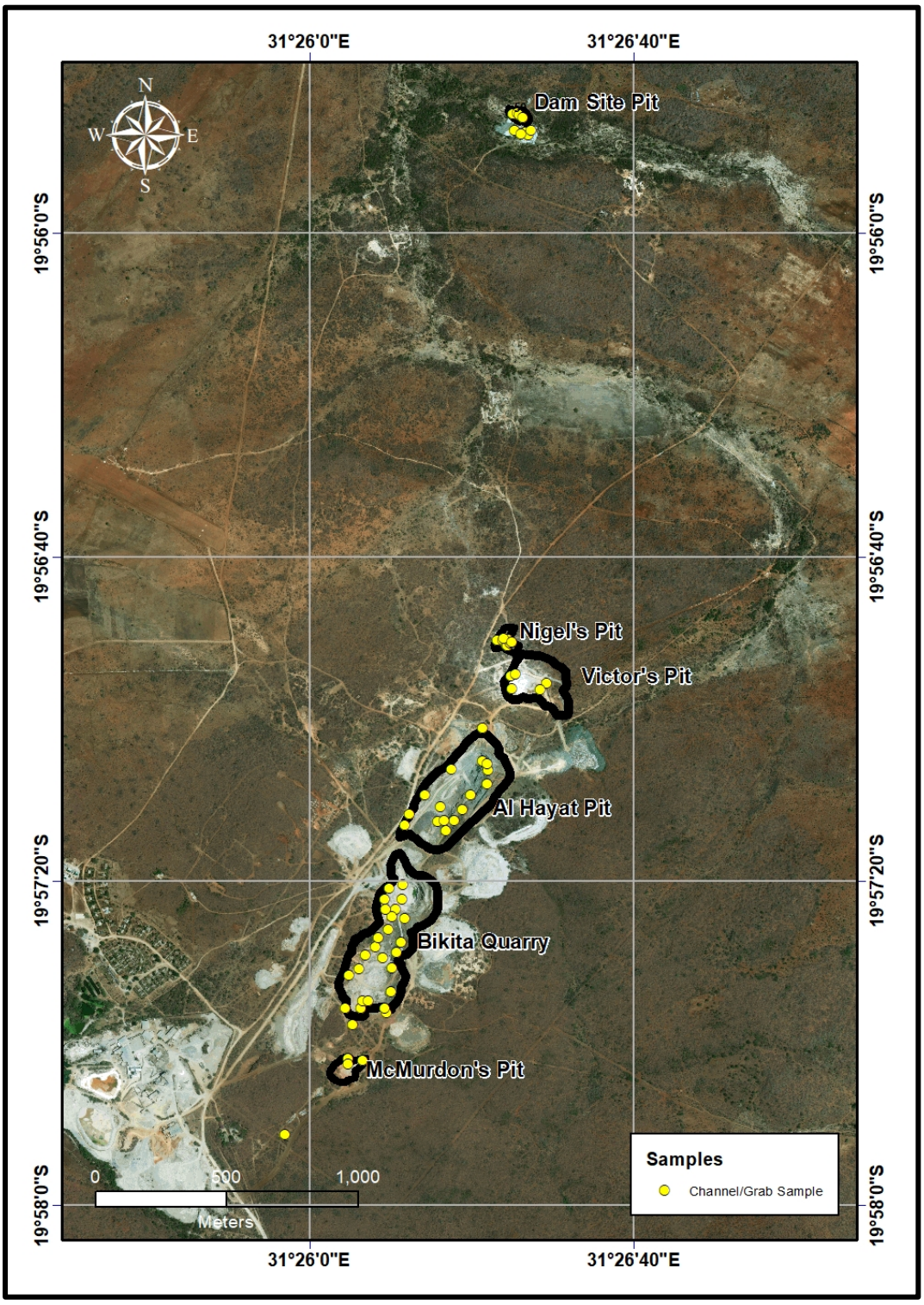

Figure 2.1*: Google Earth image of the Bikita Mine area showing individual open-cast pits and channel chip/grab sample locations*

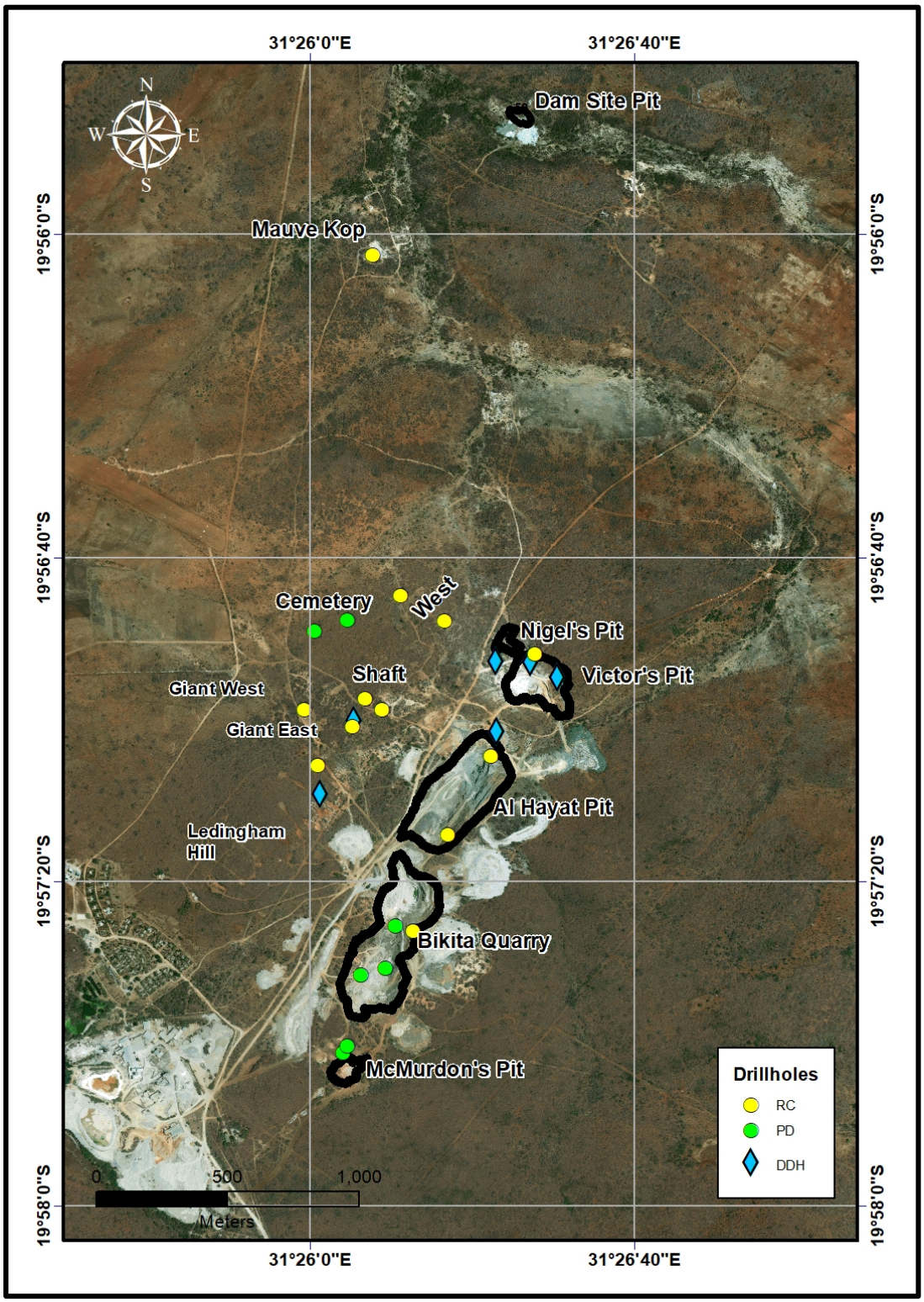

Figure 2.2: *Google Earth image of the Bikita Mine area showing individual open cast pits and various drill hole localities which were drilled in McMurdon pit, Bikita quarry, Al Hayat pit, Ledingham sector, Victor's pit, Nigel's pit, Shaft sector, West sector, Giant East sector, Mauve Kop sector and Cemetery sector.* **RC**-Reverse Circulation; **PD**-Percussion Drilling; **DDH**-Diamond Drill Hole

2.3 Sample selection

A geochemical summary of the dataset used in this report is shown in Table 2.1. These samples came from the various pegmatite bodies and were selected for geochemical analyses in order to investigate the outlined aims and objectives for the study. The samples were collected only on pegmatite intersections. The selection of these drill holes was based mainly on AAS whole-rock geochemistry and the geological logging database of the samples from the various pegmatite bodies. XRF was used to confirm the presence of other mineral constituents apart from the major elements (Li, Cs, Rb) as these elements could not be detected by AAS (Ta, Sn). The boreholes and channel or grab samples selected were based on their contiguous location within the mining lease in order to be representative, thus allowing for the comparison of the different lithologies on the relevant horizons. The following categories were used to select the drill holes:

- Drill holes where lithium is present but absent in others
- The drill holes that host varying bulk pegmatite minerals i.e. some of the drill holes must have high lithium values (above 1%) whilst others must have medium to low lithium values (below 1%)
- Those drill holes where lithium wasn't logged and yet having other mineral species like cassiterite, tantalite, and beryl
- The drill holes that are scattered in order to be representative of the various mineralogical behaviours within the pegmatite bodies
- Selection and logging of drill holes that are on the same lines in order to produce cross-sections

The description of rock types and textures, and samples collected to characterise pegmatite bodies, was mostly carried from in-situ occurrences intercepted by drill cores and chips from the localities: McMurdon, Bikita, Al Hayat, Ledingham, Victor's, Nigel's, Shaft, West, Giant East, Mauve Kop, Dam Site and Cemetery. The details for the geochemical data sets used in the report are summarised in Table 2.1.

***Table 2.1**: Geochemical dataset summary.*

Locality (Pit,Quarry, Sector)	Sample type	Number of Drill holes	Number of samples
McMurdon	Channel chip		6
	Percussion drill chip	2	45
Bikita	Channel chip		25
	RC chip	1	49
	Percussion chip	3	83
Al Hayat	Channel chip		16
	RC chip	2	90
	Diamond Drill Core	1	112
Ledingham	Diamond Drill Core	2	249
	RC chip	1	43
Victor's	RC chip	1	37
	Channel chip		5
	Diamond Drill Core	2	158
Nigel's	Channel chip		9
	Diamond Drill Core	1	63
Shaft	RC chip	3	138
West	RC chip	2	38
Giant East	RC chip	1	36
Mauve Kop	RC chip	1	13
Dam Site	Channel chip/Grab		9
Cemetery	Percussion drill chip	2	17
Total		**25**	**1241**

2.4 Geochemical sampling and logging

The main objective of conducting geochemical sampling was to understand mineralisation patterns, distributions, and zoning within the pegmatite bodies.

2.4.1 Whole-rock channel chip/grab sampling and logging

This involved taking representative fresh rock in-situ samples of economic mineralisation horizons from various pits using a chisel and hammer. Grab samples were mainly collected in the Dam Site locality where a small pit has been opened looking for extensions of the pollucite that was found there. These samples were then crushed, coned and quartered until a representative sample for assay had been obtained. The field sampling of existing exposed pit openings focused on the detailed description of economic mineralogy present in these different pegmatite bodies across the mining lease. During the logging, descriptions were made on the different rock species sampled and Table 2.2 shows how the logging was done. Details of these logging descriptions are shown in Appendix 1a.

***Table 2.2**: Preliminary channel chip log sheet.*

Sample Name	Description
MK-001	Medium to coarse grained pale lilac feldspathic lepidolite with minor quartz inclusions
MK-002	Medium to coarse grained deep mauve lepidolite intermixed with albite and quartz
MK-003	Feldspathic friable lepidolite intermixed with minor quartz inclusions
MK-004	Fine to medium grained deep mauve lepidolite with albite and quartz inclusions
MK-005	Fine grained matrix of feldspathic lepidolite, tourmaline and quartz (wall-rock altered zone)
MK-006	Medium grained pale lilac lepidolite with slicken sides showing movement of blocks (fault zone)
BS-001	Dark medium grained lepidolite
BS-002	White amblygonite
BS-003	Pink SQI with coarse needles
BS-004	Pale purple fine-grained lepidolite
BS-005	Grey petalite
BS-006	Coarse grained lepidolite
BS-007	Medium grained lepidolite

2.4.2 Whole-rock drill chip sampling and logging

This involved the collection of chip samples/powder produced from percussion and reverse circulation drilling. Samples are collected at every one-metre interval within the pegmatite intersections. Two sets of samples are obtained through riffle splitting for representativeness with the main purpose of performing chemical analysis from these one-metre intervals and this includes a geo-reference and a lab sample. The chips are first sieved using an 850 microns sieve in order to get rid of the finer particles and then placed into clearly labelled chip trays (Figure 2.3).



***Figure 2.3:** Photograph of a typical sample chip tray and its labelling*

Once in chip trays, the chips were logged per sampling intervals noting down all the identifiable mineral species within that metre, sample positions, colour changes as well as all the other relevant information from the drilling. After logging the one-metre intervals, the different zones are then grouped in order to categorise the change in zoning over a drill hole as well as aiding in the construction of drill sections. The verification of fluorescent minerals

especially eucryptite was done using a UV (Ultra-Violet) light. Log sheets detailing the sampling and logging are shown in Appendix 1c.

2.4.3 Whole-rock diamond drill core sampling and logging

Detailed diamond core logging was done to have a better geological understanding of mineralisation in the different pegmatite bodies. The logging of the core is vital on any project as the eye of a geologist will help in the interpretation with regards to the drill intersections. Initially, the drill cores were cleaned and clearly marked showing the different zones based on lithologies (Figure 2.4). Once detailed descriptions are done, the logs are then used to produce lithostratigraphic drill profiles (Figure 2.5). The diamond drill log sheets are presented in Appendix 1d.



Figure 2.4: *Preliminary diamond drill core photo from the Shaft pegmatite body showing how the different lithological boundaries were marked.* Black lines show core orientation markings and black numbers represent the metre markings and red letters are abbreviations for the different lithologies.

Drill core logging was done on each borehole to obtain information about the lithologies (zones), main mineral characteristics, alteration, weathering, grain size, lithological contacts and any other relevant information obtained from the drill holes in order to establish and classify the different varieties of the lithologies encountered in the boreholes. This was done by identifying the different mineral species and the change in lithologies with the depth of the drill hole. It is vital to make note of the contacts and transitions during logging as this helps in knowing where the mineral species occur within the different pegmatite bodies. The verification of fluorescent minerals especially eucryptite was done using a UV (Ultra-Violet) light. Core sampling was then carried out after logging. Due to complexities in the pegmatite zoning, it was agreed by the geology department that core sampling was done on every 50 cm intervals regardless of changes in lithologies. The sampling started from the hangingwall contact to the footwall contact. About a quarter size of the core was collected from core boxes. These small pieces

were put into plastic bags for geochemical sample analysis at the laboratory and the weight of each sample was recorded. Once detailed descriptions are done, a summary of the logging was created in order to derive lithostratigraphic diamond drill profiles (Figure 2.5) which then aided in producing cross-sections. Also depicted on the drill profiles are sample positions prefixed with an "A". The rest of the lithostratigraphic diamond drill profiles are presented in Appendix 4.

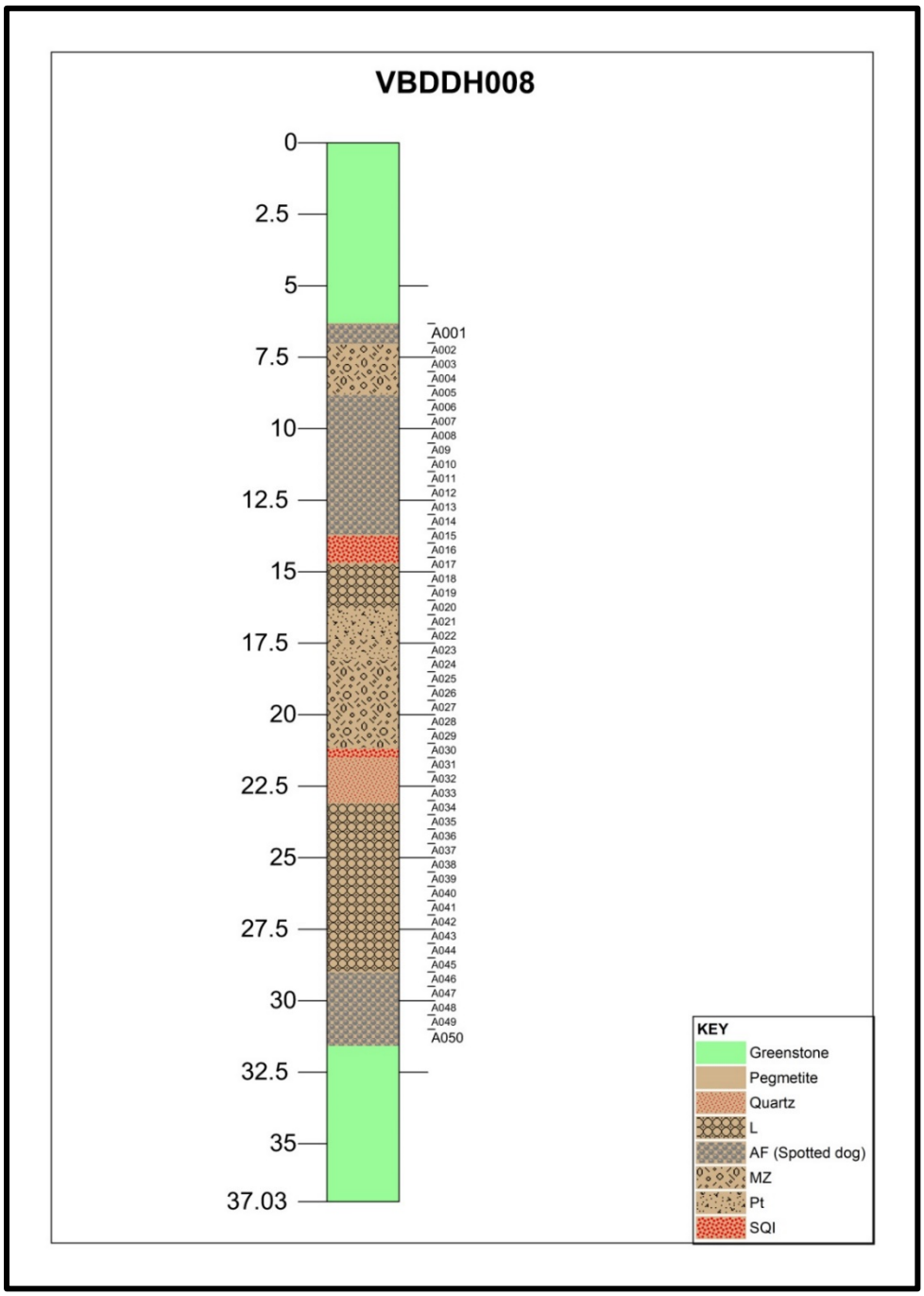

Figure 2.5: *Preliminary lithostratigraphic diamond drill profile for VB-DDH-008.* **L** represents lepidolite, **AF** represents albite feldspar, **MZ** represents mixed zone, **Pt** represents petalite and **SQI** represents spodumene.

2.4.4 Laboratory work and techniques

Representative samples from each drill hole were submitted for sample preparation. The samples were prepared according to standard procedures. Appendix 7 shows the sample preparation procedure.

2.4.5 Sample geochemical analysis

The whole-rock geochemical analyses involved a combination of AAS and XRF techniques that were employed in the determination of major and trace elements. A total of 1143 samples were analysed for major (>1 wt %), minor (<1 wt % to >100 ppm) and trace (<100 ppm) elemental composition using AAS whilst a total of 441 samples were analysed by INNOV-X XRF. These samples were analysed by the Bikita Minerals laboratory at the mine. Each AAS sample was analysed for (weight %) Li_2O, K_2O, Na_2O, Al_2O_3, Cs_2O, Fe_2O_3 and Rb_2O whilst the XRF samples were analysed for Ta, Sn, Nb, Fe, Rb and Sr. At Bikita minerals, the XRF machine is used mainly for the analysis of tantalite-bearing samples and three analyses are made on the pulverised sample and then an average is used for reporting. For the higher concentration of tantalite, the machine is set to the mining mode and units will be in percentages whilst for trace concentration of tantalite, the INNOV-X machine is set to the soil mode where units will be in ppm (parts per million). Sample points and drill holes were captured in CSV-format and imported into ArcGIS by firstly converting the file into a database file in ArcCatalog. The lithology shapefiles and sample points were then used to generate various maps.

2.5 Geological mapping

Geological mapping is the first step to have a better understanding on any project and in this case it was vital in reviewing the geology and mineralisation around the Bikita pegmatite bodies. This involved the gathering of data to update the geological map and generation of sections for the main and active Bikita pegmatite bodies in order to understand their geology. The main activities involved map digitisation, structural and lithological field investigation by integration of radiometric and ground magnetic data and interpretation of remote sensing satellite image. Ground truthing as well as interpretation of the existing regional and local geological maps was done to ensure accuracy in the captured geological data so as to help in the final data integration and interpretation.

2.5.1 Map generation

The main objective of digitising the local geology map was to obtain a digital map that can be edited so that new data can be easily updated. The georeferenced geology map was imported into an ArcGis project. The project file (mxd) was set to WGS84 Geographic Coordinate System. The various lithology units on the geology map were then digitised and saved as shapefiles for ease of manipulation. The regional geology was also loaded onto the project file and georeferenced. The local geophysical data was obtained from the mine in the form of MapInfo Tab files, these were then converted into shapefiles so that they are useable in ArcGIS. All the tiles were then merged together into a single file.

2.5.2 Structural field investigations

The field investigation that were carried out involved field structural data measurements of bedding orientations, bedding locations of fractures with a Silva compass clinometer, a Garmin map 64 GPS recording the coordinates of every structure point, a measuring tape, and a Huawei P8 Lite phone camera. About 27 structural measurements (Appendix 5) were recorded from the existing pit faces where they have better preservation and plotted with the

appropriate strike-dip symbol, then rotated accordingly to represent the strike and dip angle of that unit on the digitised local geological map.

2.5.3 Designing the ground magnetic and radiometric geophysical survey

The surveys were designed to cover the majority of the Bikita Mining Lease at 100 metre line spacing in the outlying areas for broader geological mapping, with a more detailed area surrounding the current mining pit areas to be surveyed at 50 metre line spacing to give high-resolution mapping area around the main pegmatites. The plant area and village areas were excluded from the survey area due to excessive electrical noise (electricity and metal structures) which would affect the equipment and thus the data quality. The objective of using the geophysical work was to map all of the pegmatite bodies in the area in as great a detail as possible and to create a new structural and geological map. The survey lines were laid out at 290° in order to cross the geological strike at right angles (Figure 2.6).

GEM GSM-19 Walkmags were used for the magnetics survey with a station (reading) spacing of 10 metre, thus creating a highly detailed dataset. A base station magnetometer was placed in a stable area outside of the survey area in order to monitor and remove diurnal effects and to allow for level survey data between different days. For the radiometric, a Radiation Solutions RS125 spectrometer was used, also with a 10 metre station spacing. This spectrometer measures total gamma counts as well as potassium (K) in %, thorium (Th) in ppm and uranium (U) in ppm.

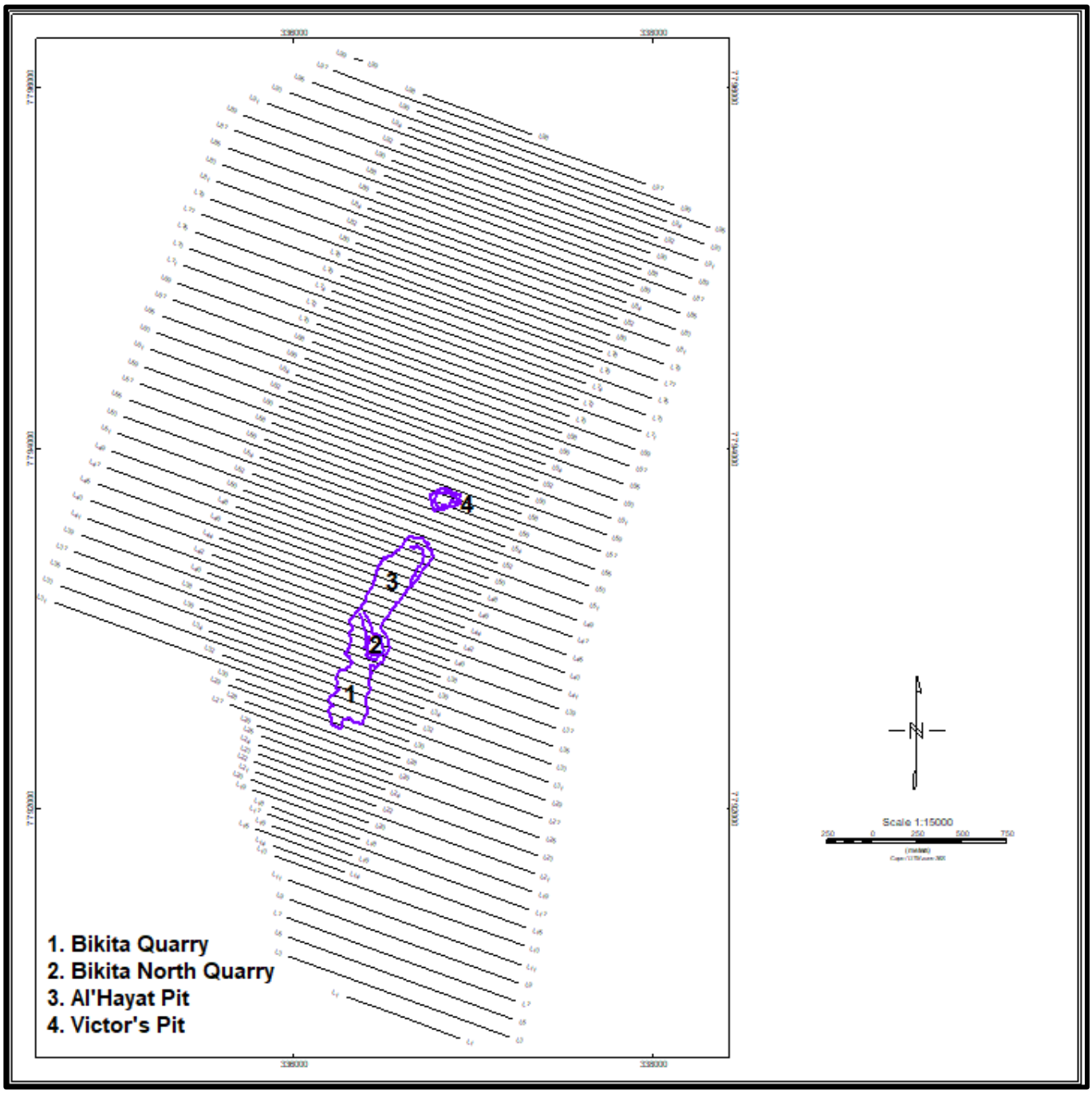

Figure 2.6: *Planning diagram showing the layout of the Bikita ground magnetic and radiometric survey.* Current pits are shown in purple.

2.5.4 Remote sensing satellite image data collection

Remote sensing has been a useful tool in mapping structures since they give a regional synoptic view of areas of interest. A Landsat 7 Enhanced Thematic Mapper (ETM+) satellite image dated 2000-10-09 comprising 8 bands which covered the project area was downloaded from the USGS website using EarthExplorer (http://earthexplorer.usgs.gov/) to further study these pegmatites as well as delineating the synoptic view of major structures cutting across the rocks in order to map the geology and have a better understanding on these structures and produce a structural map of the area. It was noted that the best image for mineral exploration

mapping is the one acquired during winter when the vegetation growth is at its lowest point so as to provide the clearest view of the underlying geology. The historic geological maps (local and regional) were used for ground-truthing and then these were combined with the geophysics data before being imported into QGis and composited into a single file using only bands 1, 2, 3, 4, 5 and 7 into an ArcGIS database. QGis software application was used for processing remote sensing images, whereas ArcGIS (ArcMap 10.3) software was used for georeferencing, editing, creating maps, and handling of the different datasets by comparing them with each other and finally integrating these datasets into final images that highlighted the features of interest. The composite image was used to create various false colour images by alternating the band combinations. Structural lineaments from the literature were also digitised in order to provide comparisons with the remote sensing work.

Satellite data processing has been exercised in order to have a synoptic regional coverage of the project area. Images captured from space usually have a hazy appearance due to the way the atmosphere transmits visible light as a result of inter-atmospheric gases and aerosols which absorb and scatter the light. The visibility (visible spectrum) of images is mainly based on red, green and blue (RGB) pixels in decreasing wavelength order of the electromagnetic spectrum. These images definitely don't have infrared or ultra-blue pixels so when dealing with maps, they are assigned bands from a multispectral image to the red, green and blue pixels thereby producing a false-colour image (in other words making the invisible visible) and true-colour images in the process. The choice of Landsat images for delineation of structures in this research work is based on the fact that they are free and produce meaningful information when processed. Landsat images also tend to get preference because of their large spectral resolution (many bands) and their appropriate spatial resolution. In this study, the satellite imagery was mainly used for structural mapping in order to identify and characterise the structural expressions such as faults, folds, and lineaments that provide an insight as to how the Bikita pegmatites have been emplaced.

2.5.5 Section generation

The sections were useful in defining lithostratigraphic columns of the pegmatite bodies. For this research, the sections were generated based on intersections and logs from percussion, reverse circulation and diamond drill sections and represent the Victor's and Nigel's, Shaft and Ledingham pegmatite bodies. The borehole lithologic logs with summary logs showing the number of geologic units are provided in Appendix 6. Interpretation of the summary logs then aided in the joining of points between boreholes as it was necessary to determine which units to merge together versus those units to be split apart based on the available geologic units. Solid lines were used to indicate reasonably certain relations between discrete data points whereas dashed lines were used to indicate uncertainty or inferred data. A legend is then incorporated into the section to explain the types of geologic formations present. The legend was placed at the bottom of the section profile.

CHAPTER 3:

LOCAL GEOLOGICAL SETTING AND FIELD RELATIONSHIPS

3.1 Introduction

This chapter involves previous work and updates from this research report, focuses on giving a detailed account and description of the local geological setting of each sector including the 15 denoted pegmatites within the Bikita Minerals mining lease as well as the related field relationships. The descriptions will cover geology of the Main pegmatite, Spodumene pegmatite, Boomerang pegmatite, East pegmatite, Shaft pegmatite, West pegmatite, Giant pegmatites, Mauve Kop pegmatites, Dam Site pegmatite, Nigel pegmatites, Ranga pegmatite and Cemetery pegmatite.

3.2 The geological setting of the Bikita pegmatites

The greisenised, sheeted, lenticular, individual pegmatite bodies found within the Bikita Minerals mining lease have intruded the greenstone-epidiorite country rocks. These are presumed to be metamorphosed basic volcanic rocks with interbedded metamorphosed sediments comprising calcareous and semipelitic schist, siliceous granulite and banded ferruginous quartzite (Tyndale-Biscoe, 1951). These rocks belong to the Bulawayan System of the Basement Complex (Macgregor, 1947). Amongst other rock types within the area are lenticular bodies of serpentinite probably representing ultrabasic intrusions in the greenstones, and strongly foliated hornblende schists (Tyndale-Biscoe, 1951). The youngest geological formation within these rocks are probably the dolerite dykes which cut across the pegmatite bodies clearly seen on the northern end of the mining lease (Tyndale-Biscoe, 1951) (Figure 3.1).

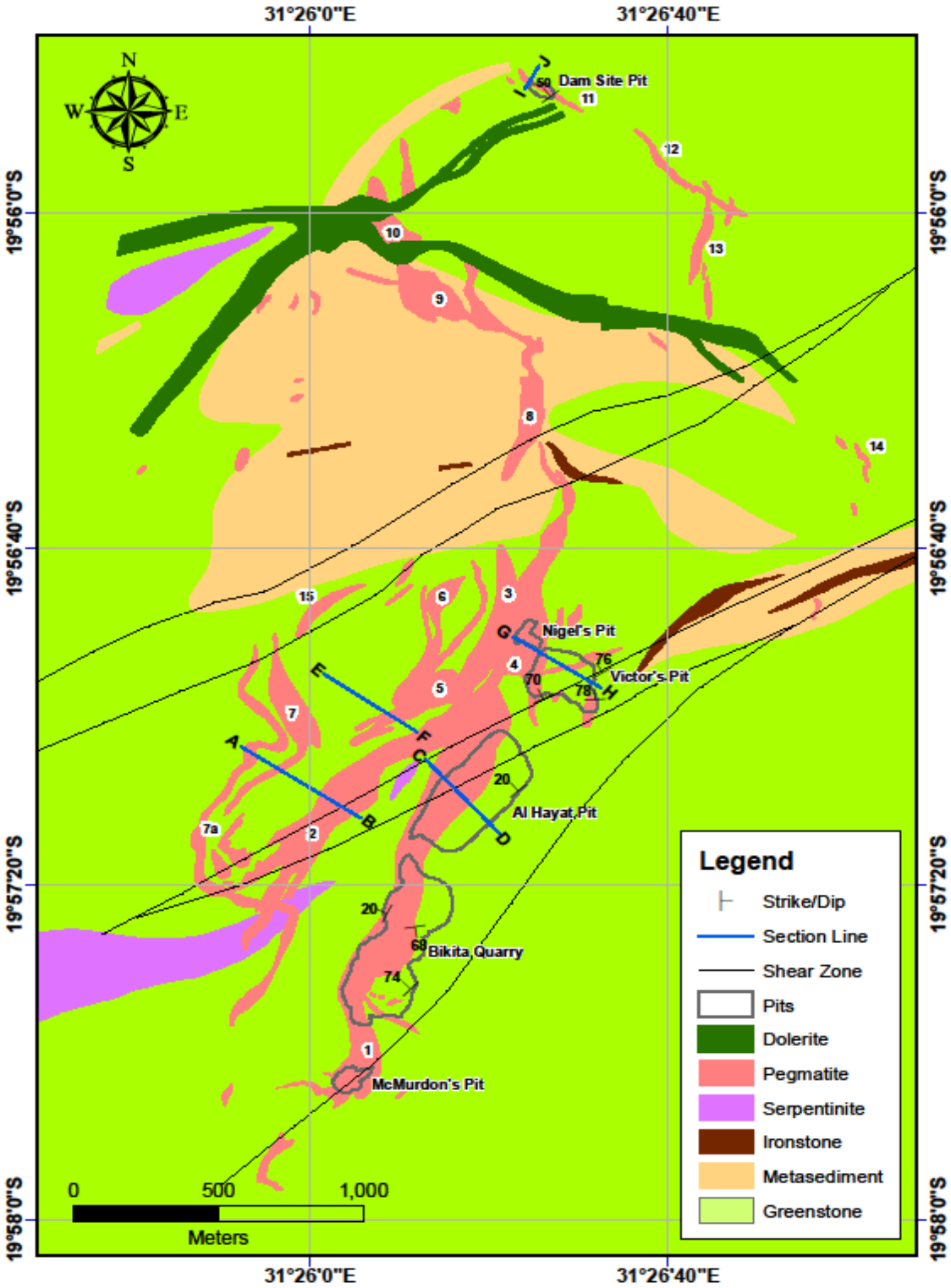

Figure 3.1*: A local geological map of the Bikita Tinfield showing the distribution of the pegmatites and the associated rocks. Also depicted are section lines, mine pits, dips/strikes and shear zones (Modified after Martin, 1964).* The numbers 1-15 (circled in white) represent the depicted pegmatite names and Table 3.1 shows the link between these numbered pegmatites and their respective names.

Table 3.1: *Table of the denoted Bikita Pegmatites with the associated pits showing their economic mineralisation after (Martin, 1964)*

Pegmatite Number	Pegmatite Name	Economic Mineralogy
1	Main (McMurdon pit, Bikita quarry and Al Hayat pit)	Petalite, SQI, pollucite, amblygonite, cassiterite, tantalite, beryl, lepidolite, bikitaite, eucryptite, hectorite
2	Spodumene (Ledingham sector)	SQI, petalite, lepidolite, hectorite, tantalite
3	Boomerang	Petalite, SQI, lepidolite, tantalite
4	East (Victor's pit and Nigel's pit)	Petalite, eucryptite, SQI, beryl, pollucite, bikitaite, lepidolite, tantalite, hectorite
5	Shaft	Petalite, eucryptite, SQI, lepidolite, hectorite, tantalite
6	West	Lepidolite, petalite, eucryptite, beryl, cassiterite
7a 7	Giant East Giant West	Petalite, SQI, Eucryptite Petalite, SQI
8	Mauve Kop South	Lepidolite
9	Mauve Kop Middle	Lepidolite
10	Mauve Kop North (Mdara mine)	Lepidolite, tantalite, beryl
11	Dam Site	Pollucite, petalite, amblygonite, lepidolite, beryl
12	Nigel North	Cassiterite, pollucite
13	Nigel South	Cassiterite
14	Ranga	Cassiterite
15	Cemetery	Petalite, lepidolite, eucryptite

The pegmatites mostly have the form of inclined sheets striking north-south and dipping east or west at angles varying from nearly horizontal to about 45° (Tyndale-Biscoe, 1951) and stretching for approximately 4 kilometres in a sporadic fashion and not as continuous masses. They are typically coarse-grained, light coloured and largely composed of albite with muscovite and quartz masses. Besides cassiterite, the ore-bodies contain tantalum-bearing minerals which include manganotantalite, microlite, and simpsonite. Lithium minerals comprise in order of abundance lepidolite, petalite, spodumene, eucryptite, bikitaite, and amblygonite. All these minerals are mainly concentrated in the southern part of the field and tend to decrease going north. Lithium, caesium, tantalum, tin and beryllium ore minerals have been proved within an explored Mining Lease which covers an area of about 1.539 Hectares (Figure 1.2). These minerals vary in proportion and distribution depending on the zonation patterns within the individual pegmatite bodies. The pegmatites are predominantly confined to upper greenschist and amphibolite-facies metabasalts of the Mesoarchean Bulawayan Group (Dittrich, 2017). The initial pegmatite mapping was done by Martin (1964) when the various individual pegmatites were distinguished within the Bikita mining area and the major pegmatite outcrops were denoted and numbered 1 to 15 (Figure 3.1 and Table 3.1). The largest of these pegmatites is the Main pegmatite (1) and smallest is the Dam Site pegmatite (11). These pegmatites have a total strike length of about 4 kilometres.

These complex pegmatites are zoned lithium-caesium-tantalum (LCT) pegmatites and their zoning indicates crystallisation in stages and in a closed system where no addition or loss of material took place (Tyndale-Biscoe, 1951). The individual pegmatite bodies contain different minerals and different proportions of the same minerals and are described in detail based on the observations by Martin (1964) together with the present observations from various drilling programs done to date.

3.2.1 Internal structure of the pegmatites

The Bikita pegmatites are a classic example of complexly zoned pegmatites. They show pronounced internal zoning that is asymmetrical with respect to the walls (Cooper, 1964). The zoning within the pegmatites consists of all four zones; the border, wall, intermediate and core zones. The economic mineralisation tends to be concentrated within the intermediate and core zones. The border zones are relatively fine-grained selvedges of mica and quartz-albite ranging from 3 to 5 centimetres thick. The wall zones are much coarser and thicker than the border zones with albite sometimes rhythmically banded, quartz, and minor beryl. The intermediate zones are between the border and wall zones are highly variable in shapes and sizes containing albite, petalite, SQI, and pollucite. The core zone is the innermost zone, commonly elongated or lenticular mainly with lepidolite and quartz. The internal zones of the pegmatites can be distinguished by the different mineral compositions, textures, and locations within the pegmatite. A summary of the economic mineralogical composition (Table 3.1) presents the 15 pegmatites found within the Bikita mining lease.

3.3 Mineralisation of the Bikita pegmatites

The Bikita pegmatites are heterogeneous with a complex mineralogical composition. The most abundant economic ore minerals within these pegmatites are lepidolite, petalite, spodumene, tantalite, pollucite, eucryptite and beryl whereas bikitaite, cassiterite, hectorite, amblygonite and apatite are sparsely distributed within the pegmatites. Other constituent minerals in these pegmatites include microcline feldspar, albite feldspar, quartz, muscovite, biotite, tourmaline, zinnwaldite, garnet, tourmaline and epidote. Significant Sn and Ta mineralisation (Figure 3.2) tends to occur in replacement units showing intensive albitisation and greisenisation of the pegmatites.

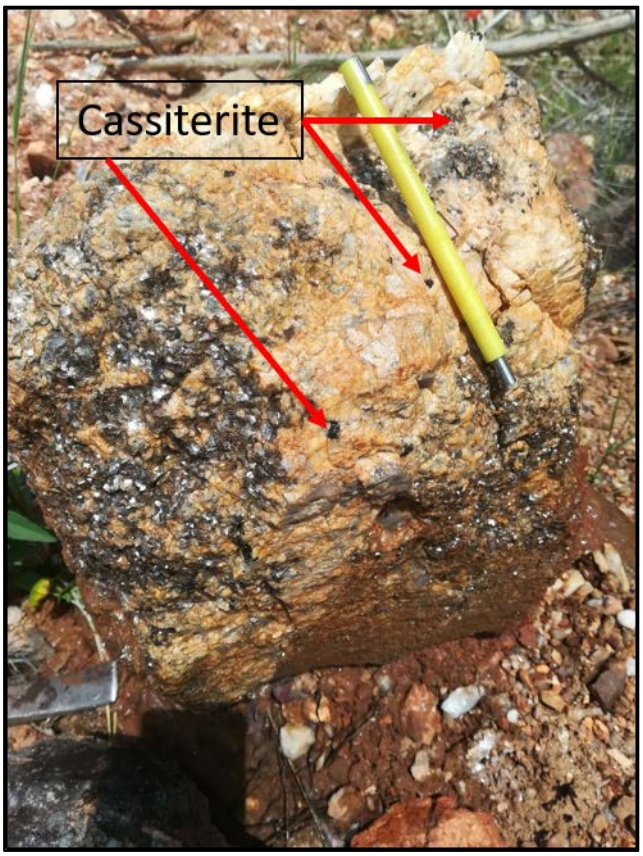

Figure 3.2: *Photograph showing disseminated cassiterite crystals (black) within a matrix of muscovite, quartz and albite feldspar.*

3.4 The Bikita Main pegmatite (1)

The Bikita Main pegmatite was discovered as a Tinfield in 1909 (Martin, 1964). Early production of tantalum, tin, beryllium, lithium and caesium minerals came from this pegmatite and as a result removed much of the pegmatite (Symons, 1961). The pegmatite has been the main source of almost all the minerals found within the Bikita Minerals mining lease and this includes the large bodies of various lithium minerals (Martin, 1964). From north to south, the tabular pegmatite has been exploited by the McMurdon pit, Bikita quarry and the Al Hayat pit (Figure 3.1). The main pegmatite is the largest and most extensively worked of all the pegmatites and strikes northeast-southwest, having been exposed for approximately 2000 metres, varying in width from 30 to 70 metres, and dipping 15° to 60° mainly to the east. This pegmatite is associated with three offshoot dykes with two of them diverging from the main dyke at an acute angle whilst the third is separated by a lenticular block of greenstone about 100 metres long (Figure 3.1).

3.4.1 The Bikita quarry

This quarry stretches for about 450 metres along strike and averages about 65 metres in width dipping mainly to the east. Lepidolite is dominant in the footwall Intermediate Zone of Bikita quarry where it occurs as the fine-grained core, feldspathic lepidolite, and dominantly lepidolite footwall unit. In the footwall Intermediate Zone lepidolite is associated with lesser amounts of petalite, SQI, tantalite, amblygonite, and beryl. Tantalite occurs in irregular crystal aggregates in fan-shaped twins within the Bikita quarry and it is black with occasional brown mangano-tantalite. The other tantalite variety is white in colour (microlite) and mostly found in lepidolite. The

occurrence of tantalite is sporadically distributed and found in the quartz-albite units of the Upper Intermediate Zone with some occasional occurrences in the Lower Intermediate Zone that has proved to be uneconomic. In the Bikita quarry pollucite with its characteristic lepidolite and quartz veining has a patchy or lensoidal distribution confined to the hangingwall Intermediate Zone. The zoning within the Bikita quarry is quite complex.

3.5 Detailed internal zoning within the Bikita quarry

According to Martin (1964), Cooper (1964) and Symons (1961) all four zones are present with varying subdivisions made based on different mineral assemblages. A total of 9 to 13 zones in separate segments of the pegmatite were distinguished and main subdivisions were made into the Border, Upper Wall, Upper-Intermediate, Core, Lower Intermediate, and Lower Wall Zones (Cooper, 1964). The internal structure seems to be layered rather than concentric, with distinct vertical asymmetries exhibited particularly in the Intermediate Zones. Within the Bikita quarry the complex internal zoning is shown in Table 3.2.

Table 3.2*: Table showing the zones of the pegmatite within the Bikita quarry*

Hangingwall Greenstone	
Zone	**Mineral Assemblage**
Border Zone	Albite + quartz selvage
Wall Zone	1. Muscovite band
	2. Hangingwall feldspar zone
Upper Intermediate Zone	1. Petalite + microcline
	2a. Massive SQI
	2b. Mixed SQI
	3. Pollucite
	4. Feldspar + quartz
	5. Mixed zone
Core Zone 1a	1a. Massive lepidolite (high grade ore)
	1b. Massive lepidolite (nearly pure)
	2. Lepidolite quartz shell – predominantly lepidolite
	3. Lepidolite quartz shell-predominantly amblygonite
Lower Intermediate Zone	1. Cobble zone
	2. Feldspathic lepidolite
Wall Zone	1. Footwall feldspar, rhythmically banded beryl zone
	2. Footwall feldspar, muscovite band
	3. Footwall feldspar, spotted dog
Footwall Greenstone	

3.5.1 Border Zones

This zone occurs on either side of the hangingwall or footwall greenstone to pegmatite contacts and consists of an albite-quartz-muscovite selvage with varying widths. The footwall Border Zone is usually blocky, sometimes weathered and containing clay minerals. This zone is a persistent marker ranging from 0.6 to 3 metres wide and sometimes accompanied by a thin mica band 2 to 10 centimetres in width. The hangingwall Border Zone is a thin

zone with a somewhat sharp contact (Figure 3.3) with the wall zone of up to 15 centimetres consisting of albite or microcline and quartz with minor zinnwaldite.

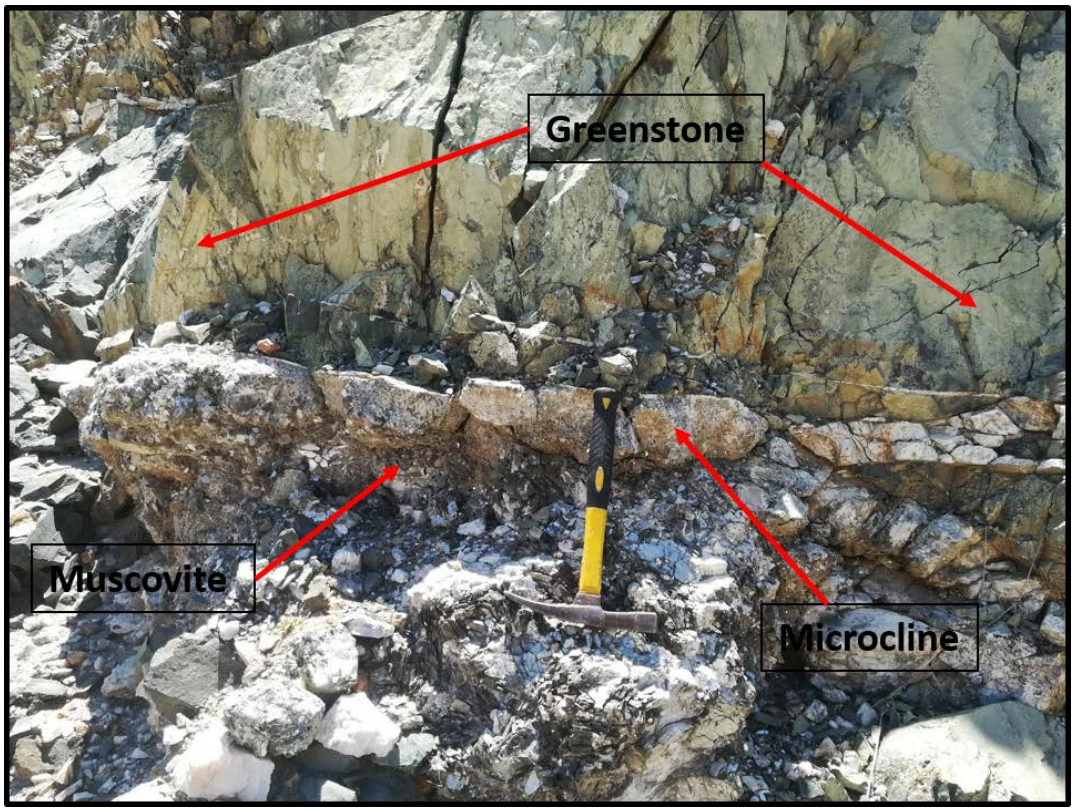

Figure 3.3: *Photograph showing the Border Zone mineralisation on the sharp greenstone and pegmatite marginal contact*

3.5.2 Wall Zones

i) The hangingwall Beryl Zone is characterised by regular, rhythmic undulating bands of fine-grained lepidolite and albite varying to about 10 centimetres in width. This zone appears to mark a transition from albite-lepidolite-albite probably due to rapid fluctuations in the conditions of crystallisation. Here the beryl occurs in albite cores showing domed structures surrounded by concentric banding with some rare associations of tantalite.

ii) Irregular muscovite bands of up to about 45 centimetres in width found together with minor quartz and pale green beryl.

iii) The “Spotted dog” zone consisting of fine-grained albite associated with scattered muscovite blebs and quartz (Figure 3.4). The footwall contact with the greenstone is sharp and with no recognised selvage.

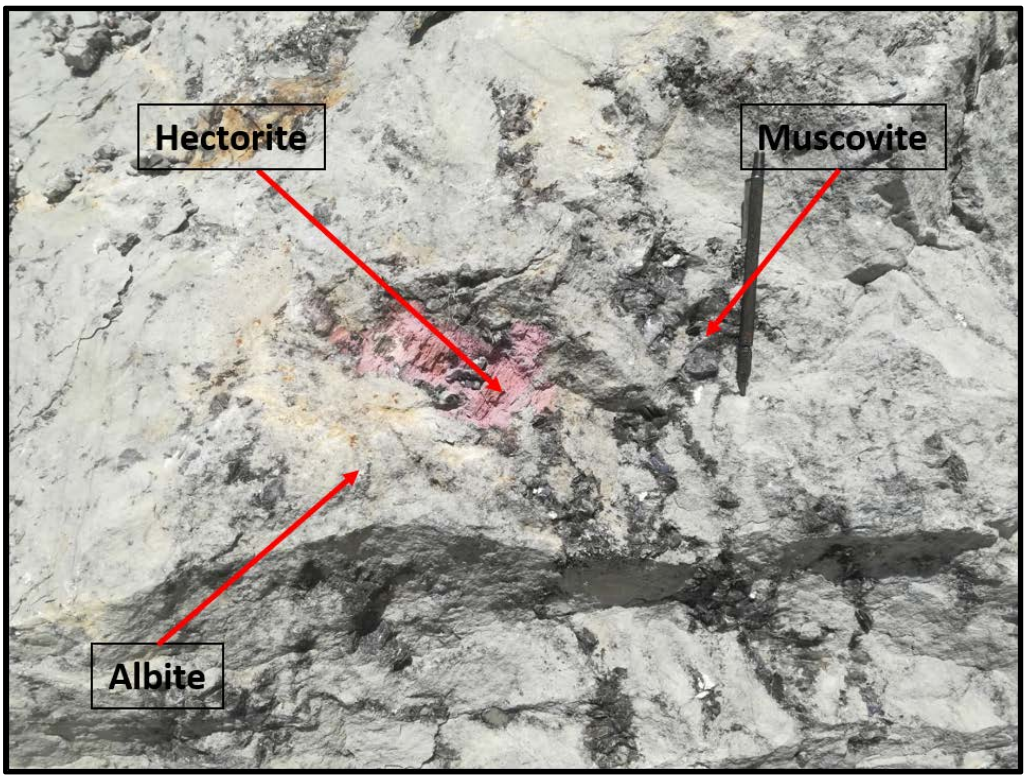

***Figure 3.4**: Photograph showing the typical "spotted dog" (matrix of albite, quartz and muscovite) with petalite being altered to hectorite (pink)*

3.5.3 Upper Intermediate Zones

i) The petalite-microcline feldspar zone contains giant crystals, up to 2 metres in length, of petalite and microcline set in a matrix of albite, quartz, and muscovite.

ii) The SQI zone occurs as acicular intergrowths of spodumene with quartz (Figure 3.5). The massive portions have blocks separated by a lepidolite-quartz matrix whilst the mixed portions have SQI in a matrix of albite (cleavelandite), lepidolite and quartz.

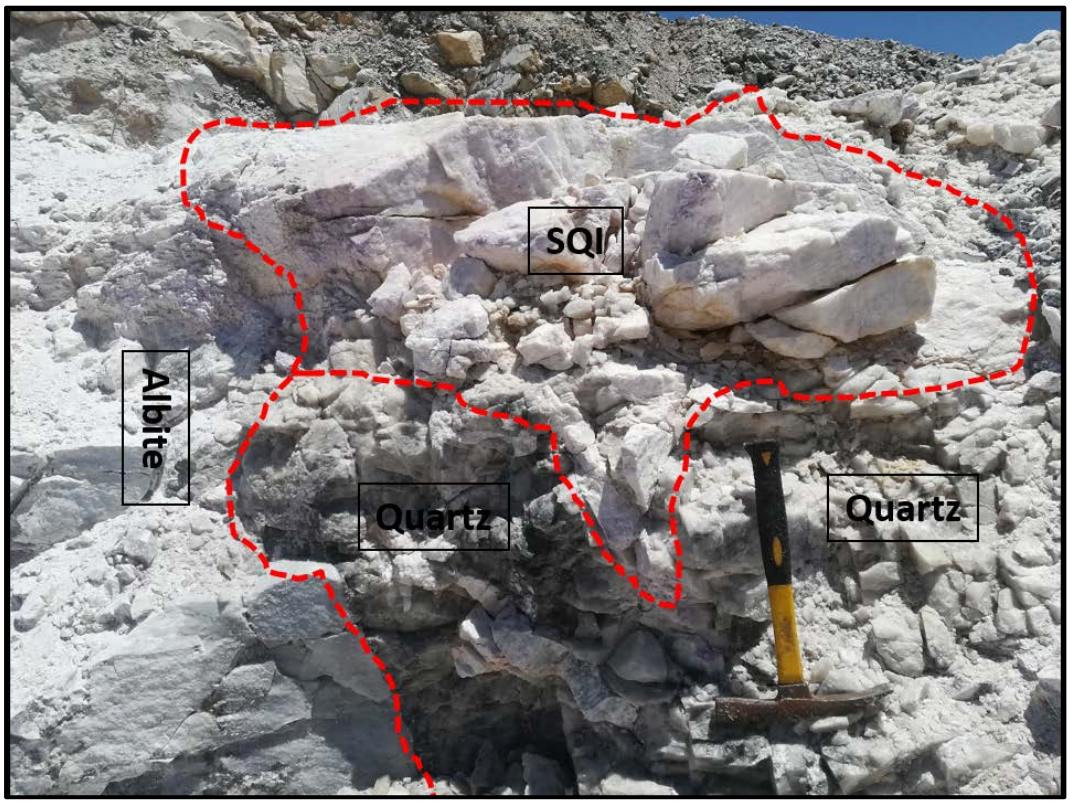

***Figure 3.5**: Photograph showing the association of albite, SQI and quartz within the Upper Intermediate Zone of the Bikita quarry*

iii) The Pollucite Zone consisting of massive pollucite traversed by irregular lepidolite veinlets.

iv) "All mix" zone consisting of microcline, coarse lepidolite, petalite, and SQI (Figure 3.6).

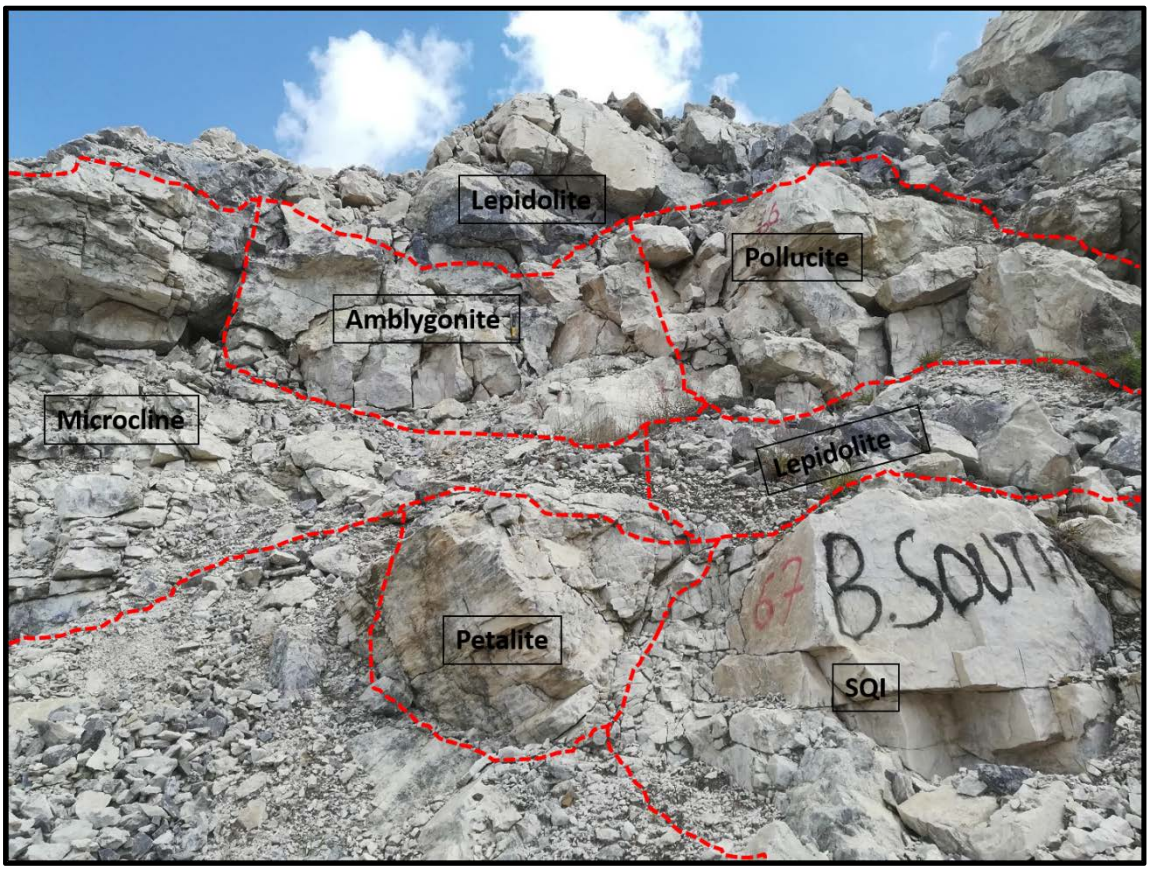

***Figure 3.6**: Photograph showing typical All Mixed Zone showing the association of various mineral species within the Bikita quarry*

3.5.4 Core Zone

This is the most economic zone of the Bikita quarry. Lepidolite is the main constituent of the Core Zone together with quartz. The other economic constituents of this Core Zone are SQI, petalite, and amblygonite which tend to occur with the quartz (Figure 3.7) in the form of irregular masses up to 6 metres across showing sharp contacts with the quartz. The gradation from the Upper Intermediate Zone into the Core Zone is marked by a decrease in the quantities of admixed quartz and albite with a corresponding increase in the lithium mineralisation. The lepidolite core is associated and surrounded by a discontinuous quartz shell of about 3 metres width.

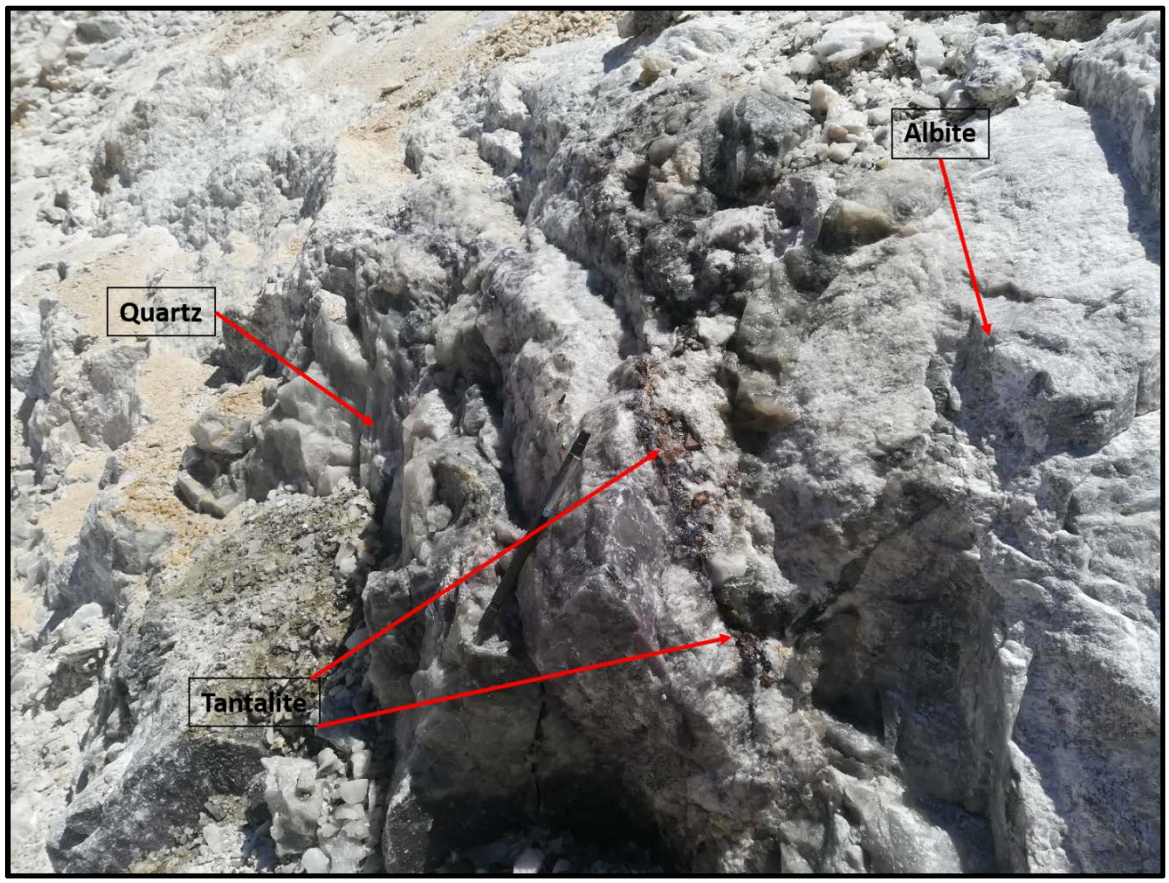

***Figure 3.7**: Photograph showing the association of tantalite mineralisation with albite and quartz within the Core Zone of the Bikita quarry*

3.5.5 Lower Intermediate Zones

These zones are found below the core zone and consist of;

i) The Cobble Zone which comprises of lenses of pure lepidolite in a matrix of fine-grained albite, disseminated lepidolite, and quartz (Figure 3.8). The cobbles range in size from 8 to 10 centimetres.



***Figure 3.8**: Typical Cobbled Zone which consists of a matrix of albite feldspar partly replaced by lepidolite forming spherical masses of various sizes within the Bikita quarry*

ii) The Feldspathic Lepidolite Zone (Figure 3.9) consists of fine-grained albite, disseminated lepidolite, and quartz. In this zone, lepidolite partly replaces the original feldspar.

iii) The footwall Beryl Zone normally extends up to or near the footwall greenstone contact.



Figure 3.9*: Photograph of the typical Lower Intermediate Zone showing feldspathic lepidolite within the footwall of Bikita quarry*

3.6 The Al Hayat pit

The Al Hayat pit is situated on the northern part of the Bikita Main pegmatite (Figure 3.1) and it is the source of petalite and microlite together with subordinate SQI and eucryptite. This pegmatite on the Al Hayat pit area has an easterly dip of between 20 to 45° and stretches for approximately 650 metres in strike length over an average width of about 60 metres.

3.6.1 Zoning within the Al Hayat pit

This pit exhibits a much simpler internal zoning succession compared to that of the Bikita quarry. In the Al Hayat pit, large masses of petalite are predominant with smaller centrally placed lenses of SQI, eucryptite, and lepidolite. It has an irregular and patchy intermediate zone containing economic lithium minerals, sharp and persistent wall contacts. Microlite is found in isolated patches of muscovite-quartz greisen (Macgregor, 1946). The Core Zone is absent from this pit. From the hangingwall to the footwall, the zoning if the Al Hayat pit is as follows:

3.6.1.1 Border Zone

This consists of fine-grained albite with quartz stringers and muscovite with a thickness of 15 to 60 centimetres.

3.6.1.2 Wall Zones

These zones from the hangingwall inwards are:

i) A mica band which consists of consistent coarse muscovite with interstitial quartz for almost the entire

strike length of the pegmatite in this pit.

ii) A hangingwall feldspar zone composed of white to cream-coloured microcline in a matrix of quartz and mica ranging from 3 to 6 metres in width.

3.6.1.3 Intermediate Zones

These zones constitute the economic portion of the Al Hayat pit and consist of:

i) A petalite and microcline zone. This is the largest of the intermediate zones consisting of massive petalite and microcline crystals set in a matrix of fine-grained albite, muscovite and minor quartz. The petalite occurs as laths up to 2 metres long and about 45 centimetres thick with the tendency towards orientation at right angles to the walls of the pegmatite. The laths decrease both in both size and abundance towards the footwall.

ii) The Minor Intermediate Zones. These contain SQI and lepidolite with eucryptite and bikitaite occurring as alteration products.

iii) "All Mix" Zone. This is when all the principal minerals occur together with no individual zones being distinguished.

3.6.1.4 Footwall Feldspar Zone

This is dominated by fine-grained albite, quartz and muscovite with some bands of coarse muscovite-quartz intergrowth. The zone has an overall width of about 9 metres. Well-developed rhythmically banded greisens are seen on the Al Hayat Northwest (Figure 3.10).



Figure 3.10*: Typical footwall spotted dog albite zone in the Al Hayat pit showing rhythmic banding*

Recent drilling within this sector has enabled the section of this pit to be updated (Figure 3.11).

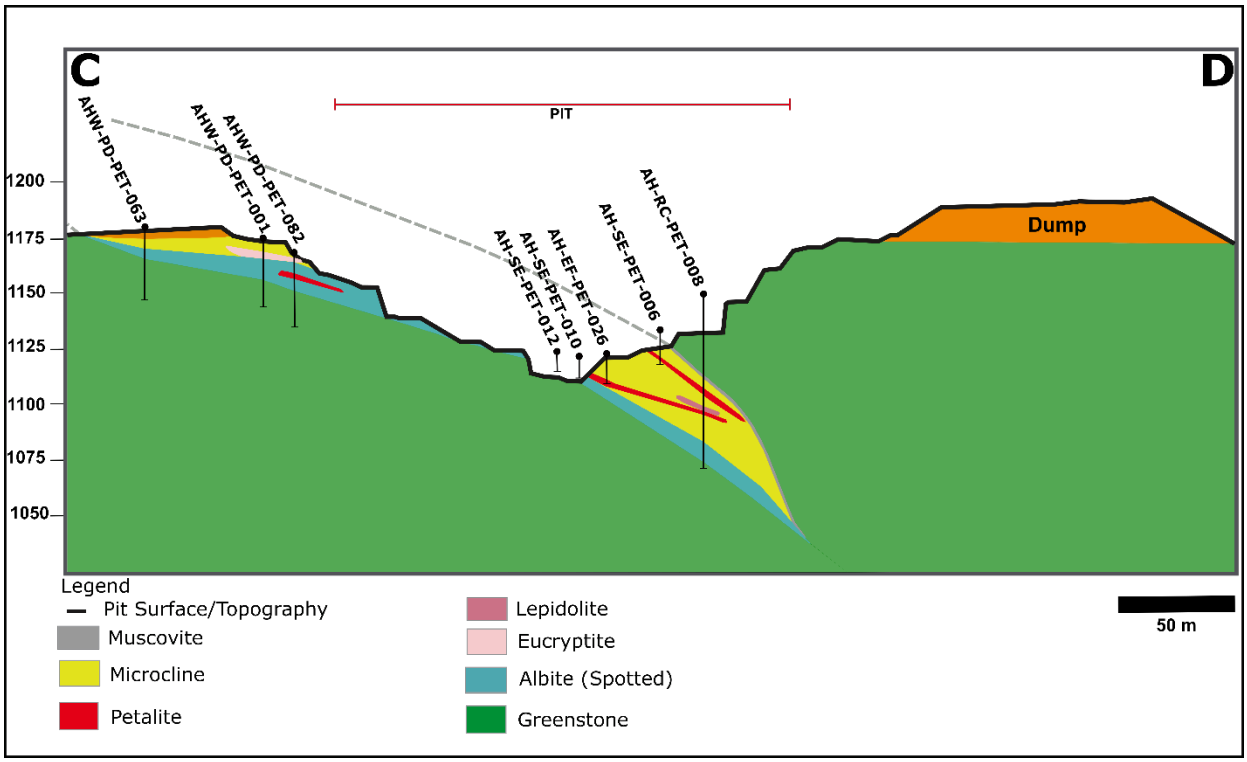

Figure 3.11: *Schematic cross section through the Al Hayat pit area from north to south*

3.7 The McMurdon pit

This pit marks the southern extremity of the Bikita Main pegmatite (Figure 3.1) and is characterised by a quartz-lepidolite core, (up to 20 metres wide). The quartz is highly fractured. The sector has been exploited for beryl, tantalite-columbite, lepidolite and cassiterite in the past and contains brown-black tantalite possibly manganotantalite which is confined to the hanging wall and footwall intermediate zones of the pegmatite. Mineralisation is associated with aplitic albite+/-lepidolite+/-quartz and muscovite units. Tantalite also occurs as large crystals at the quartz core margin (Figure 3.12). Channel chip samples that were picked from different locations within this pegmatite are given in Appendix 1a.

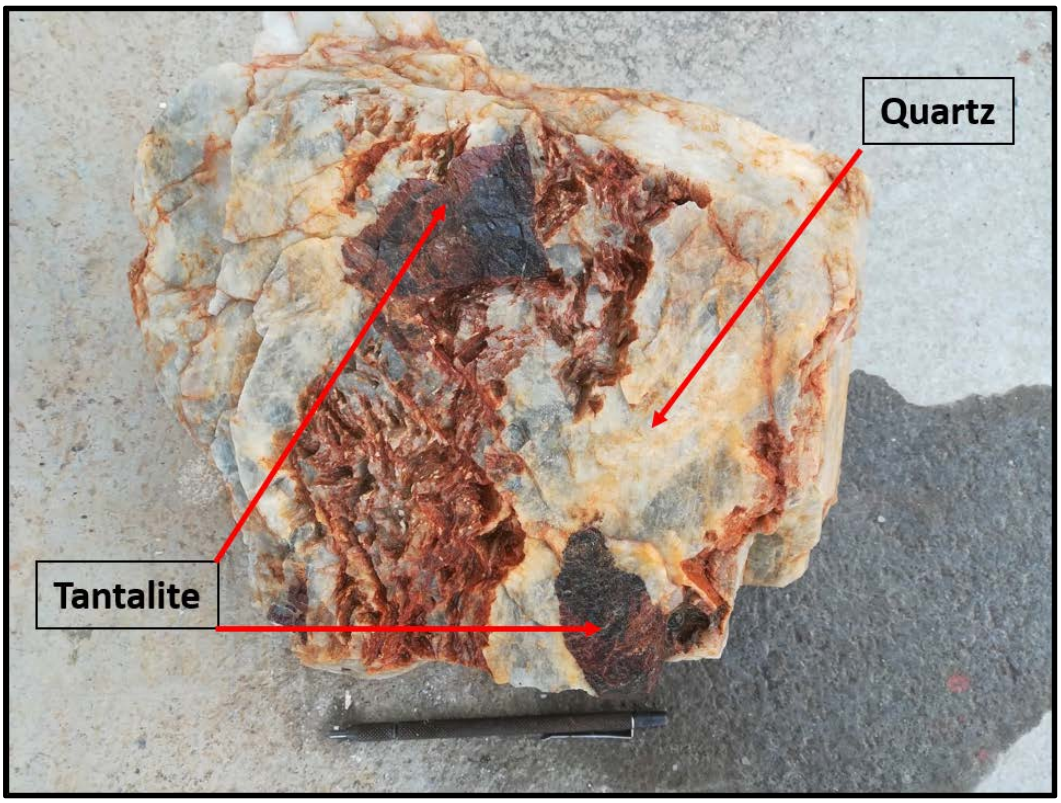

***Figure 3.12**: Photograph showing the association of mangano-tantalite and fractured quartz within the McMurdon pit*

3.8 The Spodumene pegmatite (2)

This pegmatite was emplaced in a synformal structure (Figure 3.15) on Ledingham Hill which was named after an early prospector who once owned the claim (Figure 3.1). It is about 1200 metres long striking NNE averaging 40 to 60 metres wide. The dip varies from 20 to 75° to the west. This pegmatite consists of abundant SQI with subordinate petalite and eucryptite occurrences towards its northern end. Borehole SQI DDH 44 on the old tantalite plant towards the northern extremity of the Spodumene pegmatite (Figure 3.13) intersected good quality petalite which triggered the current investigation of the Shaft pegmatite and this illustrated the considerable distribution of lithium mineralisation away from the Main pegmatite.

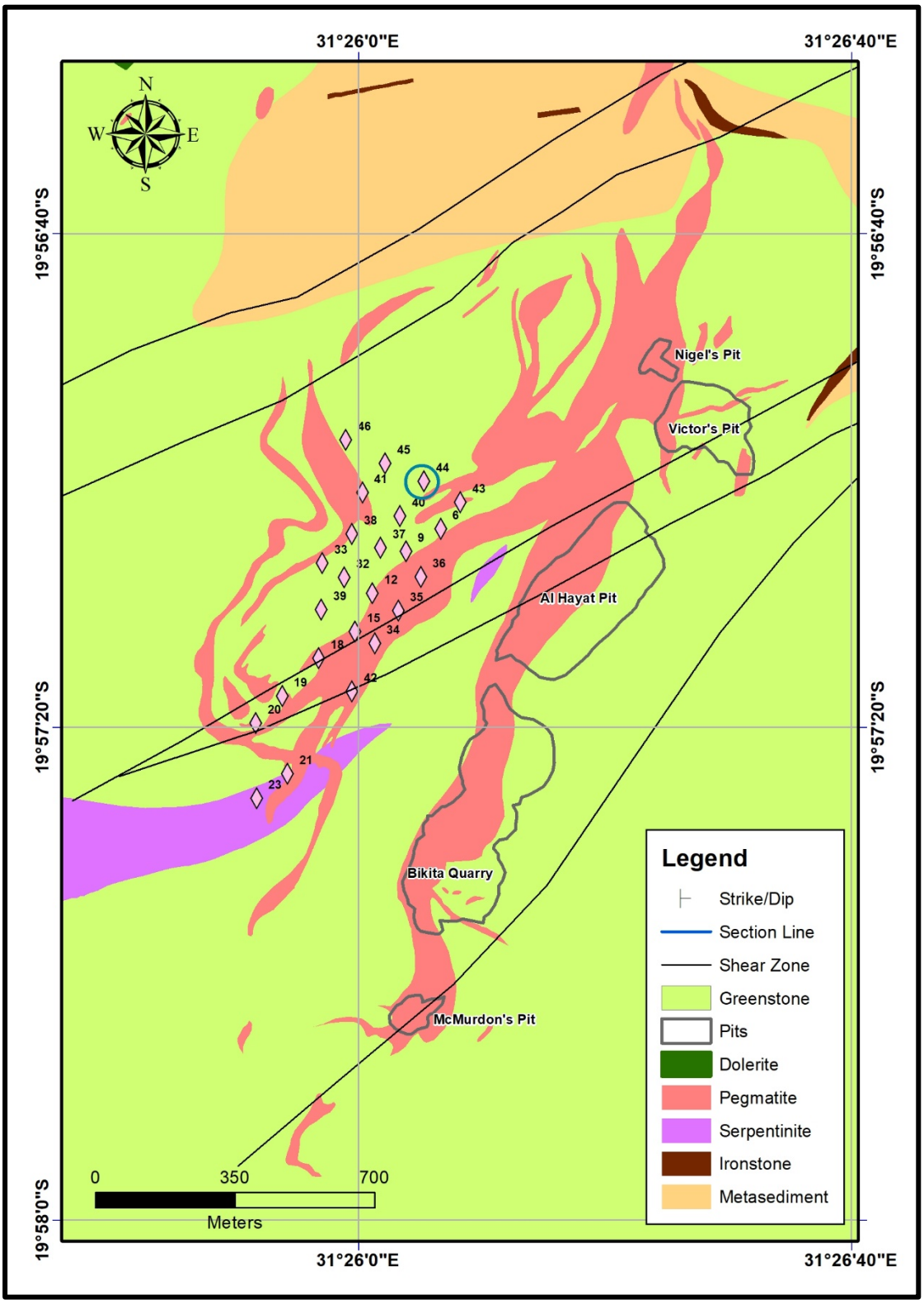

***Figure 3.13**: Borehole layout plan of the Ledingham sector showing the location of SQI_DDH44 (circled).*

A typical clean SQI core sample from the Spodumene pegmatite (Figure 3.14) shows the distinctive elongated acicular crystals associated with the style of mineralisation.



***Figure 3.14**: Core sample from the Spodumene pegmatite showing massive SQI indicated by the pink colour with distinctive elongated acicular crystals of spodumene*

3.8.1 Zoning of the Spodumene pegmatite

All holes used for the interpretation of the pegmatite are shown on the section (Figure 3.15). Based on these interpretations and observations, a synformal structure is clearly visible as well as splitting of the pegmatite into two towards the west. Zones that could be clearly demarcated and traced throughout all holes are shown, these are mainly the spotted footwall feldspar and the hangingwall microcline/feldspar zones. The middle zone comprises feldspar (both microcline and albite), SQI, petalite and hectorite. These could not be correlated between holes and so it was decided to group them into one lithology (mixed), however the dominant minerals in the zone are feldspar and spodumene.

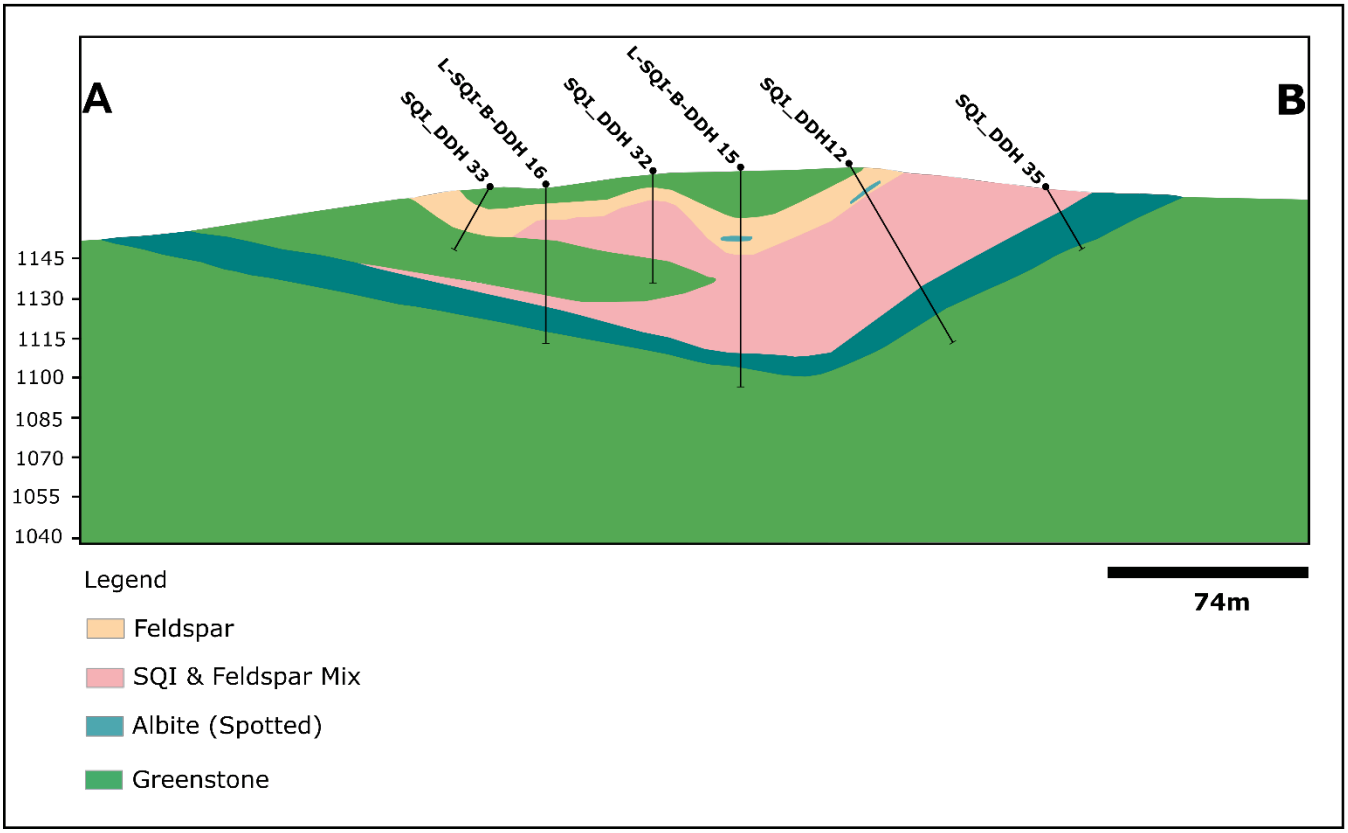

***Figure 3.15**: Schematic cross section through the Spodumene pegmatite. The location of section line A-B is shown in Figure 3.1.*

3.9 The Boomerang pegmatite (3)

This pegmatite is probably the northern continuation of the spodumene pegmatite on its northern side (Figure 3.1) and appears to cut through it whilst overriding the East pegmatite (Martin, 1964). It is about 400 metres long and 15 to 20 metres wide with a shallow dip of about 20° to the west. It is composed of petalite, SQI, cassiterite, and beryl in decreasing order of abundance. The lithium content is mainly concentrated in the south and this further decreases in a northerly direction. It is mineralogically similar to the Spodumene pegmatite and differs only by a lesser spodumene content.

3.10 The East pegmatite (4)

This pegmatite seems to start on the northern end of the Main pegmatite (1) suggesting a possible continuation of the latter. It is about 900 metres in length on a north strike dipping at 15 to 75° to the east. The lithium mineralisation consists of massive petalite associated with eucryptite, lepidolite, and SQI in order of abundance. Traces of tantalite and beryl are noticeable. Recently occurrences of pollucite have been found from the Nigel's and Victor's pits which are situated directly on this pegmatite and the results of the grab pollucite samples and channel chips of various mineral species samples picked from the two pits are given in Appendix 1a.

3.10.1 Zoning of the East pegmatite

The offshoot dykes show a quartz core with intermediate zones of albite containing beryl and tantalite. Thus they differ from pegmatites 2, 3 & 5 which do not possess distinct quartz cores and are poorly zoned. The best face exposure showing the typical zoning is on Nigel's pit (Figure 3.16).

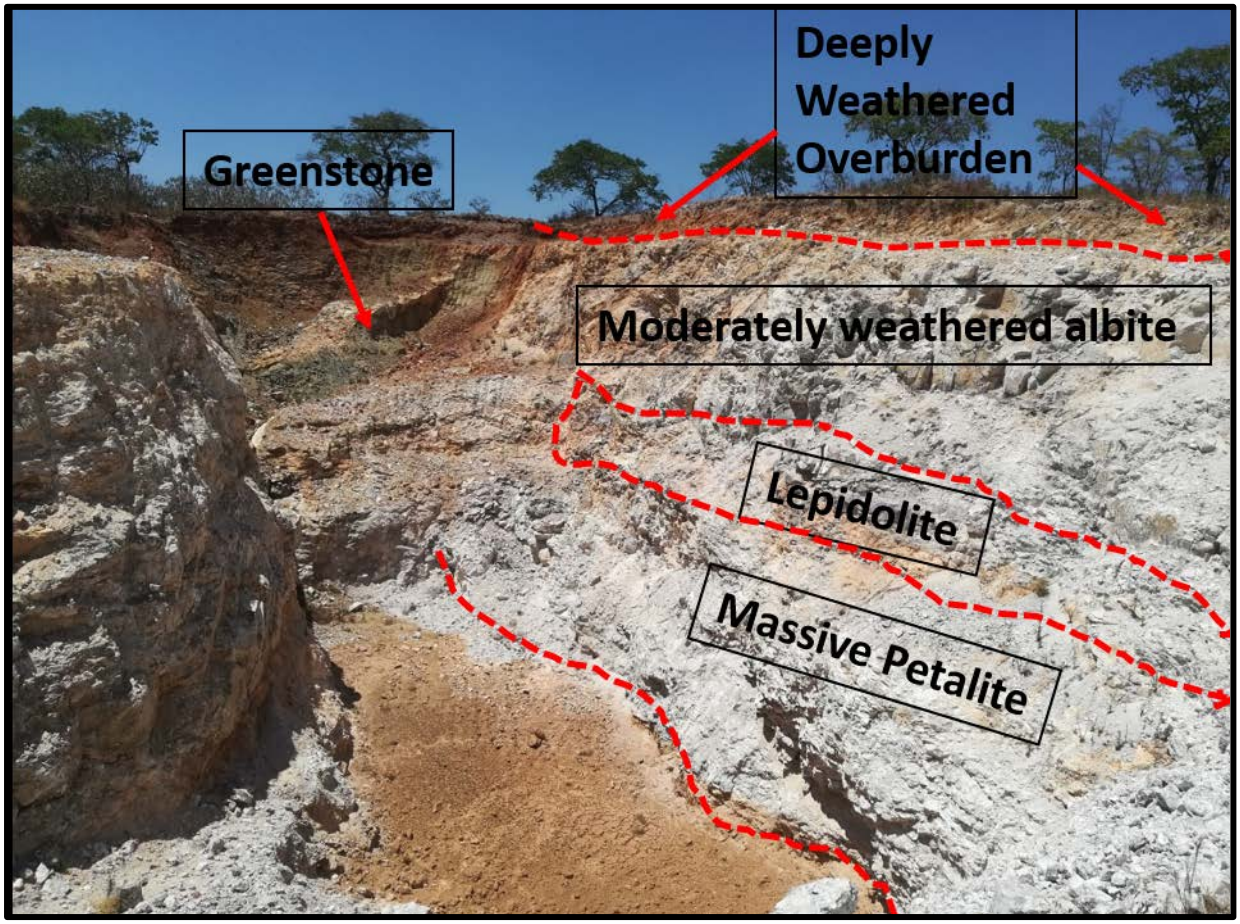

***Figure 3.16**: Overview picture of the Nigel's pit (view to south west) showing typical mineral zoning*

Drilling in the Victor's and Nigels' pit areas allowed correlation between boreholes and an interpretation of the zoning (Figure 3.17). The zoning of this sector is not as well pronounced as that of the Bikita quarry. The Footwall is mainly composed of highly weathered friable feldspar dominated by albite which shows rhythmic banding with minor microcline and this zone is about 10 metres in thickness. Above the Footwall albite is the Upper Intermediate Zone of lepidolite and petalite. Greenstone xenoliths occur just above the core which is dominated by quartz and lepidolite. Below the core is the massive petalite zone with minor inclusions of SQI and eucryptite. Below this petalite zone is the spotted dog albite zone which is in contact with the Hangingwall greenstone.

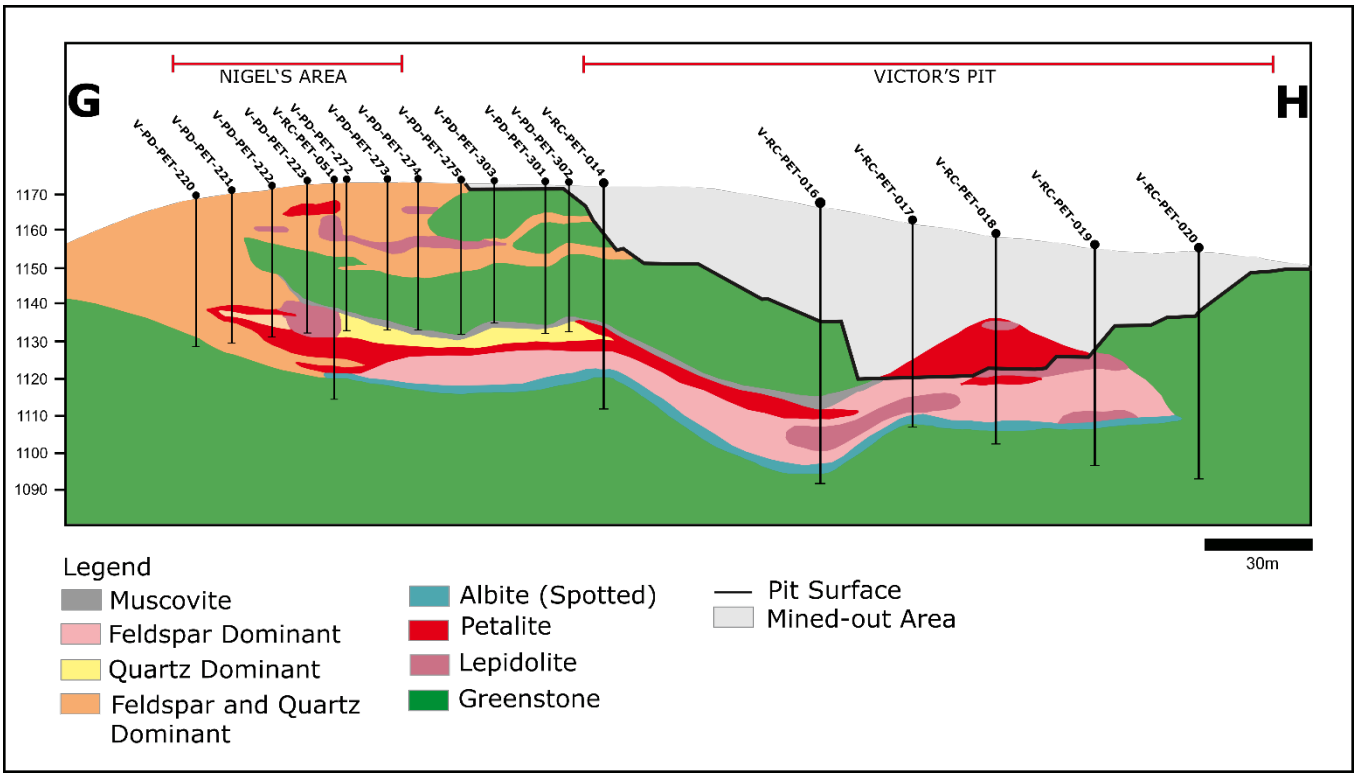

***Figure 3.17**: Schematic cross section through the East pegmatite showing the different lithologies. The Quartz Core is depicted in yellow.*

3.11 The Shaft pegmatite (5)

This pegmatite is an offshoot from the Spodumene and Boomerang pegmatites (Figure 3.1). It is about 15 metres wide on surface, and 400 metres long with some traces of petalite and SQI as well as tantalite. It appears to be trough-shaped and occurs as the topmost pegmatite in the epidiorite (Martin, 1964). It dips approximately 22° towards the northwest. There is an old tantalite plant erected by George Nolan (1950-1960) to process the relatively weathered low-grade tantalite ore found on this pegmatite. Currently, there is no mining activity on this pegmatite but exploration is in progress. Various logs from the recent drilling on this pegmatite are presented in Appendix 1c. The recent drilling of 15 boreholes has been used for a new interpretation of the pegmatite (Figure 3.18). Based on the borehole logging the pegmatite has been simplified into two zones based on the mineralogy and abundance of feldspar and petalite. Eucryptite is also found in significant quantity whilst the SQI and lepidolite observed are insignificant. The feldspar is generalised based on logging (albite and microcline) and albite is the more dominant of the two. There are two pegmatite bodies shown in the cross-section: the Upper and the Lower. The Lower (main) pegmatite shows clearly the synformal structure (Figure 3.18) that is also observed at Ledingham Hill. The fault shown is interpreted hence indicated with a question mark, however the displacement is clearly visible in both the Upper and Lower pegmatite.

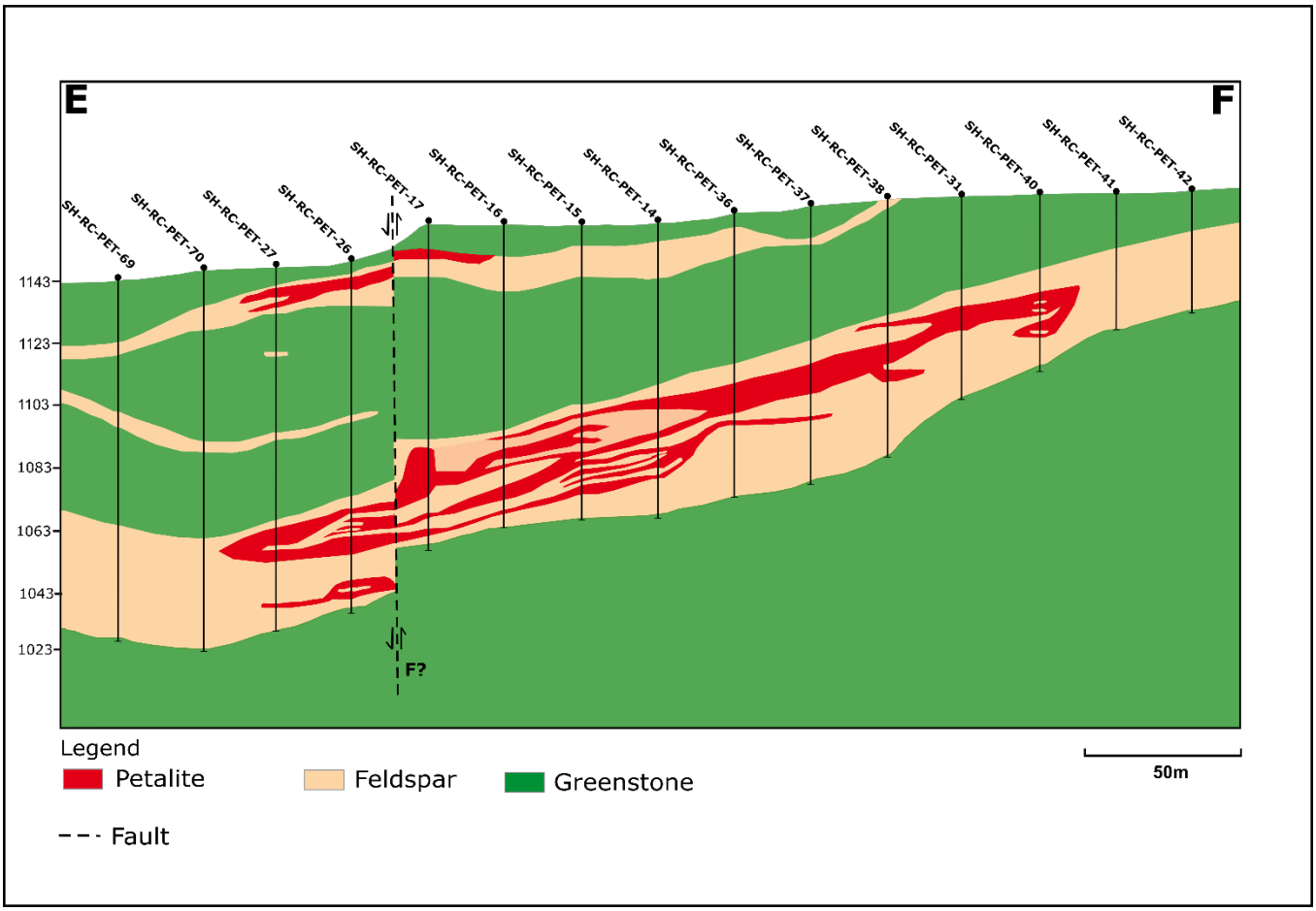

***Figure 3.18**: Schematic cross section through the Shaft pegmatite showing the different lithologies*

3.12 The West pegmatite (6)

Adjoining the Shaft pegmatite is the West pegmatite (Figure 3.1), dipping westerly in its western limbs and easterly in its eastern limb. Lithium mineralisation is poor with a few traces of lepidolite and petalite. It used to be a prolific beryl producer. Cassiterite and tantalite usually occur as finely disseminated lenses at the base of the pegmatite embedded in muscovite and quartz (Martin, 1964).

3.13 The Giant pegmatites (7)

This pegmatite appears to be an offshoot from the Spodumene pegmatite (Figure 3.1) and consists of two dykes namely Giant East (7) and Giant West (7a). The Giant East shows traces of SQI and quartz whilst the Giant West shows traces of petalite together with feldspar. There is no mining activity currently but exploration is in progress.

3.14 The Mauve Kop pegmatites (8-10)

Three distinct pegmatites are known within the Mauve Kop area shown in the northern concession of the mine lease area (Figure 3.1) and these are: Mauve Kop South (8), Mauve Kop Middle (9) and Mauve Kop North (10). The Old Mdara tantalite mine occurs on the Mauve Kop North pegmatite which shows the most well-defined persistent lithologies mainly those of the deep mauve lepidolite. The Mauve Kop South and Middle pegmatites are separated by the Ranga stream whilst the Mauve Kop Middle and the Mauve Kop North are separated by a double dolerite dyke intrusion dipping sub-horizontally towards the north-west. These pegmatites strike north-south and dip at

about 15 to 45° to the east, 15 to 20 metres in width and have a total strike length of about 1300 metres. According to Tyndale-Biscoe, (1951), all these pegmatites were capped by a mass of lepidolite greisen of a beautiful deep mauve colour (Figure 3.19a). In other sectors of these pegmatites, radial columnar aggregates of lepidolite embedded in quartz and albite are a common phenomenon (Figure3.19b).

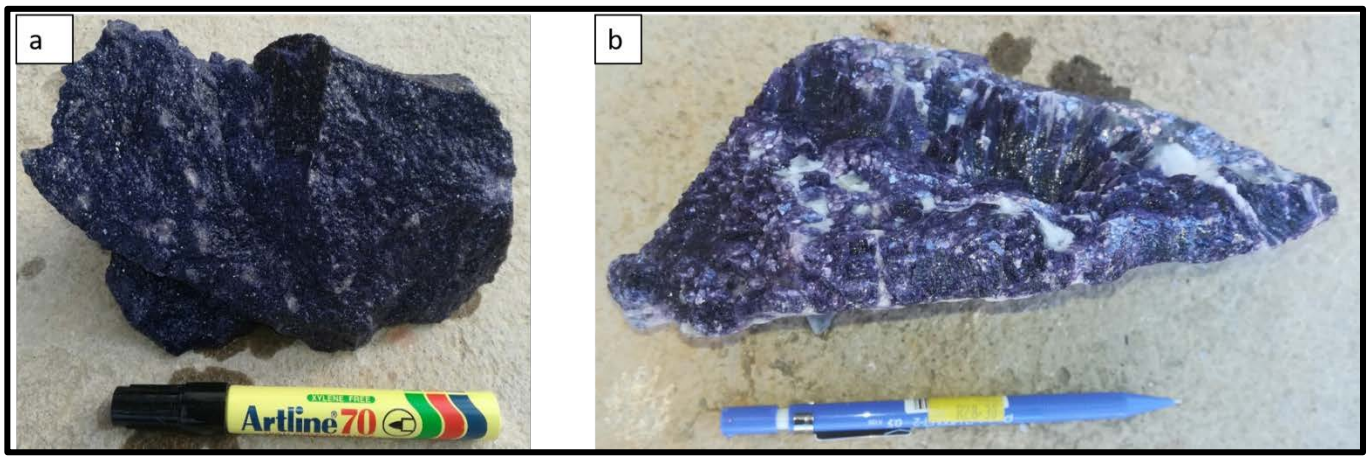

***Figure 3.19**: Lepidolite varieties. (a) Photograph showing the beautiful deep mauve lepidolite (b) Photograph showing the radial morphology on lepidolite embedded in quartz and albite.*

Apart from the deep mauve lepidolite, these pegmatites are also host to tantalite and subordinate beryl with massive fine-grained albite which is probably a replacement of the original very coarse microcline and very large masses of quartz associated with irregular pockets of beryl (Tyndale-Biscoe, 1951). The albite is the major tantalite carrier. Drill hole logs from these pegmatites are included at Appendix 1c.

3.15 The Dam Site pegmatite (11)

This pegmatite marks the northern extremity of the mineralisation within the mining lease (Figure 3.1). It probably represents the northern extension of the NW–SE trending branch of the Nigel Tin pegmatites and it contains petalite, lepidolite, amblygonite, beryl and pollucite in small lenses. It dips 15 to 40° to the north (Figure 3.20). Recent excavations were undertaken to try and find an extension of pollucite mineralisation (Figure 3.20). Details of chip and grab samples collected from this pegmatite are included at Appendix 1a.

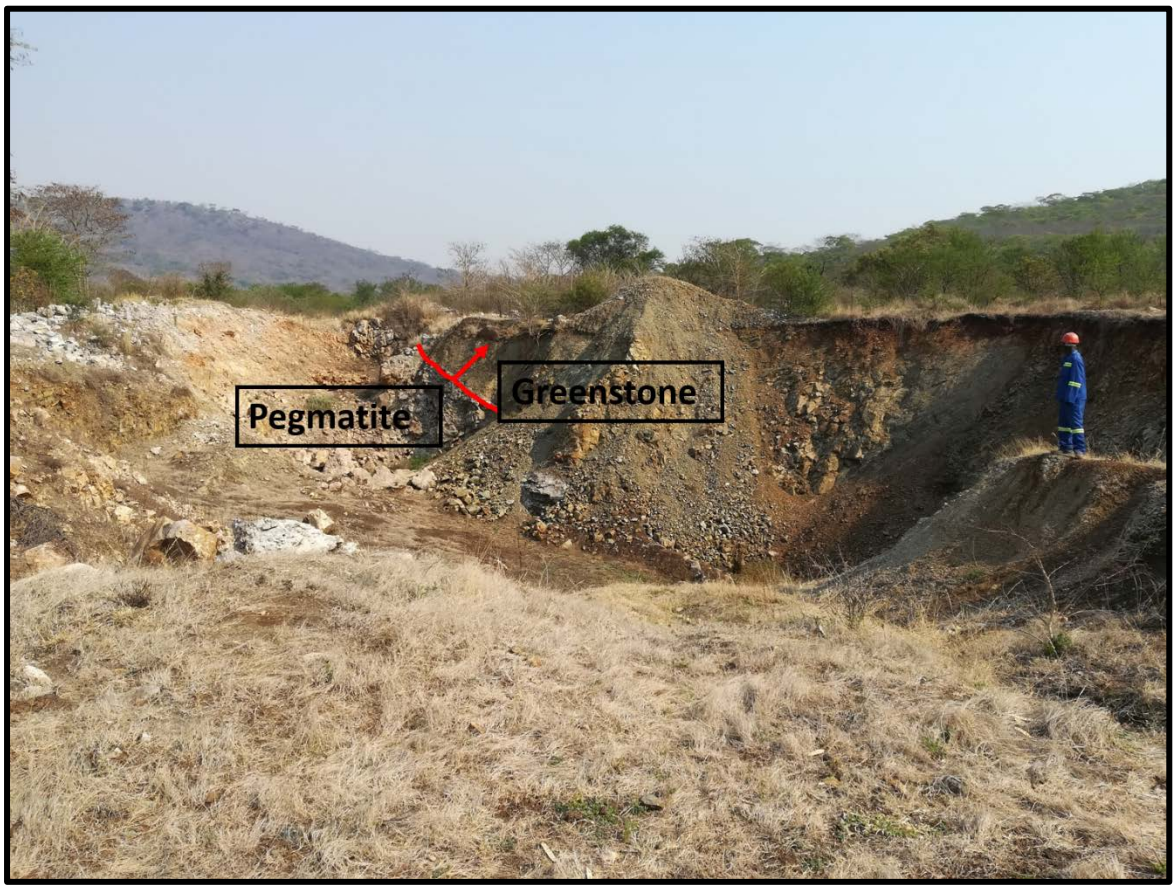

Figure 3.20*: Photograph showing the outline of the Dam Site pegmatite with a view to the north.* The red line shows the pegmatite-greenstone contact and the arrow shows the dip direction of the pegmatite

Some drilling information obtained from this pegmatite helped in generating the cross-section (Figure 3.21) which shows the lenticular nature of this pegmatite. The section is based on observations from the drilling that has been conducted to date.

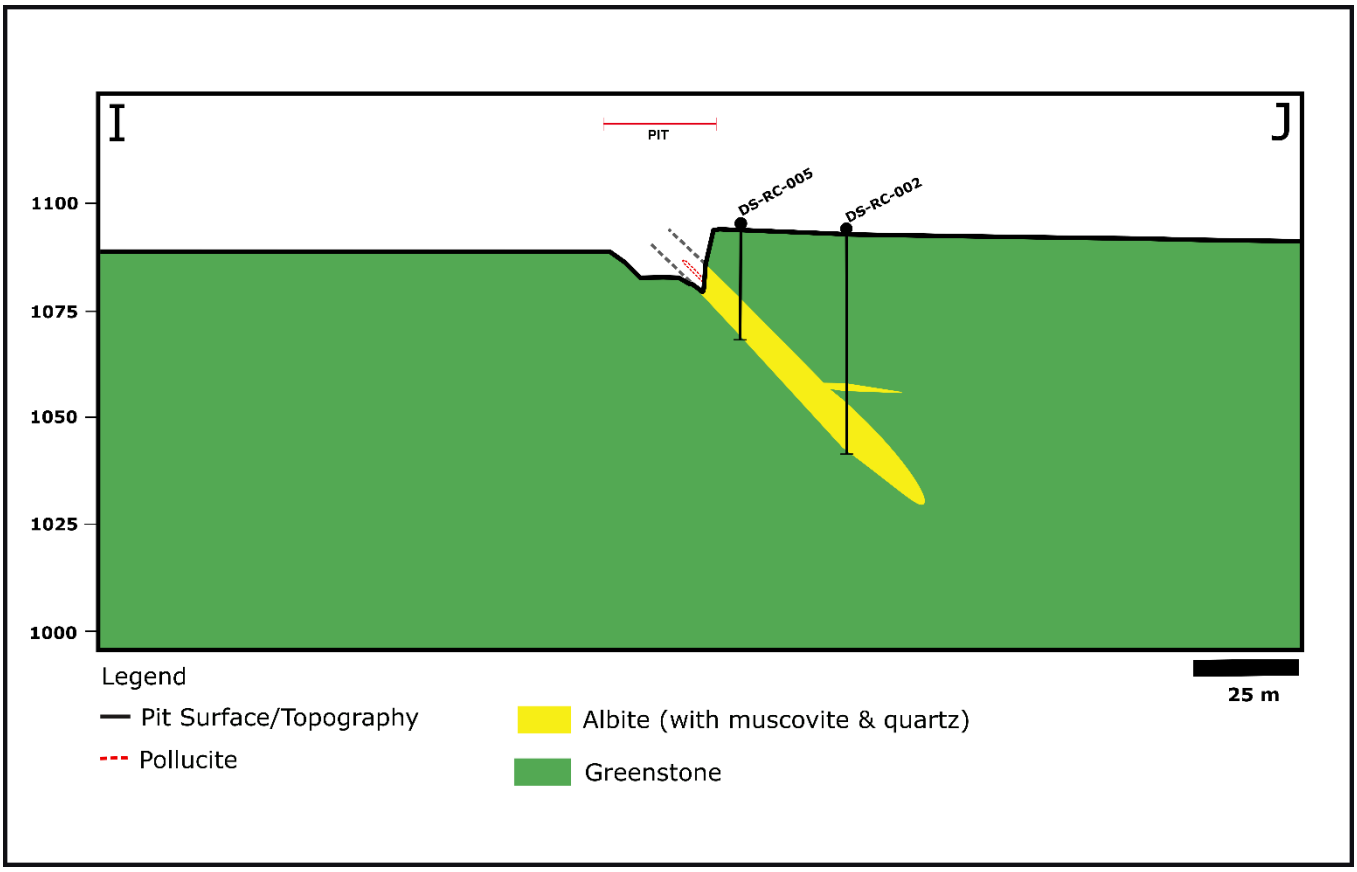

Figure 3.21: *Schematic cross section through the Dam Site pegmatite showing the associated lithologies*

3.16 The Nigel pegmatites (12 &13)

These pegmatites are situated on the northern extremity on the mining lease (Figure 3.1) and consists of Nigel North (12) where the old Nigel Tin mine occurs and Nigel South (13) which cuts across the Nigel North pegmatite at an angle of about 120° and this places it on the same strike as the Main pegmatite (1) and the East pegmatite (4). These pegmatites were hosts to lenses of cassiterite, lepidolite, and pollucite with dips varying from 65 to 90° to the north for about 500 metres (Tyndale-Biscoe, 1951). Currently, there is no mining activity taking place on these pegmatites.

3.17 The Ranga pegmatite (14)

The pegmatite is situated on the north eastern extremity of the mining lease (Figure 3.1) and follows the same strike as that of the Main pegmatite (1). It consists of a series of shallow workings and some subsequent underground workings, it used to produce cassiterite and tantalite and at some stage microlite. The pegmatite intruded into metasediments and greenstones (Tyndale-Biscoe, 1951). At the present moment, there is no mining activity on this pegmatite since the closure of the Ranga shaft.

3.18 The Cemetery pegmatite (15)

This pegmatite is situated between the Giant and West pegmatites (Figure 3.1). Based on the percussion drilling done recently on this pegmatite, it shows that petalite is present suggesting a continuation from the Shaft and Giant pegmatites. Currently, no mining activities are being carried out on this pegmatite.

3.19 Alteration in the Bikita pegmatites and relationship with the country wall-rocks

Generally, the pegmatite-country rock contacts are easily discernible and mostly irregular in shape (Figure 3.22). There is partial to extensive alteration in the Bikita field pegmatites which resulted in the development of fine-grained saccharoidal-textured type albite and acicular cleavelandite. Cleavelandite is secondary albite identifiable with a characteristic radiating morphology. The albitisation process involved replacement of microcline by sodic-rich fluids and the microcline is partially or completely destroyed. In addition to albitisation, there is the development of localised mica-rich zones or pods. London (1990) recognised that there is a spatial association of rare-element concentration (e.g. Be, Li, Rb, Cs, Nb, Ta, Sn, and U) with albitisation and muscovite replacement in rare-element pegmatites (e.g. Ta, Nb in the Tanco pegmatite).

The hangingwall greenstone of the Bikita quarry is marked by the conspicuous occurrence of a black tourmaline metasomatic selvage (Figure 3.23) and sometimes biotite. The tourmaline occurs as bladed radiating grains varying in length from 20 to 40 centimetres and also occurs as smaller grains. This tourmalinisation probably resulted from fluid wall-rock interaction during the pegmatites emplacement. Within the East pegmatite on Victor's pit, the greenstone shows some hydrothermal alteration as evidenced by chloritisation, silicification and disseminated sulphidation (Figure 3.24). Xenoliths of wall-rock greenstone also occur varying in size from 2 to 5 metres within the marginal parts of the pegmatite such as in the Al Hayat pit (Figure 3.25). According to Martin (1964), wall-rock alteration is a result of the low temperature of the intrusion. Wall-rocks are altered to hydrobiotite and zinnwaldite, with black tourmaline, apatite, rutile and diopsidic pyroxene (Tyndale-Biscoe 1951).

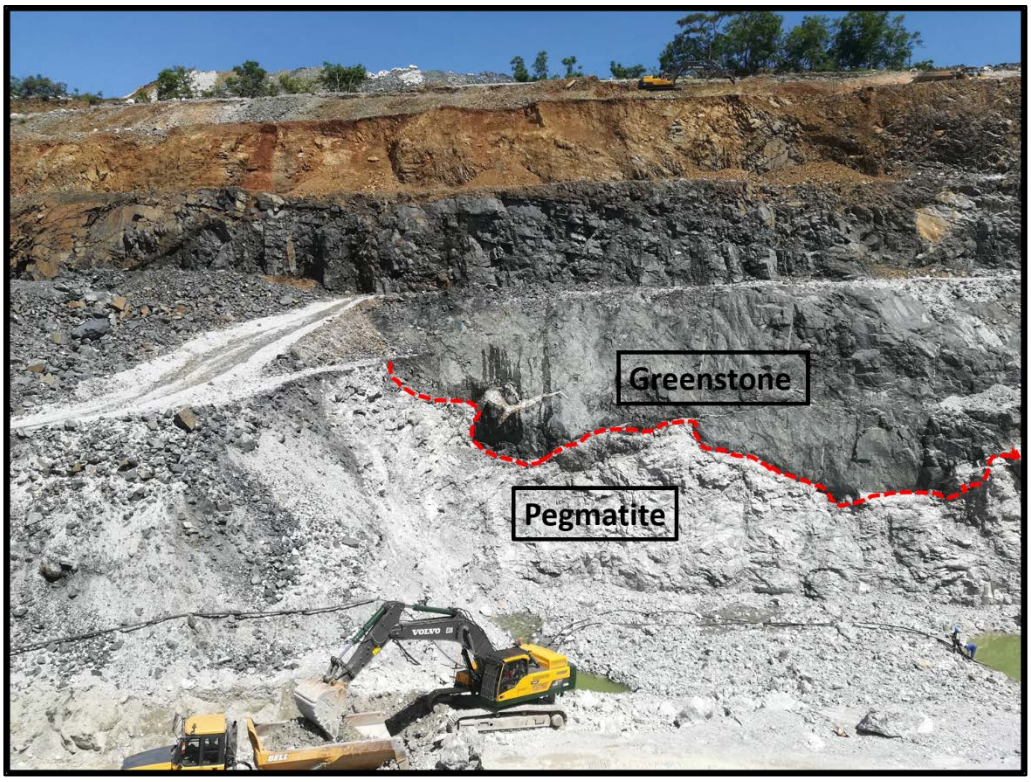

Figure 3.22: *Photograph showing an undulating contact between the greenstone and the pegmatite in Al Hayat pit with a view to the south east*

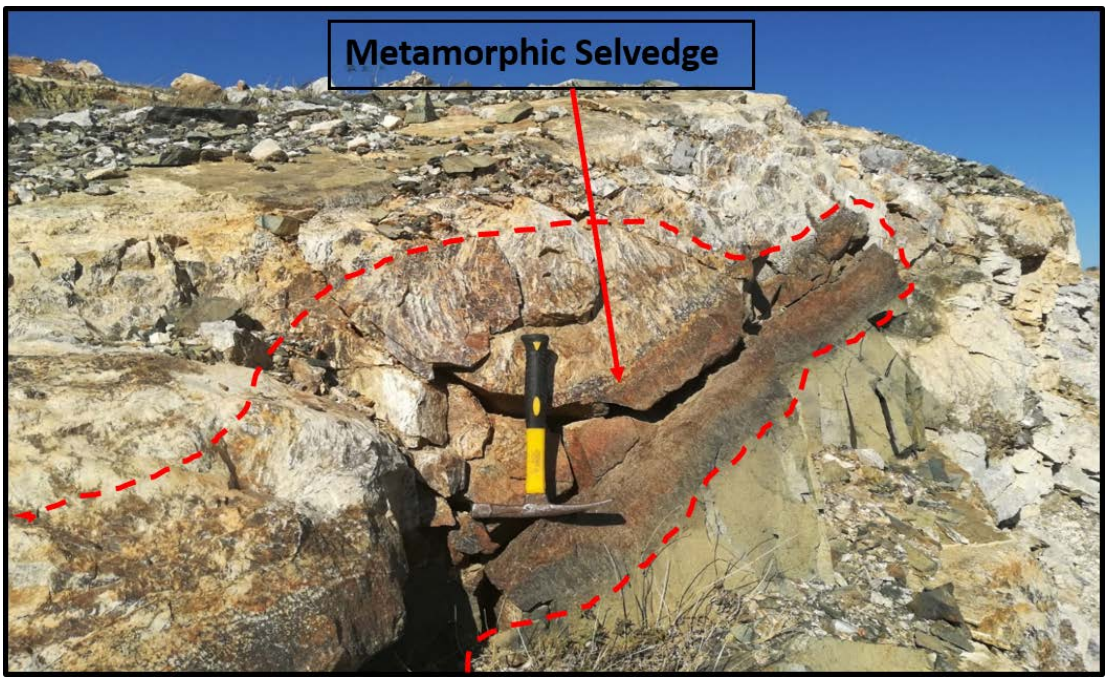

Figure 3.23: *Metamorphic selvedge of tourmaline in the Bikita quarry (marginal contact)*

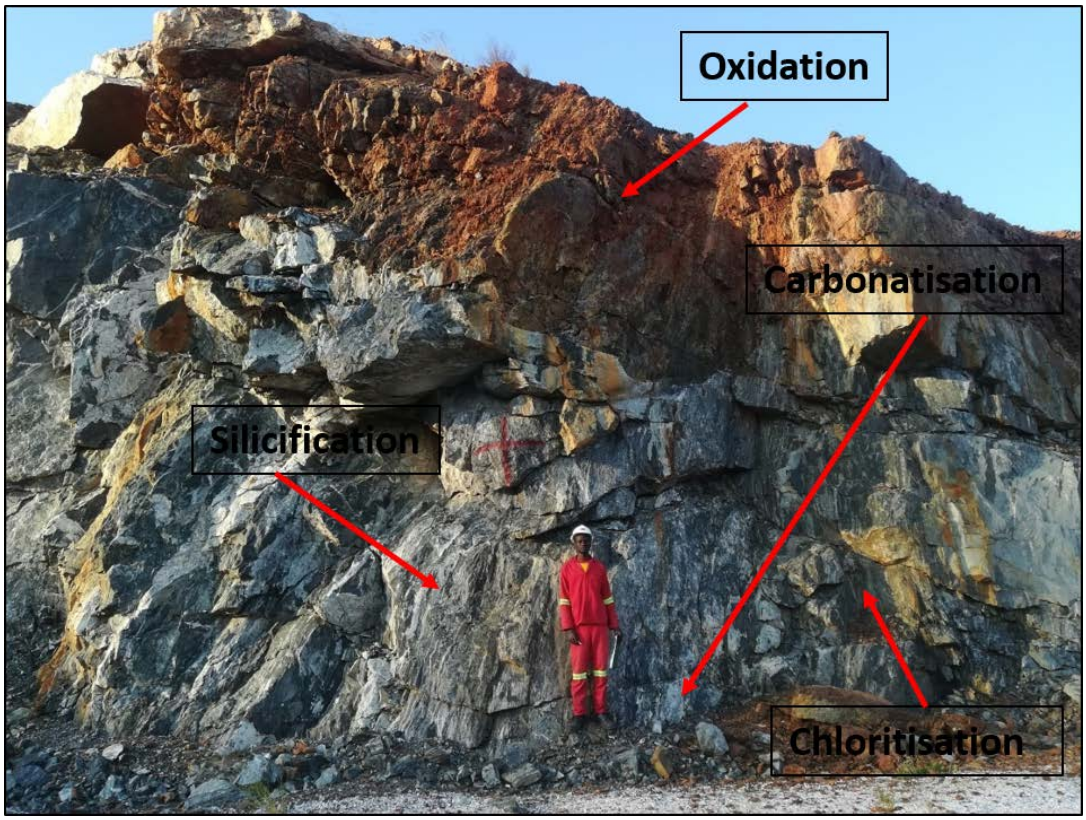

Figure 3.24: *Photograph showing typical wall-rock alteration within the Victor's pit showing carbonatisation, oxidation, silicification and chloritisation with disseminated suphidation*

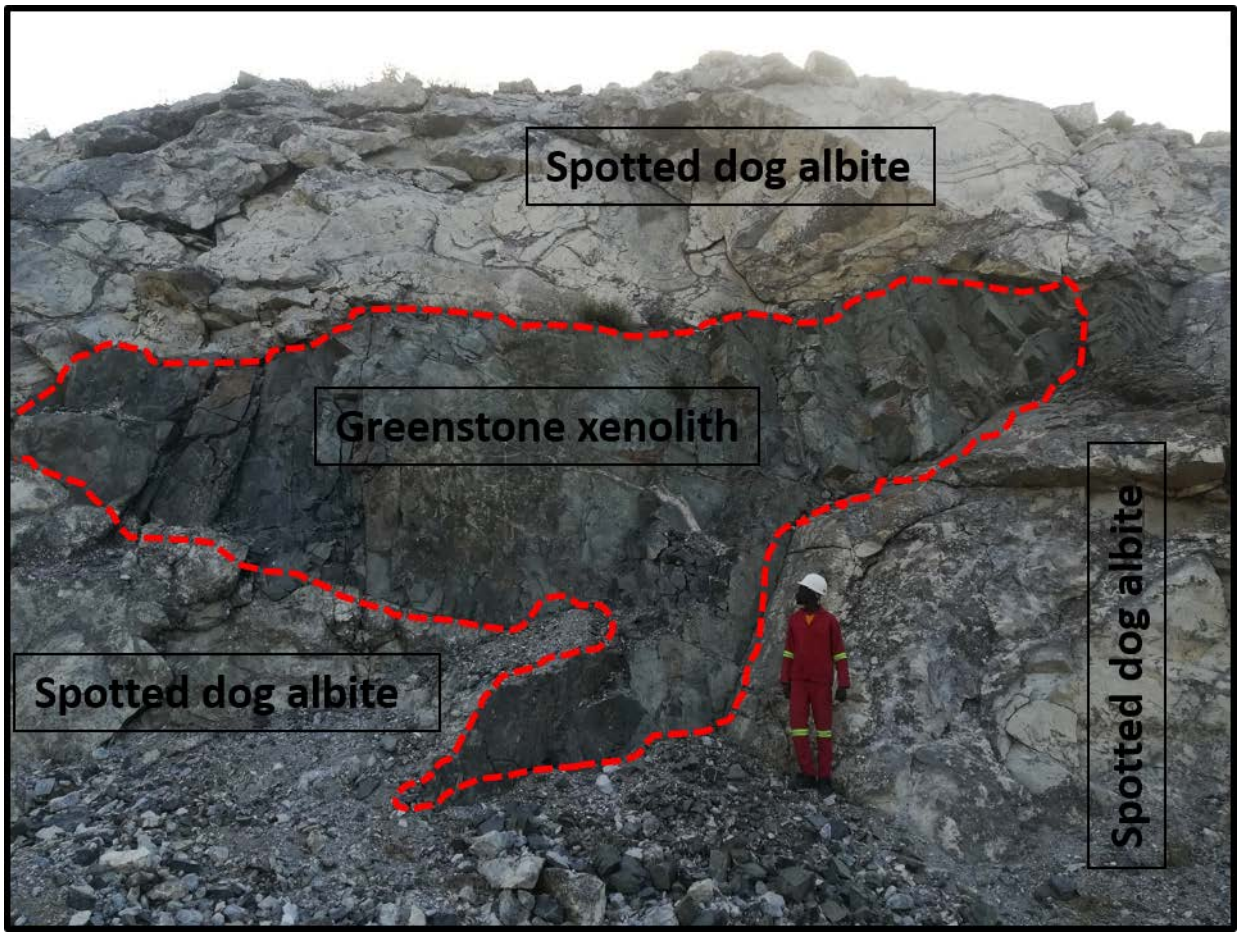

Figure 3.25: *Photograph showing a greenstone xenolith embedded within the spotted dog albite on the haulage ramp on the Al Hayat pit with a view to the west*

3.20 Age of the Bikita pegmatites

The Bikita field and particularly the Main Bikita pegmatite has been subjected to different dating techniques by various workers (e.g. Herzog et al. 1960; Melcher et al., 2015). Herzog et al (1960) obtained an age range from 2.570-2.630 Ma on dating a lepidolite from the Bikita Main pegmatite through averaging of four inter-laboratory Rb–Sr results. Melcher et al., (2015) obtained an age of 2.617 Ma on columbite and this age coincides with the intrusion of the Chilimanzi Suite of granites that were emplaced at 2.601 Ma (Jelsma et al., 1996). Generally, the pegmatites are poorly dated but recent work by Dittrich (2017), is suggesting that these pegmatites are Meso to Neoarchean in age (approximately 2.625 Ma).

3.21 Geological summary of the Bikita pegmatites

This summary presents the possible connections and links between the 15 mapped pegmatites on the Bikita Mine Lease Area (Refer to Table 3.1 and Figure 3.1 for the pegmatite names and numbers). It has also been assumed that the East (4) and Boomerang (3) pegmatites which are on the same strike and dip direction with the Main pegmatite (1) represent the northern-most extension of the main lithium mineralisation and as such, are extensions of the Main pegmatite. Moreover, since the Spodumene pegmatite (2) and the Shaft pegmatite (5) are on the same strike and dip direction, it has been assumed that they join in depth as shown on the cross-sections (Figures 3.16 and 3.19). The Giant East (7) and Giant West (7a) are probably offshoot dykes of the Spodumene

pegmatite suggesting that there is a connection between these three pegmatite bodies with more enrichment of spodumene on the east side and petalite on the west side. The Boomerang pegmatite appears to be a single body and possibly the northern continuation of the Spodumene pegmatite. This pegmatite appears to have an arcuate appearance in plan and appears to cut the Spodumene pegmatite and overlapped the East pegmatite. Many smaller pegmatites roughly parallel to the major bodies, lie further west of the West pegmatite (6) and these include the Cemetery pegmatite (15). All these western pegmatites are relatively poor in lithium, although they contain a few small bodies of lepidolite and petalite.

The East pegmatite is fairly lithium-rich although much less so than the Spodumene pegmatite. The Mauve Kop pegmatites, (8-10) presents the northern continuation of the pegmatites with a northerly strike. In the Nigel Valley, a series of smaller pegmatites strikes roughly north-west and comprises the old Nigel Tin Mine (12) and the Dam Site pegmatite (11). The Dam Site pegmatite (11) shows higher lithium contents, but is on a cross-cutting east-north-east-strike direction and may be part of the earliest lithium mineralisation. It is noteworthy that a second series of pegmatites (Nigel South) cuts these at an angle of 120° and is thus on the strike of the Bikita Main and East pegmatites. Since they dip at 25 to 40° to the east, it is therefore conceivable that further bodies of high lithium content may occur in the soil-covered Ranga Valley between the Al Hayat section and Nigel Tin Mine. Both the Dam Site (11) and the Nigel North (12) pegmatites contain lepidolite and pollucite in smaller lenses. The Ranga Mine which is 1500 metres north-east of Al Hayat consists of a series of shallow workings and some subsequent underground workings, which were used to produce cassiterite and tantalite and in later years some microlite.

CHAPTER 4:

GEOCHEMISTRY OF THE PEGMATITES

4.1 Introduction

This chapter presents the results obtained using the analyses determined by methodology discussed in the previous chapters. This includes data from core logging that is used to assess mineralisation potential of an area which was obtained through whole-rock geochemical analysis, a review of the project geology.

4.2 Whole-rock geochemical data

The whole-rock geochemical dataset consists of AAS and XRF analyses for major and trace elemental composition, made up of samples from various pegmatite bodies. The dataset analysed by the AAS technique is comprised of 1143 samples with 7 major element oxides in (%) whereas the dataset analysed by the XRF technique consists of 441 samples with 6 minor and trace elements (Ta, Nb, Sn, Fe, Rb and Sr) reported in parts per million (ppm) (Table 4.1).

The results from these geochemical analyses are important to confirm the mineral species present that may have been missed during logging interpretations. The data is treated statistically using geochemical plots in order to show sample variations and correlations. These results are then used to ascertain the chemical composition of the samples in terms of related pegmatite mineralisation and then plot geochemical patterns that will provide a guideline for any conclusions on understanding the geology and mineralisation of the different pegmatite bodies and discussions about the comparisons are done in the data interpretation and discussions section. A summary of the results of the analyses are presented in Appendix 3 and the detection limits for the various major elements analysed are presented in Appendix 8. Bivariate x-y diagrams were used to determine the relationships between major and trace element data variables. For the major element geochemical data, a comparison is then done on the elemental averages combined (Table 4.2 and Figure 4.13).

Table 4.1*: Whole-rock geochemical dataset summary showing the total numbers of samples analysed by the different methods.*

Sample Type	AAS (major elements) samples	XRF (trace elements) samples
Channel chip/grab	70	64
Percussion Drilling	100	45
Reverse Circulation	393	332
Diamond Drilling	580	0
Totals	**1143**	**441**

4.2.1 Major element geochemistry

Major element analysis by AAS can be used to examine the behaviour of Li and Cs, two of the important economic elements at Bikita. Major element bivariate x-y diagrams (Figures 4.1 to 4.13) are used in this section to display the behaviour of K_2O, Na_2O, Al_2O_3, Fe_2O_3, Cs_2O and Rb_2O with respect to Li_2O on the individual pegmatite bodies and some points have been noted with reference to these figures.

The bivariate x-y diagram of Figure 4.1 represents results from the McMurdon pit where Li_2O values range from 2.25 to 3.63 %. Li_2O shows a positive correlation with K_2O, Al_2O_3 (forms a well-defined linear trend) and tends to show no relationships with Na_2O, Fe_2O_3, Cs_2O and Rb_2O.

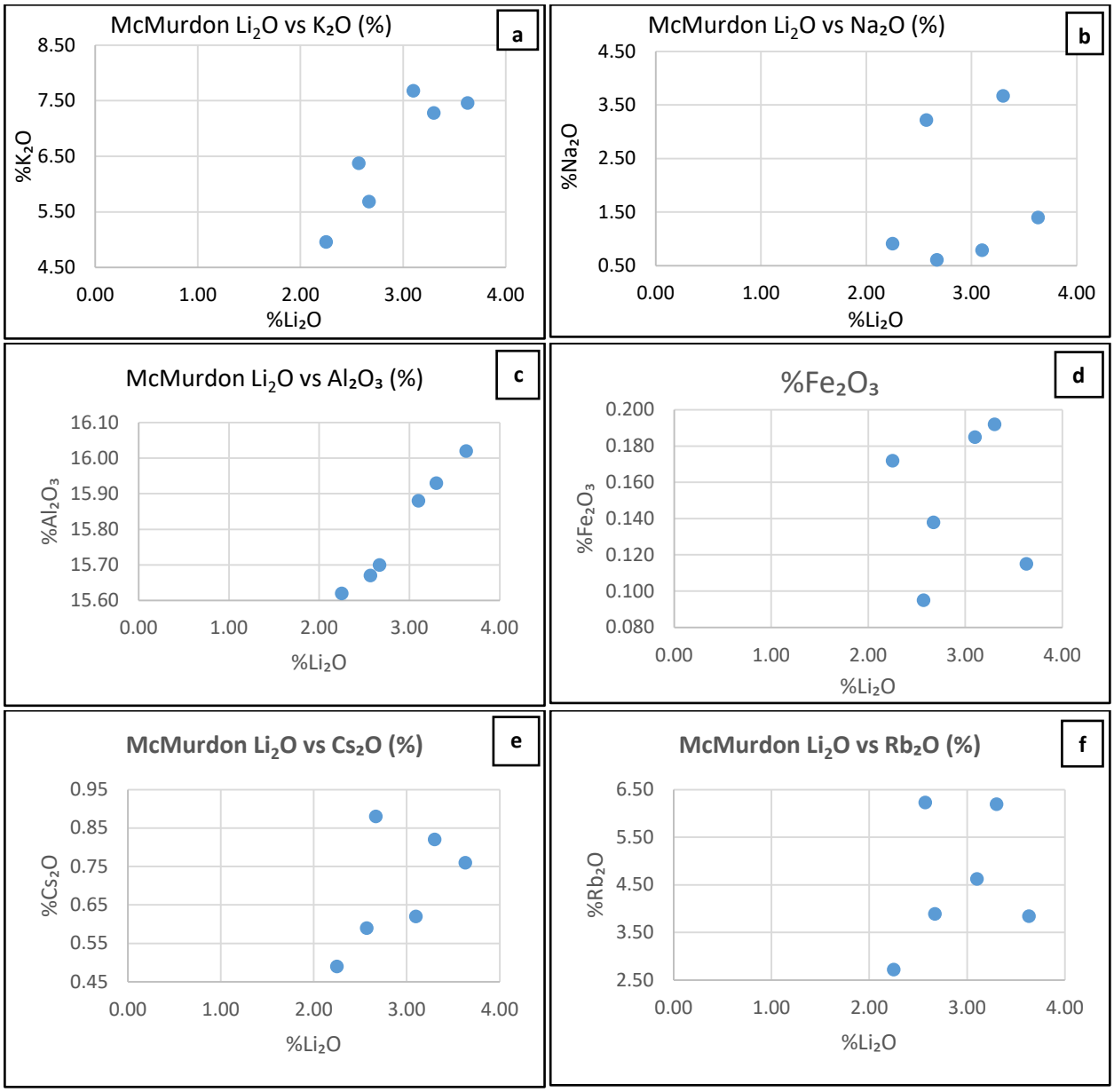

Figure 4.1: *Major element bivariate x-y diagram for the McMurdom pit pegmatite body.* See Appendix 3 for details

The main pegmatite (1) having been the most exposed and worked, it has been easy to obtain more comprehensive data to represent this part of the pegmatite body in Bikita quarry and it has proved to have the best behaved dataset. The comparison of the variations in mineralogical compositions obtained through drilling are presented in the consolidated bivariate plots. Figure 4.2 presents the plot of Li_2O versus K_2O for analysed samples from the Bikita quarry locality. Typical rock-forming mineral compositions are shown in green boxes. Three trends shown by the data correspond to specific mineral control, with the data points representing progressive enrichment in the end-member minerals. There is a positive correlation of Li_2O and K_2O contents from channel and percussion drilling but there is a scatter on reverse perhaps due to dilution effects.

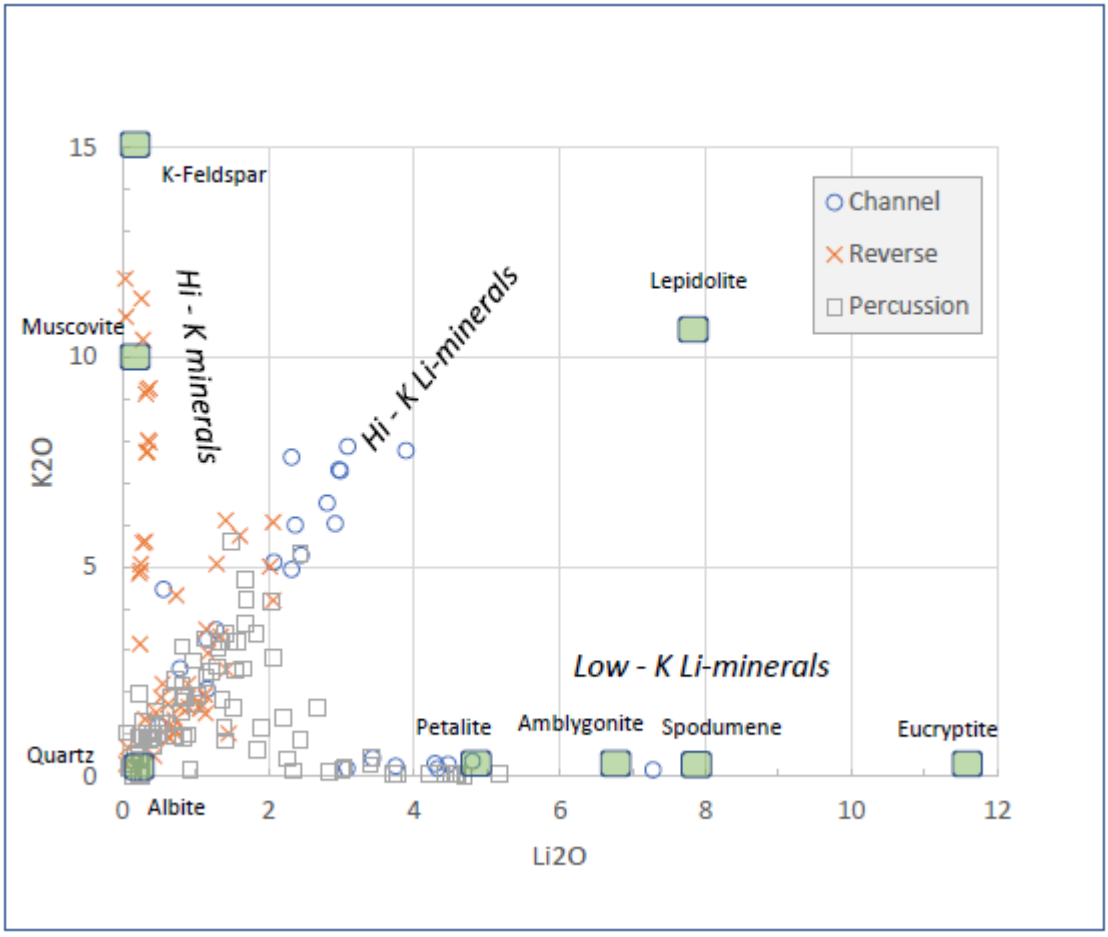

Figure 4.2**:** *Li_2O vs K_2O major element bivariate x-y diagram for the Bikita quarry pegmatite body.* See Appendix 3 for details

Figure 4.3 presents the plot of Li_2O versus Na_2O for analysed samples from the Bikita quarry locality. Typical rock-forming mineral compositions are shown in green boxes. Na_2O and Li_2O are negatively correlated and the compositions indicate that albite is a predominant host mineral.

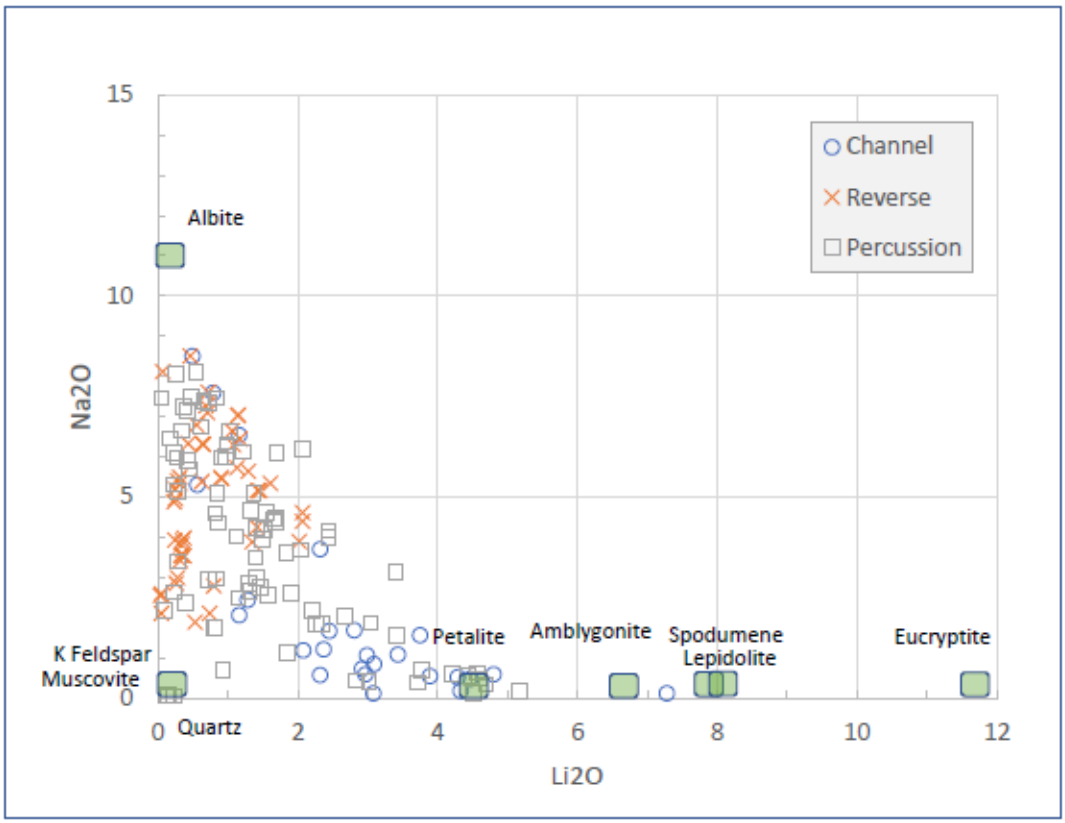

Figure 4.3: *Li_2O vs Na_2O major element bivariate x-y diagram for the Bikita quarry pegmatite body. See Appendix 3 for details*

In Figure 4.4, the plot of Li_2O versus Al_2O_3 for analysed samples from the Bikita quarry locality is presented and typical rock-forming mineral compositions are shown in green boxes. There is a shallow positive slope across three sampling techniques showing correlation of Li_2O vs Al_2O_3. Overlap of the high and low K Li minerals causes a condensed pattern, but the compositions indicate feldspars are predominant host minerals with only one sample containing significant quartz. The Li-Al plot tends not to be overly diagnostic, as all the Li minerals contain Al, but the pattern in the context of the constituent minerals is particularly instructive.

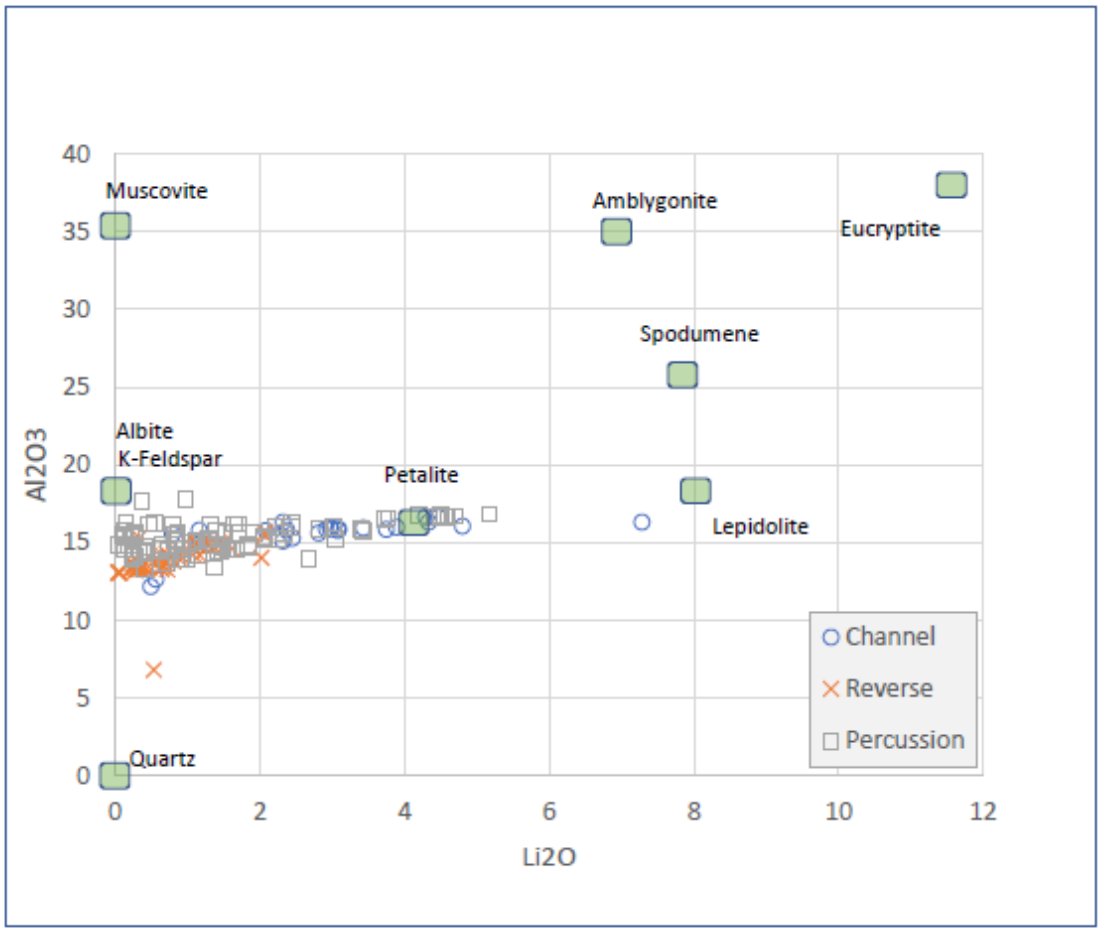

Figure 4.4: *Li_2O vs Al_2O_3 major element bivariate x-y diagram for the Bikita quarry pegmatite body. See Appendix 3 for details*

The bivariate x-y diagram presented in Figure 4.5 shows results from the Al Hayat pit where Li_2O values range from 2.35 to 5.69 %. Li_2O is showing no relationships with K_2O, Na_2O, Fe_2O_3, Cs_2O, and Rb_2O, while showing a positive correlation with Al_2O_3.

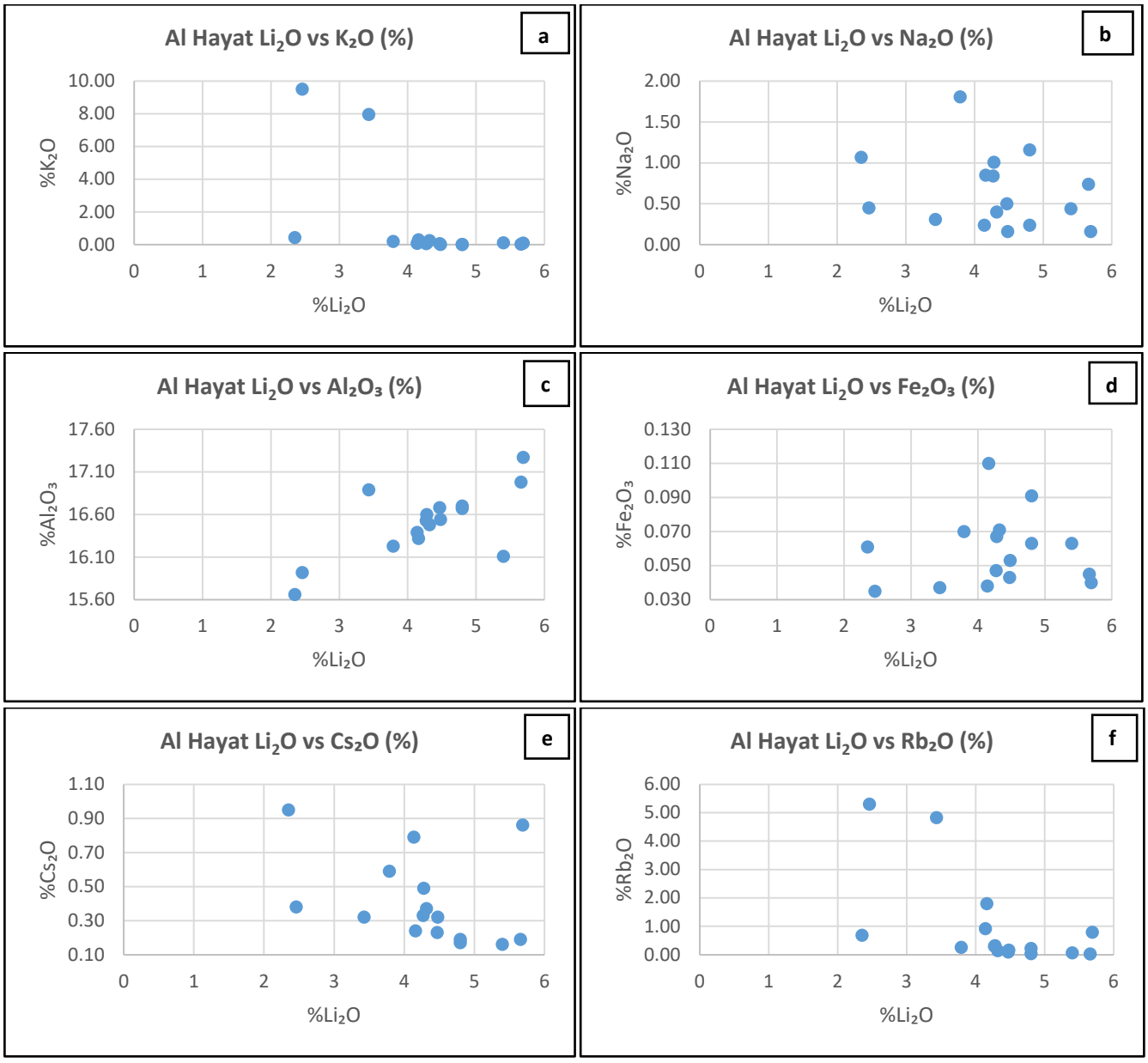

Figure 4.5: *Major element Harker variation diagram for the Al Hayat pit pegmatite body.* See Appendix 3 for details

In Figure 4.6, the bivariate x-y diagram shows results from the Ledingham pegmatite body where Li_2O is content of the samples varies from 0.10 to 4.51 %. There is a negative correlation between Li_2O and K_2O and Na_2O, where as there is a positive correlation with Al_2O_3 forming a well-defined linear trend and no relationships with Fe_2O_3, Cs_2O and Rb_2O.

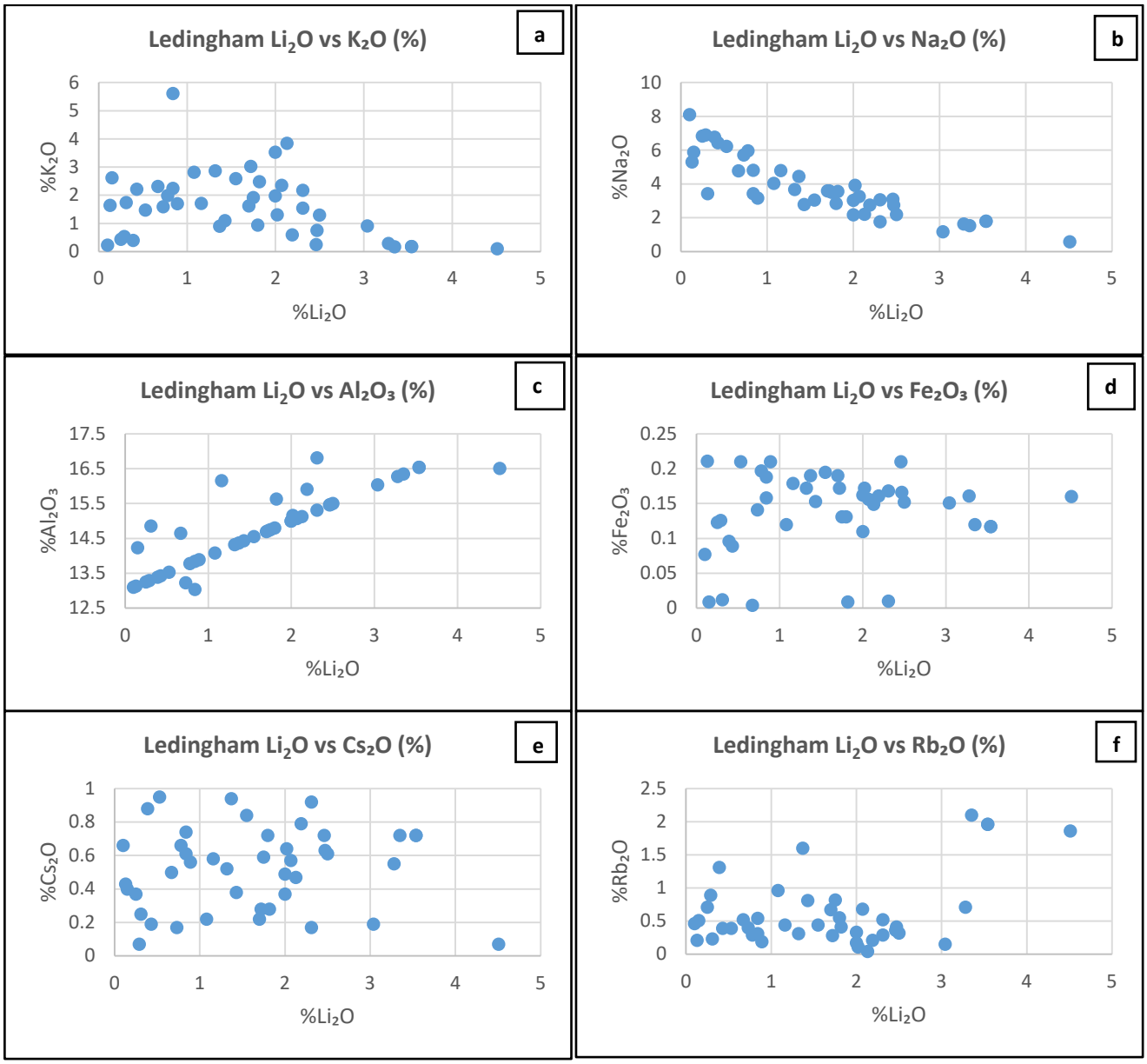

Figure 4.6: *Major element bivariate x-y diagram for the Ledingham sector pegmatite body.* See Appendix 3 for details

The bivariate x-y diagram presented in Figure 4.7 represents results from the Victor's pit where Li_2O values range from 0.33 to 2.56 % whilst Cs_2O content varies little between 26.15 to 26.78 %. Li_2O values show a positive correlation with K_2O and Rb_2O, a negative correlation with Na_2O and Al_2O_3, and shows no relationships with Fe_2O_3 and Cs_2O.

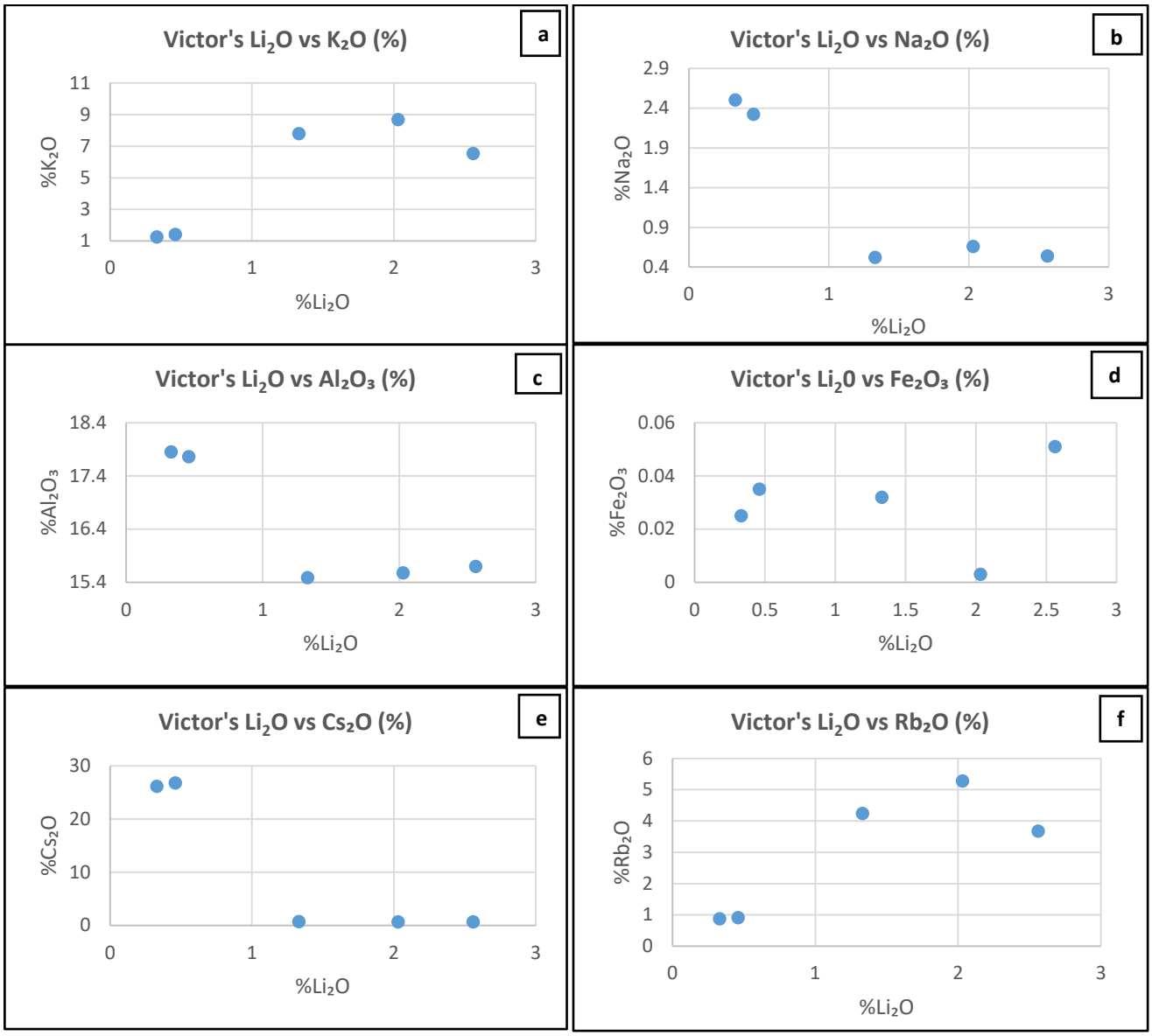

Figure 4.7: *Major element bivariate x-y diagram for the Victor's pit pegmatite body.* See Appendix 3 for details

In Figure 4.8, the bivariate x-y diagram of data from the Nigel's pit shows a variation of Li_2O from 0.43 to 5.44 % whilst Cs_2O has a wide range of 0.16 to 20.24 %. The Li_2O abundance shows no relationships with K_2O, Al_2O_3, Fe_2O_3 and Cs_2O and a negative correlation with Na_2O and Rb_2O.

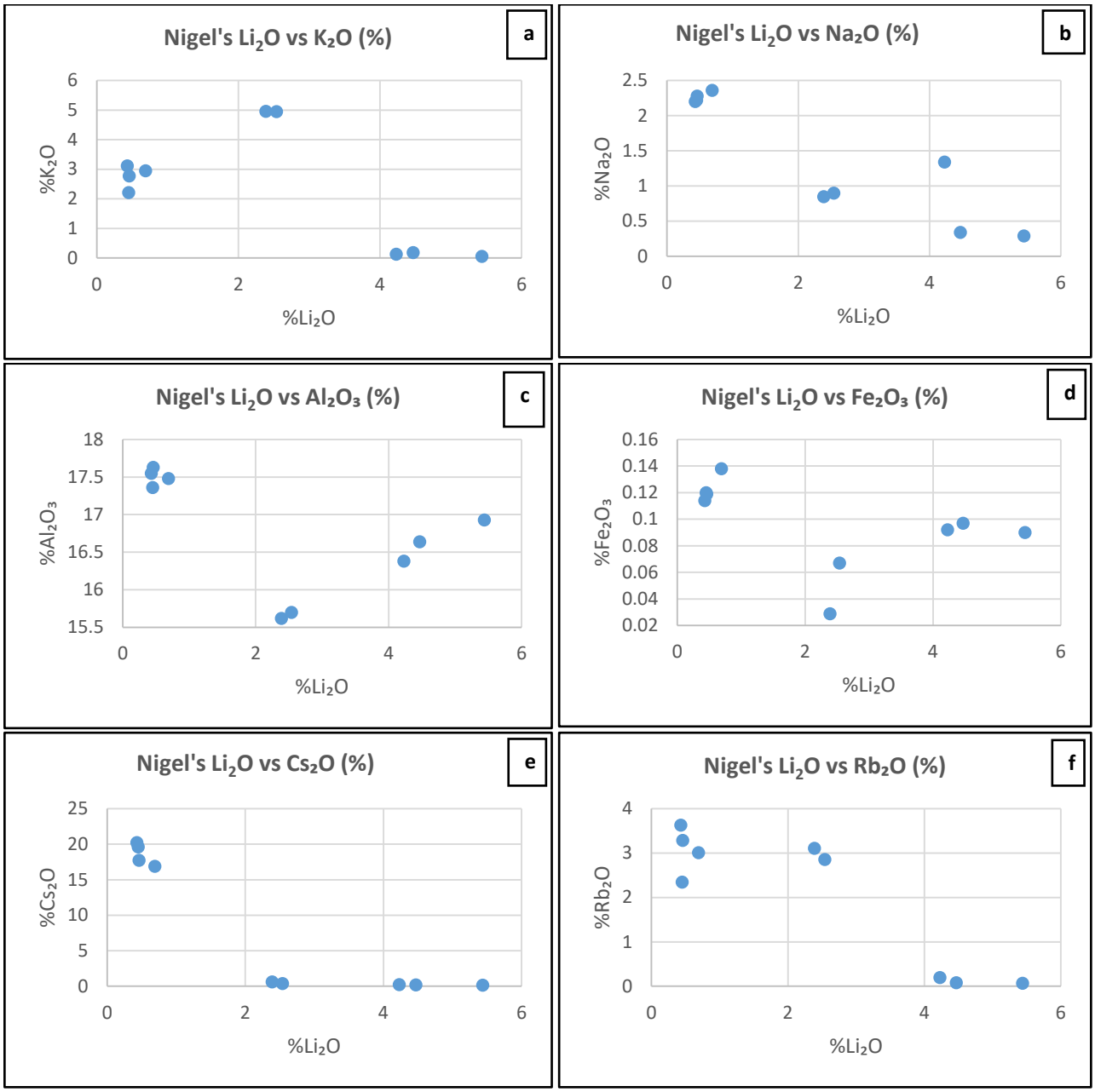

Figure 4.8: *Major element bivariate x-y diagram for the Nigel's pit pegmatite body.* See Appendix 3 for details

In Figure 4.9, the bivariate x-y diagram of data from the Shaft pegmatite body shows a Li_2O variation from 0.02 to 4.3 %. There is negative correlation between Li_2O and K_2O, Rb_2O and Na_2O, a positive correlation with Al_2O_3 and no relationships with Fe_2O_3 and Cs_2O.

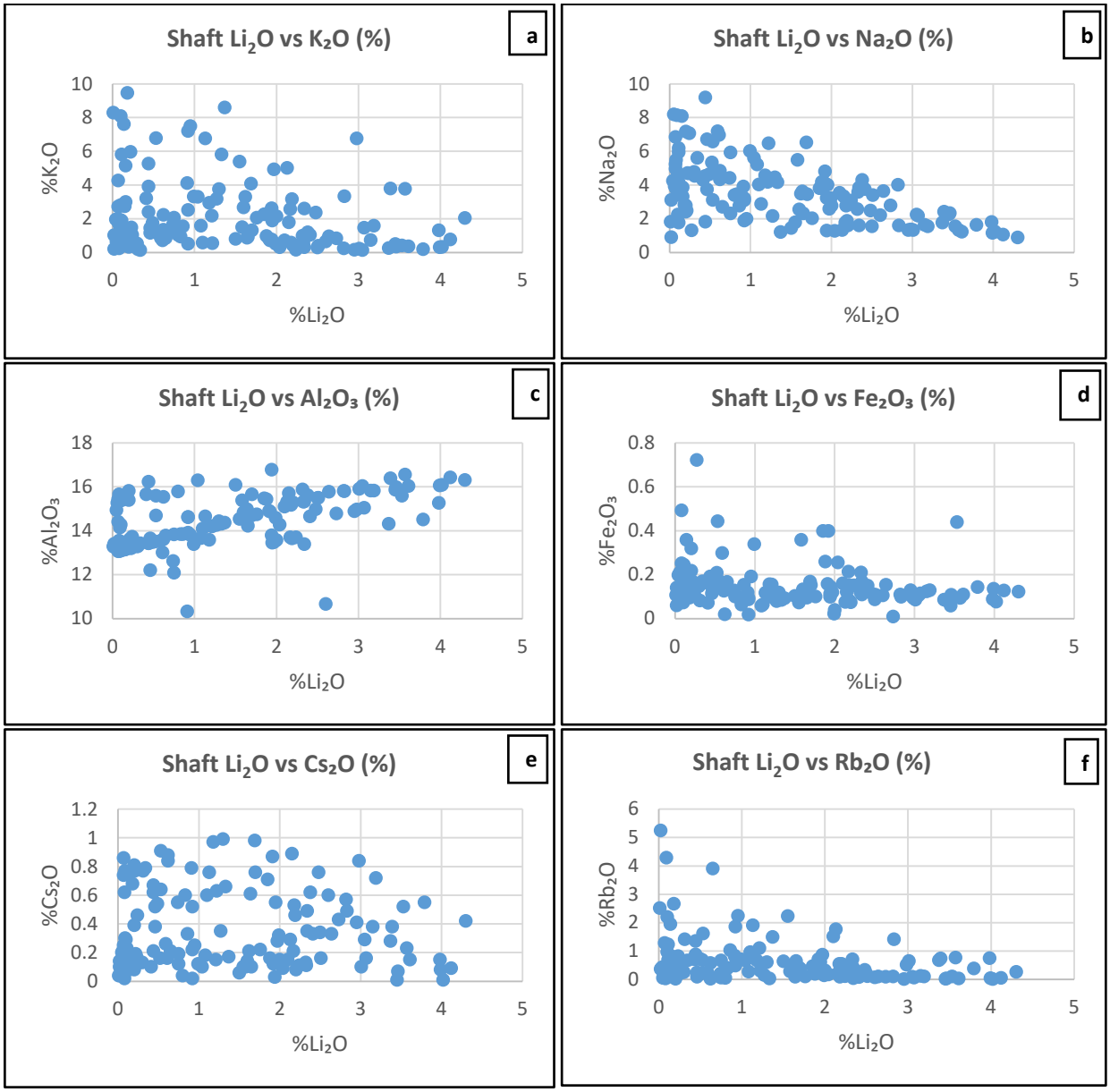

Figure 4.9: *Major element bivariate x-y diagram for the Shaft sector pegmatite body.* See Appendix 3 for details

The bivariate x-y diagram of Figure 4.10 represents data from the West pegmatite body where Li_2O values are ranging from 0.08 to 3.1 %. There is no relationship between Li_2O and K_2O, Fe_2O_3 and Cs_2O, a negative correlation with Na_2O and whilst there is a positive correlation with Al_2O_3 and Rb_2O.

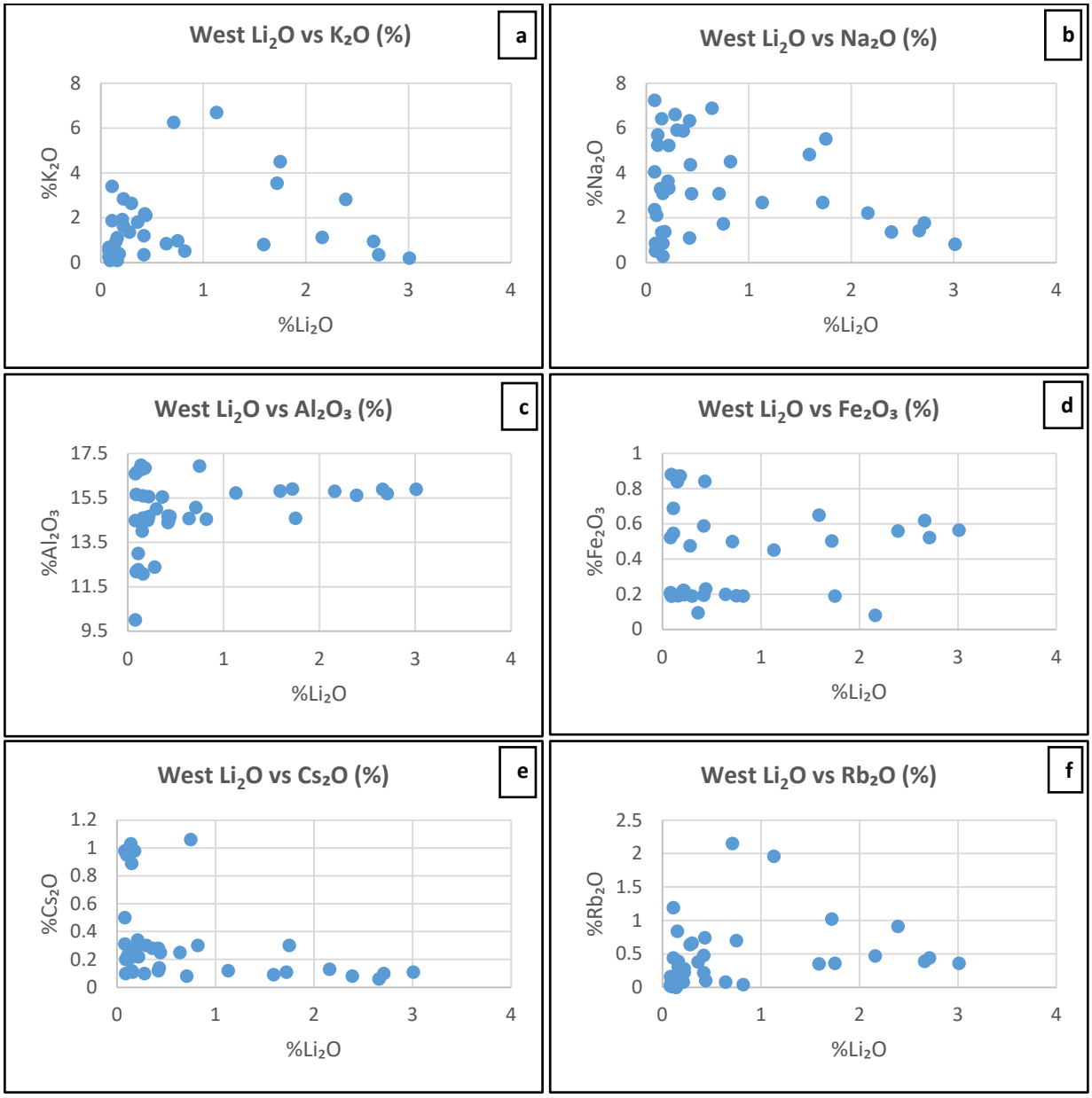

Figure 4.10: *Major element bivariate x-y diagram for the West sector pegmatite body.* See Appendix 3 for details

The bivariate x-y diagram for the Giant East pegmatite body, shown in Figure 4.11, indicates that the Li_2O content of the samples ranges from 0.13 to 4.89 %. The Li_2O shows a negative correlation with K_2O, Fe_2O_3 and Na_2O, a positive correlation with Al_2O_3 and no relationships with Cs_2O and Rb_2O.

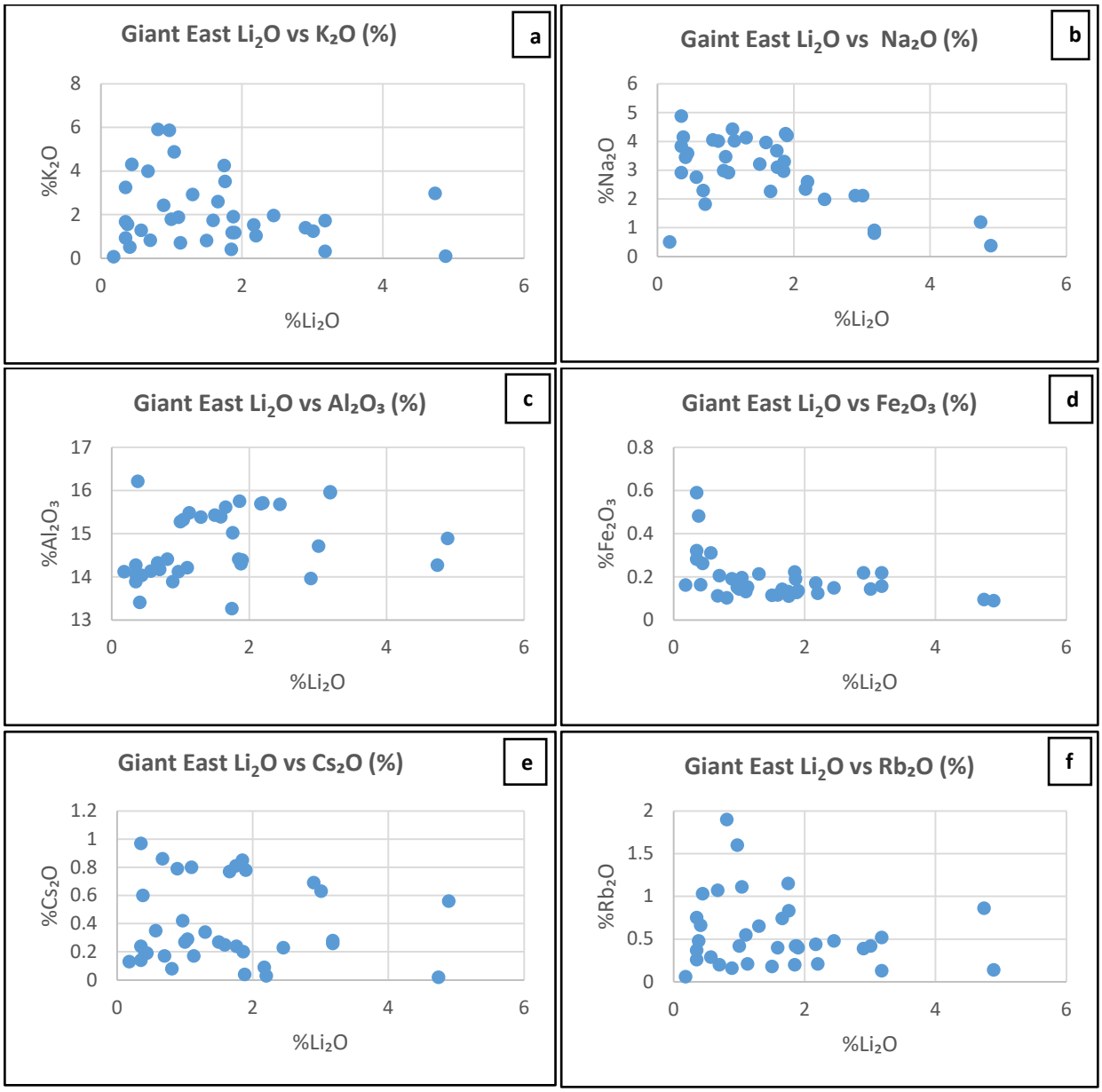

Figure 4.11: *Major element bivariate x-y diagram for the Giant East sector pegmatite body.* See Appendix 3 for details

The bivariate x-y diagram presented in Figure 4.12 represents data from the Mauve Kop pegmatite body where Li_2O values are low and vary from 0.10 to 0.46 %. Although values are low, there does appear to be a positive correlation between Li_2O content and that of K_2O, Fe_2O_3, Cs_2O and Rb_2O, with a negative correlation with Al_2O_3 and shows no relationship with Na_2O.

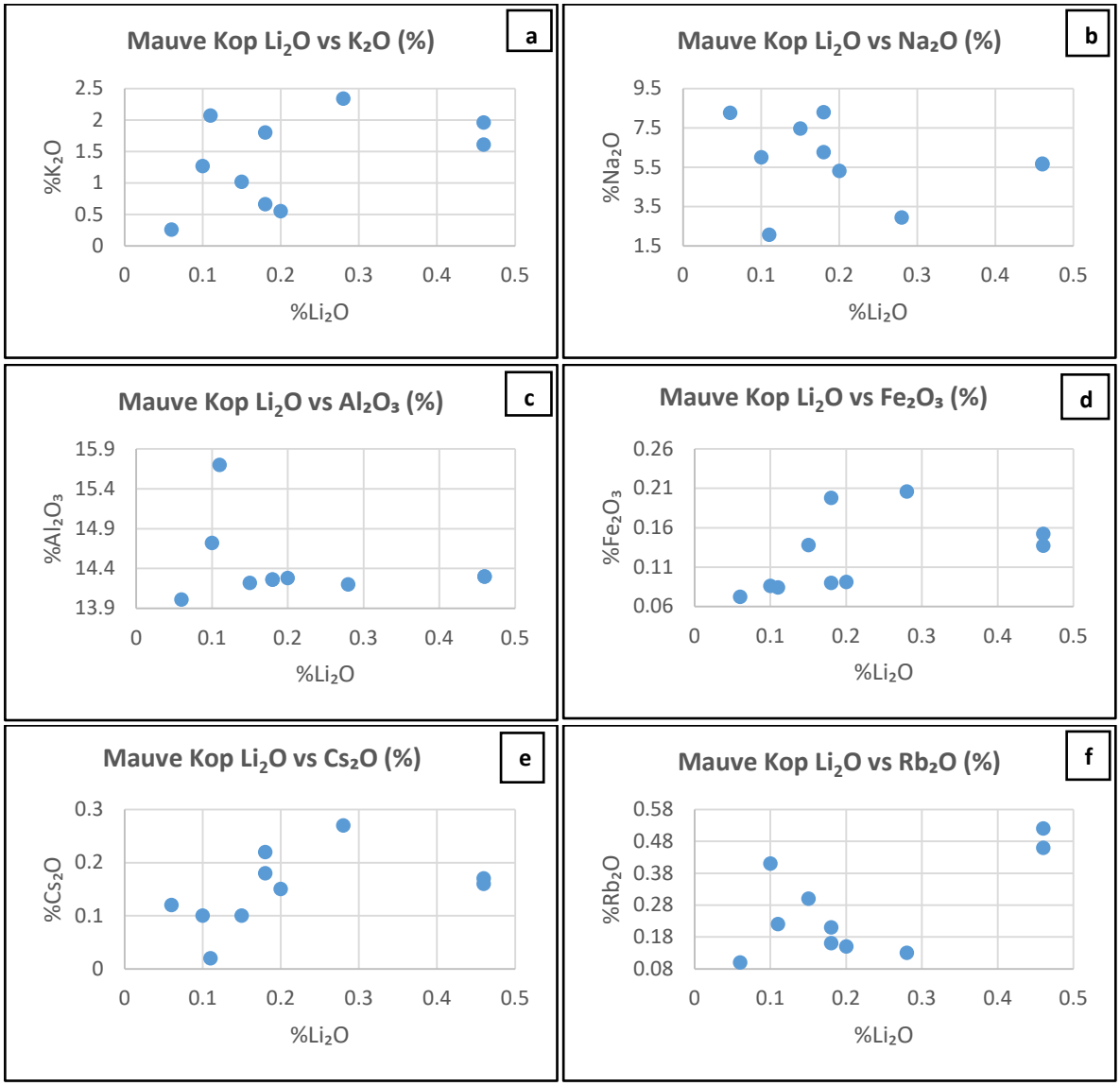

Figure 4.12*: Major element bivariate x-y diagram for the Mauve Kop sector pegmatite body.* See Appendix 3 for details

The bivariate x-y diagram for the Dam Site pit is shown in Figure 4.13. In this plot, Li_2O shows a variation from 0.65 to 8.63 %, and Cs_2O with a high range from 0.11 to 23.1 %. For Li_2O there is a negative correlation with K_2O, Na_2O, Cs_2O and Rb_2O, and no relationship with Al_2O_3 and Fe_2O_3.

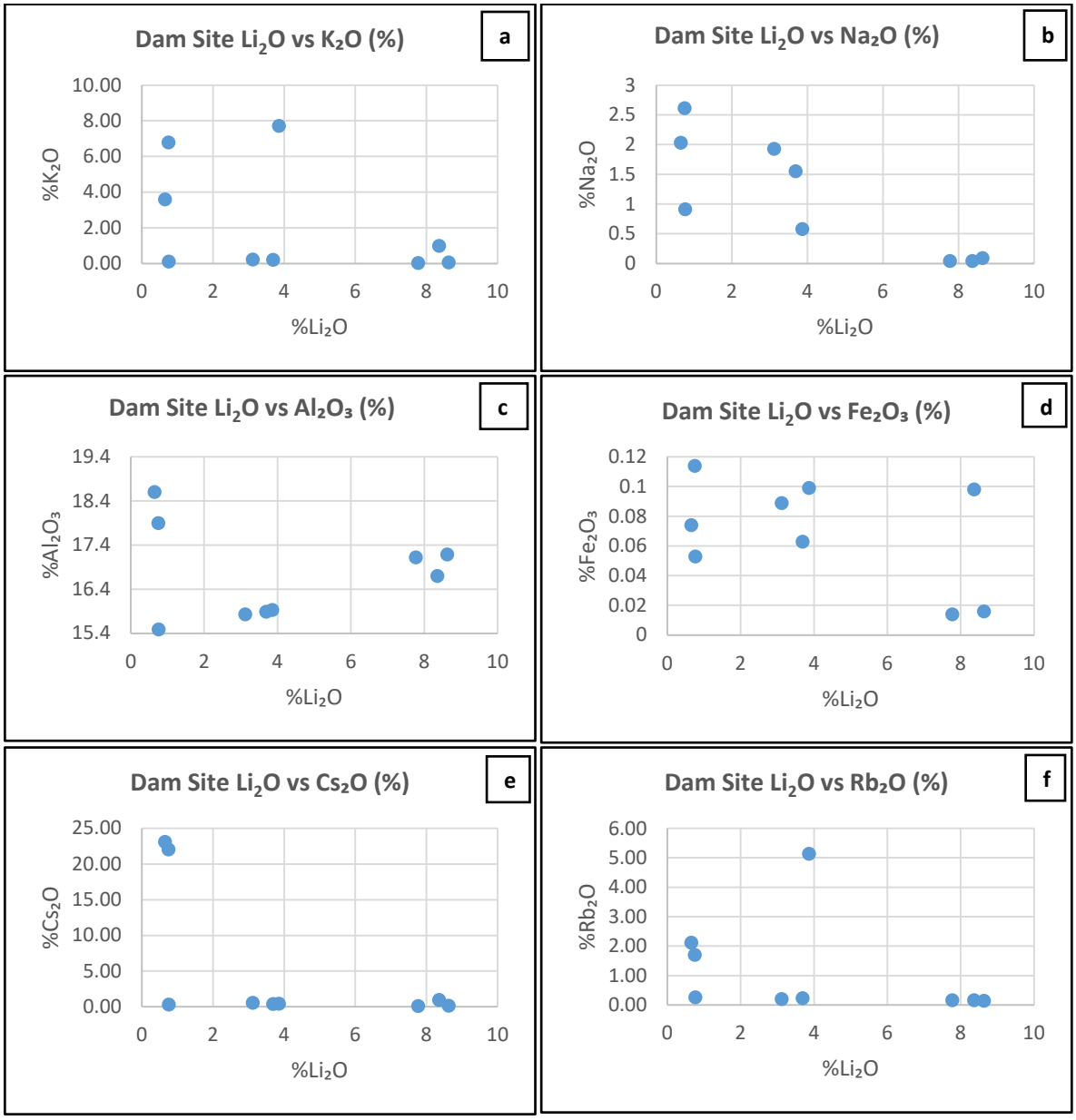

Figure 4.13: *Major element bivariate x-y diagram for the Dam Site pit pegmatite body.* See Appendix 3 for details

For the Cemetery pegmatite body, the Li_2O content varies from 0.13 to 3.49 % (Figure 4.14) and shows no relationship with K_2O, Fe_2O_3 and Rb_2O, a negative correlation with Na_2O and positive correlations with Al_2O_3 and Cs_2O.

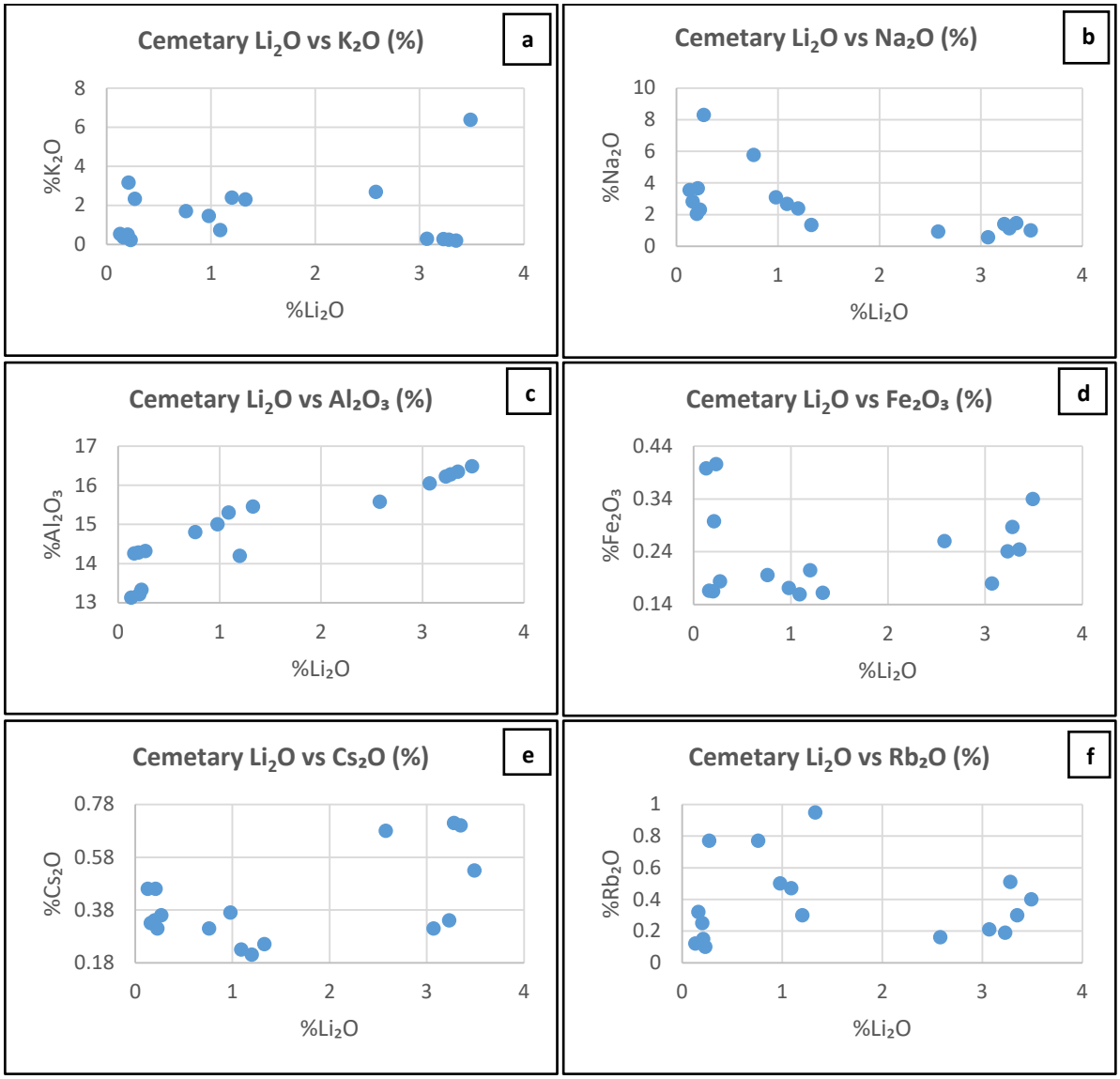

Figure 4.14: *Major element bivariate x-y diagram for the Cemetery sector pegmatite body.* See Appendix 3 for details

In Figure 4.15 represents results from all the sampled pegmatite bodies combined with Li_2O having an average of 2.08 % and Cs_2O averaging 2.48 %. Li_2O shows no relationship with K_2O, Cs_2O and Rb_2O, there is a negative correlation with Na_2O and Fe_2O_3 and a positive correlation with Al_2O_3. Table 4.2 shows the details for the data.

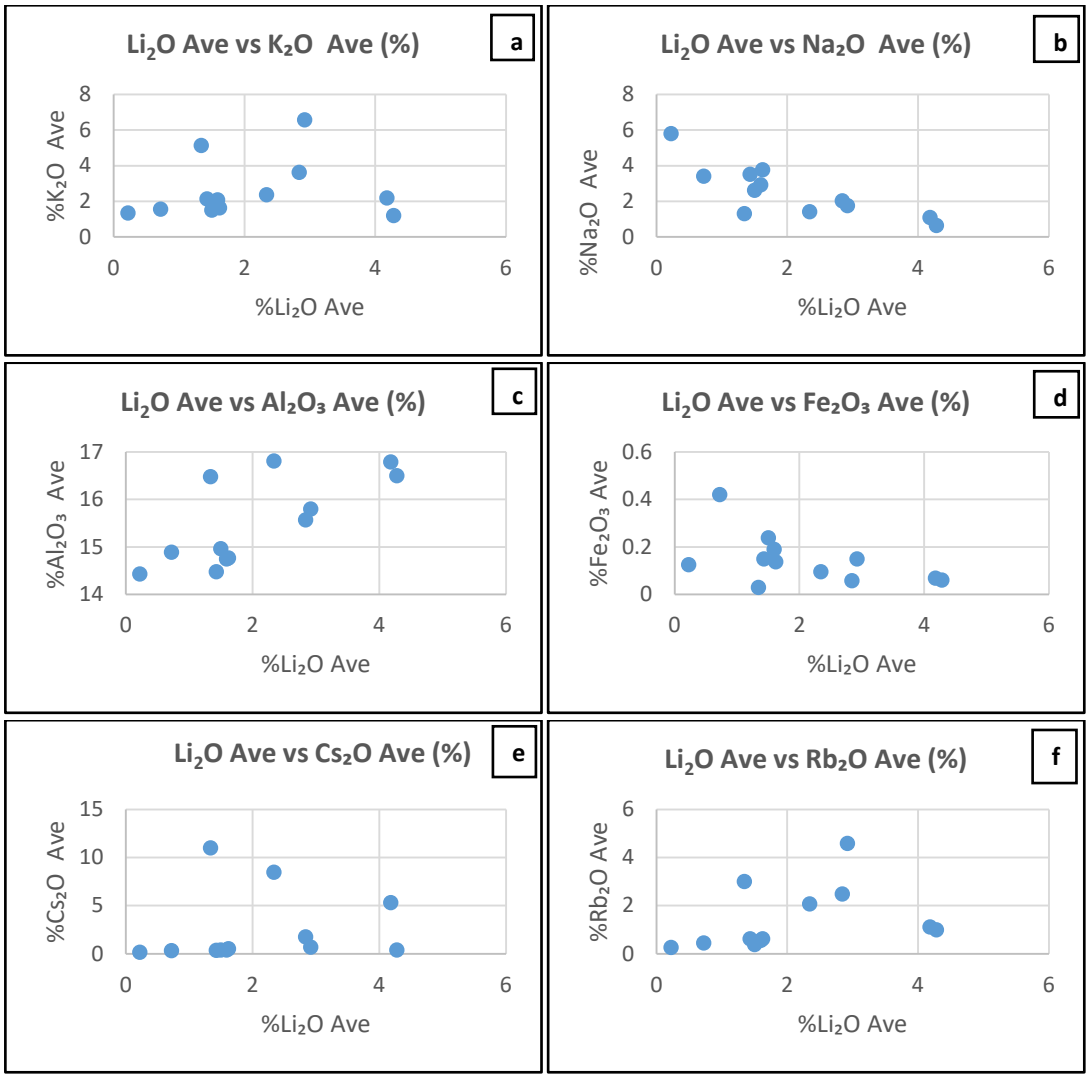

Figure 4.15: *Major element bivariate x-y diagram for all the pegmatite bodies combined as derived from Table 4.2.* See Appendix 3 for details

Table 4.2: *Combined major element variations for the various pegmatite bodies*

Pegmatite Section	%Li_2O Ave	%K_2O Ave	%Na_2O Ave	%Al_2O_3 Ave	%Fe_2O_3 Ave	%Cs_2O Ave	%Rb_2O Ave
McMurdon	2.92	6.58	1.77	15.8	0.15	0.69	4.58
Bikita	2.84	3.64	2.03	15.57	0.058	1.75	2.48
Al Hayat	4.28	1.21	0.65	16.5	0.06	0.41	1
Ledingham	1.62	1.63	3.77	14.77	0.138	0.52	0.62
Victor's	1.34	5.14	1.31	16.48	0.029	11	3
Nigel's	2.34	2.37	1.42	16.81	0.096	8.46	2.07
Shaft	1.43	2.14	3.52	14.48	0.15	0.36	0.63
West	0.72	1.56	3.42	14.89	0.42	0.32	0.45
Giant East	1.59	2.08	2.94	14.75	0.19	0.39	0.56
Mauve Kop	0.22	1.35	5.8	14.43	0.125	0.15	0.27
Dam Site	4.18	2.19	1.09	16.79	0.069	5.32	1.12
Cemetery	1.5	1.52	2.62	14.96	0.239	0.41	0.38
Total Averages	**2.08**	**2.62**	**2.53**	**15.52**	**0.144**	**2.48**	**1.43**

4.2.1.1 Variation plots major element chemostratigraphy

The geochemical data from the AAS analysis of borehole samples were also plotted together with the borehole core logs to consider and illustrate any variation between the AAS results and the core logging. These logs show variations in the behaviours of Li_2O, K_2O, Na_2O, Al_2O_3, Fe_2O_3, Cs_2O and Rb_2O. The plots allow for insights to be drawn into the vertical compositional variation of the major elements and the geochemical relationships and contrasts between the mineralised and barren intervals. The chemostratigraphy variation plots (Figures 4.14 and 4.15) shows the relationship between lithologies, mineral abundance, whole-rock geochemistry and the behaviour of certain elements with depth in the drill intersections. Refer to appendix 6 for lithologic contacts summaries and the other variation plot diagrams.

The variations in AAS data for the Ledingham sector on the Spodumene pegmatite through intersection of drill hole SQIDDH44 is shown in Figure 4.16. Through the core, Li_2O is generally low (< 1 wt %) from the top pegmatite where Na_2O dominates reflecting the abundance of albite feldspar in this intersection 6 to 15 metres. K_2O is generally low with a high value up to 7 %. Al_2O_3 varies between 15 to 17 wt %, as the amount of mica varies while Fe concentration is constantly low at <0.2 wt %. At the base for the main pegmatite intersection, Li_2O varies with high values up to 4.5 wt %. Cs_2O is generally low (< 0.1 wt %) with a few exceptions where values of 4 to wt 9 % are recorded. Na_2O is higher than K_2O within this sector of the pegmatites. Fe_2O_3 is generally low (< 0.2 wt %) with one exception where it is 2.1 wt %.

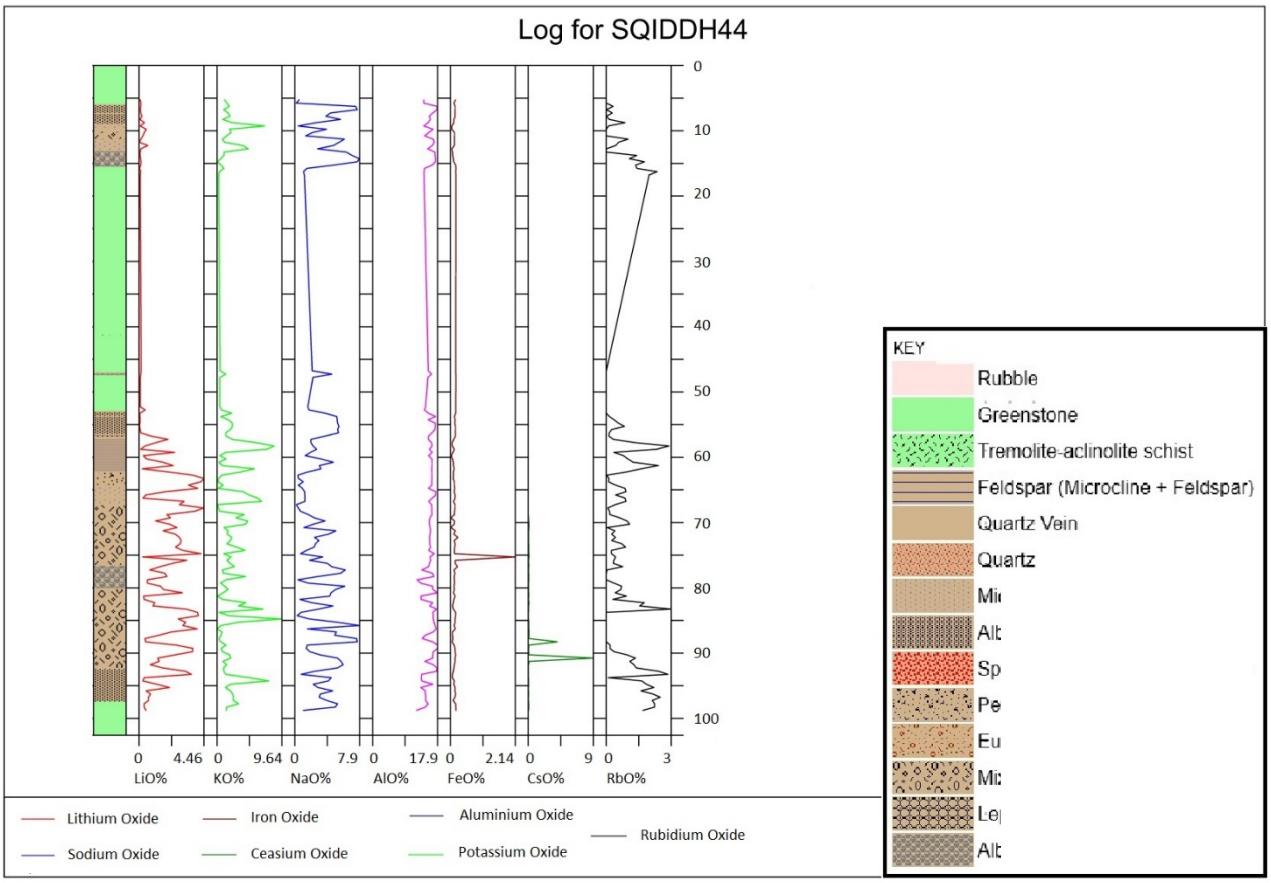

Figure 4.16: *Major element oxides chemostratigraphy variation plot for borehole SQIDDH44.* See Appendix 6C for details of lithological profile summaries.

Figure 4.17 shows the variations in AAS data from the Al Hayat sector on the Main pegmatite through drill hole AHHDDH002. Clearly Li_2O varies downhole through the different zones but values of economic significance are within the petalite and mixed zones of the intersections. There is a drop in Li_2O concentration towards the footwall contact with the greenstone. Cs_2O is generally low with high values of up to 0.9 wt %. Na_2O is lower than K_2O. Fe_2O_3 is generally low (< 0.2 wt %). Rb_2O is high (up to 6.28 wt %) in some intersections. Al_2O_3 varies between 13 and 17 wt %.

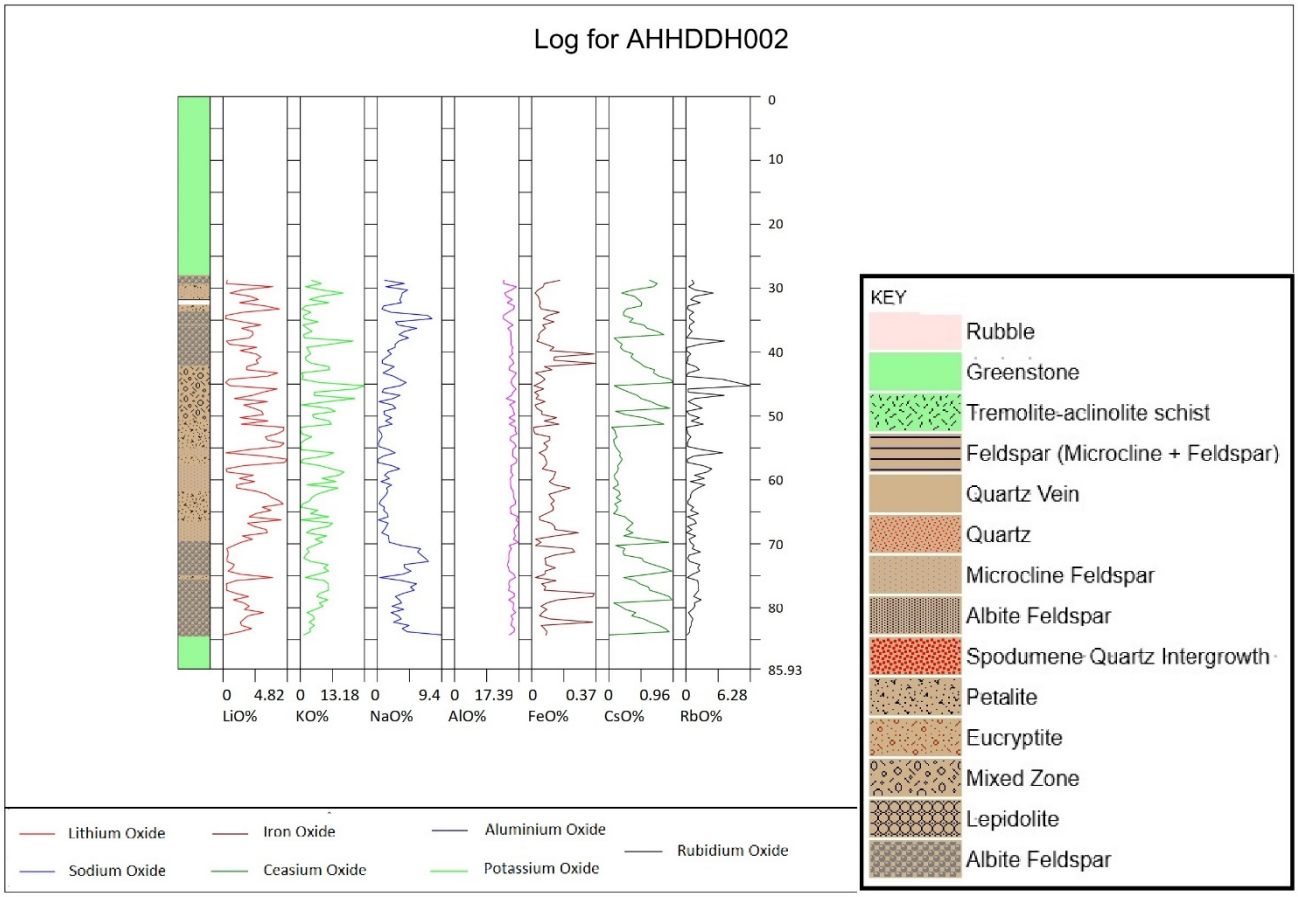

Figure 4.17*: Major element oxides chemostratigraphy variation plot for borehole AHHDDH002.* See Appendix 6C for details of lithological profile summaries.

4.2.2 Trace element geochemistry

The main objective of undertaking XRF analysis on the selected samples was to help in identifying the other elemental constituents of the pegmatites apart from lithium and caesium. Figures 4.18 to 4.27 have been used to show the variations on pegmatite bodies between Ta, Sn, Nb, Rb and Sr.

The bivariate x-y diagram of Figure 4.18 represents results from the McMurdon pit where Ta shows a positive correlation with Sn and Nb, Sn shows a positive correlation with Nb and Rb also has a positive correlation with Sr. On the Ta vs Sn plot, there is one outlier for series (1157, 1924) and (3708, 620) for the Ta vs Nb plot.

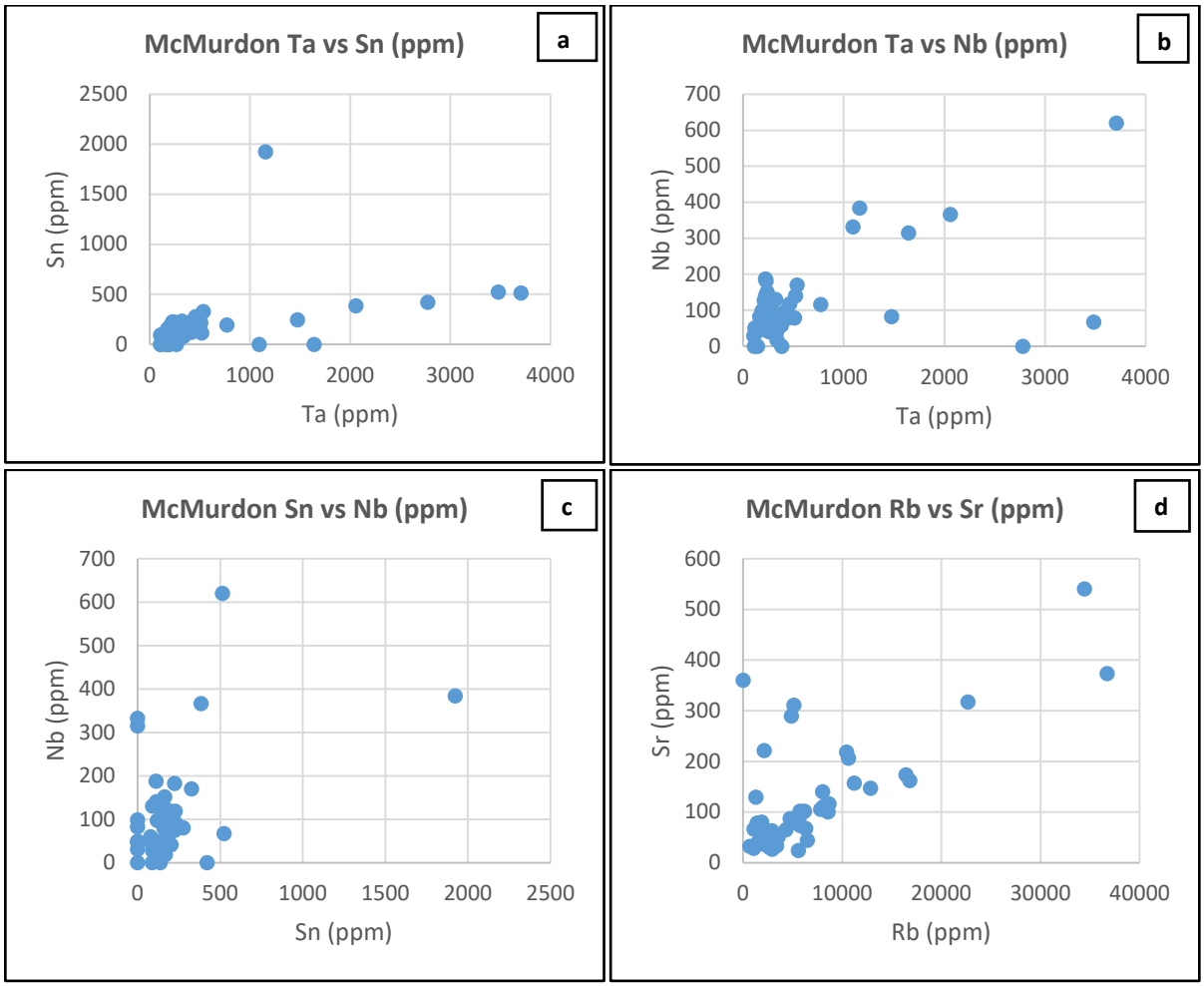

Figure 4.18: *Trace element bivariate x-y diagram for the McMurdorn pit pegmatite body.* See Appendix 2 for details

The bivariate x-y diagram shown in Figure 4.19 represents results from the Bikita quarry where Ta vs Sn, Ta vs Nb, Sn vs Nb and Rb vs Sr are all positively correlated. Outliers (18860, 9701) for Ta vs Sn, (18860, 2623) for Ta vs Nb, (9701, 2623) for Sn vs Nb and (19629, 119) for Rb vs Sr have been included from the plots.

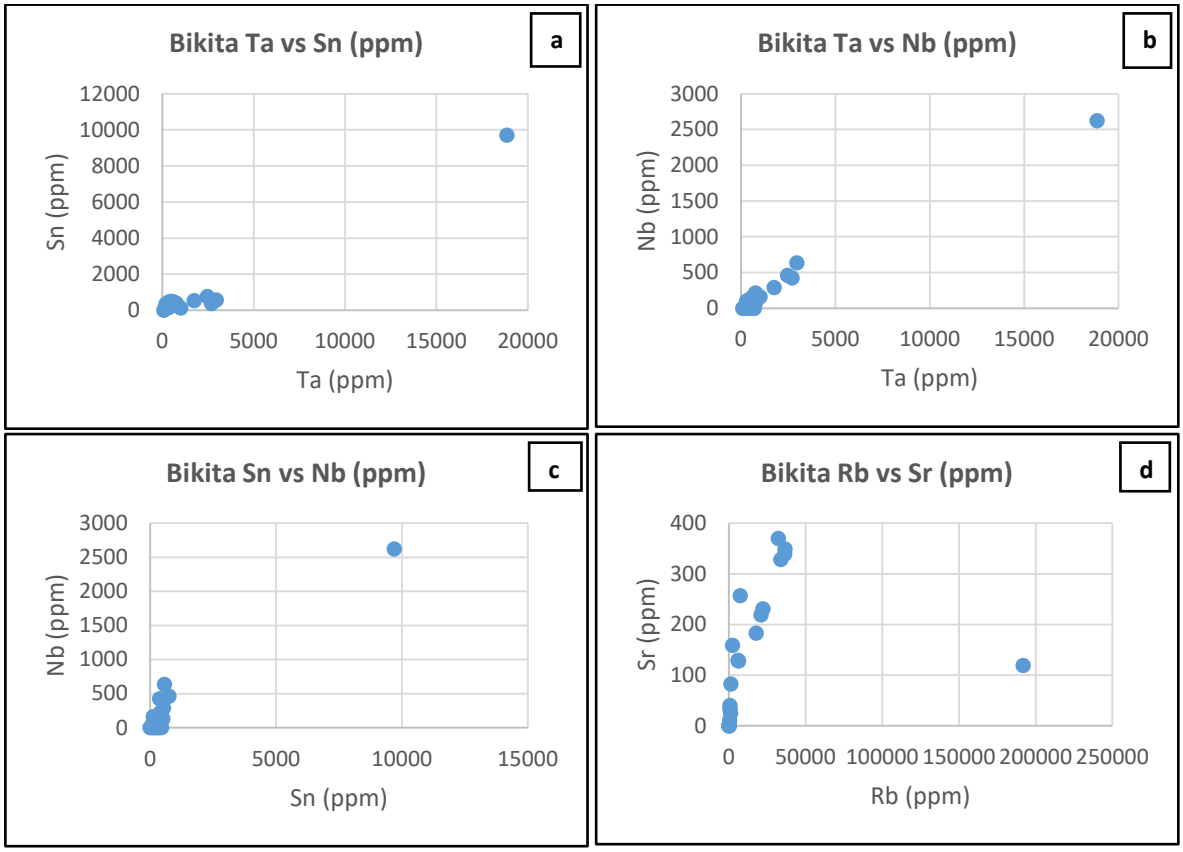

Figure 4.19: *Trace element bivariate x-y diagram for the Bikita quarry pegmatite body.* See Appendix 2 for details

The bivariate x-y diagram shown in Figure 4.20 represents results from the Al Hayat pit where Ta vs Sn (forms a well-defined linear trend), Ta vs Nb, Sn vs Nb and Rb vs Sr are all positively correlated. Outliers (176, 870) for Ta vs Nb and (0, 870) for Sn vs Nb plots have been included.

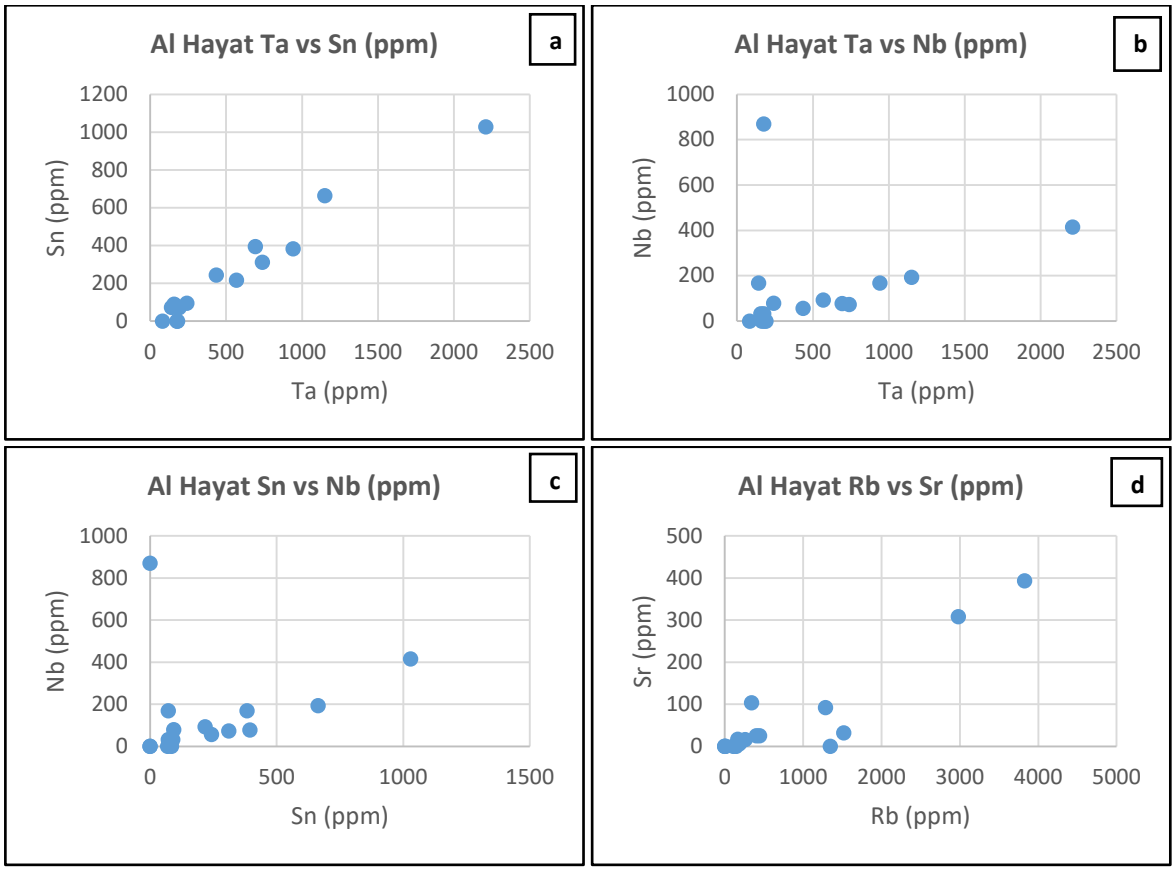

Figure 4.20: *Trace element bivariate x-y diagram for the Al Hayat pit pegmatite body.* See Appendix 2 for details

In Figure 4.21, the bivariate x-y diagram shows results from the Ledingham pegmatite body where Ta vs Sn, Ta vs Nb and Sn vs Nb shows no relationship whilst there is a positive correlation between Rb vs Sr. The Ta vs Sn plot has an outlier (178, 3077), (238, 307) for Ta vs Nb and (88, 307; 3077, 51) on the Sn vs Nb plots have been included.

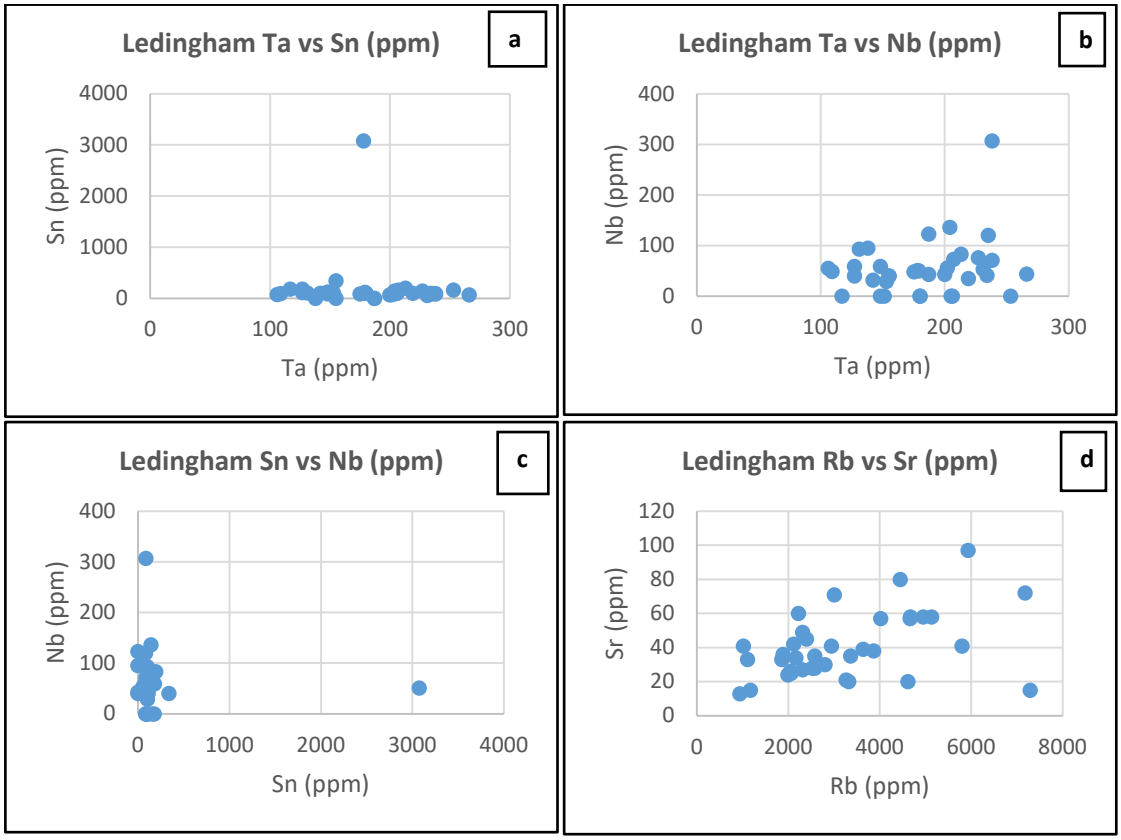

Figure 4.21: *Trace element bivariate x-y diagram for the Ledingham sector pegmatite body.* See Appendix 2 for details

The bivariate x-y diagram presented in Figure 4.22 represents results from the Victor's pit where Ta vs Sn, Ta vs Nb, Sn vs Nb and Rb vs Sr are all positively correlated. Some of the outliers were that were included were (2119, 125) for Ta vs Sn and (2119, 119) Ta vs Nb.

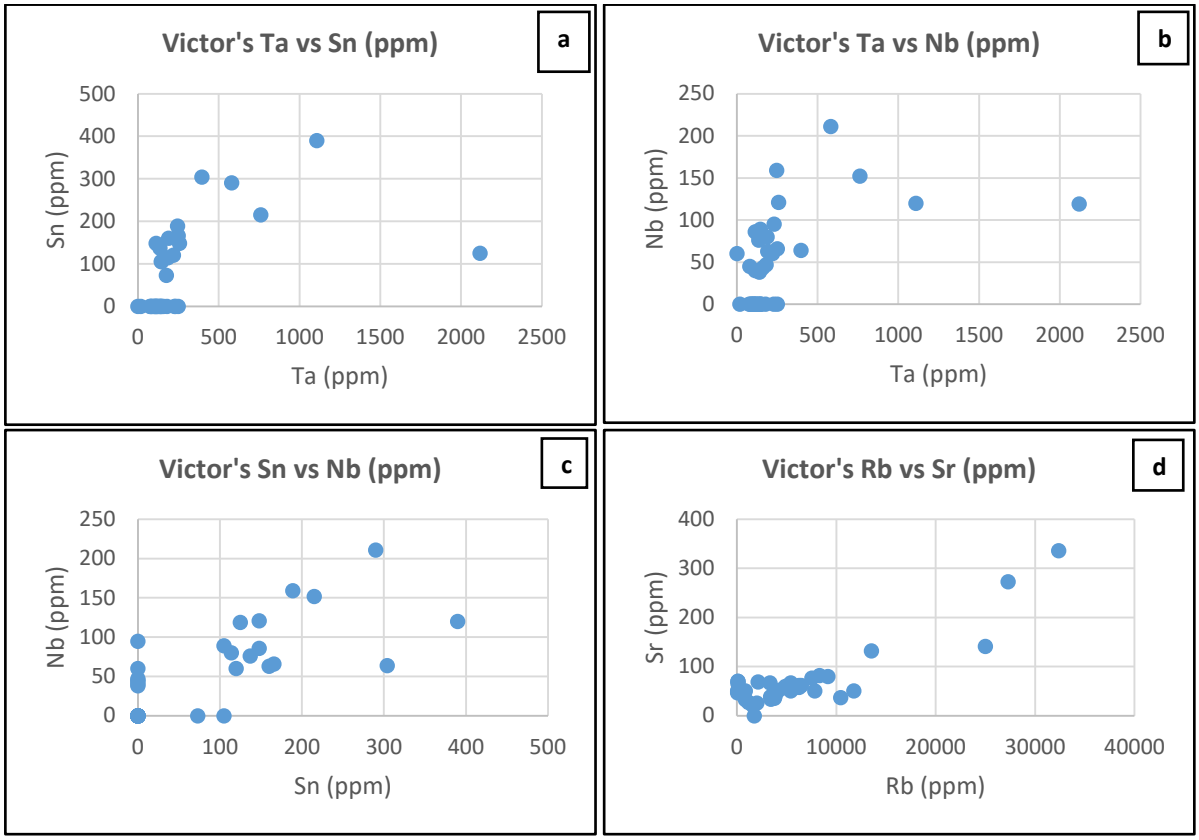

Figure 4.22: *Trace element bivariate x-y diagram for the Victor's pit pegmatite body.* See Appendix 2 for details

In Figure 4.23, the bivariate x-y diagram of data from the Nigel's pit shows there is a strong association of the elements Ta vs Sn, Ta vs Nb, Sn vs Nb and Rb vs Sr as they are all positively correlated.

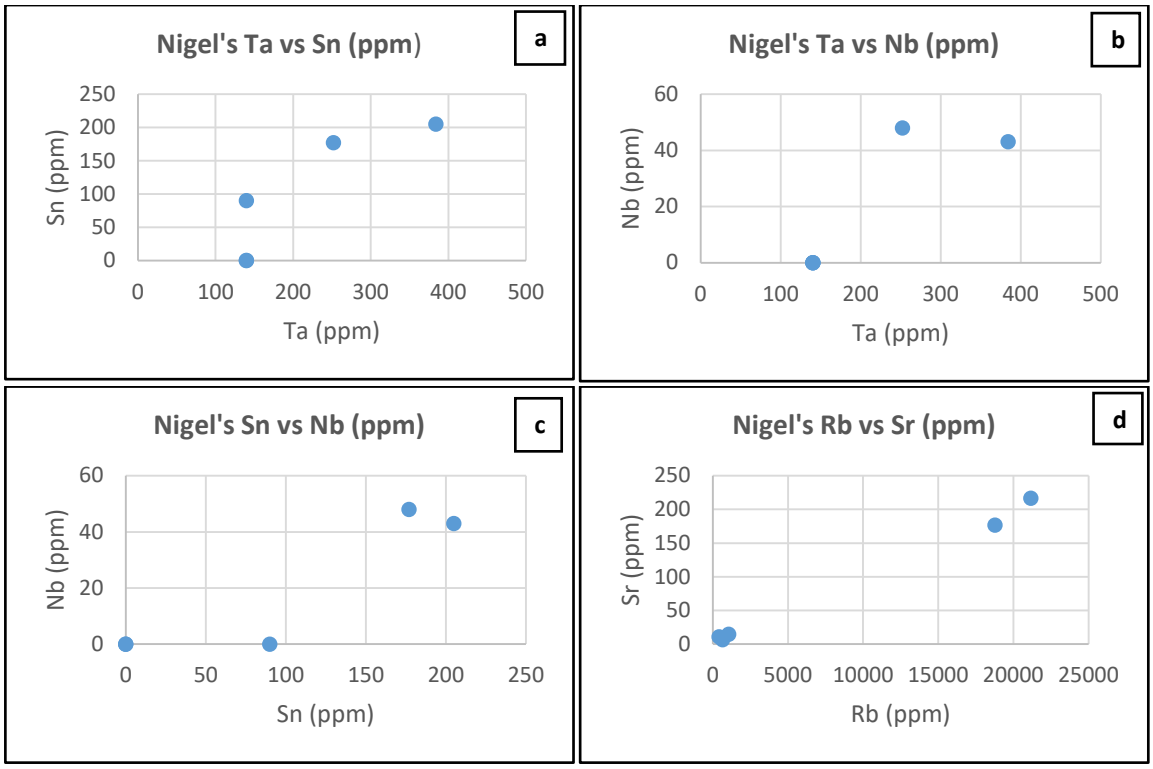

***Figure 4.23**: Trace element bivariate x-y diagram for the Nigel's pit pegmatite body.* See Appendix 2 for details

In the Shaft pegmatite body, the bivariate x-y diagram (Figure 4.24) show positive correlations between Ta vs Sn, Ta vs Nb and Rb vs Sr whilst there is no relationship between Sn vs Nb. There were outliers (243, 1390; 3047, 342) for Ta vs Sn, (109, 463; 3047, 841) for Ta vs Nb and (342, 841; 0, 463; 1390, 110) for Sn vs Nb that were included on the plots.

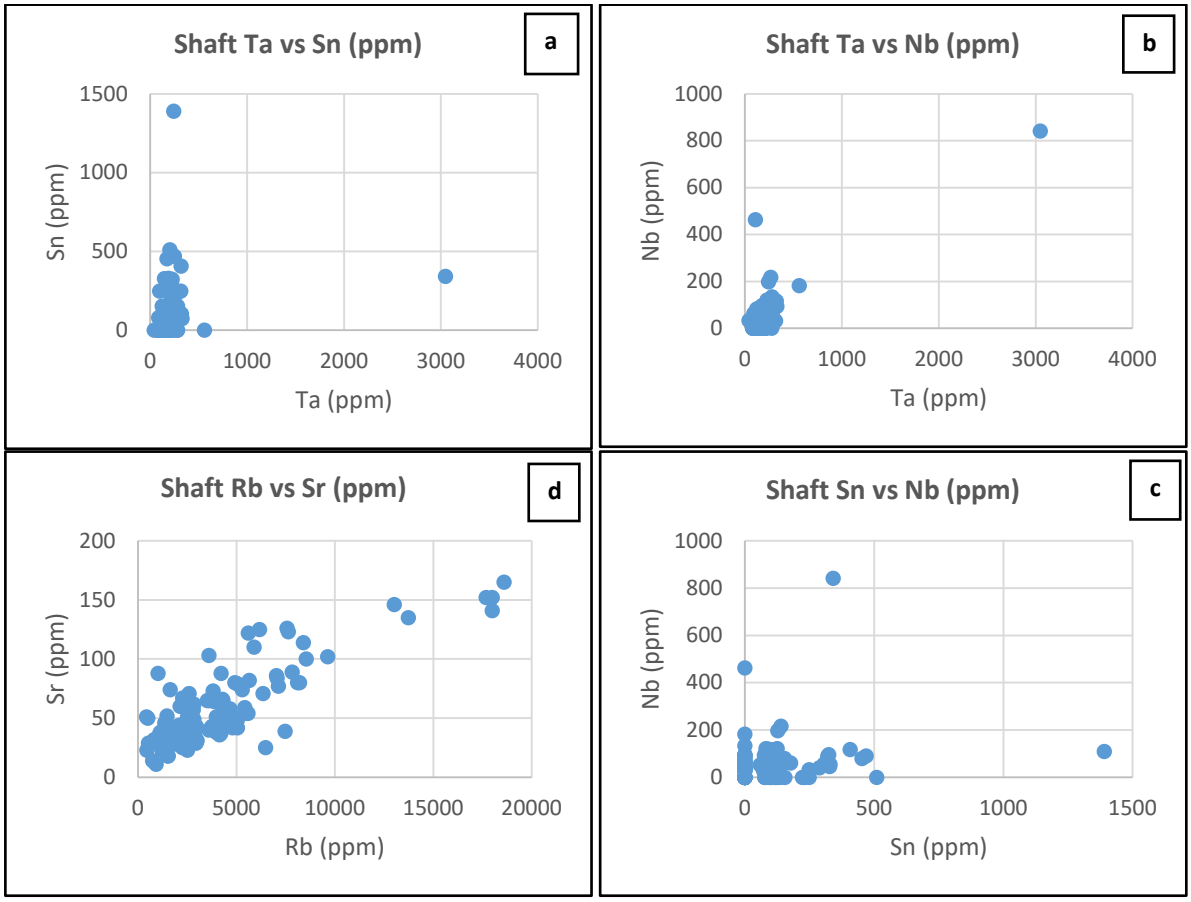

***Figure 4.24**: Trace element bivariate x-y diagram for the Shaft sector pegmatite body.* See Appendix 2 for details

Trace element data for the West pegmatite body shows a strong association between Ta vs Sn, Ta vs Nb, Sn vs Nb and Rb vs Sr (Figure 4.25). Outliers were (1575, 28291) for Ta vs Sn, (1575, 856) for Ta vs Nb, (28291, 856) and (8834, 36) for Rb vs Sr.

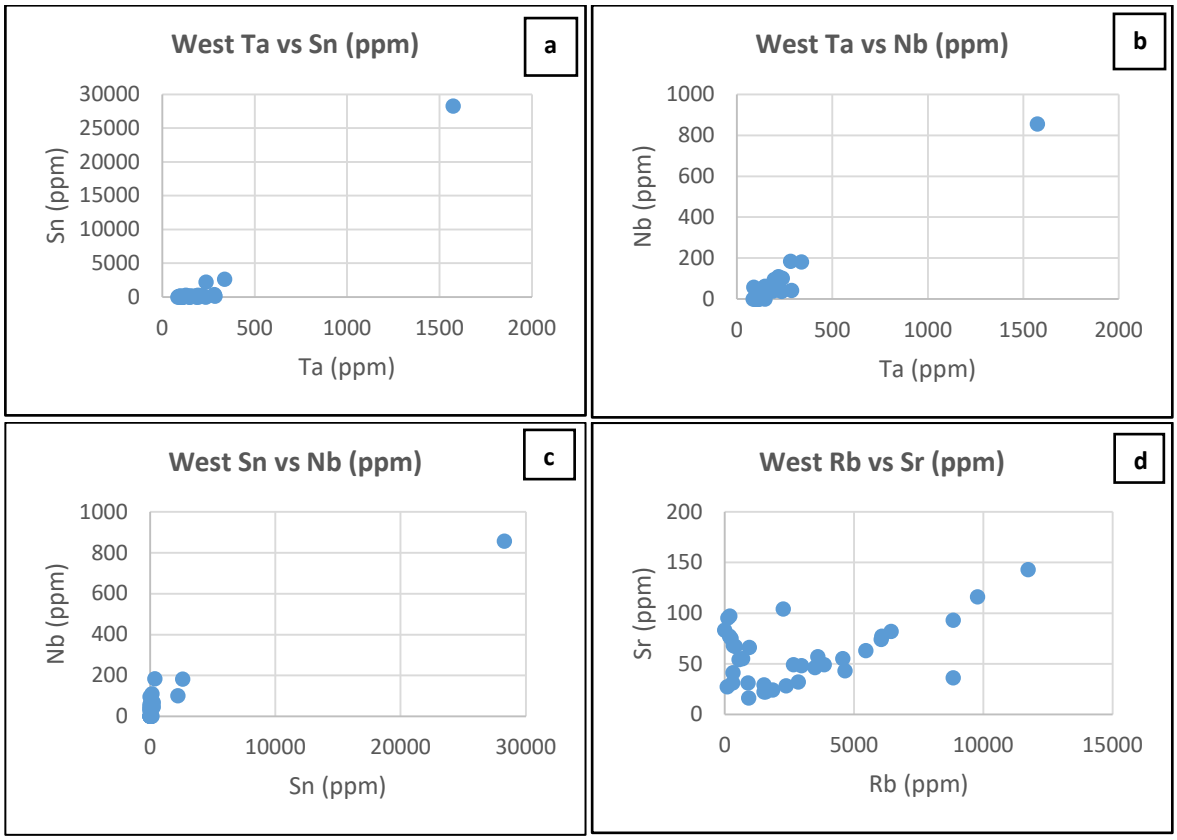

Figure 4.25: *Trace element bivariate x-y diagram for the West sector pegmatite body.* See Appendix 2 for details

The bivariate x-y diagram, shown in Figure 4.26 present data from the Mauve Kop pegmatite body. There is a strong association between Ta vs Nb and Rb vs Sr whilst there is no relationship between Ta vs Sn and Sn vs Nb. Outliers within the plots included (186, 1117) for Ta vs Sn, (117, 84) for Sn vs Nb and (2063, 110) for Rb vs Sr.

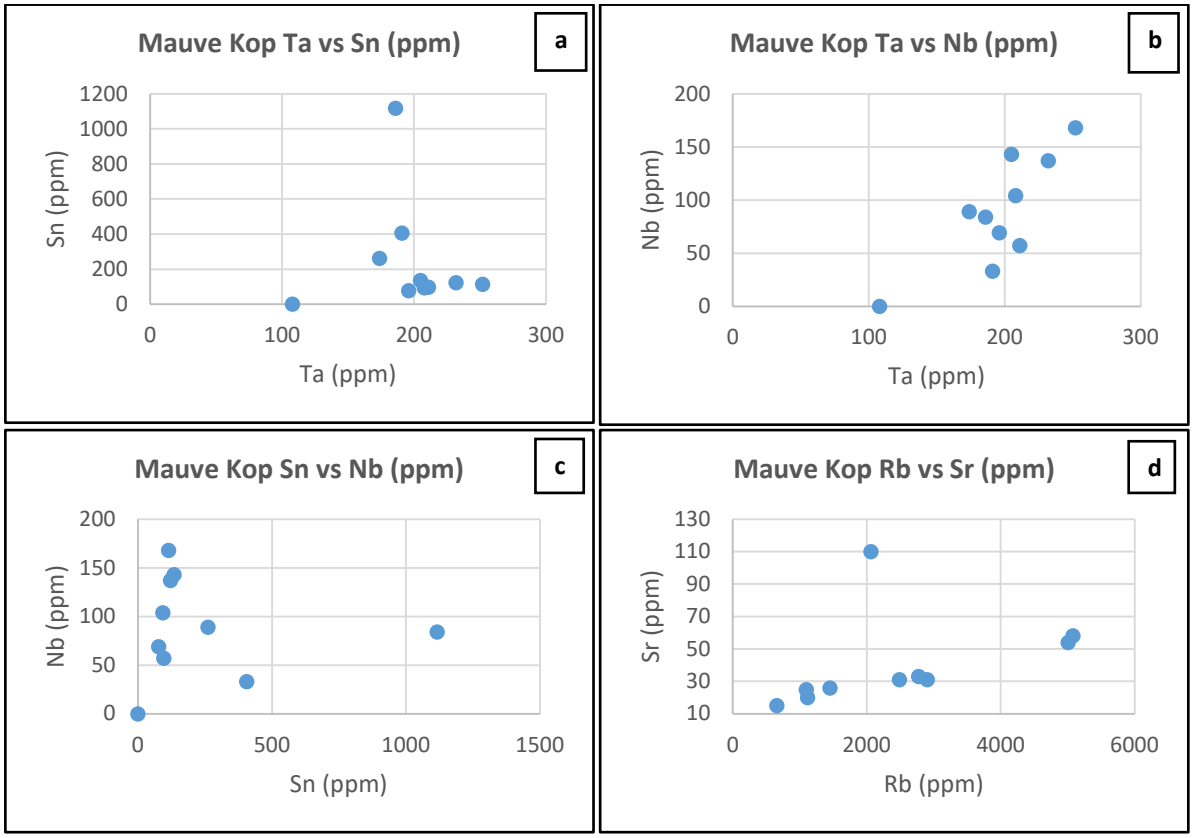

Figure 4.26: *Trace element bivariate x-y diagram for the Mauve Kop sector pegmatite body.* See Appendix 2 for details

For the Dam Site pit, there a strong association between Ta vs Sn, Ta vs Nb, Sn vs Nb and Rb vs Sr (Figure 4.27). There are outliers on the Rb vs Sr plot for series (162, 331; 121, 236 and 121, 222).

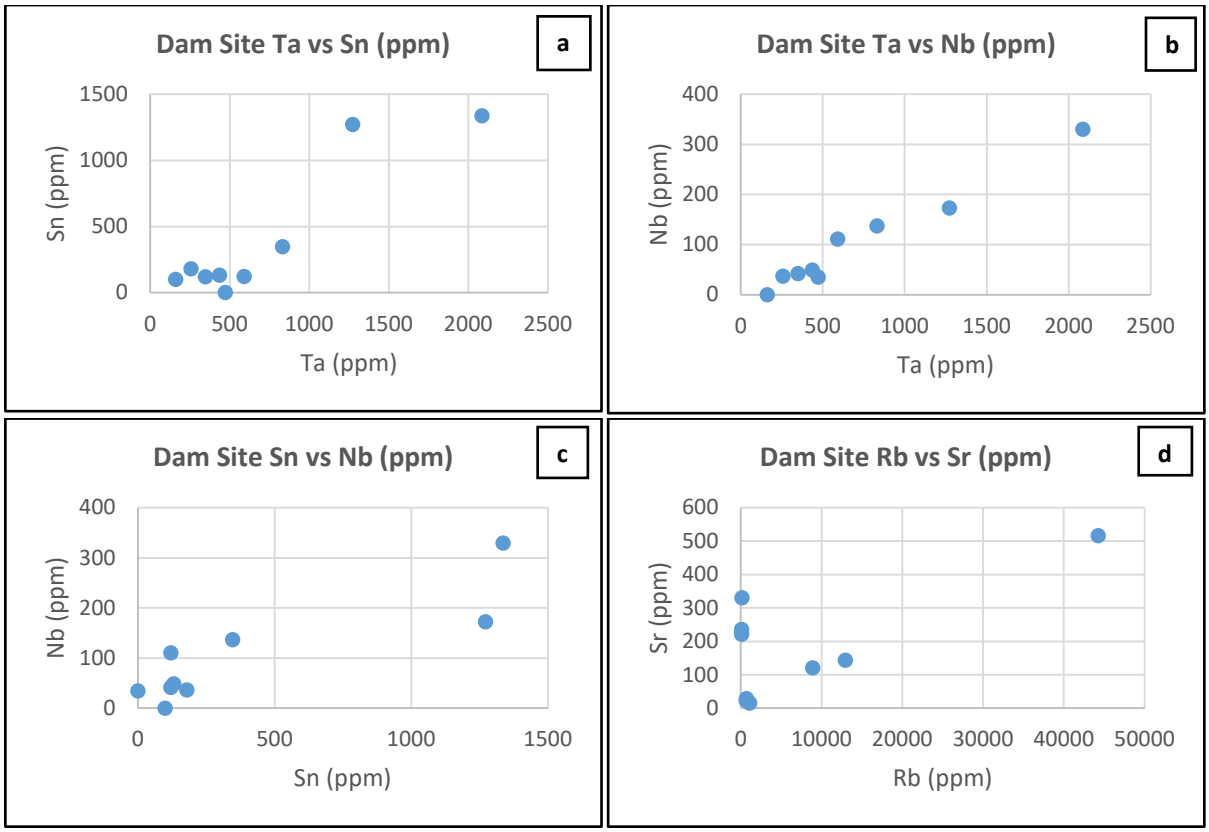

Figure 4.27: *Trace element bivariate x-y diagram for the Dam Site pit pegmatite body.* See Appendix 2 for details

When the Bikita quarry locality data are plotted and annotated (Figure 4.28) with real petrogenetic pathways and concepts a very interesting story emerges. A plot of Sr versus Rb for analysed samples from the Bikita quarry locality is presented and the behaviour of Sr and Rb during feldspar dominated fractionation of a typical parental granite magma is shown. The pair of arrows represent the liquid line of descent ("melt") and the composition of the solid crystallate ("crystals"), based on typical crystal – liquid distribution coefficients (e.g. Reid and Barton, 1983). "Ms" and "Lep" plot at typical mineral compositions that would crystallise out of a highly fractionated granite melt with 1000 ppm Rb and 20 ppm Sr.

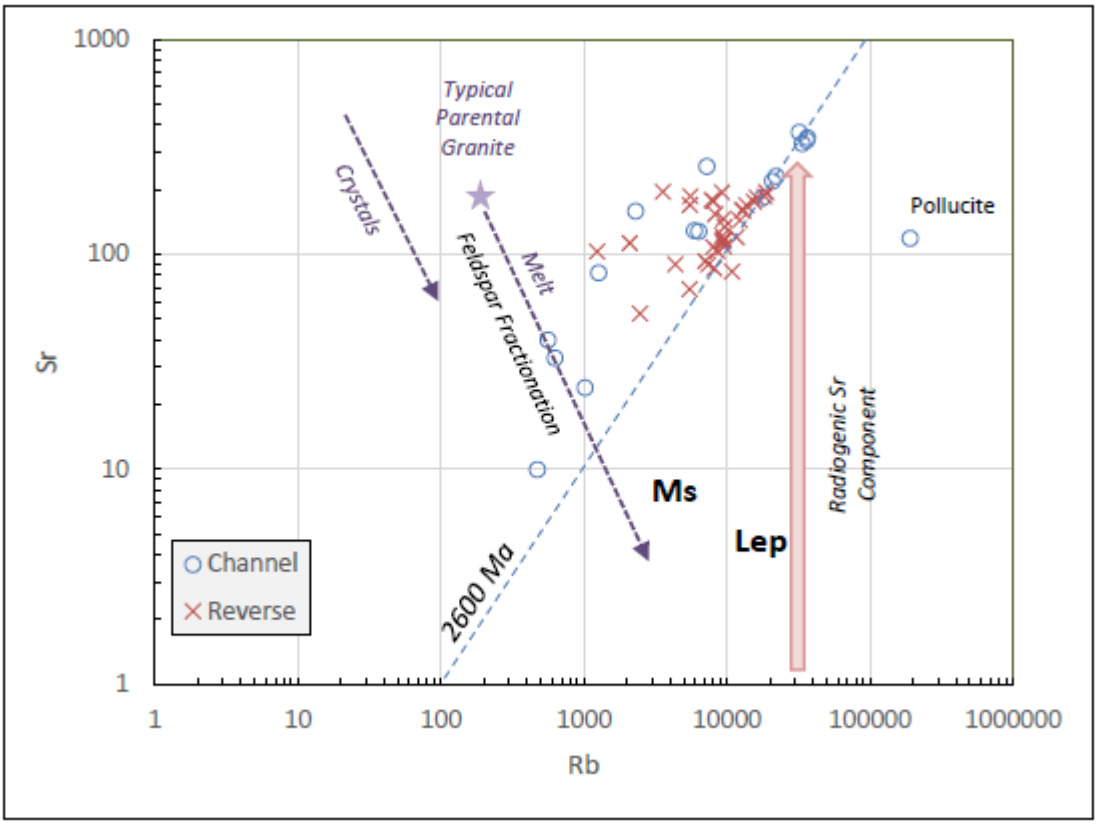

Figure 4.28: *Plot of Sr versus Rb for analysed samples from the Bikita quarry locality*

The geochemical analysis of the database has helped in understanding the behavioural characteristics of the Bikita pegmatite mineralisation.

CHAPTER 5:

GEOPHYSICAL STUDY AND REMOTE SENSING

5.1 Introduction

Geophysical survey test work involving ground magnetics and radiometrics was carried on the project area to estimate applicability of geophysical methods for surface mapping of tectonic faults, zones of excessive fracturing and mapping of new pegmatite bodies. On a more local scale ground magnetics was chosen to assist in mapping the geology and the local structural lineaments whereas ground radiometrics was used to map pegmatite/granite outcrops. Ground magnetics was also used to try and isolate the main structures of interest into which hydrothermal magnetite and/or pyrrhotite have been introduced, causing them to have a magnetic signature. Certain other structures had to be inferred, or interpreted, by the offsets which they create in other magnetic units or structures. Sometimes these more subtle structures are the more important ones. Likewise, any later brittle fractures which cross-cut and offset the shears or splays, are highlighted.

5.2 Ground magnetics survey results

The range of magnetic values obtained in the ground survey is around 5,400 nanotesla which is very large. The magnetic field data are highly variable and very busy in certain areas, which is in-keeping with areas with scree on surface where magnetic rock types such as magnetite quartzites, lavas, greenstone areas and BIF are present. Processing of the ground magnetics image so that it can more easily be interpreted often involves de-striping and smoothing of the data to a degree, and the calculation of vertical and horizontal derivatives which highlight the areas of greatest change in the field, as well as the analytical signal. In the case of the Bikita ground data, the data were so well levelled as to not require de-corrugation to remove mild line-striping. Processing of these data was undertaken in order to highlight structure. Vertical derivative is commonly applied to total magnetic field data to enhance shallow geological features. It suppresses the deeper features and helps to identify closely spaced sources by giving a better resolution. Colour and grey scale shaded images of the vertical derivative help to identify and interpret linear features like faults and joints/fractures. They are useful in outlining the boundaries of linear structural features, which are not clearly visible in the total magnetic grid. Form lines have also been added, which are interpreted from the magnetic texture within each unit. These give an idea of whether the unit is completely folded in its interior, and general strike of the foliation.

The geophysical data shows NE-trending structures with a strong WNW-trending anomaly in the north and another, similar one in the south and the total field ground magnetics result for the survey (Figure 5.1). Faults are recognised by relative shifts and interruptions along the continuity of linear geologic features. Based on these characteristics linear features like faults and dykes are interpreted from the colour shaded relief image of vertical derivative. NE-trending shears and dolerite dykes are shown on the Figure 5.2. The horizontal gradient in a NW direction, with structural interpretation and brittle fractures oriented EW and ENE are shown in Figure 5.3.

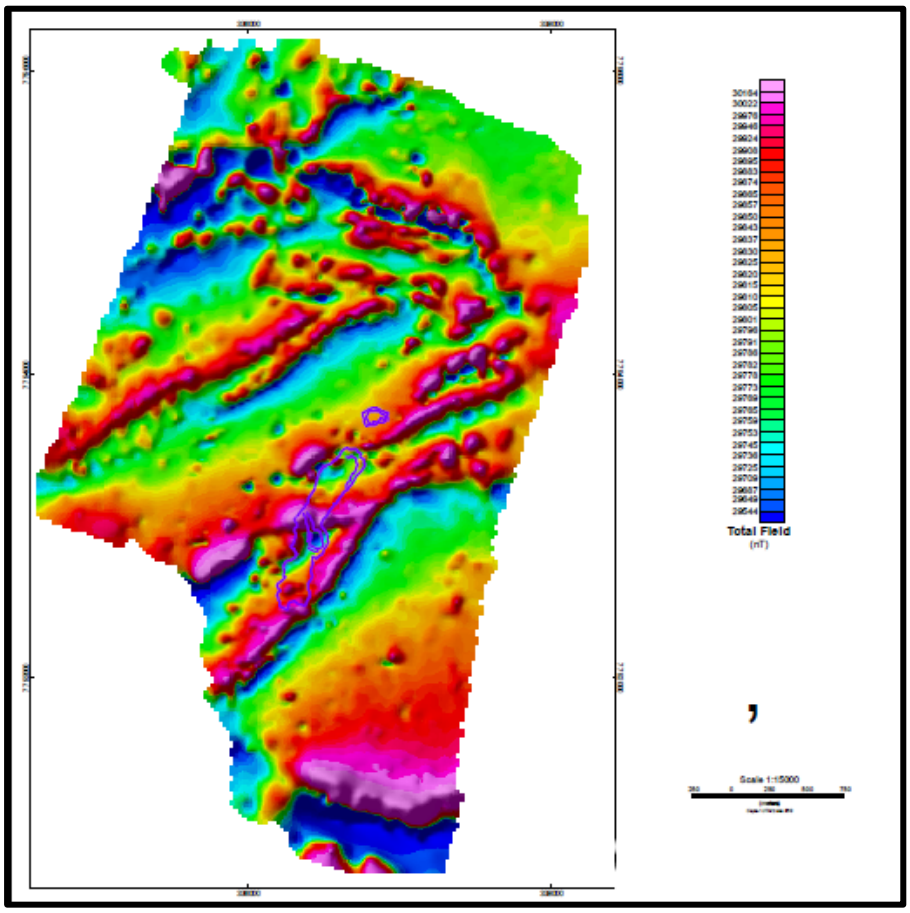

***Figure 5.1**: Total field magnetics showing clear, mainly NE-trending, structures with a strong WNW-trending anomaly in the north and another, similar one in the south.*

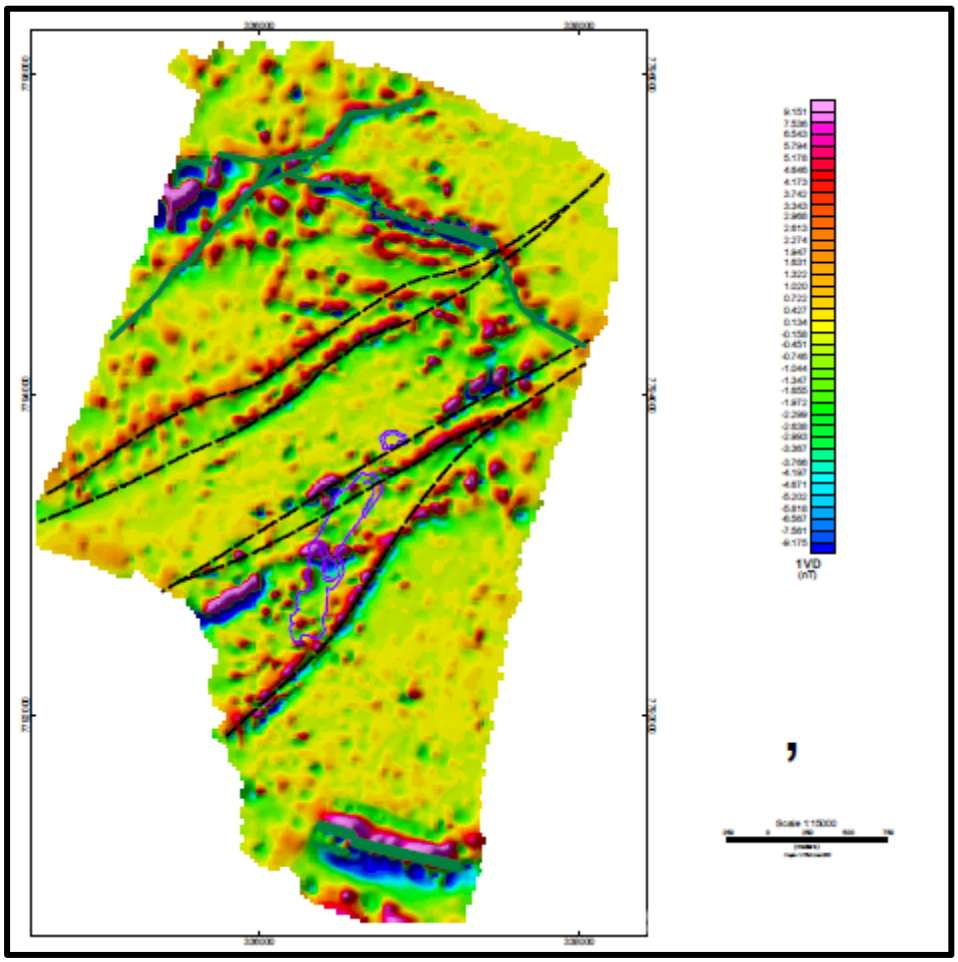

Figure 5.2: *First vertical derivative of the Bikita ground magnetics data with interpreted NE shears and dolerite dykes overlaid in dark green*

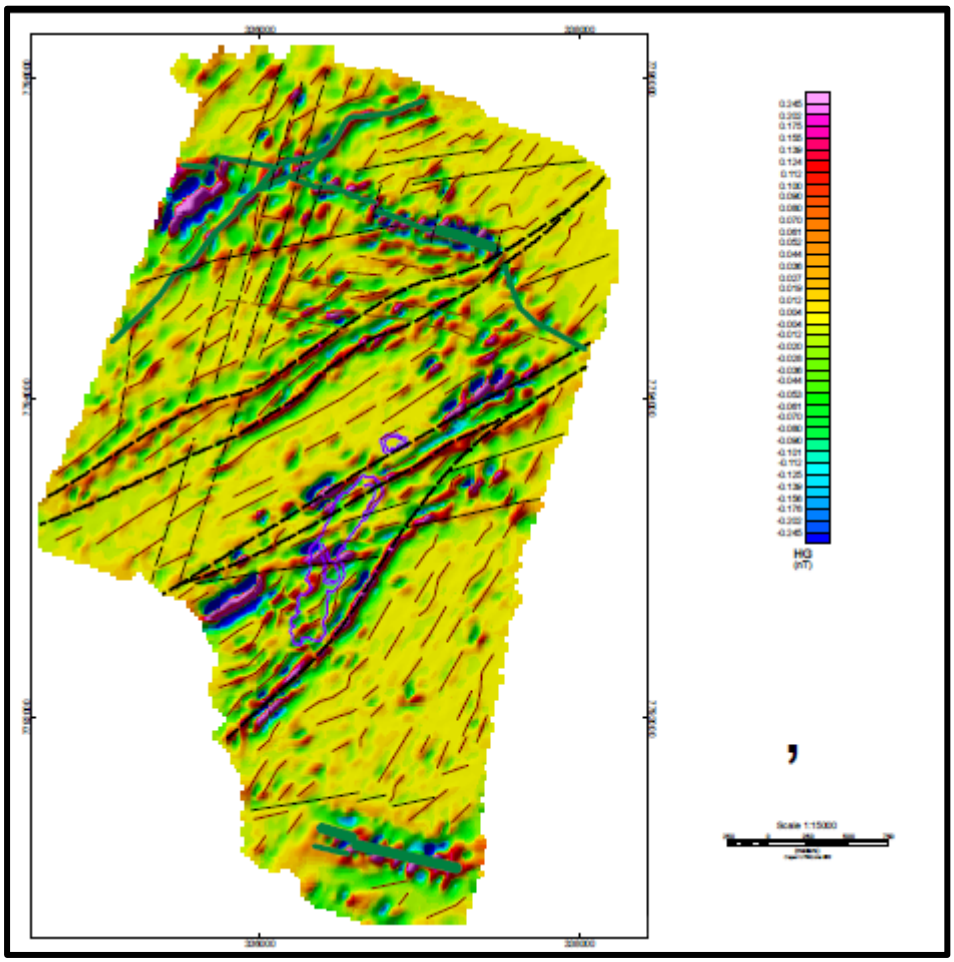

***Figure 5.3**: NW horizontal gradient of the Bikita ground magnetics data, perpendicular to strike. Interpreted NE shears, dolerite dykes, EW and ENE brittle fractures, and form lines overlaid.*

5.3 Radiometric survey results

In terms of radiometrics data, all rock types have a variable K, Th and U content, and in many cases the ratios between these elements are helpful in typifying a lithological signature and interpreting the geology. In particular, a K-Th-U ternary RGB image is often used to discriminate geological units. In order for the radiometrics to be really useful, a thin soil cover veneer is required since gamma rays start to become attenuated by approximately 20 cm of soil and deep weathering profiles are also detrimental. The high potassium values was an indication of having detected new pegmatite bodies that are probably under soil cover. Figure 5.4 shows the K-response for the survey area, with interpreted pegmatites overlaid.

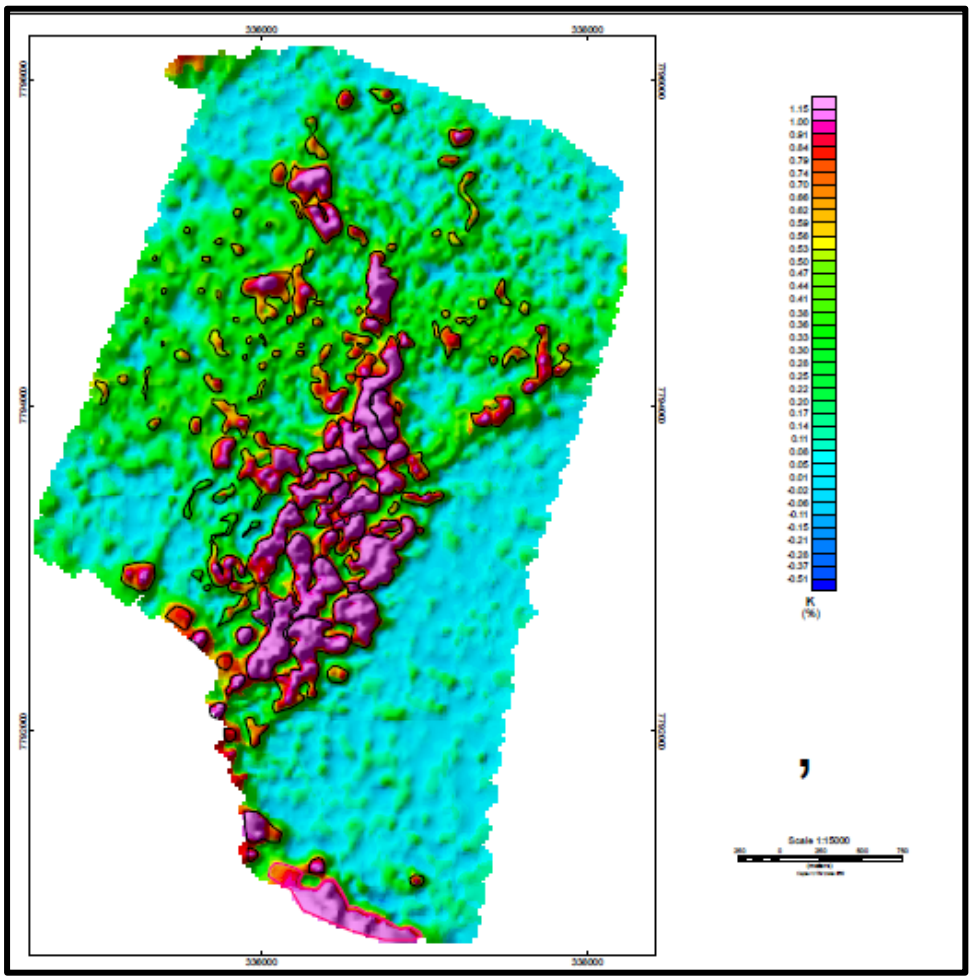

Figure 5.4: *Potassium (K) percentage with interpreted pegmatites (in purple) overlaid*

5.4 Combination of radiometrics and magnetics data

In terms of mapping the general geology of the rest of the area, it was important to integrate the radiometrics and the magnetics data together as this is useful to distinguish between lithologies and map surface geology. A K-Th-U ternary radiomerics image (Figure 5.5) shows some geological units and the analytical signal of the ground magnetics (Figure 5.6) shows some distinctly magnetically busy and quiet areas.

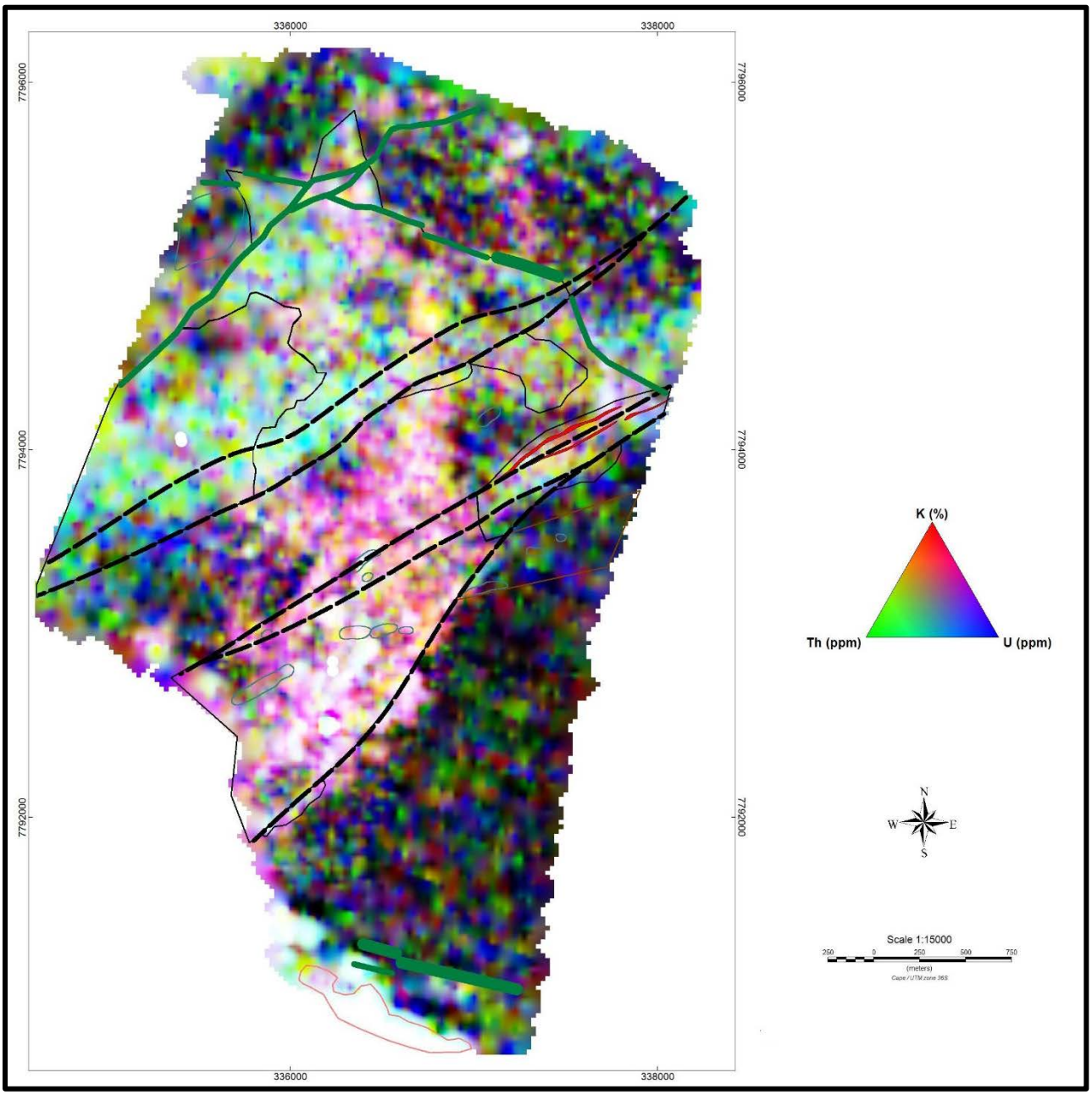

Figure 5.5*: Ternary radiometrics image showing the different lithologies within the project area.* In this RGB, Red represents K, Green represents Th and Blue represents U

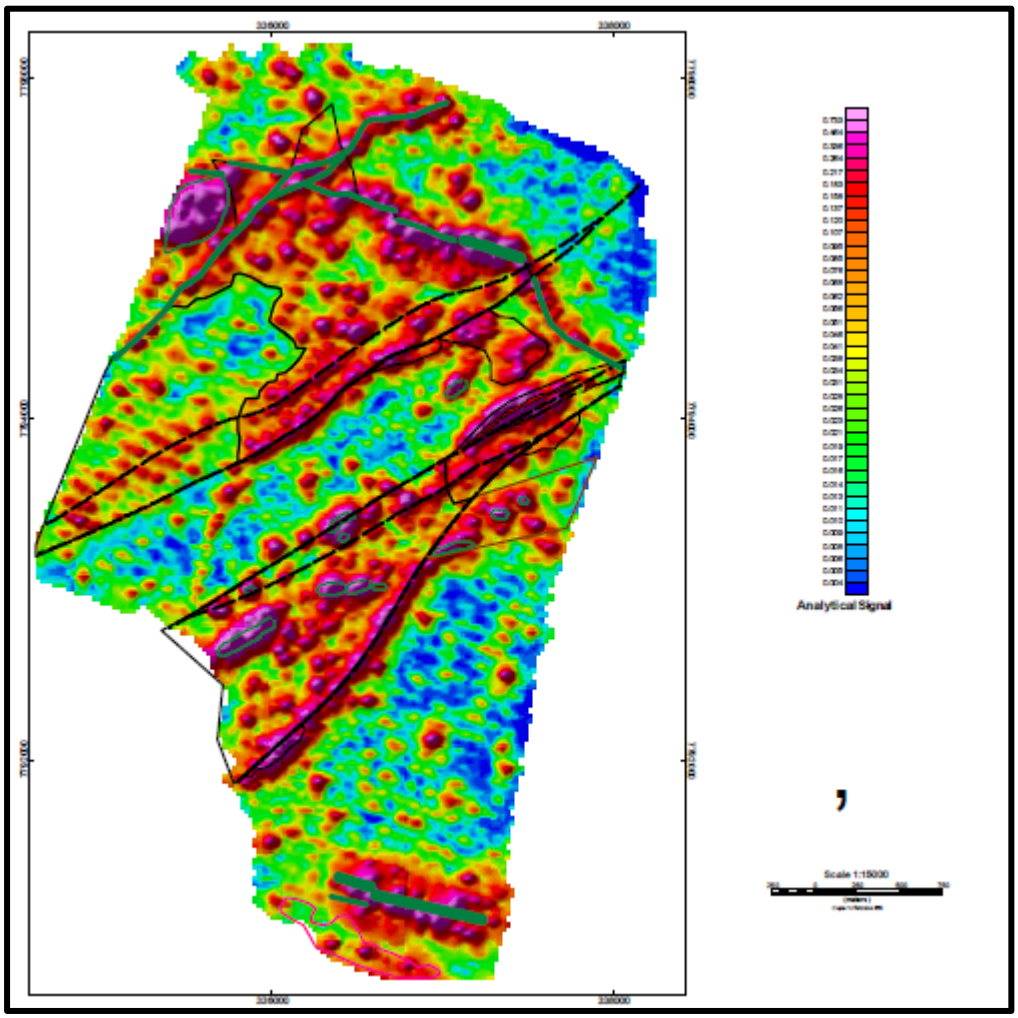

***Figure 5.6**: Analytical signal of the ground magnetics of the project area.*

5.5 Landsat 7 ETM+ Image processing

Image processing is required for the manipulation of remotely sensed data to improve their appearance and in order to create new modified images that contain more information to help ease the visual interpretations of features of interest. Landsat 7 ETM+ satellite data of multispectral bands (1, 2, 3, 4, 5, & 7) were utilised in the course of digital image processing techniques. In order to achieve better image interpretation, image processing was done using QGis. This was done using band combinations to extract and enhance spectral information from the structures within the study area. The patterns recognised in the digitally processed satellite images assist in delineating the regional structural features. Based on the above mentioned digital image processing and enhancement techniques the images became more interpretable as shown in images below.

Lineament analysis and identification requires the best images that can then be enhanced using a combination of band-ratio techniques such as linear and Gaussian nonlinear stretching and principal component analysis (PCA). In order to enhance the lineaments contained in the images, a series of directional edge enhancement filters were applied. Visual assessment of the images was done to determine the best combination for mapping

linear features. The geological lineaments of interest are usually identified as lines or linear structures that tend to be significantly brighter or darker than the background pixels.

5.5.1 Landsat True colour composite (RGB) 321

The band combination 321 was displayed for true colour visual analysis of features within the study area. The idea behind the selection of a true colour composite (Figure 5.7), is for the visible bands to be carefully chosen and allocated to their corresponding colours in order to attain an image that approximates true colour. The visible bands estimate the range of vision for the human eye, and therefore they seem to be close to a normal photograph (Kaasheka, 2018). True colour tends to appear flat and have low contrast due to the electromagnetic (EM) radiation in the blue visible region being more susceptible to atmospheric scattering (Robert, 1997). These main features are different rock types, water sources and vegetation cover.

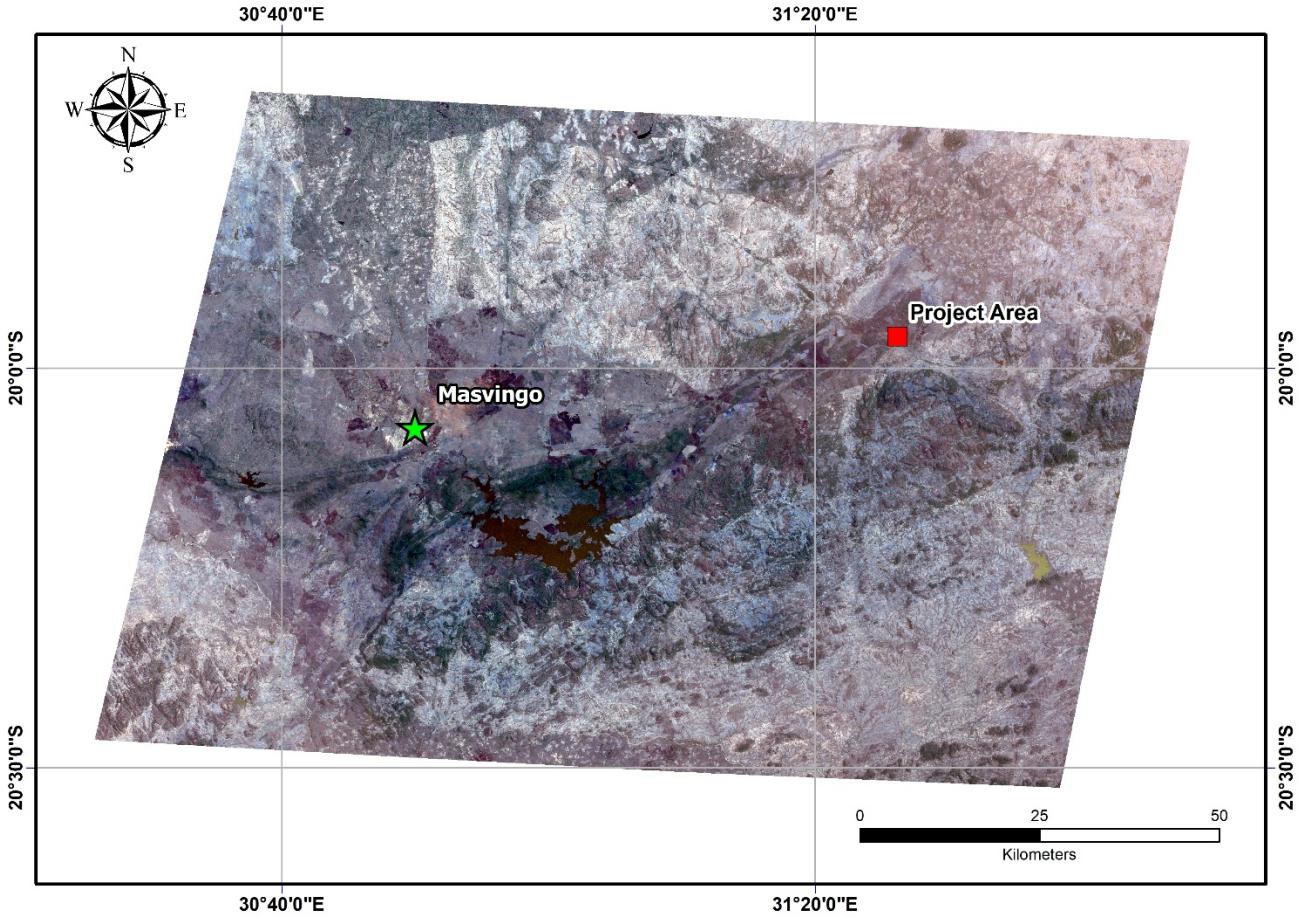

Figure 5.7: *A Landsat map covering the Masvingo Greenstone Belt produced from true colour composite image of bands 321 showing the main features within the study area.*

5.5.2 Landsat False colour composite (RGB) 432

The use of band combination 432 enables the visual discrimination and easy recognition of structural features and this false colour composite shows different rock types of the study area (Figure 5.8). The white background shows the late granites, the dull red-brown background shows the older granites and gneisses whilst the deep red are the greenstones. Figure 5.9 below shows the correlation between the geology and a section of the overlay on the MGB as the light blue part shows the greenstones whilst the green part shows the granite.

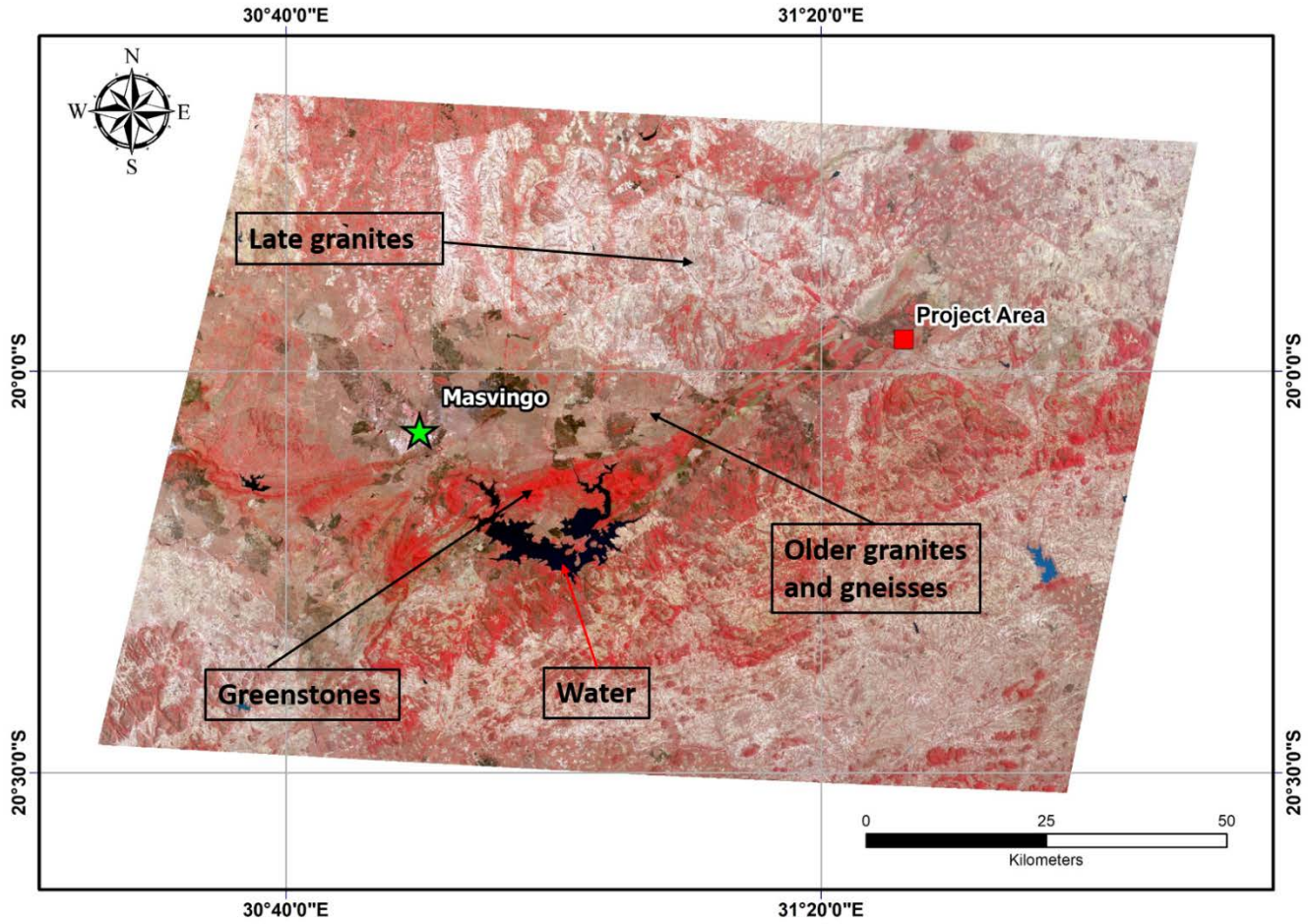

Figure 5.8: *A Landsat map covering the Masvingo Greenstone Belt produced from false-colour composite image of bands 432 showing the main geological formations and signatures.*

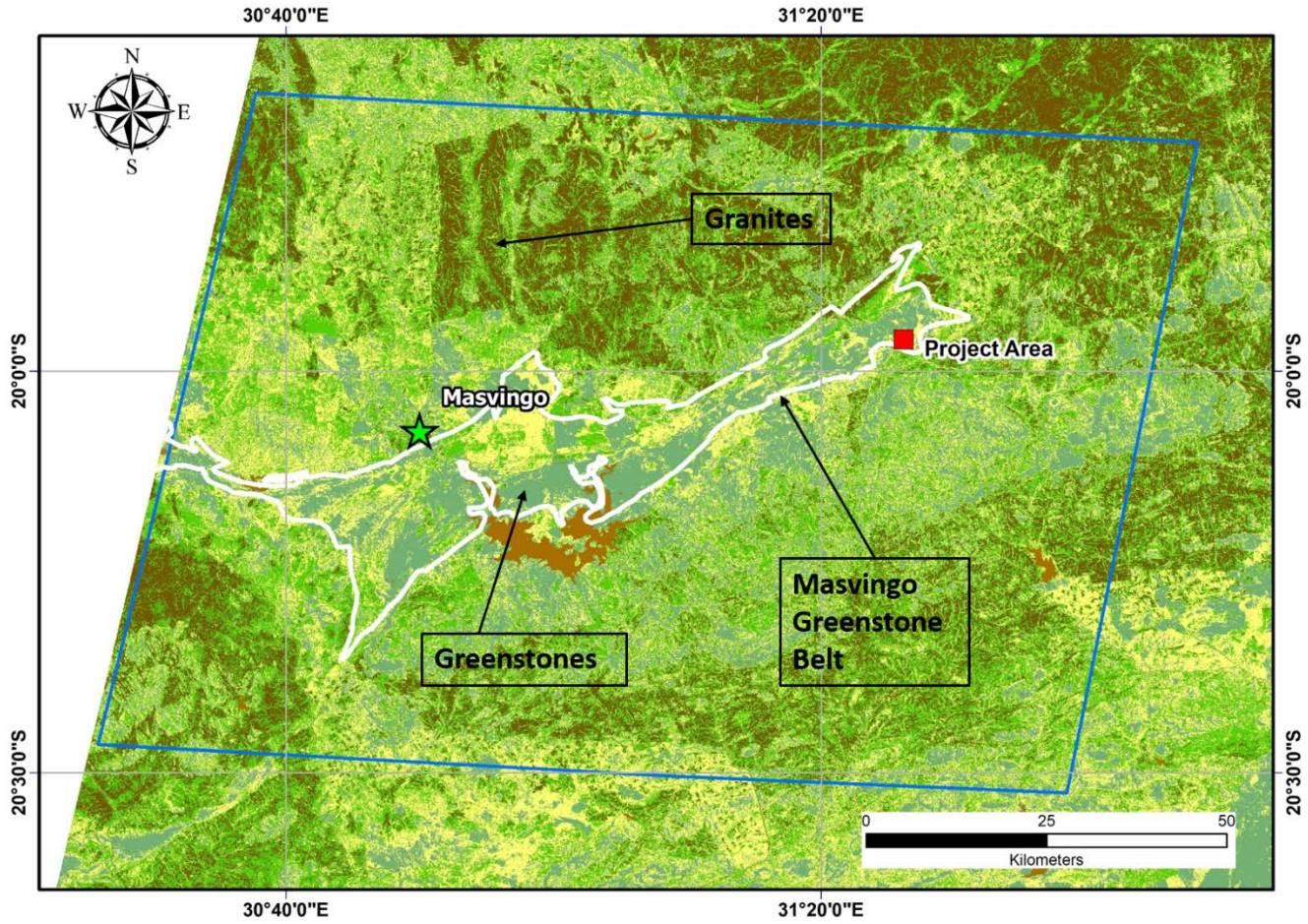

Figure 5.9: *A Landsat map covering the Masvingo Greenstone Belt showing correlations between the geology produced from unsupervised classification. The white outline shows the trend of the MGB.*

5.5.3 Principle Component Analysis (PCA) and lineament determination

The Principal Component Analysis technique is mainly used as a data compression tool in remote sensing. In this study, the edge enhancement filters and principal component analysis were used to enhance the lineaments. In order to interpret large datasets the PCA method is useful in the sense that it drastically reduces the dataset dimensionality in order to ease the interpretation whilst at the same time preserving the dataset information. This technique was exercised as it allows the extraction of new information from an image and in this case it aided the identification of the structural lineaments in great detail considering its usefulness in transforming remote sensing data to reveal the most important features of the image.

Lineament extraction (Figure 5.10) was done manually through photo interpretation by analysing the channels of the satellite data involving edge detection and line extraction. The lineaments were defined as line features or patterns interpreted on a remote sensing image. The lineaments of interest were those displaying or reflecting geological structures and in this case, it was considered to discriminate lineament extraction from other line features that are not due to geological structures. Some of the criteria that were used in lineament determination involved looking at abrupt topographic discontinuities of landforms, sudden shifts of drainage courses, offsets of layers, depressions and discontinuities in lithologies.

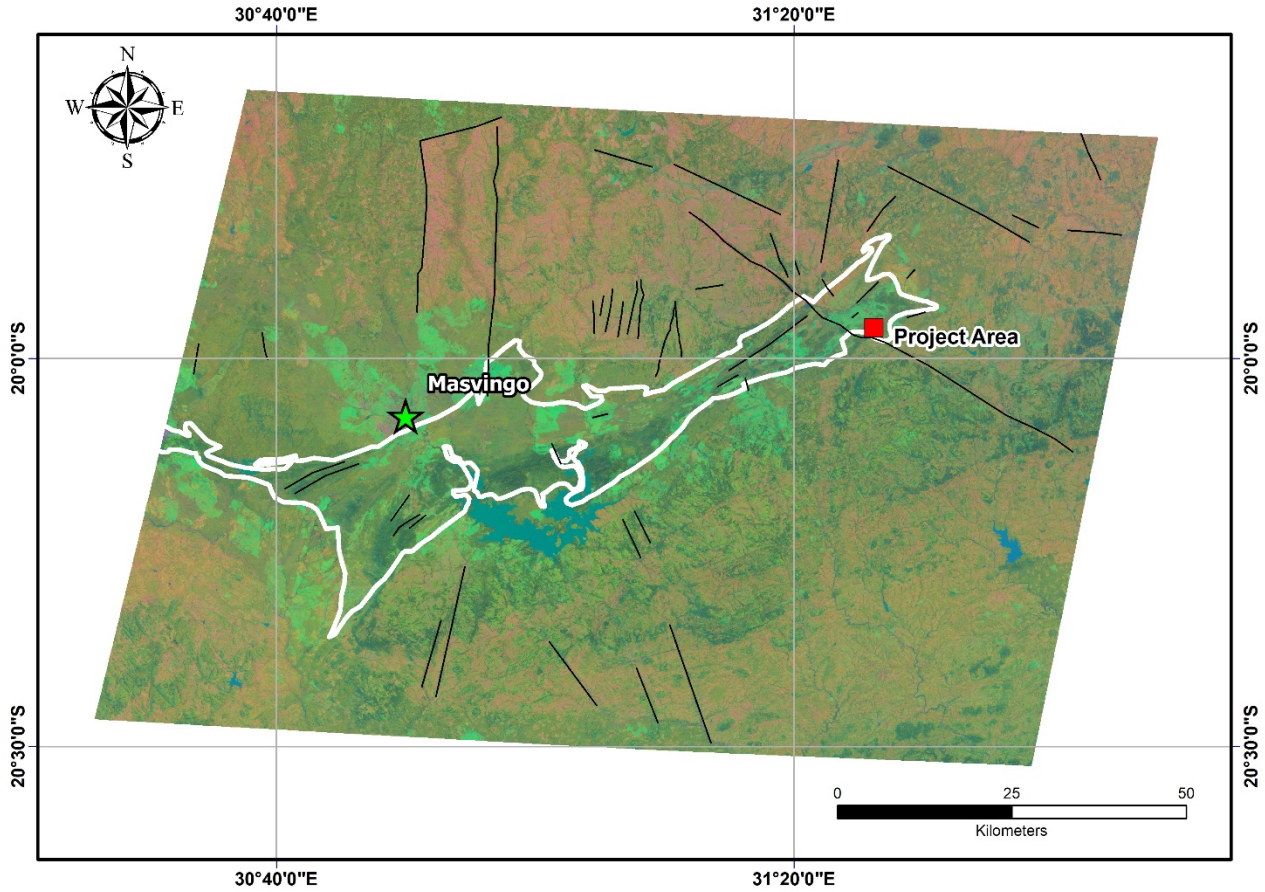

Figure 5.10: *A Landsat map covering the Masvingo Greenstone Belt in white outline produced from principle component transformation showing the delineation of structural lineaments shown in black lines*

The major limitation in manual interpretation is that the visual acuity does not allow full identification of all spectral differences in an image. It is very difficult to determine and visualise the satellite image lineaments hence, it requires good expertise in image interpretation. The remote sensing image lineaments within the study area were defined as line features and patterns. The study identified and mapped forty seven lineaments with their prevalent orientations drawn on the image (Figure 5.10) and it shows that the orientation of lineaments was dominated by NW-SE, NE- SW and N-S features.

CHAPTER 6:

DATA INTERPRETATION AND DISCUSSION

6.1 Introduction

The geochemical and geophysical characteristics, mineralisation spatial distribution across the pegmatite bodies, structural controls and the possible mechanisms on the genesis and emplacement of the Bikita pegmatites are discussed in this chapter.

6.2 Geochemical data

Based on the AAS dataset, the mineralisation is spatially distributed within the pegmatite along its strike length. Lithium is found in most of the pegmatites in the form of lepidolite, petalite, SQI, and a lesser abundance of amblygonite and eucryptite. Lithium is the most important element of interest for the mining operations. Looking at the results from Bikita quarry locality, the position of various Li mineral phases is consisant with their formulars e.g. lepidolite has both K and Li in its mineral structure, whereas eucryptite and amblygonite lack K. The typical mineral compositions have helped to ascertain mineral deportment and there are two main definable trends, a "high K trend" governed by micas (Lepidolite), and a "low K trend" thereby illustrating the control by petalite (already highlighted as the other major Li-bearing phase at Bikita). All the other Li-Al minerals (spodumene, amblygonite, eucryptite) associate with this low K trend. Displaying some of the major rock forming minerals (quartz, feldspars, and muscovite) and bulk compositions has helped the interpretations, such as the influence of albite (late stage albitisation), microcline (K-Feldspar) and muscovite (greisenisation).

The Li_2O average abundance across all the pegmatites studied is 2.08 wt % and its distribution is highly variable from pit to pit. In the McMurdon, and the Mauve Kop pegmatite body, Li_2O occurrence is restricted to lepidolite with values ranging from 0.10 to 2.63 wt %, with the highest grade in McMurdon pit. In the Victor's pit, lithium is found in a wide range of ore minerals that include petalite, lepidolite, SQI and eucryptite with the highest grade being 5.69 wt %. In the Ledingham pegmatite body, the Li_2O (0.10 to 4.51 wt %) occurs in SQI and petalite, whereas in the Cemetery and the West pegmatite bodies the Li_2O occurs in both petalite and lepidolite with values ranging from 0.08 to 3.49 wt % with the highest grade in the Cemetery body. In the Shaft, Nigel's pit, Al Hayat pit and Giant East pegmatite bodies the Li-bearing mineralogy is more varied and Li_2O occurs in SQI, eucryptite, petalite and lepidolite with values ranging from 0.02 to 5.69 wt % with the highest grade in the Al Hayat pit. The highest overall grades of lithium occur in the Bikita quarry (0.49 to 7.28 wt %) and the Dam Site pegmatite pit (8.63 wt %) where Li_2O occurs in petalite, amblygonite and lepidolite. This is because although it is less abundant, amblygonite has the highest lithium concentration. In Bikita quarry these minerals are also accompanied by SQI. Table 6.1 shows where the major element abundances obtained from each pegmatite body are highest.

Table 6.1: *Highest major element abundances for each pegmatite body*

Pegmatite Section	%Li_2O	%K_2O	%Na_2O	%Al_2O_3	%Fe_2O_3	%Cs_2O	%Rb_2O
McMurdon	3.63	7.68	3.67	16.02	0.192	0.88	6.23
Bikita	7.28	11.88	8.50	17.71	0.387	20.97	5.70
Al Hayat	5.69	13.18	7.98	17.27	2.18	0.99	6.28
Ledingham	5.47	7.69	8.10	17.90	2.14	9	3
Victor's	5.69	8.75	8.69	17.88	0.68	26.78	5.55
Nigel's	5.44	9.17	7.77	17.63	0.138	20.24	4.64
Shaft	4.12	8.60	8.19	16.79	0.219	0.98	5.25
West	3.01	6.69	7.24	16.98	0.872	1.06	2.15
Giant East	4.89	5.91	4.88	16.21	0.484	0.97	1.90
Mauve Kop	0.46	2.34	8.30	15.70	0.206	0.27	0.52
Dam Site	8.63	7.72	2.61	18.60	0.114	23.1	5.13
Cemetery	3.49	6.38	5.77	16.49	0.406	0.71	0.77

Caesium is the second important element apart from lithium for the mining operations. The Cs_2O average abundance across all the pegmatites studied is 2.48 wt %. Cs_2O occurrence is mainly restricted to pollucite within the Bikita quarry where it occurs in patches across the pegmatite body whilst sporadic occurrences are found within the Victor's, Nigel's and Dam Site pits. In the Victor's and Nigel's pits, pollucite was discovered as flying rocks after blasting which led to samples being taken for analysis to confirm its occurrence. In the Bikita quarry, Victor's, Nigel's and Dam Site pits Cs_2O ranges from 0.02 to 26.78 wt %, with the highest grade coming from Victor's pit for sample V-POL-001 as shown in Appendix 3a.

A key difference between the mineralised and barren pegmatite intersections is the relative abundances of feldspars (microcline and albite). Plagioclase generally doesn't accommodate other elements in its structure due to small radius and ionic charge of Na ion. Where the feldspars dominate then the lithium mineralisation is generally poor and vice versa. In the barren intersections, the concentrations of Na_2O in the Victor's pit are as high as 8.69 % whereas K_2O is as high as 13.18 % in the Al Hayat pit. When Na_2O is higher than K_2O it suggests that there was more albitisation within that sector of the pegmatites. Rubidium has a strong association with lepidolite getting concentrations as high as 6.28 wt % from the Al Hayat pit. Aluminium concentration is relatively high up to 18.60 wt % on the Dam Site pit probably as a result of abundant micas whereas iron is relatively low with the highest value at 2.18 wt % on the Al Hayat pit. Aluminium concentration is relatively high up to 18.60 wt % on the Dam Site pit probably as a result of abundant micas, feldspars and low K-Li minerals (petalite) whereas iron is relatively low with the highest value at 2.18 wt % on the Al Hayat pit.

The plotting of the Sr versus Rb samples from the Bikita quarry with the most important feature being that in these Rb-enriched samples of great geological age (~2600 Ma), practically all the Sr is radiogenic and thus was not present at the time of formation! Essentially all samples show mineralogical control by muscovite and mainly lepidolite (correcting for the build up of radiogenic Sr) exerting a strong influence on Rb contents of extremely differentiated melts containing practically no original Sr. Since Lepdolite would carry negligible initial Sr, the Bikita compositions are subject to augmentation by radiogenic 87Sr build up by the radioactive decay of 87Rb since formation at 2600 Ga, recorded by the labelled dashed line (Figure 4.28), which shows how much Sr has been

produced as a function Rb content. Samples with >1% Rb have essentially only radiogenic Sr today, while original contents would plot closer to the "Lep" position. The pollucite rich sample with > 10% Rb and plots below the radiogenic line, suggesting radiogenic Sr loss after formation, or a much younger age of formation.

Ta generally displays a comparable behaviour to Nb although the later seem to have lower concentrations which rarely exceeds 2623 ppm. The correlation between these elements probably reflects the occurrence of microlite. Enrichment of both Ta and Sn within the pegmatites show a strong association with increasing sodium abundance. It reflects that these ore minerals developed during a late stage albitisation phase. Rb which can substitute for K in microcline or mica shows the abundance of lepidolite. Where there is lots of feldspar and little mica there should be higher Sr than Rb and where there is a lot of microcline or lepidolite then the Rb might be greater than Sr. Sr is present through the radioactive decay of Rb in lepidolite due to the Archean age. Table 6.2 shows where the trace element abundances obtained from each pegmatite body are highest.

***Table 6.2**: Highest trace element abundances for each pegmatite body*

Pegmatite Section	Ta (ppm)	Sn (ppm)	Nb (ppm)	Rb (ppm)	Sr (ppm)
McMurdon	3708	1924	620	36700	540
Bikita	18 860	9701	2623	36564	349
Al Hayat	2211	1029	870	16836	493
Ledingham	266	3077	307	7288	97
Victor's	2119	390	211	32350	336
Nigel's	384	205	48	21159	217
Shaft	3047	1390	841	18592	165
West	1575	28 291	856	11731	143
Mauve Kop	252	1117	168	5080	110
Dam Site	2086	1336	330	44 283	517

The pegmatites of the Bikita area have been classified as rare metal (Ĉerný et al, 2003) and LCT pegmatites (Bradley and McCauley, 2013). Ĉerný et al., (1985) made an observation that extreme fractionation of lithophile elements such as Rb and Cs is a common geochemical feature of the granitic pegmatites, especially the rare-metal bearing types. While enrichment in Rb is an indicator of the degree of fractionation in the granitic pegmatites, enrichment in caesium appears to be the most important discriminator of the rare-metal pegmatites. This observation correlates with the typical geochemical characteristics of the Bikita pegmatites as shown by enrichment of these elements. Generally, the Bikita pegmatites are highly fractionated as indicated by their high Rb values (36 700 to 44 283 ppm) from McMurdon pit and Dam Site pit respectively.

The combined whole-rock geochemical database has enabled the distinction of the various pegmatite bodies into the different mineral commodities that they host. The geochemical data interpretations have proved that mineralisation within the Bikita pegmatites is dominated by lithium (mostly petalite) followed by caesium, tantalum and tin concentrations and this varies from pit to pit. The highest lithium concentration is within the Dam Site pit, the highest caesium concentration is at Victor's pit, the highest tantalum and beryllium concentrations are at Bikita

quarry and the highest tin concentration is at the West pegmatite body. The variability in distribution of lithium, caesium, tantalum and tin is shown in Figure 6.1 and it is also shown that both ends of the mining lease (Main and Dam Site pegmatites) are enriched in lithium-caesium and tantalum.

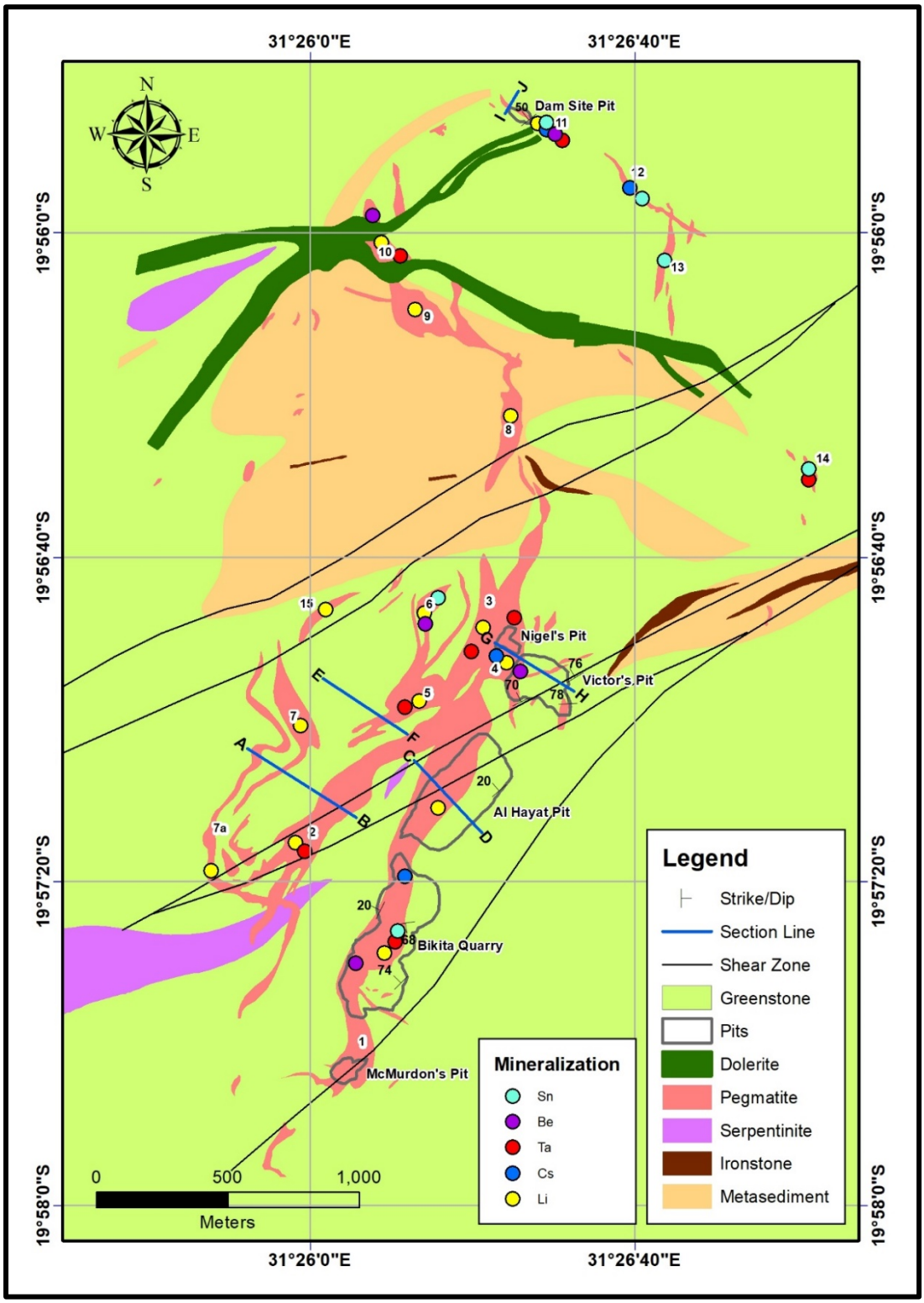

Figure 6.1: *Geological map of the Bikita Tinfield showing pegmatite mineralisation distribution patterns.* Numbers 1-15 in circles are pegmatite names and those around the pits are dip angles

6.3 Geophysical and Remote Sensing data interpretations

Pegmatites in general have a strong radiometric response and in the case of the Bikita pegmatites, there is a particularly strong K-response when compared with Th and U because of the abundance of microcline and lepidolite, and this made it easy to map them (Figure 5.4). The ternary radiometrics image (Figure 5.5) shows some clear geological units, with radiometrically dark units that are greeny black and, interpreted as greenstone volcanics, and radiometrically light units (light blue, interpreted as greenstone sediments), but the pink signature in the centre, reflect the pegmatites, and this signal tends to swamp the area. For this reason it is helpful to refine the interpretation using the analytical signature of the pegmatites. In the analytical signal of the ground magnetics (Figure 5.6), it can be seen that the magnetically busy areas and the quiet areas have been demarcated with black lines and these are often bounded by NE shear zones. Some of the radiometrically light areas are magnetically busy, whilst others are quiet. The same holds true for the radiometrically dark areas. These units have therefore been geophysically classified as dark-marginally busy area and light-marginally busy area. Geologically, the classifications are interpreted to be magnetic-greenstone-sediments and non-magnetic-greenstone sediments etc. Figure 6.2 shows the resulting broad scale structural interpretation of the survey area.

The interpreted structural lineaments show a complex structural picture involving a set of four main trends. These are NE-trending arcuate shears and brittle N-S, NNE and ENE faulting. The latter appear to play a major role in offsetting the pegmatites within the current pits. The N-S faults and the NNE-trending fractures appear to modify the shape of the main pegmatite occurrence. The NE shears have shaped the contacts of the geology and changed their shapes forming the main contacts between the greenstone sediments and volcanics. It is also possible that the main shear corridors created volumetric space in the form of N-S tension gashes into which the pegmatite swarm could intrude. This type of geometry could potentially be realised by overall sinistral movement between the northern shear corridor and the southern one.

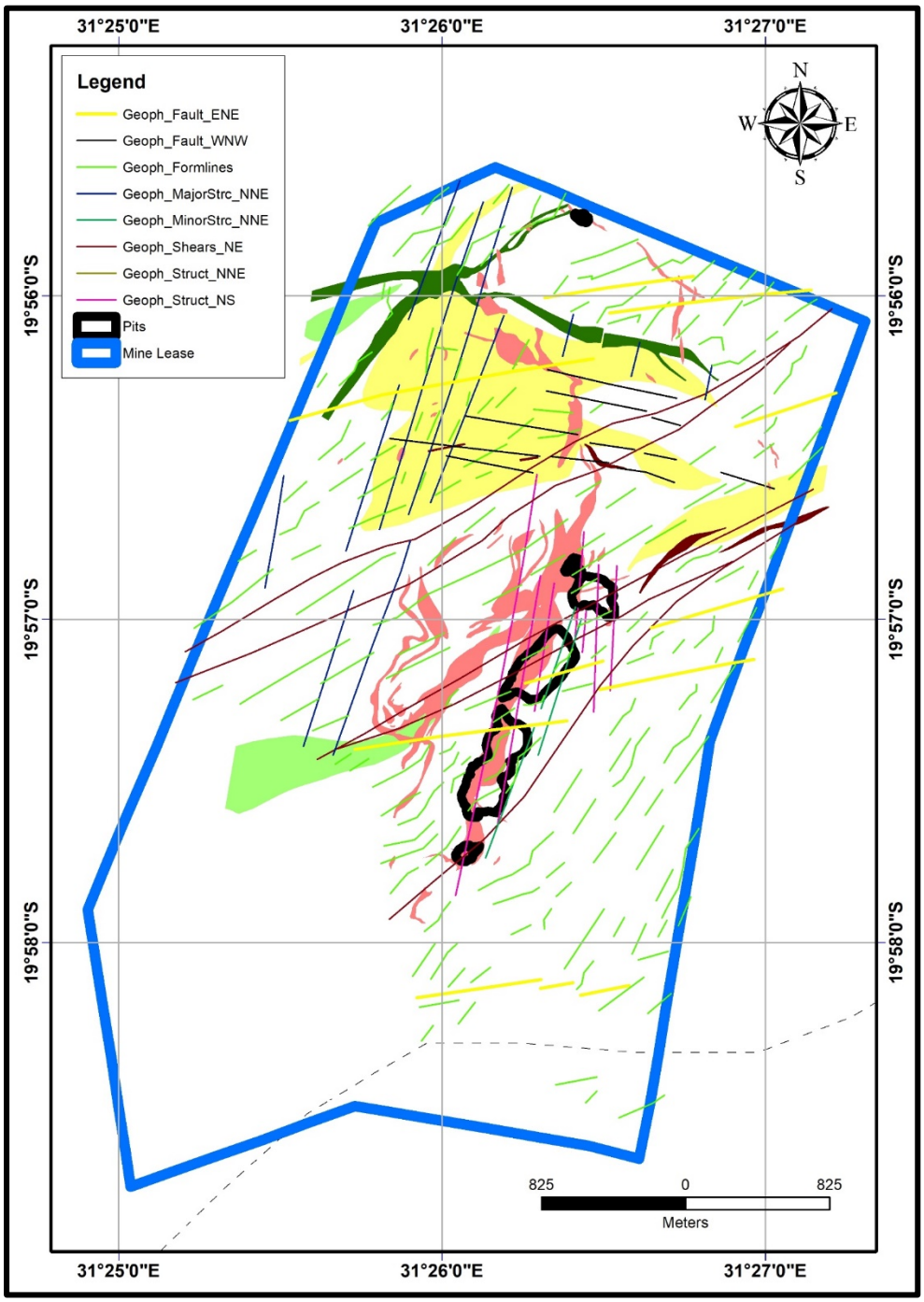

Figure 6.2: *A map of the Bikita Tinfield showing a ground magnetic broad-scale local structural lineament interpretation*

When the K-response interpretation is compared with the geologically mapped pegmatites (Figure 6.3) it is clear there is good correlation, but that the radiometric data are detecting some small new pegmatites in a number of areas which because of their small size don't change much on the existing geological map. The strong K-response presented on Figure 5.4 provides a good correlation with the distribution of known pegmatites when the spread of the interpreted pegmatites is overlain. The pegmatite swarm dominates the centre of the area.

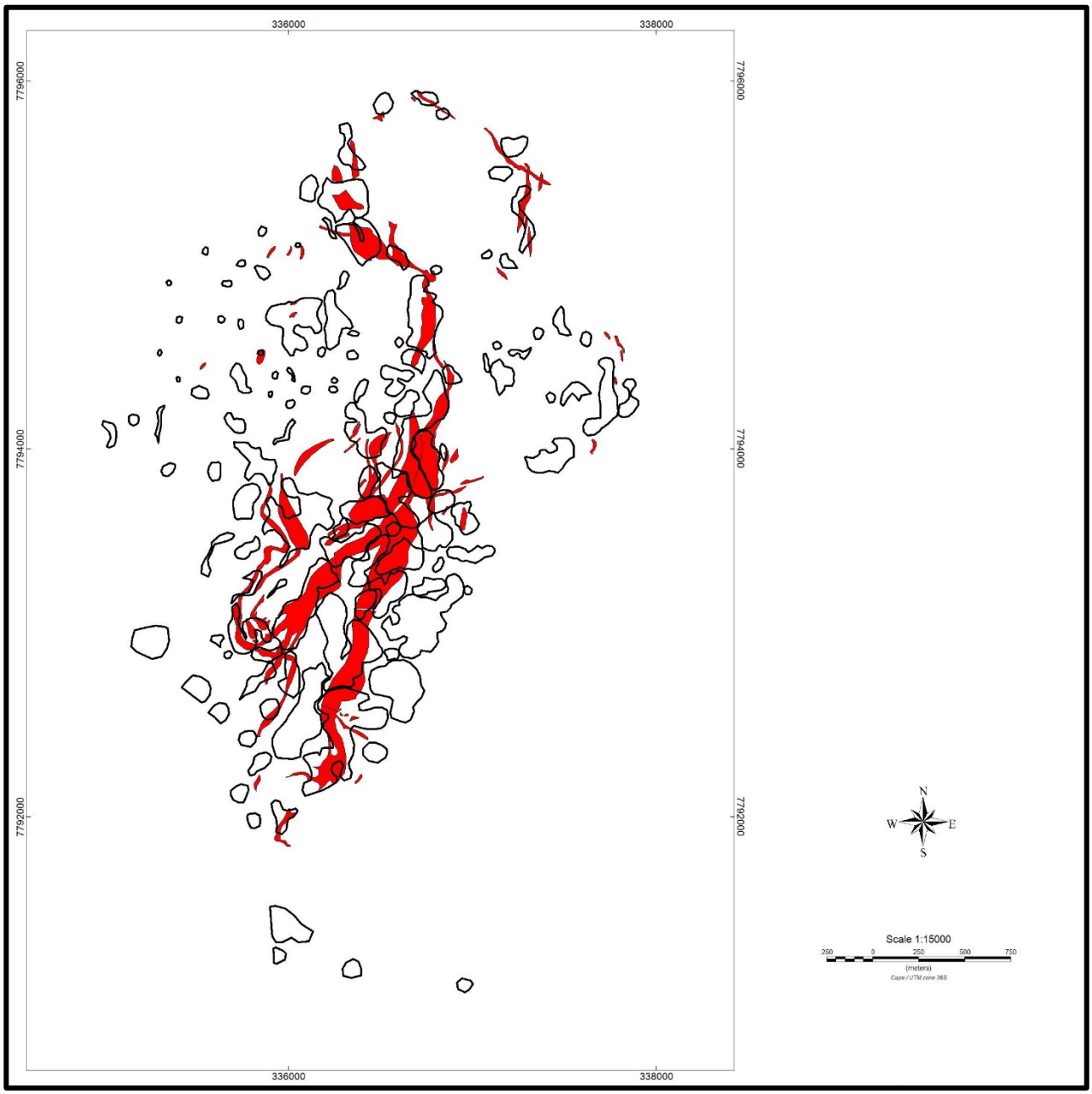

***Figure 6.3**: Interpreted pegmatites (from K %) in black outline, overlaid on mapped pegmatites in red.*

6.4 Structural controls

6.4.1 Regional structural controls

The structural lineaments from the geophysical work done by Gwavava and Ranganai (2009) together with those on the regional geology map of the project area done by Wilson (1964) were digitised and then combined with the current remote sensing work. The idea was to identify correlations between these 3 methods. The combined lineament maps (Figure 6.4) shows a positive correlation as in most cases the lineaments look more or less the same. The processing and interpretation of the satellite imagery data sets has provided new structural information in the quest to delineate the structural controls on the emplacement of the Bikita pegmatites. The comparison

was useful in delineation of the lineaments in the final map (Figure 6.5).

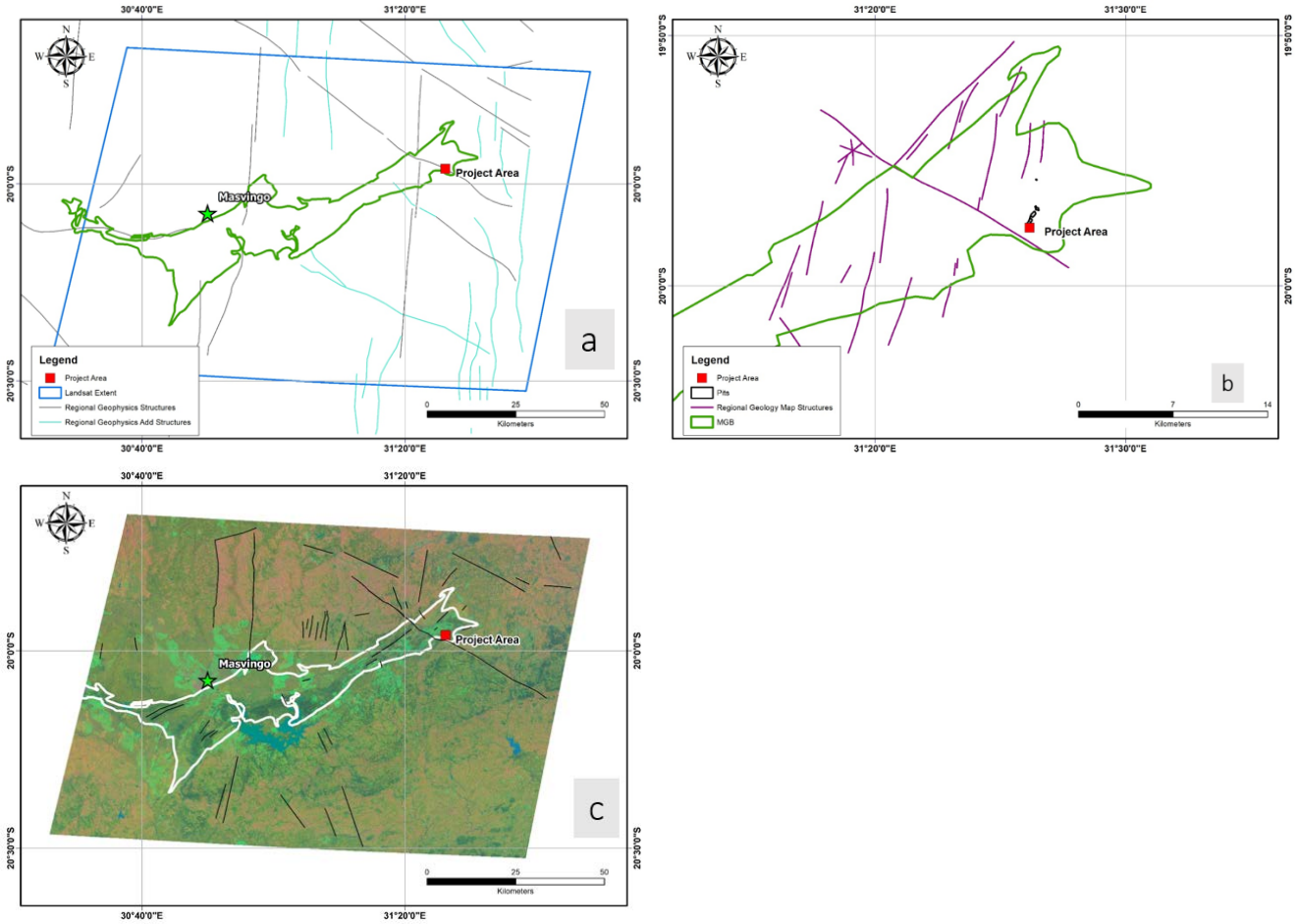

Figure 6.4: *Comparison images of satellite, regional geophysics. Adapted from Gwavava and Ranganai (2009) and regional geology lineaments. After Wilson (1990).* a) Regional geophysics structures b) Regional geology map lineaments c) Landsat lineaments

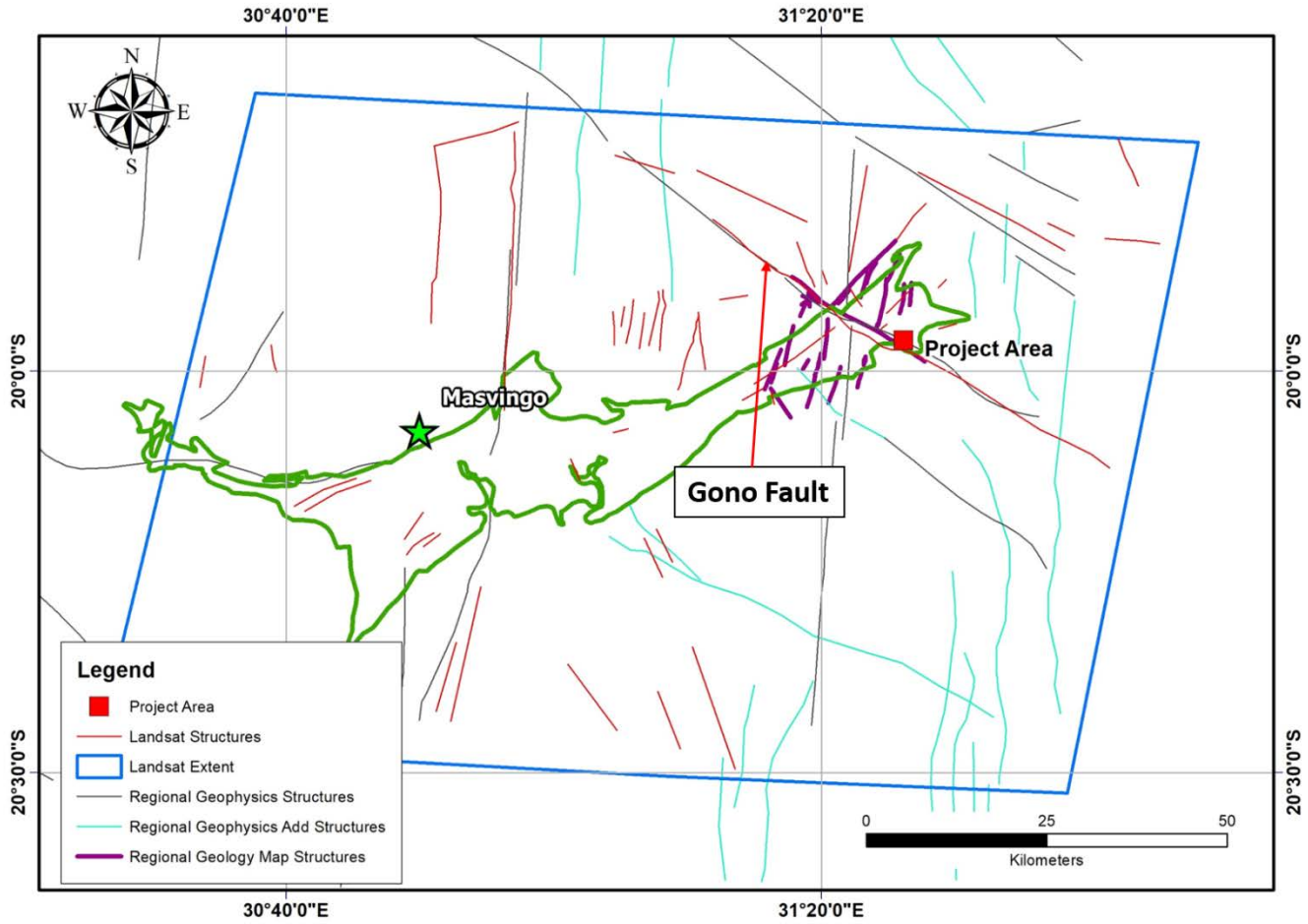

***Figure 6.5**: Final interpretation map showing the Masvingo Greenstone Belt and combined regional structural lineaments*

The NW–SE trending Gono fault (Figure 6.5) in the eastern part of the Masvingo Greenstone Belt is the main structural feature around the Bikita pegmatite district. It is a normal fault that displays some degree of dextral shearing associated with the formation of a second order set of N–S striking normal faults found predominantly on its northern side. This type of structural setting is favourable for the emplacement of pegmatite melts. These structures are interpreted to have resulted from the extensional tectonic regime during which the Chilimanzi Suite granites were emplaced into the surrounding gneisses. The extensional tectonics provided the pathways for the pegmatite forming melts. The Gono fault separates the Bikita pegmatite field in the hanging wall from the Riverton pegmatite field in its footwall and exhibits dextral shearing (Dittrich, 2017). Widespread pegmatite-hosted mineralisation (mostly Archaean) appears to be associated with genetically late-tectonic Chilimanzi suite granites (Broderick, 1981). The pegmatites are thought to have been derived from the post-Shamvaian granites which surrounds the greenstone belt (Wilson, 1981). The greenschist to amphibolite facies grade of metamorphism presents the favourable environment for pegmatite emplacement and this can only happen after intensive rock deformation of the country rock. The other major structural feature is the Popoteke fault (Figure 1.5) which cuts right across the Masvingo Greenstone Belt from north to south with an almost NNE orientation and parallel to the Bikita pegmatites to suggest a structural control.

6.4.2 Local structural controls

The Bikita pegmatites have sharp contact relationship with enclosing host rocks suggesting that the metal rich pegmatitic magma intruded into cold rocks. At Bikita, field evidence suggests that the pegmatites passively invaded the fractures as structurally controlled sheets without any significant alteration of the enclosing rocks. Interaction with country rock is minimal and restricted to tourmaline-rich metasomatic selvedges of approximately 25-30 cm in thickness. Field evidence suggests that most of the structures within the mining lease are in the same strike as the pegmatites therefore cutting across the fabric of the country rock. However, field observation evidence (Figure 6.6) shows that some of the structures/fabrics (faults, shear zones and fractures) in the greenstone country-rock could have acted as pathways for fluids and magma.

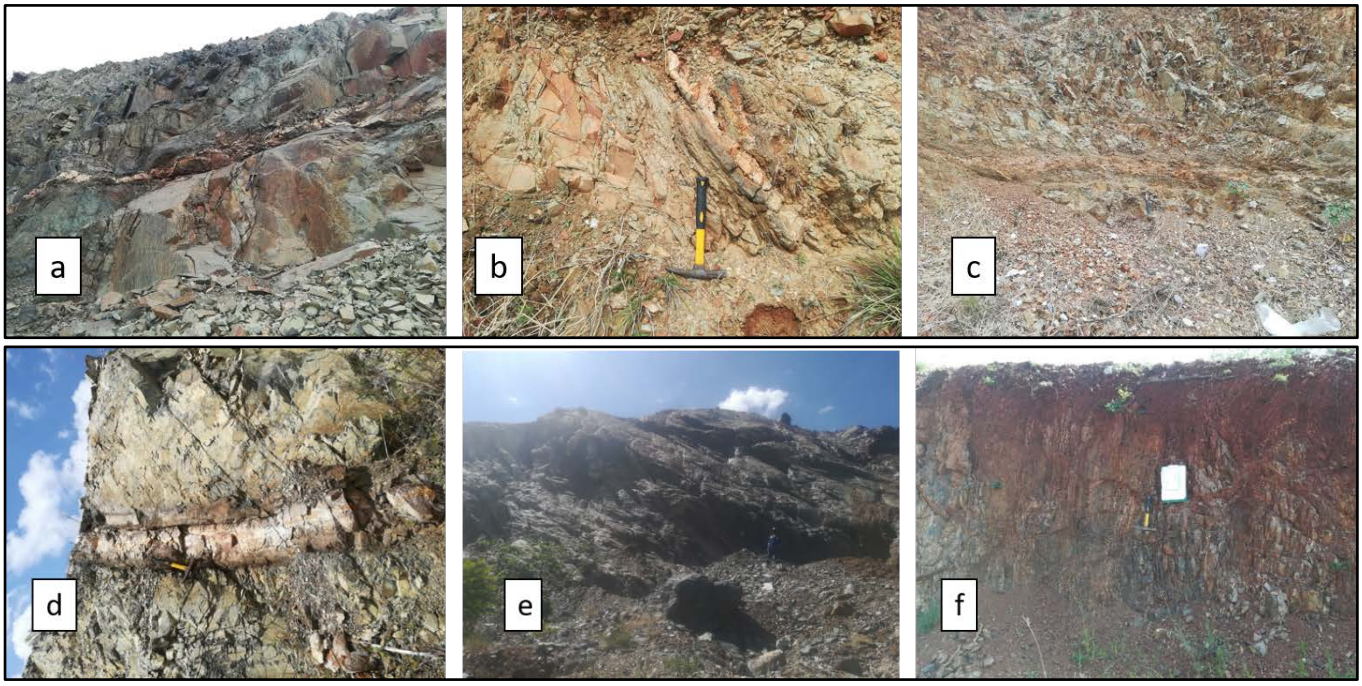

Figure 6.6: *Field evidence for possible local emplacement along lineaments of the pegmatites.* a) Photograph of a fracture filled by pegmatitic material within the Bikita quarry b) Photograph of a shear zone with quartz vein infill c) Photograph of a fracture cutting across the country rock fabric d) Photograph of a fracture filled by pegmatitic material with hydrothermal alteration of black tourmaline within the F/W of Bikita quarry e) Photograph of a huge shear zone within the Al Hayat pit f) Photograph of a huge shear zone trending N-S from the Victor's pit.

6.5 Possible mechanisms regarding the genesis and emplacement of the Bikita pegmatites

Typically the spatial relationship between the source granites and pegmatites can often be clearly identified, showing that rare metal pegmatite bodies are mostly no more than 5 kilometres away from their parent post-tectonic granites, and rarely more than 10 kilometres at the most (Breaks and Tindle 1997). Those pegmatites situated far from the source are highly fractionated while those close to the source and least evolved in an LCT environment contain the ordinary mineralisation of an S-type granite. Baker (1996) has experimentally confirmed this observation, by modelling the escape of the pegmatite melt from their parent plutons, providing the plutons are of sufficient size to heat adjacent host rocks. Additionally, this model confirms that the most differentiated and evolved (lowest viscosity) pegmatites are the most distant from their parent granites. It has also been noted that rare metal deposits within Archaean cratons tend to be emplaced along margins of greenstone belts where their localisation is probably controlled by deep-reaching marginal faults and this seems to be the case for the Bikita pegmatites (Senzani, 1992).

The emplacement of LCT pegmatites is essentially structurally controlled and that the locus of these intrusions exploit zones of structural weakness that include lithological contacts, foliation planes, shear zones and faults (Ĉerný 1989a; London 2008). Most of these pegmatites if not all are emplaced within mountain belts dominated by metasedimentary and granitic rocks, and mostly at the times of assembly of supercontinents over the Earth's history (McCauley & Bradley 2014; Bradley et al. 2016, 2017). Also considering that the pegmatites are spatially associated with shear zones, it is suggested that the shear zones (possible large-scale dilatant zones) may have acted as a planes of weakness along which magma could have ascended through the crust. According to previous studies (e.g. Senzani, 1992), there is a clear relationship that exists between local structure and pegmatite emplacement and the related deposits occupy graben structures, faults, shear zones and hinges, domes, or areas where faults cross together with pre-existing voids. As a result of this relationship, it becomes easier for intruding magma to follow zones of crustal weakness or relatively reduced pressure. Individual pegmatites and pegmatite groups take on a variety of morphologies, which are controlled by an interplay of fluid pressure of the pegmatite melt, host rock rheology and anisotropy, lithostatic and directed stress conditions, pore water pressures, and dilational directions (Brisbin, 1986). Pegmatite intrusions are achieved by forceful emplacement, where the pegmatites fluid pressure overcomes compressive and tensile strengths of the host rocks (Brisbin, 1986).

The Bikita pegmatites are hosted mainly within the upper greenschist to lower amphibolite facies which have low pressure mineral assemblages. According to Cerny (1991), pegmatites of the lithium-caesium-tantalum (LCT) family are associated with this type of metamorphic environment. Little has been published regarding the genesis of the Bikita pegmatites but it is believed that the intrusion of these pegmatites is probably related to the Chibi batholith which encompasses the Masvingo Greenstone Belt. It is believed that the pegmatite melts represent highly fractionated residual melts derived from the crystallisation of the younger surrounding granites belonging to the Chilimanzi or Sesombi Suites (e.g., Martin, 1964, Grubb, 1985; Melcher et al., 2015). Based on the complexity in zoning in particular that of the Main pegmatite (1), the crystallisation must have happened in a series of stages within a closed system. However, considering that the intrusions were emplaced into granites as internal pegmatites and extend into the greenstone belt, there is another suggestion that the Bikita pegmatites might have been emplaced at 600 °C or above (Grubb, 1985) thereby further suggesting crystallisation to have taken place essentially in an open system and the crystallisation history is associated with varying degrees of structural movements and the intrusion of late predominantly sodic hydrothermal solutions.

The emplacement of the magma is considered to have been through regional shear and thrust zones (i.e., Gono and Popoteke faults) as channel-ways for the fluid-rich residual magmas. Consequently, these slow and interrupted cooling conditions were able to contribute substantially to extensive replacement events (Grubb, 1985). The Bikita pegmatites are massive, which shows that they intruded after the main regional foliation event. They however display horizontal and vertical faulting. They are emplaced into pre-existing fractures which have flat-lying to gentle geometry which formed by yet unknown processes. In addition, Grubb (1985) was of the opinion that most mineralised pegmatites tend to be concentrated within the peripheral region of the craton (e.g., Bikita pegmatite field) and thus may likewise have been influenced by events associated with the adjoining mobile belts like the Limpopo and Zambezi belts.

According to interpretations by Dittrich (2017), the geochemically highest evolved portions of the LCT pegmatite field are represented by the massive pollucite mineralisation within the southernmost extension of the Bikita

pegmatite field exposed within the Bikita quarry. He further noted that structural geological constraints within the Bikita pegmatite district points to the NW-SE striking Gono fault which exhibits a normal character with dextral movement, in addition to a second conjugated N-S striking system of faults. These N-S striking faults point towards the location of the assumed source granite and are therefore interpreted to be have played a pivotal role as conduits for the emplacement of the Bikita LCT pegmatites. The notion of probably having a source granite towards the NE of the Masvingo greenstone belt was supported by Gwavava & Ranganai (2009) when they gave evidence of this region exhibiting a low vertical gravity anomaly reflecting the presence of granitoid intrusive bodies and also as conduit for the source granite.

CHAPTER 7:

CONCLUSION AND RECOMMENDATION

7.1 Conclusion

Having studied the Bikita pegmatites in great detail, some assumptions have been made based on a combination of field observations and literature. Lithium is the most important element of interest for the mining operations and having a closer look at the results from Bikita quarry locality which has shown the best behaved dataset, the typical mineral compositions have helped to ascertain mineral deportment and the main definable trends are a high K trend governed by micas i.e. lepidolite and a low K trend which appears to be illustrating the control by petalite. The other Li-Al minerals (spodumene, amblygonite, eucryptite) associate with this low K trend. Displaying some of the major rock forming minerals (quartz, feldspars, and muscovite) and bulk compositions has been useful in the interpretations, such as the influence of albite (late stage albitisation), microcline (K-feldspar) and muscovite (greisenisation). Essentially all samples show mineralogical control by muscovite and mainly lepidolite (correcting for the build up of radiogenic Sr) exerting a strong influence on Rb contents of extremely differentiated melts containing practically no original Sr.

Spatial data processing, analysis and integration using Remote Sensing, geophysics, geochemistry and GIS applications were useful in understanding the geology, mineralisation and structural controls on emplacement of the Bikita pegmatites. Geochemical work applied in this report work has proved that the Bikita pegmatites are richly endowed in lithium ore minerals with lepidolite and petalite being the most dominant. Amblygonite is now found as remnants within the Bikita sector and Dam Site whilst alteration minerals (eucryptite and bikitaite) remain as by-products within the lithium-rich zones. Ta is found in most of the pegmatite bodies mainly concentrated in lepidolite with varying proportions.

Caesium is now found in smaller patches within the Bikita quarry as most of it has been mined out. Whole-rock geochemical data processing and interpretation was helpful in determining the composition of the pegmatites which aided the plotting of mineralisation distribution patterns (Figure 6.1). The major and trace element geochemical compositions clearly show that the sampled pegmatites within the mining lease are all mineralised with lithium being the most dominant element. It was also noted that partially to-completely albitised K-feldspar units show a higher grade of-mineralisation as opposed to unalbitised units which are poorly mineralised. Field observations, together with whole-rock geochemical data, have shown that both the northern extremity (Dam Site pegmatite) and the southern extremity (main pegmatite on Bikita quarry) of the project area are highly enriched in lithium, caesium and tantalum probably suggesting multiple magma sources.

This study showed that geophysical and remote sensing data processing and interpretation were helpful in identifying the possible structural controls on emplacement of the Bikita pegmatites. Structural analysis suggests that the NE–SW trending Gono fault together with the N-S trending Popoteke fault are the major structural features on a regional scale. These are understood to have played a vital role in the emplacement mechanism of the pegmatites as this kind of structural setting is most favourable for the emplacement of pegmatite melts. On a local structural scale, fractures and shears are the most dominant structures mapped in the study area. The most

important structures are those which have the same trend as that of the pegmatites (NE, N-S, NNE and ENE). In other cases these structures were subsequently filled by pegmatitic material showing that these zones of weakness were utilised as a locus when the pegmatites were being emplaced within the greenstone. Some of the ground truthed structural lineaments have been updated on the local geology map (Figure 7.1).

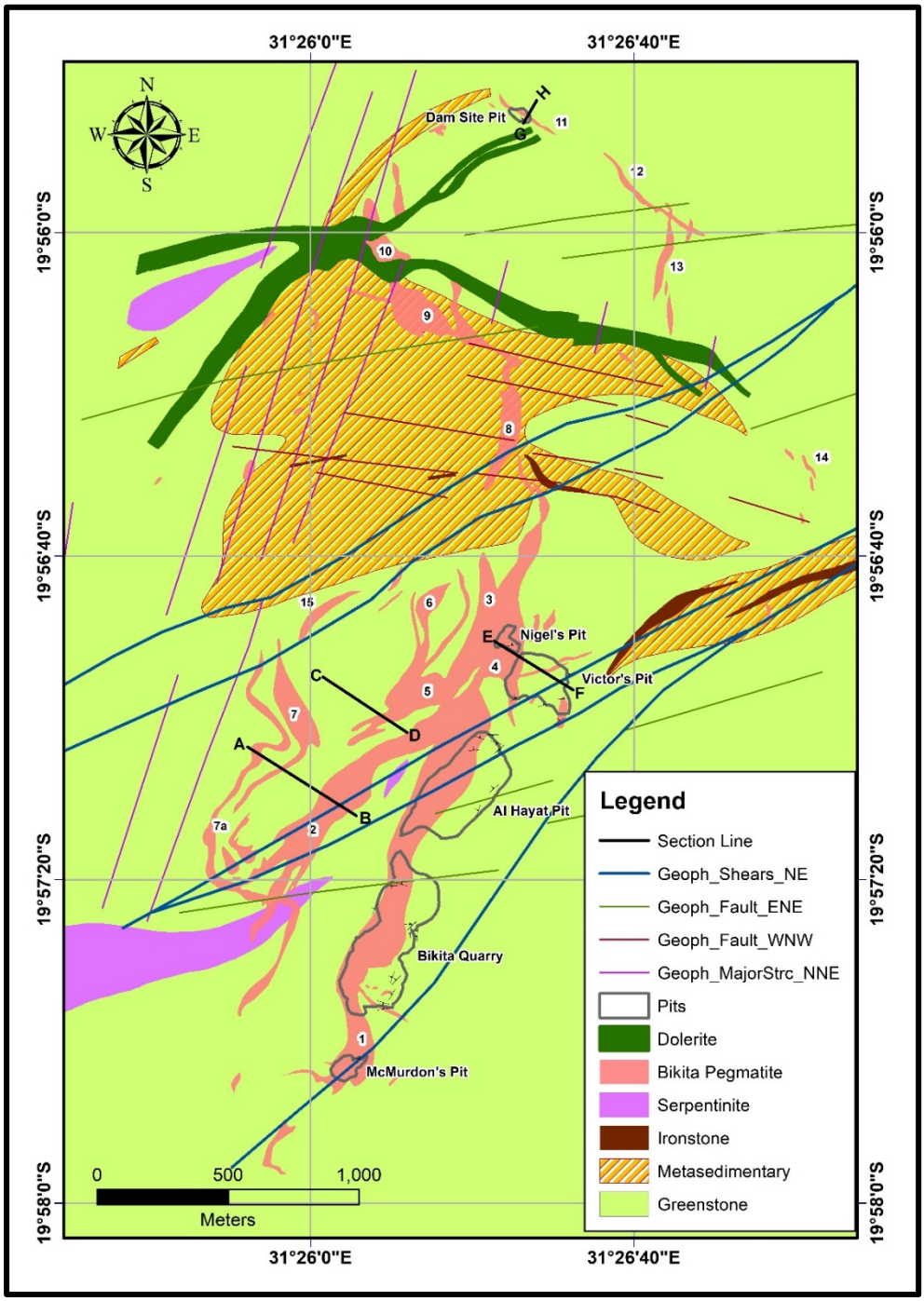

Figure 7.1: *Final interpretation geological map of the Bikita Tinfield showing the updated structures and section lines.* The sections are in chapter 3 on Figures 3.11, 3.15, 3.17, 3.18 and 3.21.

7.2 Recommendation

There are several outstanding questions surrounding the origin and source of the Bikita pegmatites. Such information is vital to come up with their genetic and emplacement models. Also considering that both the southern end (Bikita sector) and northern end (Dam Site) of the mining lease area (Figure 6.1) show the presence of lithium, caesium and tantalite it therefore becomes difficult to tell where the source pluton could be located. Consequently it is thus suggested that geochronological studies be done in order to address this gap. The internal zoning within the Bikita pegmatites is somehow very complex and not easy to understand. It is therefore, recommended that for better understanding of the internal relationship and connection between these pegmatites, isotopic studies be done as this will go a long way in constraining the possible mechanisms that would have controlled the complex zoning within the pegmatites. Exploration must try and cover the other pegmatites (Boomerang, Giant West, West and Cemetery) where little work has been done in order to increase the knowledge regarding their full potentials. Of particular interest will be the Cemetery pegmatite to see if the petalite mineralisation observed from the Shaft pegmatite will be continuous since these pegmatites are adjacent to each other (Figure 3.1). In order to increase the life of mine, other abandoned orebodies like the Victor's and Nigel's need to be revisited by doing XRD analysis on the reference exploration samples as the visual logging of these samples show some potential mineralisation.

References

Anhaeusser, C.R., 1976. The nature and distribution of Archaean gold mineralisation in Southern Africa. *Mineral Science Engineering 8,* 46–48.

Baker, D.R., 1996. Granitic melt viscosities: Empirical and configurational entropy models for their calculation. *American Mineralogist* 81, 126-134.

Bickle, M.J., Martin, A. and Nisbet, E.G., 1975. Basaltic and peridotitic komatiites, stromatolites and a basal unconformity in the Belingwe greenstone belt, Rhodesia. *Earth Planet Science Letter, 27*: 155–162.

Blenkinsop, T.G., Frei, R., 1997. Dating the intrusion of the Razi Granites, Zimbabwe: tectonic implications for the Northern Marginal Zone of the Limpopo Belt and the Zimbabwe craton. *In: Conference Abstract Volume, Harare, Zimbabwe, Intraplate magmatism and tectonics of southern Africa, and the 17th Colloquium on African Geology*, 4.

Blenkinsop, T.G., Martin, A., Jelsma, H.A., Vinyu, M.L., 1997. The Zimbabwe Craton. *In: de Wit, M.J., Ashwall, L. (Eds.), Greenstone Belts. Oxford University Monograph on Geology and Geophysics 35*, 567–580.

Bliss, N.W. and Stidolph, P.A., 1969. A review of the Rhodesian basement omplex. *Geological. Society. South. Africa; Special. Publication. 2*; 305–333.

Bradley, D.C. and McCauley, A., 2013. A preliminary deposit model for lithium-cesium-tantalum pegmatites. *U.S. Geological Survey Open-File Report 2013–1008, 1–7.*

Bradley D.C., Shea E., Buchwaldt R., Bowring S., Benowitz J., O'Sullivan P. & McCauley A., 2016. Geochronology and tectonic context of lithium-cesium-tantalum pegmatites in the Appalachians. *The Canadian Mineralogist, **54**(4),* 945-969.

Bradley D.C., McCauley A.D. & Stillings L.M., 2017. Mineral-deposit model for lithium-cesium-tantalum pegmatites. *U.S. Geological Survey Scientific Investigations Report 2010–5070*, 48.

Breaks, F.W. and Tindle, A.G., 1997. Rare-element exploration potential of the Separation Lake area: an emerging target for Bikita-type mineralization in the Superior Province of Ontario: *Ontario Geological Survey, Open File Report 5966*, 27.

Brisbin, W.C., 1986. Mechanics of pegmatite intrusion: *American Mineralogist,* volume 71, 644–651.

Broderick, T.J., 1981. The Zambezi Metamorphic Belt in Zimbabwe in Hunter, D.R. Developments in *Precambrian Geology Volume ii: The Precambrian of the southern hemisphere. Amsterdam, Elsevier*, 739-742.

Campbell, S.D., Pitfield, P.E.J., 1994. Structural controls of gold mineralisation in the Zimbabwe craton-Exploration guidelines. *Zimbabwe Geological Survey Bulletin* 101, 6–10.

Černý, P., 1989a. Exploration strategy and methods for pegmatite deposits of tantalum. *In Lanthanides, Tantalum, and Niobium*. Edited by P. Moller, P. Černý and F. Saupe. Springer-Verlag, New York, 274-302.

Černý, P., 1991. Rare-element granitic pegmatites. Part I, Anatomy and internal evolution of pegmatite deposits. *Geoscience Canada 18,* 49-67.

Černý, P., Meintzer, R. E. and Anderson, A. J., 1985. Extreme fractionation in rare-element granitic pegmatites: selected examples of data and mechanisms; *Canadian Mineralogist 23*: pp. 381-421.

Ĉerný, P., Anderson, A. J., Tomascak, P. B., & Chapman, R., 2003. Geochemical and morphological features of beryl from the Bikita granitic pegmatite, Zimbabwe. *The Canadian Mineralogist: 41(4):* 1003-1011.

Cooper, D.G., 1964. "The Geology of the Bikita Pegmatite". In: *The Geology of Some Ore Deposits in Southern Africa*. Ed. by S.H. Haughton. Volume. 1–2. Johannesburg: Geological Society of South Africa, 441–462.

Coward, M.P., and James, P., 1974."The deformation patterns of two Archaean greenstone belts in Rhodesia and Botswana". *In: Precambrian Research 1.4,* 235–258.

Dirks P.H.G.M and Jelsma H.A., 1998. Horizontal accretion and stabilisation of the Archean Zimbabwe craton. Geology 26:11–14.

Dittrich, T., 2017. Meso to Neoarchaean Lithium-Cesium-Tantalum (LCT) Pegmatites (Western Australia, Zimbabwe) and a Genetic Model for the Formation of Massive Pollucite Mineralisations. *PhD Dissertation. TU Bergakademie Freiberg,* 47–62.

Grubb, P.L.C., 1985. "Pegmatite mineralisation patterns in the Zimbabwe Craton". *In: The Crust-The Significance of Granites Gneisses in the Lithosphere.* Ed. by W. Liren, Y. Taiming, Y. Kuirong, J. Didiers, J.K. Greenberg, G.R. Lowell, X. Hongyouan, Y. Shoujun & Augustithis, S.S.. Athens (Greece): Theophrastus Publication S.A., 669–690.

Gwavava, O., and Ranganai R.T., 2009. The geology and structure of the Masvingo greenstone belt and adjacent granite plutons from geophysical data, Zimbabwe Craton. *South African journal of geology, 2009, volume 112*, 277-290

Hamilton, P.J., 1977. Sr isotope and trace element studies of the Great Dyke and Bushveld mafic phase and their relationship to early Proterozoic magma genesis. *In: Southern Africa Journal of Petrology, 18*, 24–52.

Herzog, L.F., II, Pinson, W.H., JR. and Hurley, P.M., 1960. Rb–Sr analyses and age determinations on certain lepidolites, including an international inter-laboratory comparison suite. *American Journal of Science. 258,* 191-208.

Hickman, M.H., 1978. Isotopic evidence for crustal reworking of the Rhodesian Archaean craton, Southern Africa. Geology, 6; 214–216

Kaasheka, E.K., 2018. The use of Geographic Information Systems (GIS) and Remote Sensing on the Matchless Amphibolite Belt (MAB), Gorob-Hope area, Namibia. *University of the Witwatersrand MSc Thesis.*, 29-37.

London, D., 1990. "Internal differentiation of rare–element pegmatites; A synthesis of recent research". *In: Geological Society of America –Special Paper 246*, 35–50.

London, D., 2008. Pegmatites: *The Canadian Mineralogist Special Publication* 10. *ISBN: 978-0-921294-47-4.*

McCauley A. & Bradley D.C., 2014. The global age distribution of granitic pegmatites. *The Canadian Mineralogist, **52**,* 183-190.

Macgregor, A. M., 1946. "Simpsonite and other tantalates from Bikita, Southern Rhodesia." *Mineral Magazine, XXVII,* 1946, 157-165.

Macgregor, A. M., 1947. "An outline of the geological history of Southern Rhodesia." *Southern Rhodesia Geological Survey Bulletin 38*, Salisbury.

Macgregor, A.M., 1951. Some milestones in the Precambrian of southern Rhodesia. *Geological Society of South Africa Proceedings 54,* 27–71.

McCourta, S., and Vearncombe., J.R., 1992. Shear zones of the Limpopo Belt and adjacent granitoid-greenstone terranes: implications for late Archaean collision tectonics in southern Africa. In: D.D. van Reenen, C. Roering, L.D. Ashwal and M.J. de Wit (Editors), *The Archaean Limpopo Granulite Belt: Tectonics and Deep Coustal Processes. Precambrian Research*, 55–70.

Martin, H.J., 1964. "The Bikita Tinfield". In: *Bulletin - Southern Rhodesia Geological Survey 58,* 114–131.

Melcher, F., T. Graupner, H.-E Gabler, M. Sitnikova, F. Henjes-Kunst, T. Oberthur, A. Gerdes and Dewaele, S., 2015. "Tantalum-(niobium-tin) mineralisation in African pegmatites and rare metal granites: Constraints from Ta-Nb oxide mineralogy, geochemistry and U-Pb geochronology". *In: Ore Geology Reviews 64*, 667–719.

Murahwi, C.Z., 1995. The geology of the Unki platinum-base metal deposit Selukwe subchamber, Great Dyke, Zimbabwe. *Rhodes University MSc Thesis*, 26-30.

Reid, D.L. Barton, E.S., 1983. Geochemical characterisation of grantoids in the Namaqualand geotraverse. *Special. Publication. Geological. Society. South Africa, 10, 67-82)*

Robert A., S., 1997. Remote Sensing, Models and methods for image processing, *Academic Press second edition*, p. 229-286.

Senzani, F.E.D., 1992. Pegmatite-Hosted Mineral Deposits of Central and Southern Africa: Regional Geological Settings and Preliminary Exploration Target Considerations. *Rhodes University Master of Science in Mineral Exploration Dissertation*, 70-80

Symons, R., 1959. A description of Bikita Mineral's mining operations" *Chamber of Mines Journal Volume 1* 22-6.

Symons, R., 1961. Operation at Bikita Minerals (Private), Ltd., Southern Rhodesia. *Institute of Mining Metallurgy, Bulletin 661*, 129-172.

Treloar, P.J., Blenkinsop, T.G., 1995. Archaean deformation patterns in Zimbabwe: true indicators of Tibetan-style crustal extrusion or not? In: Coward, M.P., Ries, A.C. (Eds.), *Early Precambrian Processes. Geological Society Special Publication 95,* 87–108.

Tyndale-Biscoe, R., 1951. The geology of the Bikita Tin-Field, Southern Rhodesia. *Transactions of the Geological Society of South Africa, volume 54,* 11-23.

van Roij, A., 2006. Integration of airborne geophysical data and spaceborne multispectral data for geological mapping and mineral potential mapping in a poorly exposed region : A case study of the kibi area, Ghana. 126 p. *Utrecht University (UU), ITC, Utrecht, Enschede.*

Wilson, J.F., 1964. The geology of the country around Fort Victoria and the Bikita Tinfield, *Southern Rhodesia Geological Survey Bulletin 58*, Salisbury, 147.

Wilson, J.F., 1979. A preliminary reappraisal of the Rhodesian Basement Complex. *Special. Publication. Geological. Survey. South. Africa,* ***5*****,** 1–23.

Wilson, J.F., 1981. The granitic-gneiss greenstone shield: Zimbabwe in Hunter, D.R. (1981). Developments in Precambrian Geology Volume II: *The Precambrian of the southern hemisphere. Amsterdam, Elsevier,* 454-492.

Wilson, J.F., 1990. A craton and its cracks: some of the behaviour of the Zimbabwe block from the late Archaean to the Mesozoic in response to horizontal movements, and the significance of some of its mafic dyke fracture patterns. *Journal of African Earth Sciences 10*, 483–501.

Wilson, J.F., Jones, D. and Kramers, J.D., 1987. Mafic dyke swarms in Zimbabwe. In Mafic dvke swarms Halls, H.C. and Fahrig, W.E., eds., Special Paper Geological Association of Canada., 34, 433 - 444.

Wilson, A.H. and Prendergast, M.D., 1989. The Great Dyke of Zimbabwe.I: Tectonic setting, stratigraphy, petrology, structure, emplacement and crystallisation. In Magmatic Sulphides-The Zimbabwe Volume, Prendergast M.D. and Jones, M.J., eds.*The Institution of Mining and Metallurgy, London,* 1-20.

Appendices

Appendix 1a: Channel Chip Log Sheets

Sample Name	Description	Easting	Nothing
MK-001	Medium to coarse grained pale lilac feldspathic lepidolite with minor quartz inclusions	335980	7791708
MK-002	Medium to coarse grained deep mauve lepidolite intermixed with albite and quartz	336202	7791998
MK-003	Feldspathic friable lepidolite intermixed with minor quartz inclusions	336203	7791977
MK-004	Fine to medium grained deep mauve lepidolite with albite and quartz inclusions	336217	7792128
MK-005	Fine grained matrix of feldspathic lepidolite, tourmaline and quartz (wall-rock altered zone)	336339	7792174
MK-006	Medium grained pale lilac lepidolite with slicken sides showing movement of blocks (fault zone)	336255	7791993
BS-001	Dark medium grained lepidolite	336190	7792190
BS-002	White amblygonite	336246	7792190
BS-003	Pink SQI with coarse needles	336254	7792217
BS-004	Pale purple fine-grained lepidolite	336204	7792315
BS-005	Grey Petalite	336239	7792340
BS-006	Coarse grained Lepidolite	336263	7792393
BS-007	Medium grained Lepidolite	336296	7792424
BS-008	Fine grained Lepidolite	336306	7792458
BS-009	Fine grained Lepidolite	336343	7792489
BS-010	Pollucite with purple stockworks	336391	7792441
BS-011	Medium grained Lepidolite	336373	7792404
BS-012	Pink SQI with coarse needles	336323	7792382

BS-013	White Petalite	336359	7792344
BS-014	Medium grained Lepidolite	336281	779298
BS-015	Pollucite with purple stockworks	336274	7792218
BS-016	Feldspar intemixed with altered greenstone and tourmaline filling a fault	336356	7792255
BS-017	Albite feldspar mixed with greenstone and tourmaline	336332	7792192
BN-001	Medium-grained deep mauve lepidolite with 10 % albite feldspar and 5 % quartz inclusions	336369	7792567
BN-002	Grey to white Petalite	336403	7792532
BN-003	Medium grained pale lilac feldspathic lepidolite with 30 % albite feldspar and 10 % quartz inclusions	336390	7792606
BN-004	Medium grained pale lilac feldspathic lepidolite with 60 % albite feldspar and 10 % quartz inclusions	336394	7792661
BN-005	Medium grained pale lilac feldspathic lepidolite with 60 % albite feldspar and 5 % quartz inclusions	336354	7792539
BN-006	Petalite with minor lepidolite veinlets	336332	7792566
BN-007	Eucryptite	336329	7792606
BN-008	Medium grained deep mauve lepidolite mixed with quartz, apatite and minor albite feldspar	336345	7792645
AH-001	Petalite intermixed with grey muscovite	336397	7792886
AH-002	Eucryptite	336415	7792927
AH-003	Hectorite mixed with albite feldspar and muscovite	336471	7793002
AH-004	Petalite mixed with muscovite	336563	7793100
AH-005	Petalite-massive	336526	7792957
AH-006	SQI mixed with muscovite	336516	7792900
AH-007	Eucryptite with iron/manganese dendrites	336545	7792866
AH-008	Petalite-massive	336574	7792905
AH-009	Petalite mixed with muscovite	336605	7792947

AH-010	Petalite mixed with muscovite	336635	7793003
AH-011	Petalite-massive	336691	7793044
AH-012	Pink SQI with coarse needles	336696	7793098
AH-013	Petalite-massive	336675	7793134
AH-014	Petalite mixed with muscovite-Transitional Petalite Ore (TPO)	336673	7793258
AH-015	Medium grained lepidolite with about 30 % quartz inclusions	336691	7793122
AH-016	Medium grained slickensided lepidolite with calcic joint infill material about 30 % quartz inclusions	336541	7792905
NG-001	Medium grained lepidolite intermixed with albite and quartz inclusions	336723	7793593
NG-002	Petalite mixed with muscovite	336743	7793593
NG-003	Eucryptite	336756	7793576
NG-004	Medium grained dark purple lepidolite	336760	7793570
NG-005	SQI mixed with minor lepidolite	336763	7793594
NG-POL-001	Pollucite with purple stockworks	336770	7793582
NG-POL-002	Pollucite with purple stockworks	336762	7793595
NG-POL-003	Pollucite with purple stockworks	336745	7793598
NG-POL-004	Pollucite with purple stockworks	336776	7793584
DS-001	Medium grained pale purple lepidolite	336761	7795591
DS-002	Grey Petalite	336779	7795595
DS-003	Grey Petalite	336783	7795585
DS-004	Grey amblygonite	336798	7795577
DS-005	Pollucite with grey stockworks	336769	7795529
DS-006	Peach Beryl	336807	7795521

DS-007	Pollucite with grey stockworks	336817	7795512
DS-008	Cleavelandite with big coarse lepidolite flacks	336826	7795528
DS-009	Pollucite with grey stockworks	336790	7795513
VP-001	Medium grained friable lepidolite with about 10 % feldspar inclusions	336778	7793409
VP-002	Medium grained friable lepidolite with about 20 % quartz and 15 % feldspar inclusions. Possible beryl phenocrysts?	336903	7793430
VP-003	Pale lilac fine-grained lepidolite with about 10 % quartz inclusions and possibly Ta inclusions?	336775	7793457
V-POL-001	Pollucite with purple stockworks	336880	7793405
V-POL-002	Pollucite with purple stockworks	336791	7793465

Appendix 1b: Percussion Drilling Log Sheets

BIKITA MINERALS (PVT) LIMITED

DRILL LOG & SAMPLING FORM Page 1 of 1 pages

BIKITA MINERALS

DATE:	29/09/2018	**NO. LAB SAMPLES:**	20	**SAMPLER:**	M.N
SECTOR:	Bikita South	**NO. GEO SAMPLES:**	22	**GEO:**	ASG
HOLE NO.:	BS-PD-SQI-008				
TYPE*	PD	**DATUM:**	WGS 84		
EOH:	22	**X:**	336240.91		
Inclination:	-90	**Y:**	772319.24	*Type: * PD; RC; DD (core)*	
Azimuth:	0	**Z:**	1180.755M	'Colour: *** Brown (B); Red (R); Grey (Gy); Green (Gr); Pink (Pk); Purple (Pl); White (W) Black (Bk); Yellow (Y).	

Geology**

OB	Overburden/rubble	**A**	Amblygonite	**L**	Lepidolite	**Hect**	Hectorite
W	Weathered	**SQI**	Spodumene	**Be**	Beryl	**D**	Dolerite

F	Fresh	**Pt**	Petalite	**Ta**	Tantalite	**AF**	Albite Feldspar
Q	Quartz	**Pol**	Pollucite	**C**	Cassiterite	**MF**	Microcline Feldspar
BM	Biotite Mica	**MM**	Muscovite Mica	**Gst**	Greenstone	**Eucr**	Eucryptite

From (m)	To (m)	Lab Spl. No	Geo sample (X)	colour***	Geology** (E.g. Q + F)	From (m)	To (m)	Lab Spl. No	Geo sample (X)	colour***	Geology** (E.g. Q + F)
0	1	-1		B	OB(Q ,L ,Rubble)	25	26	-26			
1	2	A001-2	BS-PD-SQI-008	W	SQI ,Pol? ,Q	26	27	-27			
2	3	-3		W	SQI ,Pol? ,L ,AF	27	28	-28			
3	4	-4		W	SQI ,Eucr	28	29	-29			
4	5	-5		W	SQI ,Q	29	30	-30			
5	6	-6		W	Pt ,Q ,SQI	30	31	-31			
6	7	-7		W	Pt ,Q ,MM	31	32	-32			
7	8	-8		W	AF ,L ,Q	32	33	-33			
8	9	-9		W	AF ,L	33	34	-34			
9	10	-10		W	AF ,L	34	35	-35			
10	11	-11		W	AF ,L	35	36	-36			
11	12	A011-12	BS-PD-SQI-008	W	AF ,L	36	37	-37			
12	13	-13		W	L ,AF ,Q	37	38	-38			
13	14	-14		W	L ,AF ,Q	38	39	-39			

14	15	-15		PL	L ,AF ,Q	39	40	-40			
15	16	-16		PL	L ,Q ,AF	40	41	-41			
16	17	-17		W	AF ,Q ,L	41	42	-42			
17	18	-18		W	AF ,Q ,MM	42	43	-43			
18	19	-19		GY	MM ,AF	43	44	-44			
19	20	-20		GY	AF ,Q ,MM	44	45	-45			
20	21	A020 - 21	BS-PD-SQI-008	Gr	Gst ,AF ,Q	45	46	-46			
21	22	-22		Gr	Gst	46	47	-47			
22	23	-23				47	48	-48			
23	24	-24				48	49	-49			
24	25	-25				49	50	-50			

BIKITA MINERALS

BIKITA MINERALS (PVT) LIMITED **DRILL LOG & SAMPLING FORM** Page 1 of 1 pages

DATE: 18/07/17 **NO. LAB SAMPLES:** 30 **SAMPLER:** M .N & A.S.G

SECTOR:	BIKITA SOUTH	**NO. GEO SAMPLES:**	30	**GEO:**	JPA
HOLE NO.:	BS-PD-POL-041				
TYPE*	PD	**DATUM:**	WGS 84		
EOH:	30	**X:**	336327		
Inclination:	-90	**Y:**	7792349	*Type: * PD; RC; DD (core)*	
Azimuth:	0	**Z:**		'Coluor: *** Brown (B); Red (R); Grey (Gy); Green (Gr); Pink (Pk); Purple (Pl); White (W) Black (Bk); Yellow (Y).	

Geology**							
OB	Overburden/rubble	**A**	Amblygonite	**L**	Lepidolite	**Hect**	Hectorite
W	Weathered	**SQI**	Spodumene	**Be**	Beryl	**D**	Dolerite
F	Fresh	**Pt**	Petalite	**Ta**	Tantalite	**AF**	Albite Feldspar
Q	Quartz	**Pol**	Pollucite	**C**	Cassiterite	**MF**	Microcline Feldspar
BM	Biotite Mica	**MM**	Muscovite Mica	**Gst**	Greenstone	**Eucr**	Eucryptite

	To (m)	**Lab Spl. No**	**Geo sample (X)**	**colour*** **	**Geology** (E.g. Q + F)**	**From (m)**	**To (m)**	**Lab Spl. No**	**Geo sample (X)**	**colour*** **	**Geology** (E.g. Q + F)**
0	1		BS-POL - 041-1031	W	Q	25	26	-26	BS-PD-POL-041-1056	PL	L ,AF ,Q
1	2	-2		W	Q	26	27	-27		PL	L ,Q ,AF
2	3	-3		W	Q	27	28	-28		W	Q ,AF ,L ,MM

3	4	-4		W	Q	28	29	-29		W	Q ,AF ,MM ,L
4	5	-5		W	Q	29	30	-30	BS-PD-POL-041-1060	W	AF ,MM ,Q
5	6	-6		W	Q ,AF ,L	30	31	-31			
6	7	-7		W	Q ,AF ,SQI? ,L	31	32	-32			
7	8	-8		W	L ,AF ,Q	32	33	-33			
8	9	-9		W	L ,AF ,Q	33	34	-34			
9	10	-10		W	L ,AF ,Q	34	35	-35			
10	11	-11		PL	L ,AF ,Q	35	36	-36			
11	12	-12		PL	AF ,L ,Q	36	37	-37			
12	13	-13		PL	L ,AF ,Q	37	38	-38			
13	14	-14		PL	L ,AF ,Q	38	39	-39			
14	15	-15		PL	L ,Q ,AF	39	40	-40			
15	16	-16		PL	L ,AF	40	41	-41			
16	17	-17		PL	L ,AF	41	42	-42			
17	18	-18		GY	L ,AF	42	43	-43			
18	19	-19		GY	L ,AF	43	44	-44			
19	20	-20		GY	L ,AF ,Q	44	45	-45			
20	21	-21		W	L ,AF	45	46	-46			
21	22	-22		W	AF ,L ,Q	46	47	-47			
22	23	-23		W	AF ,L ,Q	47	48	-48			
23	24	-24		W	L ,AF ,Q	48	49	-49			

24	25	-25	BS-POL - 041-1055	PL	L ,AF ,Q	49	50	-50			

BIKITA MINERALS

BIKITA MINERALS (PVT) LIMITED **DRILL LOG & SAMPLING FORM** Page 1 of 1 pages

DATE:	30/01/18	**NO. LAB SAMPLES:**	33	**SAMPLER:**	LM ,ASG
SECTOR:	BN	**NO. GEO SAMPLES:**	40	**GEO:**	JPA
HOLE NO.:	BN-PD-SQI-009				
TYPE*	PD	**DATUM:**	WGS 84		
EOH:	40M	**X:**	336362		
Inclination:	-90	**Y:**	77925505	*Type: * PD; RC; DD (core)*	
Azimuth:	0	**Z:**	1173M	'Coluor: *** Brown (B); Red (R); Grey (Gy); Green (Gr); Pink (Pk); Purple (Pl); White (W) Black (Bk); Yellow (Y).	

Geology**

OB	Overburden/rubble	**A**	Amblygonite	**L**	Lepidolite	**Hect**	Hectorite
W	Weathered	**SQI**	Spodumene	**Be**	Beryl	**D**	Dolerite
F	Fresh	**Pt**	Petalite	**Ta**	Tantalite	**AF**	Albite Feldspar

Q	Quartz	**Pol**	Pollucite			**C**	Cassiterite	**MF**	Microcline Feldspar		
BM	Biotite Mica	**MM**	Muscovite Mica			**Gst**	Greenstone	**Eucr**	Eucryptite		
	To (m)	**Lab Spl. No**	**Geo sample (X)**	**colour*** **	**Geology** (E.g. Q + F)**	**From (m)**	**To (m)**	**Lab Spl. No**	**Geo sample (X)**	**colour*** **	**Geology****
0	1	A001-1	BN-PD-SQI-009		AF ,L	25	26	A026-26	BN-PD-SQI-009		AF ,L
1	2	-2			AF ,L	26	27	-27			AF ,L ,MM
2	3	-3			AF ,L	27	28	-28			AF ,MM ,Q ,L
3	4	-4			AF ,L	28	29	-29			AF ,MM
4	5	-5			Pt ,AF ,MM	29	30	-30			AF ,MM ,Q
5	6	-6			Pt ,L ,Q	30	31	-31			AF ,MM ,Q
6	7	-7			AF ,MM ,Pt ,L	31	32	-32			AF ,MM
7	8	-8			Pt ,MM ,AF ,SQI	32	33	A033-33	BN-PD-SQI-009		AF ,Gst
8	9	-9			SQI ,Pt	33	34	-34			Gst weathered
9	10	-10			Pt	34	35	-35			Gst weathered
10	11	-11			Pt	35	36	-36			Gst weathered

11	12	-12			Pt	36	37	-37			Gst weathered
12	13	-13			Pt	37	38	-38			Gst weathered
13	14	-14			Pt	38	39	-39			Gst weathered
14	15	-15			Pt	39	40	-40			Gst weathered
15	16	-16			Pt	40	41	-41			
16	17	-17			Pt ,L ,MM	41	42	-42			
17	18	-18			MF ,L	42	43	-43			
18	19	-19			AF ,L	43	44	-44			
19	20	-20			L ,AF	44	45	-45			
20	21	-21			AF ,L ,Q	45	46	-46			
21	22	-22			AF ,MM ,Q	46	47	-47			
22	23	-23			Q ,AF ,L	47	48	-48			
23	24	-24			AF ,Q ,L	48	49	-49			
24	25	-25			AF ,L	49	50	-50			

DATE:	6/8/2018	**NO. LAB SAMPLES:**	8	**SAMPLER:**	L.M
SECTOR:	CEMETEREY	**NO. GEO SAMPLES:**	8	**GEO:**	A.SG
HOLE NO.:	C-PD-PET-006				
TYPE*	PD	**DATUM:**	WGS 84		
EOH:	22M	**X:**	336075		
Inclination:	-90	**Y:**	7793617	*Type: * PD; RC; DD (core)*	
Azimuth:	0	**Z:**	1133M	'Coluor: *** Brown (B); Red (R); Grey (Gy); Green (Gr); Pink (Pk); Purple (Pl); White (W) Black (Bk); Yellow (Y).	

Geology**							
OB	Overburden/rubble	**A**	Amblygonite	**L**	Lepidolite	**Hect**	Hectorite
W	Weathered	**SQI**	Spodumene	**Be**	Beryl	**D**	Dolerite
F	Fresh	**Pt**	Petalite	**Ta**	Tantalite	**AF**	Albite Feldspar
Q	Quartz	**Pol**	Pollucite	**C**	Cassiterite	**MF**	Microcline Feldspar
BM	Biotite Mica	**MM**	Muscovite Mica	**Gst**	Greenstone	**Eucr**	Eucryptite

	To (m)	**Lab Spl. No**	**Geo sample (X)**	**colour*** **	**Geology** (E.g. Q + F)**	**From (m)**	**To (m)**	**Lab Spl. No**	**Geo sample (X)**	**colour*** **	**Geology** (E.g. Q + F)**
0	1	-1		B	OB -Q ,Rubble	25	26	-26			

1	2	-2		B	Q Rubble -Doleritic Gst	26	27	-27			
2	3	-3		Gr	Doleritic Gst	27	28	-28			
3	4	-4		Gr	Doleritic Gst	28	29	-29			
4	5	-5		Gr	Doleritic Gst	29	30	-30			
5	6	-6		Gr	Doleritic Gst	30	31	-31			
6	7	-7		Gr	Doleritic Gst	31	32	-32			
7	8	-8		Gr	Doleritic Gst	32	33	-33			
8	9	-9		Gr	Doleritic Gst	33	34	-34			
9	10	A001 -10	C-PD-PET-006	Gr	Doleritic Gst	34	35	-35			
10	11	A002-11		W	AF ,Q ,MM ,Pt? ,B?	35	36	-36			
11	12	-12		W	AF ,MM ,Pt? ,Q	36	37	-37			
12	13	-13		W	Q ,Pt? ,AF	37	38	-38			
13	14	-14		W	AF ,Q	38	39	-39			
14	15	-15		W	AF ,Q	39	40	-40			
15	16	A007-16		W	AF ,Q ,MM	40	41	-41			
16	17	A008 -17	C-PD-PET-006	Gr	Doleritic Gst	41	42	-42			
17	18	-18		Gr	Doleritic Gst	42	43	-43			
18	19	-19		Gr	Doleritic Gst	43	44	-44			
19	20	-20		Gr	Doleritic Gst	44	45	-45			

20	21	-21		Gr	Doleritic Gst	45	46	-46			
21	22	-22		Gr	Doleritic Gst	46	47	-47			
22	23	-23				47	48	-48			
23	24	-24				48	49	-49			
24	25	-25				49	50	-50			

BIKITA MINERALS

BIKITA MINERALS (PVT) LIMITED **DRILL LOG & SAMPLING FORM**

DATE:	1/9/2018	**NO. LAB SAMPLES:**	9	**SAMPLER:**	LM
SECTOR:	CEMETEREY	**NO. GEO SAMPLES:**	9	**GEO:**	ASG
HOLE NO.:	C-PD-PET-016				
TYPE*	PD	**DATUM:**	WGS 84		
EOH:	3OM	**X:**	336188		
Inclination:	-90	**Y:**	7793659	*Type: * PD; RC; DD (core)*	
Azimuth:	0	**Z:**	1135M	'Coluor: *** Brown (B); Red (R); Grey (Gy); Green (Gr); Pink (Pk); Purple (Pl); White (W) Black (Bk); Yellow (Y).	

Geology**							
OB	Overburden/rubble	**A**	Amblygonite	**L**	Lepidolite	**Hect**	Hectorite
W	Weathered	**SQI**	Spodumene	**Be**	Beryl	**D**	Dolerite
F	Fresh	**Pt**	Petalite	**Ta**	Tantalite	**AF**	Albite Feldspar
Q	Quartz	**Pol**	Pollucite	**C**	Cassiterite	**MF**	Microcline Feldspar
BM	Biotite Mica	**MM**	Muscovite Mica	**Gst**	Greenstone	**Eucr**	Eucryptite

	To (m)	**Lab Spl. No**	**Geo sample (X)**	**colour*** **	**Geology** (E.g. Q + F)**	**From (m)**	**To (m)**	**Lab Spl. No**	**Geo sample (X)**	**colour*** **	**Geology** (E.g. Q + F)**
0	1	-1		Gr	Gst	25	26	A005 -26	C-PD-PET-016	W	Pt ,Q
1	2	-2		Gr	Gst	26	27	-27		W	Pt ,Q ,L
2	3	-3		Gr	Gst	27	28	-28		W	Pt ,Q ,L
3	4	-4		Gr	Gst	28	29	-29		W	Q ,Pt ,MM
4	5	-5		Gr	Gst	29	30	A009 -26	C-PD-PET-016	W	AF ,MM
5	6	-6		Gr	Gst	30	31	-31			
6	7	-7		Gr	Gst	31	32	-32			
7	8	-8		Gr	Gst	32	33	-33			
8	9	-9		Gr	Gst	33	34	-34			
9	10	-10		Gr	Gst	34	35	-35			
10	11	-11		Gr	Gst	35	36	-36			

11	12	-12		Gr	Gst	36	37	-37			
12	13	-13		Gr	Gst	37	38	-38			
13	14	-14		Gr	Gst	38	39	-39			
14	15	-15		Gr	Gst	39	40	-40			
15	16	-16		Gr	Gst	40	41	-41			
16	17	-17		Gr	Gst	41	42	-42			
17	18	-18		Gr	Gst	42	43	-43			
18	19	-19		Gr	Gst	43	44	-44			
19	20	-20		Gr	Gst	44	45	-45			
20	21	-21		Gr	Gst	45	46	-46			
21	22	A001 -22	C-PD-PET-016	Gr	Gst	46	47	-47			
22	23	-23		Gy	Gst ,AF	47	48	-48			
23	24	-24		W	AF ,MM ,Q ,Pt	48	49	-49			
24	25	A004 - 25	C-PD-PET-016		Pt ,MM	49	50	-50			

BIKITA MINERALS

BIKITA MINERALS (PVT) LIMITED **DRILL LOG & SAMPLING FORM** Page 1 of 1 pages

DATE:	3/3/2019	**NO. LAB SAMPLES:**	21	**SAMPLER:**	VM
SECTOR:	MCMURDON	**NO. GEO SAMPLES:**	21	**GEO:**	AG
HOLE NO.:	MC-LP-PD-009				
TYPE*	PD	**DATUM:**	WGS 84		
EOH:	22M	**X:**	336183.4		
Inclination:	-90	**Y:**	7792027.6	*Type: * PD; RC; DD (core)*	
Azimuth:	0	**Z:**	1203.564M	'Coluor: *** Brown (B); Red (R); Grey (Gy); Green (Gr); Pink (Pk); Purple (Pl); White (W) Black (Bk); Yellow (Y).	

Geology**							
OB	Overburden/rubble	**A**	Amblygonite	**L**	Lepidolite	**Hect**	Hectorite
W	Weathered	**SQI**	Spodumene	**Be**	Beryl	**D**	Dolerite
F	Fresh	**Pt**	Petalite	**Ta**	Tantalite	**AF**	Albite Feldspar
Q	Quartz	**Pol**	Pollucite	**C**	Cassiterite	**MF**	Microcline Feldspar
BM	Biotite Mica	**MM**	Muscovite Mica	**Gst**	Greenstone	**Eucr**	Eucryptite

	To (m)	**Lab Spl. No**	**Geo sample (X)**	**colour*** **	**Geology** (E.g. Q + F)**	**From (m)**	**To (m)**	**Lab Spl. No**	**Geo sample (X)**	**colour*** **	**Geology** (E.g. Q + F)**
0	1	A001 - 1	MC-LP-PD-009	B	L Rubble	25	26	-26			
1	2	-2		Pl	L Rubble	26	27	-27			

2	3	-3		Pl	L Rubble	27	28	-28			
3	4	-4		Pl	L Rubble	28	29	-29			
4	5	-5		W	Q ,L	29	30	-30			
5	6	-6		Pl	L ,Q	30	31	-31			
6	7	-7		W	AF ,Q ,L?	31	32	-32			
7	8	-8		W	AF ,Q ,L	32	33	-33			
8	9	-9		Pl	L ,Q ,AF	33	34	-34			
9	10	-10		Pl	L ,AF ,Q	34	35	-35			
10	11	-11		Pl	L ,Q ,AF	35	36	-36			
11	12	-12		W	AF ,L ,Q	36	37	-37			
12	13	A013 - 13	MC-LP-PD-009	W	AF ,L ,Q	37	38	-38			
13	14	-14		W	Q ,AF	38	39	-39			
14	15	-15		W	Q ,MM	39	40	-40			
15	16	-16		W	Q ,MM	40	41	-41			
16	17	-17		Gy	MM ,Q ,AF	41	42	-42			
17	18	-18		Gy	MM ,AF	42	43	-43			
18	19	-19		Gy	MM ,Q ,AF	43	44	-44			
19	20	-20		Gy	Q ,MM	44	45	-45			
20	21	A021 - 21	MC-LP-PD-009	Gr	Gst	45	46	-46			
21	22	-22		Gr	Gst	46	47	-47			

22	23	-23				47	48	-48			
23	24	-24				48	49	-49			
24	25	-25				49	50	-50			

BIKITA MINERALS

BIKITA MINERALS (PVT) LIMITED **DRILL LOG & SAMPLING FORM** Page 1 of 1 pages

DATE:	04/03/19 - 05/03/19	**NO. LAB SAMPLES:**	24	**SAMPLER:**	T.K
SECTOR:	MCMURDON	**NO. GEO SAMPLES:**	24	**GEO:**	A.G
HOLE NO.:	MC-LP-014				
TYPE*	P.D	**DATUM:**	WGS 84		
EOH:	25M	**X:**	336196.66		
Inclination:	-90	**Y:**	7792049.1	*Type: * PD; RC; DD (core)*	
Azimuth:	0	**Z:**	1202.774M	'Coluor: *** Brown (B); Red (R); Grey (Gy); Green (Gr); Pink (Pk); Purple (Pl); White (W) Black (Bk); Yellow (Y).	

Geology**

OB	Overburden/rubble	**A**	Amblygonite	**L**	Lepidolite	**Hect**	Hectorite
W	Weathered	**SQI**	Spodumene	**Be**	Beryl	**D**	Dolerite

F	Fresh	**Pt**	Petalite	**Ta**	Tantalite	**AF**	Albite Feldspar
Q	Quartz	**Pol**	Pollucite	**C**	Cassiterite	**MF**	Microcline Feldspar
BM	Biotite Mica	**MM**	Muscovite Mica	**Gst**	Greenstone	**Eucr**	Eucryptite

	To (m)	Lab Spl. No	Geo sample (X)	colour***	Geology** (E.g. Q + F)	From (m)	To (m)	Lab Spl. No	Geo sample (X)	colour***	Geology** (E.g. Q + F)
0	1	A001 -1	MC-LP-PD-014	B	OB-AF ,L ,MM	25	26	-26			
1	2	-2		Gy	MM ,Q	26	27	-27			
2	3	-3		W	Q ,L	27	28	-28			
3	4	-4		W	Q	28	29	-29			
4	5	-5		W	MF	29	30	-30			
5	6	-6		W	MF	30	31	-31			
6	7	-7		W	Q	31	32	-32			
7	8	-8		W	AF ,Q	32	33	-33			
8	9	-9		W	AF	33	34	-34			
9	10	-10		Gy	AF ,L	34	35	-35			
10	11	-11		Gy	AF ,L	35	36	-36			
11	12	-12		Gy	AF ,L	36	37	-37			
12	13	-13		Gy	AF ,L	37	38	-38			
13	14	-14		Pl	L ,AF	38	39	-39			
14	15	-15		Pl	L ,AF ,Q	39	40	-40			

15	16	-16		Gy	AF ,L ,Q	40	41	-41			
16	17	-17		Gy	AF ,MM ,Q	41	42	-42			
17	18	-18		Gy	MM ,AF	42	43	-43			
18	19	-19		Gy	MM ,AF	43	44	-44			
19	20	-20		Gy	MM ,AF	44	45	-45			
20	21	-21		Gy	MM ,AF	45	46	-46			
21	22	-22		Gy	AF ,MM	46	47	-47			
22	23	-23		Gy	AF ,Q ,MM	47	48	-48			
23	24	A024 -24	MC-LP-PD- 014	Gy	AF ,MM	48	49	-49			
24	25	-25			Gst	49	50	-50			

Appendix 1c: Reverse Circulation drilling log sheets

BIKITA MINERALS

BIKITA MINERALS (PVT) LIMITED **DRILL LOG & SAMPLING FORM** Page 1 of 2 pages

		NO. LAB			
DATE:	10/8/2018	**SAMPLES:**	41	**SAMPLER:**	TK
		NO. GEO			
SECTOR:	AL HAYAT	**SAMPLES:**	41	**GEO:**	JPA
HOLE NO.:	AHS-RC-PET-001				
TYPE*	RC	**DATUM:**	WGS 84		
EOH:	75M	**X:**	336548		
Inclination:	-90	**Y:**	7792852	*Type: * PD; RC; DD (core)*	
Azimuth:	0	**Z:**	1152M	'Coluor: *** Brown (B); Red (R); Grey (Gy); Green (Gr); Pink (Pk); Purple (Pl); White (W) Black (Bk); Yellow (Y).	

Geology**							
OB	Overburden/rubble	**A**	Amblygonite	**L**	Lepidolite	**Hect**	Hectorite
W	Weathered	**SQl**	Spodumene	**Be**	Beryl	**D**	Dolerite
F	Fresh	**Pt**	Petalite	**Ta**	Tantalite	**AF**	Albite Feldspar
Q	Quartz	**Pol**	Pollucite	**C**	Cassiterite	**MF**	Microcline Feldspar
BM	Biotite Mica	**MM**	Muscovite Mica	**Gst**	Greenstone	**Eucr**	Eucryptite

	To (m)	Lab Spl. No	Geo sample (X)	colour***	Geology** (E.g. Q + F)	From (m)	To (m)	Lab Spl. No	Geo sample (X)	colour***	Geology** (E.g. Q + F)
0	1	-1		Gr	Gst	25	26	-26		Gr	Gst
1	2	-2		Gr	Gst	26	27	-27		Gr	Gst
2	3	-3		Gr	Gst	27	28	-28		Gr	Gst
3	4	-4		Gr	Gst	28	29	-29		Gr	Gst
4	5	-5		Gr	Gst	29	30	-30		Gr	Gst
5	6	-6		Gr	Gst	30	31	-31		Gr	Gst
6	7	-7		Gr	Gst	31	32	-32		Gr	Gst
7	8	-8		Gr	Gst	32	33	A001 -33	AHS-RC-PET-001	Gr	Gst
8	9	-9		Gr	Gst	33	34	-34		W	AF,Q,M
9	10	-10		Gr	Gst	34	35	-35		W	M,AF,Q
10	11	-11		Gr	Gst	35	36	-36		W	MF,MM
11	12	-12		Gr	Gst	36	37	-37		Gy	MF,Q,MM

12	13	-13		Gr	Gst	37	38	-38		W	MF,MM ,Q
13	14	-14		Gr	Gst	38	39	-39		W	MF,MM
14	15	-15		Gr	Gst	39	40	-40		W	MF
15	16	-16		Gr	Gst	40	41	-41		W	MF
16	17	-17		Gr	Gst	41	42	-42		Gy	MF ,Pt ,Q ,MM
17	18	-18		Gr	Gst	42	43	-43		Gy	MF
18	19	-19		Gr	Gst	43	44	-44		W	MF
19	20	-20		Gr	Gst	44	45	-45		W	MF
20	21	-21		Gr	Gst	45	46	-46		W	MF
21	22	-22		Gr	Gst	46	47	-47		Gy	MF,Pt
22	23	-23		Gr	Gst	47	48	-48		Gy	Pt
23	24	-24		Gr	Gst	48	49	-49		Gy	MF
24	25	-25		Gr	Gst	49	50	A018 -50	AHS-RC-PET-001	Gy	Pt

DATE:	10/6/2018	**NO. LAB SAMPLES:**	41	**SAMPLER:**	TK
SECTOR:	AL HAYAT	**NO. GEO SAMPLES:**	41	**GEO:**	JPA
HOLE NO.:	AHS-RC-PET-001				
TYPE*	RC	**DATUM:**	WGS 84		
EOH:	75M	**X:**	336548		
Inclination:	-90	**Y:**	7792852		
Azimuth:	0	**Z:**	1152M		

*Type: * PD; RC; DD (core)*

Coluor: *** Brown (B); Red (R); Grey (Gy); Green (Gr); Pink (Pk); Purple (Pl); White (W) Black (Bk); Yellow (Y).

Geology**							
OB	Overburden/rubble	**A**	Amblygonite	**L**	Lepidolite	**Hect**	Hectorite
W	Weathered	**SQI**	Spodumene	**Be**	Beryl	**D**	Dolerite
F	Fresh	**Pt**	Petalite	**Ta**	Tantalite	**AF**	Albite Feldspar
Q	Quartz	**Pol**	Pollucite	**C**	Cassiterite	**MF**	Microcline Feldspar
BM	Biotite Mica	**MM**	Muscovite Mica	**Gst**	Greenstone	**Eucr**	Eucryptite

From (m)	**To (m)**	**Lab Spl. No**	**Geo sample (X)**	**colour*** **	**Geology** (E.g. Q + F)**	**From (m)**	**To (m)**	**Lab Spl. No**	**Geo sample (X)**	**colour*** **	**Geology** (E.g. Q + F)**

50	51	A019 -51	AHS-RC-PET-001	PK	Pt,MF ,Eucr?	75	76	-76			
51	52	-52		Gy	MF ,L ,Q	76	77	-77			
52	53	-53		Gy	MF ,L	77	78	-78			
53	54	-54		Gy	MF,L	78	79	-79			
54	55	-55		Gy	MF,L	79	80	-80			
55	56	-56		Gy	MF,L	80	81	-81			
56	57	-57		Gy	MF ,Eucr	81	82	-82			
57	58	-58		Gy	Pt,MF	82	83	-83			
58	59	-59		Gy	Pt,L	83	84	-84			
59	60	-60		Gy	Pt ,L ,AF	84	85	-85			
60	61	-61	AHS-RC-PET-001	PK	L,AF ,Pt	85	86	-86			
61	62	-62		PK	L,Pt,AF	86	87	-87			
62	63	-63		W	Pt ,L	87	88	-88			
63	64	-64		W	MM ,Q ,AF	88	89	-89			
64	65	-65		W	MF	89	90	-90			
65	66	-66		Gy	MF	90	91	-91			
66	67	-67		Gy	MM,AF ,Q	91	92	-92			
67	68	-68		Gy	MF,MM ,Q	92	93	-93			
68	69	-69		w	AF ,MM ,Q	93	94	-94			
69	70	-70		w	AF ,MM ,Q	94	95	-95			

70	71	-71		w	AF ,MM	95	96	-96			
71	72	-72		w	AF ,MM	96	97	-97			
72	73	A041 -73	AHS-RC-PET-001	Gr	Gst	97	98	-98			
73	74	-74		Gr	Gst	98	99	-99			
74	75	-75		Gr	Gst	99	100	-100			



BIKITA MINERALS (PVT) LIMITED

DRILL LOG & SAMPLING FORM

DATE:	24/11/2017	**NO. LAB SAMPLES:**	49	**SAMPLER:**	V.M
SECTOR:	AL HAYAT	**NO. GEO SAMPLES:**	49	**GEO:**	J.P.A
HOLE NO.:	AH-RC-PET-009				
TYPE*	RC	**DATUM:**	WGS 84		
EOH:	69M	**X:**	336702		
Inclination:	-90	**Y:**	7793154	*Type: * PD; RC; DD (core)*	
Azimuth:	0	**Z:**	1139	'Coluor: *** Brown (B); Red (R); Grey (Gy); Green (Gr); Pink (Pk); Purple (Pl); White (W)	

Black (Bk); Yellow (Y).

Geology**							
OB	Overburden/rubble	**A**	Amblygonite	**L**	Lepidolite	**Hect**	Hectorite
W	Weathered	**SQI**	Spodumene	**Be**	Beryl	**D**	Dolerite
F	Fresh	**Pt**	Petalite	**Ta**	Tantalite	**AF**	Albite Feldspar
Q	Quartz	**Pol**	Pollucite	**C**	Cassiterite	**MF**	Microcline Feldspar
BM	Biotite Mica	**MM**	Muscovite Mica	**Gst**	Greenstone	**Eucr**	Eucryptite

	To (m)	**Lab Spl. No**	**Geo sample (X)**	**colour*** **	**Geology** (E.g. Q + F)**	**From (m)**	**To (m)**	**Lab Spl. No**	**Geo sample (X)**	**colour*** **	**Geology** (E.g. Q + F)**
0	1	-1		Gr	Gst	25	26	A009 -26	AH-RC-PET-009	W	Q,Pt,L
1	2	-2		Gr	Gst	26	27	-27		W	Pt,L
2	3	-3		Gr	Gst	27	28	-28		W	AF,Pt,MM
3	4	-4		Gr	Gst	28	29	-29		W	Q,MM,Pt?,MF
4	5	-5		Gr	Gst	29	30	-30		W	MF,MM,Q
5	6	-6		Gr	Gst	30	31	-31		W	Q,Pt
6	7	-7		Gr	Gst	31	32	-32		W	MF,Q
7	8	-8		Gr	Gst	32	33	-33		W	MF,Q
8	9	-9		Gr	Gst	33	34	-34		W	MF,Pt

9	10	-10		Gr	Gst	34	35	-35		W	MM,MF
10	11	-11		Gr	Gst	35	36	-36		W	MM,MF
11	12	-12		Gr	Gst	36	37	-37		W	MM,MF
12	13	-13		Gr	Gst	37	38	-38		W	Pt
13	14	-14		Gr	Gst	38	39	-39		W	Pt
14	15	-15		Gr	Gst	39	40	-40		W	Pt,Q
15	16	-16		Gr	Gst	40	41	-41		W	Pt
16	17	-17		Gr	Gst	41	42	-42		W	Pt,MM
17	18	A001 - 18	AH-RC-PET-009	Gr	Gst	42	43	-43		W	MF,Pt,MM
18	19	-19		Gr	Gst	43	44	-44		W	F,Pt
19	20	-20		Gy	Gst ,MM,Pt?	44	45	-45		W	MF,Pt,MM
20	21	-21		W	MM,Pt,MF	45	46	-46		W	Pt,MM,AF
21	22	-22		W	MF,Pt,L	46	47	-47		W	Pt,MM ,AF
22	23	-23		W	Q,Pt	47	48	-48		W	Pt
23	24	-24		W	Pt,L	48	49	-49		W	Pt,MM
24	25	A008 - 25	AH-RC-PET-009	W	Pt	49	50	A033 - 50	AH-RC-PET-009	W	Pt,MM

DATE:	24-25/11/2017	**NO. LAB SAMPLES:**	49	**SAMPLER:**	V.M
SECTOR:	AL HAYAT	**NO. GEO SAMPLES:**	49	**GEO:**	JPA
HOLE NO.:	AH-RC-PET-009				
TYPE*	RC	**DATUM:**	WGS 84		
EOH:	69M	**X:**	336702		
Inclination:	-90	**Y:**	7793154	*Type: * PD; RC; DD (core)*	
Azimuth:	0			Coluor: *** Brown (B); Red (R); Grey (Gy); Green (Gr); Pink (Pk); Purple (Pl); White (W) Black (Bk); Yellow (Y).	

Geology**

OB	Overburden/rubble	**A**	Amblygonite	**L**	Lepidolite	**Hect**	Hectorite
W	Weathered	**SQI**	Spodumene	**Be**	Beryl	**D**	Dolerite
F	Fresh	**Pt**	Petalite	**Ta**	Tantalite	**AF**	Albite Feldspar
Q	Quartz	**Pol**	Pollucite	**C**	Cassiterite	**MF**	Microcline Feldspar
BM	Biotite Mica	**MM**	Muscovite Mica	**Gst**	Greenstone	**Eucr**	Eucryptite

From (m)	To (m)	Lab Spl. No	Geo sample (X)	colour***	Geology** (E.g. Q + F)	From (m)	To (m)	Lab Spl. No	Geo sample (X)	colour***	Geology** (E.g. Q + F)
50	51	A034 - 51	AH-RC-PET-009	W	MM,MF	75	76	-76			
51	52	-52		W	MM,Q	76	77	-77			
52	53	-53		W	MM ,MF	77	78	-78			
53	54	-54		W	MM,Q	78	79	-79			
54	55	-55		W	MM,Pt	79	80	-80			
55	56	-56		W	MF,MM	80	81	-81			
56	57	-57		W	Pt,MF,MM	81	82	-82			
57	58	-58		W	MM,Q	82	83	-83			
58	59	-59		W	MM,AF	83	84	-84			
59	60	-60		W	AF,MM	84	85	-85			
60	61	-61		W	AF,Q,MM	85	86	-86			
61	62	-62		Gy	GST,Q,AF	86	87	-87			
62	63	-63		Gy	MM,AF,Gst	87	88	-88			
63	64	-64		Gy	AF,Q,Gst	88	89	-89			
64	65	-65		Gr	Gst	89	90	-90			
65	66	A034 - 66	AH-RC-PET-009	Gr	Gst	90	91	-91			
66	67	-67		Gr	Gst	91	92	-92			

67	68	-68		Gr	Gst	92	93	-93			
68	69	-69		Gr	Gst	93	94	-94			
69	70	-70				94	95	-95			
70	71	-71				95	96	-96			
71	72	-72				96	97	-97			
72	73	-73				97	98	-98			
73	74	-74				98	99	-99			
74	75	-75				99	100	-100			

BIKITA MINERALS

BIKITA MINERALS (PVT) LIMITED

DRILL LOG & SAMPLING FORM

Page 1 of 2 pages

DATE:	8/11/2018	**NO. LAB SAMPLES:**	49	**SAMPLER:**	W GARIRA
SECTOR:	BIKITA EAST	**NO. GEO SAMPLES:**	49	**GEO:**	ASG
HOLE NO.:	BE-RC-PET-001				
TYPE*	RC	**DATUM:**	WGS 84		
EOH:	84M	**X:**	336443		
Inclination:	-90	**Y:**	7792480	*Type: * PD; RC; DD (core)*	
Azimuth:	0	**Z:**	1191M	'Coluor: *** Brown (B); Red (R); Grey (Gy); Green (Gr); Pink (Pk); Purple (Pl); White (W)	

Black (Bk); Yellow (Y).

Geology**							
OB	Overburden/rubble	**A**	Amblygonite	**L**	Lepidolite	**Hect**	Hectorite
W	Weathered	**SQl**	Spodumene	**Be**	Beryl	**D**	Dolerite
F	Fresh	**Pt**	Petalite	**Ta**	Tantalite	**AF**	Albite Feldspar
Q	Quartz	**Pol**	Pollucite	**C**	Cassiterite	**MF**	Microcline Feldspar
BM	Biotite Mica	**MM**	Muscovite Mica	**Gst**	Greenstone	**Eucr**	Eucryptite

	To (m)	**Lab Spl. No**	**Geo sample (X)**	**colour*** **	**Geology** (E.g. Q + F)**	**From (m)**	**To (m)**	**Lab Spl. No**	**Geo sample (X)**	**colour*** **	**Geology** (E.g. Q + F)**
0	1	-1		Gr	Gst	25	26	-26		Gr	Gst
1	2	-2		Gr	Gst	26	27	-27		Gr	Gst
2	3	-3		Gr	Gst	27	28	-28		Gr	Gst
3	4	-4		Gr	Gst	28	29	-29		Gr	Gst
4	5	-5		Gr	Gst	29	30	-30		Gr	Gst
5	6	-6		Gr	Gst	30	31	-31		Gr	Gst
6	7	-7		Gr	Gst	31	32	-32		Gr	Gst
7	8	-8		Gr	Gst	32	33	-33		Gr	Gst
8	9	-9		Gr	Gst	33	34	-34		Gr	Gst
9	10	-10		Gr	Gst	34	35	A001 - 35	BE-RC-PET-001	Gr	Gst ,MF ,MM

10	11	-11		Gr	Gst	35	36	-36		Gy	MF ,MM
11	12	-12		Gr	Gst	36	37	-37		W	MF, Q
12	13	-13		Gr	Gst	37	38	-38		W	AF , MM ,Q
13	14	-14		Gr	Gst	38	39	-39		W	MF
14	15	-15		Gr	Gst	39	40	-40		W	MF ,MM
15	16	-16		Gr	Gst	40	41	-41		W	MF
16	17	-17		Gr	Gst	41	42	-42		W	Q
17	18	-18		Gr	Gst	42	43	-43		W	Q
18	19	-19		Gr	Gst	43	44	-44		W	Q
19	20	-20		Gr	Gst	44	45	-45		W	Q
20	21	-21		Gr	Gst	45	46	-46		W	Q
21	22	-22		Gr	Gst	46	47	-47		W	Q
22	23	-23		Gr	Gst	47	48	-48		W	Q
23	24	-24		Gr	Gst	48	49	-49		W	Q
24	25	-25		Gr	Gst	49	50	A016 - 50	BE-RC-PET-001	W	Q

DATE:		**NO. LAB SAMPLES:**	49	**SAMPLER:**	W GARIRA
SECTOR:	BIKITA EAST	**NO. GEO SAMPLES:**	49	**GEO:**	ASG
HOLE NO.:	BE-RC-PET-001				
TYPE*	RC	**DATUM:**	WGS 84		
EOH:	84M	**X:**	336443		
Inclination:	-90	**Y:**	7792480	*Type: * PD; RC; DD (core)*	
Azimuth:	0	**Z:**	1191m	Coluor: *** Brown (B); Red (R); Grey (Gy); Green (Gr); Pink (Pk); Purple (Pl); White (W) Black (Bk); Yellow (Y).	

Geology**							
OB	Overburden/rubble	**A**	Amblygonite	**L**	Lepidolite	**Hect**	Hectorite
W	Weathered	**SQI**	Spodumene	**Be**	Beryl	**D**	Dolerite
F	Fresh	**Pt**	Petalite	**Ta**	Tantalite	**AF**	Albite Feldspar
Q	Quartz	**Pol**	Pollucite	**C**	Cassiterite	**MF**	Microcline Feldspar
BM	Biotite Mica	**MM**	Muscovite Mica	**Gst**	Greenstone	**Eucr**	Eucryptite

From (m)	**To (m)**	**Lab Spl. No**	**Geo sample (X)**	**colour*** **	**Geology** (E.g. Q + F)**	**From (m)**	**To (m)**	**Lab Spl. No**	**Geo sample (X)**	**colour*** **	**Geology** (E.g. Q + F)**

50	51	A017 -51	BE-RC-PET-001	W	Q	75	76	A042 -76	BE-RC-PET-001	Pl	L ,AF ,Q
51	52	-52		W	Q	76	77	-77		Gy	AF ,L ,MM
52	53	-53		W	MF ,L	77	78	-78		Gy	AF ,MM
53	54	-54		W	Q ,L	78	79	-79		Gy	MM ,AF
54	55	-55		W	AF ,L	79	80	-80		Gy	AF ,MM ,Epid
55	56	-56		W	AF ,L	80	81	-81		Gy	AF ,MM
56	57	-57		W	AF ,L	81	82	-82		W	AF
57	58	-58		W	AF ,L ,Q	82	83	A049 -83	BE-RC-PET-001	W	MF
58	59	-59		W	AF ,Q ,B	83	84	-84		Gr	Gst
59	60	-60		W	AF ,L ,Q	84	85	-85			
60	61	-61		Pl	L ,AF	85	86	-86			
61	62	-62		Pl	L ,AF	86	87	-87			
62	63	-63		Pl	L ,AF	87	88	-88			
63	64	-64		Pl	L ,AF	88	89	-89			
64	65	-65		W	AF ,L	89	90	-90			
65	66	-66		W	AF ,L	90	91	-91			
66	67	-67		W	AF ,L	91	92	-92			
67	68	-68		W	AF ,L	92	93	-93			
68	69	-69		W	AF ,L	93	94	-94			
69	70	-70		W	AF ,L	94	95	-95			

70	71	-71		W	AF ,L	95	96	-96			
71	72	-72		Pl	L ,Q ,AF	96	97	-97			
72	73	-73		Pl	L ,Q ,AF	97	98	-98			
73	74	-74		W	Q , L ,AF	98	99	-99			
74	75	A041 -75	BE-RC-PET-001	W	Q , L ,MF	99	100	-100			

BIKITA MINERALS

BIKITA MINERALS (PVT) LIMITED

DRILL LOG & SAMPLING FORM

Page 1 of 2 pages

DATE:	10/1/2019	**NO. LAB SAMPLES:**	36	**SAMPLER:**	GEO TEAM
SECTOR:	GIANT-EAST	**NO. GEO SAMPLES:**	36	**GEO:**	A.G
HOLE NO.:	GE-RC-PET-001				
TYPE*	RC	**DATUM:**	WGS 84		
EOH:	60M	**X:**	336041		
Inclination:	-90	**Y:**	7793319	*Type: * PD; RC; DD (core)*	
Azimuth:	0	**Z:**	1139m	'Coluor: *** Brown (B); Red (R); Grey (Gy); Green (Gr); Pink (Pk); Purple (Pl); White (W) Black (Bk); Yellow (Y).	

Geology**							
OB	Overburden/rubble	**A**	Amblygonite	**L**	Lepidolite	**Hect**	Hectorite
W	Weathered	**SQI**	Spodumene	**Be**	Beryl	**D**	Dolerite
F	Fresh	**Pt**	Petalite	**Ta**	Tantalite	**AF**	Albite Feldspar
Q	Quartz	**Pol**	Pollucite	**C**	Cassiterite	**MF**	Microcline Feldspar
BM	Biotite Mica	**MM**	Muscovite Mica	**Gst**	Greenstone	**Eucr**	Eucryptite

	To (m)	**Lab Spl. No**	**Geo sample (X)**	**colour*** **	**Geology** (E.g. Q + F)**	**From (m)**	**To (m)**	**Lab Spl. No**	**Geo sample (X)**	**colour*** **	**Geology** (E.g. Q + F)**
0	1	-1		B	OB rubble	25	26	A024 -26	GE-RC-PET-001	W	AF ,Pt ,MM ,Q
1	2	-2		B	OB rubble & highly W Gst	26	27	-27		W	AF ,MM
2	3	A001 -3	GE-RC-PET-001	W	Q, AF, MM	27	28	-28		Gr	Gst ,AF
3	4	-4		W	AF ,Pt ,MM	28	29	-29		Gr	Gst ,AF
4	5	-5		W	AF ,Pt	29	30	-30		w	AF ,SQI?
5	6	-6		W	MF ,Pt	30	31	-31		w	MF ,SQI?
6	7	-7		W	Pt	31	32	-32		w	AF ,Q ,MM
7	8	-8		W	Pt	32	33	-33		w	AF, Eucr?
8	9	-9		W	Pt ,AF	33	34	-34		w	AF

9	10	-10		W	AF ,PT ,SQI?	34	35	A033 -35	GE-RC-PET-001	Gr	Gst
10	11	-11		W	AF ,Q ,SQI?	35	36	-36		Gr	Gst
11	12	-12		Gy	AF, Q	36	37	-37		Gr	Gst
12	13	-13		W	AF, Pt	37	38	-38		Gr	Gst
13	14	-14		W	AF ,Eucr	38	39	-39		Gr	Gst
14	15	-15		Gy	AF ,Gst	39	40	-40		Gr	Gst
15	16	-16		Gy	MF ,Q ,Pt	40	41	-41		Gr	Gst
16	17	-17		W	Pt ,MF ,Q ,Eucr	41	42	-42		Gr	Gst
17	18	-18		W	Pt, MF	42	43	-43		Gr	Gst
18	19	-19		W	MF ,Q ,MM	43	44	-44		Gr	Gst
19	20	-20		W	Pt, Eucr ,Q	44	45	-45		Gr	Gst
20	21	-21		W	AF ,Q ,MM	45	46	A034 -46	GE-RC-PET-001	W	MF ,Gst
21	22	-22		W	SQI ,AF	46	47	-47		W	MF
22	23	-23		W	Eucr ,SQI	47	48	A036 -48	GE-RC-PET-001	Gr	Gst ,MF
23	24	-24		W	Eucr ,SQI ,Q ,MM	48	49	-49			Gst
24	25	A023 -25	GE-RC-PET-001	W	AF ,Pt ,MM	49	50	-50			Gst

DATE:	10/1/2019	**NO. LAB SAMPLES:**	36	**SAMPLER:**	GEO TEAM
SECTOR:	GIANT-EAST	**NO. GEO SAMPLES:**	36	**GEO:**	A.G

HOLE NO.:	GE-RC-PET-001		
TYPE*	RC	**DATUM:**	WGS 84
EOH:	60M	**X:**	336041
Inclination:	-90	**Y:**	7793319
Azimuth:	0	**Z:**	

*Type: * PD; RC; DD (core)*

Coluor: *** Brown (B); Red (R); Grey (Gy); Green (Gr); Pink (Pk); Purple (Pl); White (W) Black (Bk); Yellow (Y).

Geology**

OB	Overburden/rubble	**A**	Amblygonite	**L**	Lepidolite	**Hect**	Hectorite
W	Weathered	**SQI**	Spodumene	**Be**	Beryl	**D**	Dolerite
F	Fresh	**Pt**	Petalite	**Ta**	Tantalite	**AF**	Albite Feldspar
Q	Quartz	**Pol**	Pollucite	**C**	Cassiterite	**MF**	Microcline Feldspar
BM	Biotite Mica	**MM**	Muscovite Mica	**Gst**	Greenstone	**Eucr**	Eucryptite

From (m)	To (m)	Lab Spl. No	Geo sample (X)	colour***	Geology** (E.g. Q + F)	From (m)	To (m)	Lab Spl. No	Geo sample (X)	colour***	Geology** (E.g. Q + F)
50	51	-51		Gr	Gst	75	76	-76			
51	52	-52		Gr	Gst	76	77	-77			
52	53	-53		Gr	Gst	77	78	-78			
53	54	-54		Gr	Gst	78	79	-79			
54	55	-55		Gr	Gst	79	80	-80			
55	56	-56		Gr	Gst	80	81	-81			
56	57	-57		Gr	Gst	81	82	-82			
57	58	-58		Gr	Gst	82	83	-83			
58	59	-59		Gr	Gst	83	84	-84			
59	60	-60		Gr	Gst	84	85	-85			
60	61	-61				85	86	-86			
61	62	-62				86	87	-87			
62	63	-63				87	88	-88			
63	64	-64				88	89	-89			
64	65	-65				89	90	-90			
65	66	-66				90	91	-91			
66	67	-67				91	92	-92			
67	68	-68				92	93	-93			
68	69	-69				93	94	-94			

69	70	-70				94	95	-95			
70	71	-71				95	96	-96			
71	72	-72				96	97	-97			
72	73	-73				97	98	-98			
73	74	-74				98	99	-99			
74	75	-75				99	100	-100			

BIKITA MINERALS

BIKITA MINERALS (PVT) LIMITED

DRILL LOG & SAMPLING FORM

Page 1 of 2 pages

		NO. LAB			
DATE:	5/10/2018	**SAMPLES:**	43	**SAMPLER:**	N.B.D
		NO. GEO			
SECTOR:	LEDINGHAM	**SAMPLES:**	43	**GEO:**	ASG
HOLE NO.:	LN-RC-PET-004				
TYPE*	RC	**DATUM:**	WGS 84		
EOH:	69M	**X:**	336094		
Inclination:	90	**Y:**	7793108	*Type: * PD; RC; DD (core)*	
Azimuth:	0	**Z:**	1154M	'Coluor: *** Brown (B); Red (R); Grey (Gy); Green (Gr); Pink (Pk); Purple (Pl); White (W)	

Black (Bk); Yellow (Y).

Geology**							
OB	Overburden/rubble	**A**	Amblygonite	**L**	Lepidolite	**Hect**	Hectorite
W	Weathered	**SQI**	Spodumene	**Be**	Beryl	**D**	Dolerite
F	Fresh	**Pt**	Petalite	**Ta**	Tantalite	**AF**	Albite Feldspar
Q	Quartz	**Pol**	Pollucite	**C**	Cassiterite	**MF**	Microcline Feldspar
BM	Biotite Mica	**MM**	Muscovite Mica	**Gst**	Greenstone	**Eucr**	Eucryptite

	To (m)	**Lab Spl. No**	**Geo sample (X)**	**colour*** **	**Geology** (E.g. Q + F)**	**From (m)**	**To (m)**	**Lab Spl. No**	**Geo sample (X)**	**colour*** **	**Geology** (E.g. Q + F)**
0	1	-1		Gr	Gst	25	26	A002 - 26	LN-RC-PET-004	W	AF ,M, Q
1	2	-2		Gr	Gst	26	27	-27		W	Pt ,MF
2	3	-3		Gr	Gst	27	28	-28		W	Pt ,MF
3	4	-4		Gr	Gst	28	29	-29		W	Pt ,MF
4	5	-5		Gr	Gst	29	30	-30		W	Pt
5	6	-6		Gr	Gst	30	31	-31		W	Pt , SQI ,MM
6	7	-7		Gr	Gst	31	32	-32		W	MF ,MM, Q
7	8	-8		Gr	Gst	32	33	-33		W	MF ,M
8	9	-9		Gr	Gst	33	34	-34		W	MM ,Q ,AF
9	10	-10		Gr	Gst	34	35	-35		W	AF ,MM ,Q

10	11	-11		Gr	Gst	35	36	-36		W	AF ,MM ,Q
11	12	-12		Gr	Gst	36	37	-37		W	AF ,MM
12	13	-13		Gr	Gst	37	38	-38		W	Pt ,MM
13	14	-14		Gr	Gst	38	39	-39		W	Pt ,Q
14	15	-15		Gr	Gst	39	40	-40		W	Pt ,Q
15	16	-16		Gr	Gst	40	41	-41		W	AF, Pt ,Q
16	17	-17		Gr	Gst	41	42	-42		W	AF, Pt ,Q
17	18	-18		Gr	Gst	42	43	-43		W	AF, Pt ,SQI
18	19	-19		Gr	Gst	43	44	-44		W	AF ,Q ,Pt
19	20	-20		Gr	Gst	44	45	-45		W	AF ,SQI , Eucr
20	21	-21		Gr	Gst	45	46	-46		W	AF ,Eucr
21	22	-22		Gr	Gst	46	47	-47		W	AF
22	23	-23		Gr	Gst	47	48	-48		W	AF ,Eucr ,Q
23	24	-24		Gr	Gst	48	49	-49		W	AF ,Q ,Eucr
24	25	A001 - 25	LN-RC-PET-004	W	AF ,Gst ,Q	49	50	A026 - 50	LN-RC-PET-004	W	AF ,SQI , Eucr

DATE:	5/10/2018	**NO. LAB SAMPLES:**	43	**SAMPLER:**	N.B.D
SECTOR:	LEDINGHAM	**NO. GEO SAMPLES:**	43	**GEO:**	A.S.G
HOLE NO.:	LN-RC-PET-004				
TYPE*	RC	**DATUM:**	WGS 84		
EOH:	69M	**X:**	336094		
Inclination:	90	**Y:**	7773108		
Azimuth:	0	**Z:**	1154M	*Type: * PD; RC; DD (core)* Coluor: *** Brown (B); Red (R); Grey (Gy); Green (Gr); Pink (Pk); Purple (Pl); White (W) Black (Bk); Yellow (Y).	

Geology**							
OB	Overburden/rubble	**A**	Amblygonite	**L**	Lepidolite	**Hect**	Hectorite
W	Weathered	**SQI**	Spodumene	**Be**	Beryl	**D**	Dolerite
F	Fresh	**Pt**	Petalite	**Ta**	Tantalite	**AF**	Albite Feldspar
Q	Quartz	**Pol**	Pollucite	**C**	Cassiterite	**MF**	Microcline Feldspar
BM	Biotite Mica	**MM**	Muscovite Mica	**Gst**	Greenstone	**Eucr**	Eucryptite

From (m)	**To (m)**	**Lab Spl. No**	**Geo sample (X)**	**colour*** **	**Geology** (E.g. Q + F)**	**From (m)**	**To (m)**	**Lab Spl. No**	**Geo sample (X)**	**colour*** **	**Geology** (E.g. Q + F)**

50	51	A027 - 51	LN-RC-PET-004	W	Pt ,AF ,MM	75	76	-76			
51	52	-52		W	AF ,MM ,Pt	76	77	-77			
52	53	-53		W	AF ,MM ,SQI	77	78	-78			
53	54	-54		W	AF ,SQI	78	79	-79			
54	55	-55		W	AF ,Eucr	79	80	-80			
55	56	-56		W	AF ,MM	80	81	-81			
56	57	-57		W	MF ,SQI	81	82	-82			
57	58	-58		W	MF ,Q	82	83	-83			
58	59	-59		W	AF ,SQI	83	84	-84			
59	60	-60		W	AF ,SQI	84	85	-85			
60	61	-61		W	AF ,Pt	85	86	-86			
61	62	-62		W	AF ,MM, Pt ,SQI	86	87	-87			
62	63	-63		W	AF ,MM ,Pt	87	88	-88			
63	64	-64		W	AF ,Pt ,MM	88	89	-89			
64	65	-65		W	AF ,MM ,Pt	89	90	-90			
65	66	-66		W	AF ,MM	90	91	-91			
66	67	A043 - 67	LN-RC-PET-004	W	AF ,MM, Gst	91	92	-92			
67	68	-68		Gr	Gst	92	93	-93			
68	69	-69		Gr	Gst	93	94	-94			
69	70	-70				94	95	-95			

70	71	-71				95	96	-96			
71	72	-72				96	97	-97			
72	73	-73				97	98	-98			
73	74	-74				98	99	-99			
74	75	-75				99	100	-100			

BIKITA MINERALS

BIKITA MINERALS (PVT) LIMITED **DRILL LOG & SAMPLING FORM** Page 1 of 2 pages

DATE:	13/10/2018	**NO. LAB SAMPLES:**	48	**SAMPLER:**	V.M
SECTOR:	SHAFT	**NO. GEO SAMPLES:**	48	**GEO:**	A.S.G
HOLE NO.:	SH-RC-PET-001				
TYPE*	RC	**DATUM:**	WGS 84		
EOH:	88M	**X:**	336211		
Inclination:	-90	**Y:**	7793257	*Type: * PD; RC; DD (core)*	
Azimuth:	0	**Z:**	1154M	'Coluor: *** Brown (B); Red (R); Grey (Gy); Green (Gr); Pink (Pk); Purple (Pl); White (W) Black (Bk); Yellow (Y).	

Geology**							
OB	Overburden/rubble	**A**	Amblygonite	**L**	Lepidolite	**Hect**	Hectorite
W	Weathered	**SQI**	Spodumene	**Be**	Beryl	**D**	Dolerite
F	Fresh	**Pt**	Petalite	**Ta**	Tantalite	**AF**	Albite Feldspar
Q	Quartz	**Pol**	Pollucite	**C**	Cassiterite	**MF**	Microcline Feldspar
BM	Biotite Mica	**MM**	Muscovite Mica	**Gst**	Greenstone	**Eucr**	Eucryptite

	To (m)	**Lab Spl. No**	**Geo sample (X)**	**colour*** **	**Geology** (E.g. Q + F)**	**From (m)**	**To (m)**	**Lab Spl. No**	**Geo sample (X)**	**colour*** **	**Geology** (E.g. Q + F)**
0	1	A001 - 1	SH-RC-PET-001	B	F, Q	25	26	-26		Gr	Gst
1	2	-2		B	Q ,M ,F	26	27	-27		Gr	Gst
2	3	A003 - 3	SH-RC-PET-001	Gy	Gst ,Q ,F	27	28	-28		Gr	Gst
3	4	-4		Gr	Gst	28	29	-29		Gr	Gst
4	5	-5		Gr	Gst	29	30	-30		Gr	Gst
5	6	-6		Gr	Gst	30	31	-31		Gr	Gst
6	7	-7		Gr	Gst	31	32	-32		Gr	Gst
7	8	-8		Gr	Gst	32	33	-33		Gr	Gst
8	9	-9		Gr	Gst	33	34	-34		Gr	Gst
9	10	-10		Gr	Gst	34	35	-35		Gr	Gst
10	11	-11		Gr	Gst	35	36	-36		Gr	Gst

11	12	-12		Gr	Gst	36	37	-37		Gr	Gst
12	13	-13		Gr	Gst	37	38	-38		Gr	Gst
13	14	-14		Gr	Gst	38	39	-39		Gr	Gst
14	15	-15		Gr	Gst	39	40	-40		Gr	Gst
15	16	-16		Gr	Gst	40	41	-41		Gr	Gst
16	17	-17		Gr	Gst	41	42	-42		Gr	Gst
17	18	-18		Gr	Gst	42	43	A004 - 43	SH-RC-PET-001	Gy	SQI ,AF ,Q
18	19	-19		Gr	Gst	43	44	-44			AF
19	20	-20		Gr	Gst	44	45	-45			AF
20	21	-21		Gr	Gst	45	46	-46			AF ,Q
21	22	-22		Gr	Gst	46	47	-47			AF ,L
22	23	-23		Gr	Gst	47	48	-48			AF ,MM
23	24	-24		Gr	Gst	48	49	-49			AF ,L
24	25	-25		Gr	Gst	49	50	A011 - 50	SH-RC-PET-001		AF

DATE:	13/10/2018	**NO. LAB SAMPLES:**	48	**SAMPLER:**	V.M
SECTOR:	SHAFT	**NO. GEO SAMPLES:**	48	**GEO:**	A.S.G
HOLE NO.:	SH-RC-PET-001				
TYPE*	RC	**DATUM:**	WGS 84		
EOH:	88M	**X:**	336211		
Inclination:	-90	**Y:**	7793257		
Azimuth:	0	**Z:**	1154M	*Type: * PD; RC; DD (core)*	
				Coluor: *** Brown (B); Red (R); Grey (Gy); Green (Gr); Pink (Pk); Purple (Pl); White (W) Black (Bk); Yellow (Y).	

Geology**							
OB	Overburden/rubble	**A**	Amblygonite	**L**	Lepidolite	**Hect**	Hectorite
W	Weathered	**SQI**	Spodumene	**Be**	Beryl	**D**	Dolerite
F	Fresh	**Pt**	Petalite	**Ta**	Tantalite	**AF**	Albite Feldspar
Q	Quartz	**Pol**	Pollucite	**C**	Cassiterite	**MF**	Microcline Feldspar
BM	Biotite Mica	**MM**	Muscovite Mica	**Gst**	Greenstone	**Eucr**	Eucryptite

From (m)	**To (m)**	**Lab Spl. No**	**Geo sample (X)**	**colour*** **	**Geology** (E.g. Q + F)**	**From (m)**	**To (m)**	**Lab Spl. No**	**Geo sample (X)**	**colour*** **	**Geology** (E.g. Q + F)**

50	51	A012 - 51	SH-RC-PET-001	Gy	AF ,Eucr	75	76	A037 - 76	SH-RC-PET-001	Gy	AF ,Eucr
51	52	-52		Gy	AF ,Eucr	76	77	-77		Gy	AF ,Eucr
52	53	-53		Gy	AF ,Eucr	77	78	-78		Gy	AF ,Eucr ,Pt
53	54	-54		Gy	AF	78	79	-79		Gy	AF ,Pt
54	55	-55		Gy	AF ,SQI	79	80	-80		Gy	Pt
55	56	-56		Gy	MF ,Eucr	80	81	-81		Gy	Pt
56	57	-57		Gy	MF ,Eucr	81	82	-82		Gy	Pt ,MF
57	58	-58		Gy	MF	82	83	-83		Gy	Pt ,MF,Q
58	59	-59		Gy	AF	83	84	-84		Gy	AF
59	60	-60		Gy	AF ,Eucr	84	85	-85		Gy	AF ,L
60	61	-61		Gy	AF ,Eucr	85	86	-86		Gy	AF
61	62	-62		Gy	AF ,MM	86	87	-87		Gy	AF ,Gst
62	63	-63		Gy	AF ,MM ,Eucr	87	88	A049 -88	SH-RC-PET-001	Gr	Gst
63	64	-64		Gy	Eucr ,Pt ,AF	88	89	-89			
64	65	-65		Gy	MF ,Pt ,Eucr	89	90	-90			
65	66	-66		Gy	AF ,Pt ,Eucr	90	91	-91			
66	67	-67		Gy	AF,MM	91	92	-92			
67	68	-68		Gy	AF,MM	92	93	-93			
68	69	-69		Gy	AF,MM	93	94	-94			
69	70	-70		Gy	AF	94	95	-95			

70	71	-71		Gy	AF ,Pt	95	96	-96			
71	72	-72		Gy	AF	96	97	-97			
72	73			Gy	AF ,Pt	97	98	-98			
73	74	-74		Gy	Eucr ,Pt	98	99	-99			
74	75	-75	SH-RC-PET-001	Gy	AF ,Eucr	99	100	-100			

BIKITA MINERALS

BIKITA MINERALS (PVT) LIMITED

DRILL LOG & SAMPLING FORM

Page 1 of 2 pages

		NO. LAB			
DATE:	4/12/2018	**SAMPLES:**	43	**SAMPLER:**	Tonny M
		NO. GEO			
SECTOR:	SHAFT	**SAMPLES:**	43	**GEO:**	A.G
HOLE NO.:	SH-RC-PET-020				
TYPE*	R.C	**DATUM:**	WGS 84		
EOH:	100M	**X:**	336259		
Inclination:	-90	**Y:**	7793368	*Type: * PD; RC; DD (core)*	
Azimuth:	0	**Z:**	1164M	'Coluor: *** Brown (B); Red (R); Grey (Gy); Green (Gr); Pink (Pk); Purple (Pl); White (W)	

Black (Bk); Yellow (Y).

Geology**							
OB	Overburden/rubble	**A**	Amblygonite	**L**	Lepidolite	**Hect**	Hectorite
W	Weathered	**SQl**	Spodumene	**Be**	Beryl	**D**	Dolerite
F	Fresh	**Pt**	Petalite	**Ta**	Tantalite	**AF**	Albite Feldspar
Q	Quartz	**Pol**	Pollucite	**C**	Cassiterite	**MF**	Microcline Feldspar
BM	Biotite Mica	**MM**	Muscovite Mica	**Gst**	Greenstone	**Eucr**	Eucryptite

	To (m)	**Lab Spl. No**	**Geo sample (X)**	**colour*** **	**Geology** (E.g. Q + F)**	**From (m)**	**To (m)**	**Lab Spl. No**	**Geo sample (X)**	**colour*** **	**Geology** (E.g. Q + F)**
0	1	-1		Gr	Gst	25	26	-26		Gr	Gst
1	2	-2		Gr	Gst	26	27	-27		Gr	Gst
2	3	-3		Gr	Gst	27	28	-28		Gr	Gst
3	4	-4		Gr	Gst	28	29	-29		Gr	Gst
4	5	-5		Gr	Gst	29	30	-30		Gr	Gst
5	6	-6		Gr	Gst	30	31	-31		Gr	Gst
6	7	-7		Gr	Gst	31	32	-32		Gr	Gst
7	8	-8		Gr	Gst	32	33	-33		Gr	Gst
8	9	-9		Gr	Gst	33	34	-34		Gr	Gst
9	10	-10		Gr	Gst	34	35	-35		Gr	Gst

10	11	A001 - 11	SH-RC-PET-020	W	AF ,MM ,Q	35	36	-36		Gr	Gst
11	12	-12		W	MF ,MM ,Q	36	37	-37		Gr	Gst
12	13	-13		W	MF ,MM ,Q	37	38	-38		Gr	Gst
13	14	-14		W	MM ,AF ,Q	38	39	-39		Gr	Gst
14	15	-15		W	AF, Q	39	40	-40		Gr	Gst
15	16	-16		W	MF, Q ,MM	40	41	-41		Gr	Gst
16	17	-17		W	AF ,Q ,MM ,Pt	41	42	-42		Gr	Gst
17	18	-18		W	AF, Q ,MM	42	43	-43		Gr	Gst
18	19	A009 - 19	SH-RC-PET-020	W	AF, MM	43	44	-44		Gr	Gst
19	20	-20		Gr	Gst	44	45	-45		Gr	Gst
20	21	-21		Gr	Gst	45	46	-46		Gr	Gst
21	22	-22		Gr	Gst	46	47	-47		Gr	Gst
22	23	-23		Gr	Gst	47	48	-48		Gr	Gst
23	24	-24		Gr	Gst	48	49	-49		Gr	Gst
24	25	-25		Gr	Gst	49	50	-50		Gr	Gst

		NO. LAB					
DATE:	4/12/2018	**SAMPLES:**	43	**SAMPLER:**	Tonny		
		NO. GEO					
SECTOR:	SHAFT	**SAMPLES:**	43	**GEO:**	A.G		
HOLE NO.:	SH-RC-PET-020						
TYPE*	RC	**DATUM:**	WGS 84				
EOH:	100M	**X:**	336259				
Inclination:	-90	**Y:**	773368	*Type: * PD; RC; DD (core)*			
Azimuth:	0	**Z:**	1164M	Coluor: *** Brown (B); Red (R); Grey (Gy); Green (Gr); Pink (Pk); Purple (Pl); White (W) Black (Bk); Yellow (Y).			

Geology**							
OB	Overburden/rubble	**A**	Amblygonite	**L**	Lepidolite	**Hect**	Hectorite
W	Weathered	**SQI**	Spodumene	**Be**	Beryl	**D**	Dolerite
F	Fresh	**Pt**	Petalite	**Ta**	Tantalite	**AF**	Albite Feldspar
Q	Quartz	**Pol**	Pollucite	**C**	Cassiterite	**MF**	Microcline Feldspar
BM	Biotite Mica	**MM**	Muscovite Mica	**Gst**	Greenstone	**Eucr**	Eucryptite

From (m)	To (m)	Lab Spl. No	Geo sample (X)	colour***	Geology** (E.g. Q + F)	From (m)	To (m)	Lab Spl. No	Geo sample (X)	colour***	Geology** (E.g. Q + F)
50	51	-51		Gr	Gst	75	76	A020 - 76	SH-RC-PET-020	W	AF
51	52	-52		Gr	Gst	76	77	-77		W	AF, Pt ,MM
52	53	-53		Gr	Gst	77	78	-78		W	AF,MM
53	54	-54		Gr	Gst	78	79	-79		W	AF, Q
54	55	-55		Gr	Gst	79	80	-80		W	AF ,Pt, MM
55	56	-56		Gr	Gst	80	81	-81		W	AF, MM, Q, Pt
56	57	-57		Gr	Gst	81	82	-82		W	AF ,MM
57	58	-58		Gr	Gst	82	83	-83		W	AF ,MM ,Pt
58	59	-59		Gr	Gst	83	84	-84		W	AF, MM,Q
59	60	-60		Gr	Gst	84	85	-85		W	AF,MM, Pt
60	61	-61		Gr	Gst	85	86	-86		W	MM, Q, AF, Eucry
61	62	-62		Gr	Gst	86	87	-87		W	AF ,MM ,Q ,Eucry
62	63	-63		Gr	Gst	87	88	-88		W	AF, Pt
63	64	-64		Gr	Gst	88	89	-89		W	AF ,MM
64	65	-65		Gr	Gst	89	90	-90		W	AF ,MM , Eucry

65	66	A010 - 66	SH-RC-PET-020	Gr	Gst ,AF ,MM	90	91	-91		W	MF ,MM ,Q ,Pt
66	67	-67		W	AF ,MM ,Pt	91	92	-92		W	AF ,Pt ,MM ,Q
67	68	-68		W	Pt ,MM	92	93	-93		W	AF, MM
68	69	-69		Gy	Pt ,AF ,MM	93	94	-94		W	AF, MM
69	70	-70		W	Pt ,MM	94	95	-95		W	MM,AF ,Q
70	71	-71		W	Pt ,AF ,MM	95	96	-96		W	AF ,Q ,MM
71	72	-72		W	Pt ,AF	96	97	-97		W	AF ,MM
72	73	-73		W	Pt ,AF ,MM	97	98	-98		W	AF,MM ,Q
73	74	-74		W	Pt, AF	98	99	A043 - 99	SH-RC-PET-020	W	AF ,Q ,MM, Gst
74	75	A019 - 75	SH-RC-PET-020	W	AF, Eucry	99	100	-100		Gr	Gst

BIKITA MINERALS

BIKITA MINERALS (PVT) LIMITED

DRILL LOG & SAMPLING FORM

Page 1 of 2 pages

DATE: 8/9/2019 **NO. LAB SAMPLES:** 47 **SAMPLER:** Geo team

SECTOR:	SHAFT	**NO. GEO SAMPLES:**	47	**GEO:**	A.G
HOLE NO.:	SH-RC-PET-034				
TYPE*	RC	**DATUM:**	WGS 84		
EOH:	87M	**X:**	336324		
Inclination:	-90	**Y:**	7793324	*Type: * PD; RC; DD (core)*	
Azimuth:	0	**Z:**	1169m	'Coluor: *** Brown (B); Red (R); Grey (Gy); Green (Gr); Pink (Pk); Purple (Pl); White (W) Black (Bk); Yellow (Y).	

Geology**							
OB	Overburden/rubble	**A**	Amblygonite	**L**	Lepidolite	**Hect**	Hectorite
W	Weathered	**SQI**	Spodumene	**Be**	Beryl	**D**	Dolerite
F	Fresh	**Pt**	Petalite	**Ta**	Tantalite	**AF**	Albite Feldspar
Q	Quartz	**Pol**	Pollucite	**C**	Cassiterite	**MF**	Microcline Feldspar
BM	Biotite Mica	**MM**	Muscovite Mica	**Gst**	Greenstone	**Eucr**	Eucryptite

	To (m)	**Lab Spl. No**	**Geo sample (X)**	**colour*** **	**Geology** (E.g. Q + F)**	**From (m)**	**To (m)**	**Lab Spl. No**	**Geo sample (X)**	**colour*** **	**Geology** (E.g. Q + F)**
0	1	-1		B	OB rubble peg	25	26	-26		Gr	Gst
1	2	-2		B	OB rubble peg	26	27	-27		Gr	Gst
2	3	-3		Gr	Gst	27	28	-28		Gr	Gst
3	4	-4		Gr	Gst	28	29	-29		Gr	Gst

4	5	A001-5	SH-RC-PET-034	W	AF ,Q	29	30	-30		Gr	Gst
5	6	-6		W	AF ,MM ,Q ,L	30	31	-31		Gr	Gst
6	7	A003-7	SH-RC-PET-034	Gr	Gst ,AF ,MM	31	32	-32		Gr	Gst
7	8	-8		Gr	Gst	32	33	-33		Gr	Gst
8	9	-9		Gr	Gst	33	34	-34		Gr	Gst
9	10	-10		Gr	Gst	34	35	-35		Gr	Gst
10	11	-11		Gr	Gst	35	36	-36		Gr	Gst
11	12	A004 - 12	SH-RC-PET-034	W	MM , AF, Q	36	37	-37		Gr	Gst
12	13	-13		Gr	Gst	37	38	-38		Gr	Gst
13	14	-14		Gr	Gst	38	39	-39		Gr	Gst
14	15	-15		Gr	Gst	39	40	-40		Gr	Gst
15	16	-16		Gr	Gst	40	41	-41		Gr	Gst
16	17	-17		Gr	Gst	41	42	-42		Gr	Gst ,Qtz vein
17	18	-18		Gr	Gst	42	43	-43		Gr	Gst , Qtz vein
18	19	-19		Gr	Gst	43	44	A005-44	SH-RC-PET-034	Gy	Gst, AF
19	20	-20		Gr	Gst	44	45	-45		W	AF
20	21	-21		Gr	Gst	45	46	-46		W	AF ,L
21	22	-22		Gr	Gst	46	47	-47		W	AF ,L

22	23	-23		Gr	Gst	47	48	-48		W	AF ,MM ,Q
23	24	-24		Gr	Gst	48	49	-49		W	AF ,Pt ,Hect ,MM
24	25	-25		Gr	Gst	49	50	A011 -50	SH-RC-PET-034	W	Pt ,MM

BIKITA MINERALS

BIKITA MINERALS (PVT) LIMITED

DRILL LOG & SAMPLING FORM

DATE:	9/2/2019	**NO. LAB SAMPLES:**	47	**SAMPLER:**	Geo team
SECTOR:	SHAFT	**NO. GEO SAMPLES:**	47	**GEO:**	A.G

HOLE NO.:	SH-RC-PET-034		
TYPE*	RC	**DATUM:**	WGS 84
EOH:	87M	**X:**	3363324
Inclination:	-90	**Y:**	7793324
Azimuth:	0	**Z:**	

*Type: * PD; RC; DD (core)*

Coluor: *** Brown (B); Red (R); Grey (Gy); Green (Gr); Pink (Pk); Purple (Pl); White (W) Black (Bk); Yellow (Y).

Geology**							
OB	Overburden/rubble	**A**	Amblygonite	**L**	Lepidolite	**Hect**	Hectorite
W	Weathered	**SQI**	Spodumene	**Be**	Beryl	**D**	Dolerite
F	Fresh	**Pt**	Petalite	**Ta**	Tantalite	**AF**	Albite Feldspar
Q	Quartz	**Pol**	Pollucite	**C**	Cassiterite	**MF**	Microcline Feldspar
BM	Biotite Mica	**MM**	Muscovite Mica	**Gst**	Greenstone	**Eucr**	Eucryptite

From (m)	To (m)	Lab Spl. No	Geo sample (X)	colour***	Geology** (E.g. Q + F)	From (m)	To (m)	Lab Spl. No	Geo sample (X)	colour***	Geology** (E.g. Q + F)
50	51	A012 - 51	SH-RC-PET-034	W	MF	75	76	A037 - 76	SH-RC-PET-034	W	AF ,MM ,Q
51	52	-52		W	Q	76	77	-77		W	AF ,MM
52	53	-53		W	MF	77	78	-78		W	AF
53	54	-54		W	MF	78	79	-79		W	AF ,MM ,Q ,Ta?
54	55	-55		W	MF	79	80	-80		W	AF ,MM ,Eucr
55	56	-56		W	MF ,Hect ,SQI?	80	81	-81		W	AF , MM ,Q
56	57	-57		W	MF ,Q, SQI	81	82	-82		W	AF ,Pt ,Q
57	58	-58		W	AF, Q ,Eucr? ,SQI	82	83	-83		W	AF ,MM
58	59	-59		W	AF,Eucr?	83	84	-84		W	AF
59	60	-60		W	AF , M Eucr?	84	85	-85		W	AF

60	61	-61		W	AF , Eucr ,Pt ,MM	85	86	A047 - 86	SH-RC-PET-034	W	AF
61	62	A023 - 62	SH-RC-PET-034	W	Pt ,AF ,MM	86	87	-87		Gr	Gst
62	63	-63		W	AF, Pt , MM ,Q	87	88	-88			
63	64	-64		W	AF ,MM , Pt	88	89	-89			
64	65	-65		W	AF ,MM	89	90	-90			
65	66	-66		W	AF , Pt ,MM	90	91	-91			
66	67	-67		W	AF ,MM	91	92	-92			
67	68	-68		W	Pt ,AF ,MM	92	93	-93			
68	69	-69		W	AF ,Pt , MM ,Q	93	94	-94			
69	70	-70		W	AF ,Pt , MM	94	95	-95			
70	71	-71		W	Pt ,AF ,MM	95	96	-96			
71	72	-72		W	AF, MM, Q	96	97	-97			
72	73	-73		W	AF, MM, Q, TA?	97	98	-98			
73	74	-74		W	AF ,MM ,Q	98	99	-99			
74	75	A036 - 75	SH-RC-PET-034	W	AF ,MM ,Q	99	100	-100			

DATE:	24/05/2017	**NO. LAB SAMPLES:**	37	**SAMPLER:**	V.M
SECTOR:	VICTORS	**NO. GEO SAMPLES:**	37	**GEO:**	J.P.A
HOLE NO.:	V-RC-PET-028				
TYPE*	RC	**DATUM:**	WGS 84		
EOH:	73M	**X:**	336854		
Inclination:	-90	**Y:**	7793544	*Type: * PD; RC; DD (core)*	
Azimuth:	0	**Z:**		'Coluor: *** Brown (B); Red (R); Grey (Gy); Green (Gr); Pink (Pk); Purple (Pl); White (W) Black (Bk); Yellow (Y).	

Geology**							
OB	Overburden/rubble	**A**	Amblygonite	**L**	Lepidolite	**Hect**	Hectorite
W	Weathered	**SQI**	Spodumene	**Be**	Beryl	**D**	Dolerite
F	Fresh	**Pt**	Petalite	**Ta**	Tantalite	**AF**	Albite Feldspar
Q	Quartz	**Pol**	Pollucite	**C**	Cassiterite	**MF**	Microcline Feldspar
BM	Biotite Mica	**MM**	Muscovite Mica	**Gst**	Greenstone	**Eucr**	Eucryptite

	To (m)	**Lab Spl. No**	**Geo sample (X)**	**colour*** **	**Geology** (E.g. Q + F)**	**From (m)**	**To (m)**	**Lab Spl. No**	**Geo sample (X)**	**colour*** **	**Geology** (E.g. Q + F)**

0	1	-1		B	Gst,OB,rubble	25	26	-26		Gr	Gst-Fresh
1	2	-2		Gr	Gst-Deeply weathered	26	27	-27		Gr	Gst-Fresh
2	3	-3		Gr	Gst-mod weathered	27	28	-28		Gr	Gst-Fresh
3	4	-4		Gr	Gst-mod weathered	28	29	-29		Gr	Gst-Fresh
4	5	-5		Gr	Gst-mod weathered	29	30	-30		Gr	Gst-Fresh
5	6	-6		Gr	Gst-mod weathered	30	31	-31		Gr	Gst-Fresh
6	7	-7		Gr	Gst-mod weathered	31	32	-32		Gr	Gst-Fresh
7	8	-8		Gr	Gst-mod weathered	32	33	-33		Gr	Gst-Fresh
8	9	-9		Gr	Gst-mod weathered	33	34	-34		Gr	Gst-Fresh
9	10	-10		Gr	Gst-mod weathered	34	35	-35		Gr	Gst-Fresh
10	11	-11		Gr	Gst-mod weathered	35	36	-36		Gr	Gst-Fresh
11	12	-12		Gr	Gst-mod weathered	36	37	-37		Gr	Gst-Fresh
12	13	-13		Gr	Gst-mod weathered	37	38	-38		Gr	Gst-Fresh
13	14	-14		Gr	Gst-Fresh	38	39	-39		Gr	Gst-Fresh
14	15	-15		Gr	Gst-Fresh	39	40	-40		Gr	Gst-Fresh
15	16	-16		Gr	Gst-Fresh	40	41	-41		Gr	Gst-Fresh
16	17	-17		Gr	Gst-Fresh	41	42	A009 -42	V-RC-PET-028	Gr	Gst-Fresh
17	18	A001 - 18	V-RC-PET-028	Gr	Gst-Fresh	42	43	-43		Gr	Gst-Fresh
18	19	-19		Gr	Gst-Fresh	43	44	-44		Gr	Gst,AF

19	20	-20		Gr	Gst,AF,MM	44	45	-45		Gy	AF,MF ,MM
20	21	-21		Gy	AF ,MM ,Q	45	46	-46		Gy	AF,Pt,MM
21	22	-22		Gy	AF,MM ,Q	46	47	-47		Gy	AF ,Q ,MM ,MF
22	23	-23		Gy	AF,MM ,Q ,Gst	47	48	-48		W	Pt,MM,MF ,AF
23	24	-24		Gr	Gst-Fresh	48	49	-49		Gy	MF ,Pt ,MM
24	25	A008 - 25	V-RC-PET-028	Gr	Gst-Fresh	49	50	A017 -50	V-RC-PET-028	Gy	MM,Pt,Q

BIKITA MINERALS

BIKITA MINERALS (PVT) LIMITED

DRILL LOG & SAMPLING FORM

Page 2 of 2 pages

DATE:	25-05-2017	**NO. LAB SAMPLES:**	37	**SAMPLER:**	V.M
SECTOR:	VICTORS	**NO. GEO SAMPLES:**	37	**GEO:**	J.P.A
HOLE NO.:	V-RC-PET-028				
TYPE*	RC	**DATUM:**	WGS 84		
EOH:	93M	**X:**	3336854		

Inclination:	-90	**Y:**	7793544
Azimuth:	0	**Z:**	

*Type: * PD; RC; DD (core)*

Coluor: *** Brown (B); Red (R); Grey (Gy); Green (Gr); Pink (Pk); Purple (Pl); White (W) Black (Bk); Yellow (Y).

Geology**							
OB	Overburden/rubble	**A**	Amblygonite	**L**	Lepidolite	**Hect**	Hectorite
W	Weathered	**SQI**	Spodumene	**Be**	Beryl	**D**	Dolerite
F	Fresh	**Pt**	Petalite	**Ta**	Tantalite	**AF**	Albite Feldspar
Q	Quartz	**Pol**	Pollucite	**C**	Cassiterite	**MF**	Microcline Feldspar
BM	Biotite Mica	**MM**	Muscovite Mica	**Gst**	Greenstone	**Eucr**	Eucryptite

From (m)	To (m)	Lab Spl. No	Geo sample (X)	colour***	Geology** (E.g. Q + F)	From (m)	To (m)	Lab Spl. No	Geo sample (X)	colour***	Geology** (E.g. Q + F)
50	51	A018 - 51	V-RC-PET-028	Gy	AF ,MM ,Pt	75	76	-76			
51	52	-52		Gy	AF,MM,Pt	76	77	-77			
52	53	-53		W	Pt,MF ,MM	77	78	-78			
53	54	-54		W	Pt	78	79	-79			
54	55	-55		W	Eucr,L	79	80	-80			
55	56	-56		Gy	Eucr, MF ,POL? ,L	80	81	-81			
56	57	-57		Gy	MF ,L ,POL?	81	82	-82			

57	58	-58		Gy	POL? ,L ,AF	82	83	-83			
58	59	-59		Gy	AF,Q,MM	83	84	-84			
59	60	-60		Gy	AF,Q,MM	84	85	-85			
60	61	-61		Gy	AF,Q,MM	85	86	-86			
61	62	-62		Gy	AF,Q,MM	86	87	-87			
62	63	-63		Gy	AF,Q,MM	87	88	-88			
63	64	-64		Gy	AF,Q,MM	88	89	-89			
64	65	-65		Gy	AF, MM	89	90	-90			
65	66	-66		Gy	AF,MF ,Q ,MM	90	91	-91			
66	67	-67		Gy	AF,Q,MM ,MF	91	92	-92			
67	68	-68		Gy	AF,MF ,MM	92	93	-93			
68	69	-69		Gy	Gst	93	94	-94			
69	70	A037 - 70	V-RC-PET-028	Gr	Gst	94	95	-95			
70	71	-71		Gr	Gst	95	96	-96			
71	72	-72		Gr	Gst	96	97	-97			
72	73	-73		Gr	Gst	97	98	-98			
73	74	-74				98	99	-99			
74	75	-75				99	100	-100			

BIKITA MINERALS

BIKITA MINERALS (PVT) LIMITED

DRILL LOG & SAMPLING FORM

DATE:	12/7/2017	**NO. LAB SAMPLES:**	23	**SAMPLER:**	VM/AG
SECTOR:	WEST	**NO. GEO SAMPLES:**	23	**GEO:**	JPA
HOLE NO.:	WC-RC-003				
TYPE*	RC	**DATUM:**	WGS 84		
EOH:	85M	**X:**	336375		
Inclination:	-90	**Y:**	7793760	*Type: * PD; RC; DD (core)*	
Azimuth:	0	**Z:**		'Coluor: *** Brown (B); Red (R); Grey (Gy); Green (Gr); Pink (Pk); Purple (Pl); White (W) Black (Bk); Yellow (Y).	

Geology**							
OB	Overburden/rubble	**A**	Amblygonite	**L**	Lepidolite	**Hect**	Hectorite
W	Weathered	**SQI**	Spodumene	**Be**	Beryl	**D**	Dolerite
F	Fresh	**Pt**	Petalite	**Ta**	Tantalite	**AF**	Albite Feldspar
Q	Quartz	**Pol**	Pollucite	**C**	Cassiterite	**MF**	Microcline Feldspar
BM	Biotite Mica	**MM**	Muscovite Mica	**Gst**	Greenstone	**Eucr**	Eucryptite

	To (m)	Lab Spl. No	Geo sample (X)	colour***	Geology** (E.g. Q + F)	From (m)	To (m)	Lab Spl. No	Geo sample (X)	colour***	Geology** (E.g. Q + F)
0	1	A001 -1	WC-RC-003	Gy	AF ,Q ,MM	25	26	-26		Gr	Gst
1	2	-2		Gy	Q,AF,MM	26	27	-27		Gr	Gst
2	3	-3		Gr	Gst	27	28	-28		Gr	Gst
3	4	A004 -4	WC-RC-003	Gr	Gst	28	29	-29		Gr	Gst
4	5	-5		Gr	Gst	29	30	-30		Gr	Gst
5	6	-6		Gr	Gst	30	31	-31		Gr	Gst
6	7	-7		Gr	Gst	31	32	-32		Gr	Gst
7	8	-8		Gr	Gst	32	33	-33		Gr	Gst
8	9	-9		Gr	Gst	33	34	-34		Gr	Gst
9	10	-10		Gr	Gst	34	35	-35		Gr	Gst
10	11	-11		Gr	Gst	35	36	-36		Gr	Gst
11	12	-12		Gr	Gst	36	37	-37		Gr	Gst
12	13	-13		Gr	Gst	37	38	-38		Gr	Gst
13	14	-14		Gr	Gst	38	39	-39		Gr	Gst
14	15	-15		Gr	Gst	39	40	-40		Gr	Gst
15	16	-16		Gr	Gst	40	41	-41		Gr	Gst
16	17	-17		Gr	Gst	41	42	-42		Gr	Gst
17	18	-18		Gr	Gst	42	43	-43		Gr	Gst

18	19	-19		Gr	Gst	43	44	-44		Gr	Gst
19	20	-20		Gr	Gst	44	45	-45		Gr	Gst
20	21	-21		Gr	Gst	45	46	-46		Gr	Gst
21	22	-22		Gr	Gst	46	47	-47		Gr	Gst
22	23	-23		Gr	Gst	47	48	-48		Gr	Gst
23	24	-24		Gr	Gst	48	49	-49		Gr	Gst
24	25	-25		Gr	Gst	49	50	-50		Gr	Gst

BIKITA MINERALS

BIKITA MINERALS (PVT) LIMITED

DRILL LOG & SAMPLING FORM

Page 2 of 2 pages

DATE:	12/7/2017	**NO. LAB SAMPLES:**	23	**SAMPLER:**	V.M/A.G
SECTOR:	WEST	**NO. GEO SAMPLES:**	23	**GEO:**	J.P.A
HOLE NO.:	WC-RC-003				

TYPE*	RC	**DATUM:**	WGS 84
EOH:	85M	**X:**	336375
Inclination:	-90	**Y:**	7793760
Azimuth:	0	**Z:**	

*Type: * PD; RC; DD (core)*

Coluor: *** Brown (B); Red (R); Grey (Gy); Green (Gr); Pink (Pk); Purple (Pl); White (W) Black (Bk); Yellow (Y).

Geology**							
OB	Overburden/rubble	**A**	Amblygonite	**L**	Lepidolite	**Hect**	Hectorite
W	Weathered	**SQI**	Spodumene	**Be**	Beryl	**D**	Dolerite
F	Fresh	**Pt**	Petalite	**Ta**	Tantalite	**AF**	Albite Feldspar
Q	Quartz	**Pol**	Pollucite	**C**	Cassiterite	**MF**	Microcline Feldspar
BM	Biotite Mica	**MM**	Muscovite Mica	**Gst**	Greenstone	**Eucr**	Eucryptite

From (m)	**To (m)**	**Lab Spl. No**	**Geo sample (X)**	**colour*** **	**Geology** (E.g. Q + F)**	**From (m)**	**To (m)**	**Lab Spl. No**	**Geo sample (X)**	**colour*** **	**Geology** (E.g. Q + F)**
50	51	-51		Gr	Gst	75	76	A021 - 76	WC-RC-003	Gy	Gst ,AF
51	52	-52		Gr	Gst	76	77	-77		Gr	Gst
52	53	-53		Gr	Gst	77	78	A023 - 78	WC-RC-003	Gr	Gst
53	54	-54		Gr	Gst	78	79	-79		Gr	Gst
54	55	-55		Gr	Gst	79	80	-80		Gr	Gst
55	56	-56		Gr	Gst	80	81	-81		Gr	Gst
56	57	-57		Gr	Gst	81	82	-82		Gr	Gst
57	58	-58		Gr	Gst	82	83	-83		Gr	Gst

58	59	-59		Gr	Gst	83	84	-84		Gr	Gst
59	60	A005-60	WC-RC-003	Gr	Gst	84	85	-85		Gr	Gst
60	61	-61		Gr	AF ,MM,Q ,L	85	86	-86		Gr	Gst
61	62	-62		Gy	AF , Eucr? ,B? ,L	86	87	-87			
62	63	-63		Gy	AF ,Eucr ,B ?,L	87	88	-88			
63	64	-64		Gy	AF,MM,Q,B ?	88	89	-89			
64	65	-65		Gy	AF,MM,Q,B ?	89	90	-90			
65	66	-66		Gy	AF,MM ,Q,Pt	90	91	-91			
66	67	-67		Gy	AF,MM ,Q,Pt,B?	91	92	-92			
67	68	-68		Gy	AF,MM,Q,Pt?	92	93	-93			
68	69	-69		Gy	AF,Q,MM ,Pt	93	94	-94			
69	70	-70		Gy	AF ,Q ,MM ,Pt ?,B?	94	95	-95			
70	71	-71		Gy	AF ,MM	95	96	-96			
71	72	-72		Gy	AF ,Q ,L?,MM	96	97	-97			
72	73	-73		Gy	AF ,Q ,MM ,L?	97	98	-98			
73	74	-74		Gy	AF ,MM	98	99	-99			
74	75	A020-75	WC-RC-003	Gy	AF ,Gst	99	100	-100			

BIKITA MINERALS

BIKITA MINERALS (PVT) LIMITED

DRILL LOG & SAMPLING FORM

DATE:	10/7/2017	**NO. LAB SAMPLES:**	15	**SAMPLER:**	VM/AG
SECTOR:	WEST	**NO. GEO SAMPLES:**	15	**GEO:**	J.P.A
HOLE NO.:	WC-RC-004				
TYPE*	RC	**DATUM:**	WGS 84		
EOH:	90M	**X:**	336476		
Inclination:	-90	**Y:**	7793927	*Type: * PD; RC; DD (core)*	
Azimuth:	0	**Z:**		'Coluor: *** Brown (B); Red (R); Grey (Gy); Green (Gr); Pink (Pk); Purple (Pl); White (W) Black (Bk); Yellow (Y).	

Geology**

OB	Overburden/rubble	**A**	Amblygonite	**L**	Lepidolite	**Hect**	Hectorite
W	Weathered	**SQI**	Spodumene	**Be**	Beryl	**D**	Dolerite
F	Fresh	**Pt**	Petalite	**Ta**	Tantalite	**AF**	Albite Feldspar
Q	Quartz	**Pol**	Pollucite	**C**	Cassiterite	**MF**	Microcline Feldspar
BM	Biotite Mica	**MM**	Muscovite Mica	**Gst**	Greenstone	**Eucr**	Eucryptite

	To (m)	Lab Spl. No	Geo sample (X)	colour***	Geology** (E.g. Q + F)	From (m)	To (m)	Lab Spl. No	Geo sample (X)	colour***	Geology** (E.g. Q + F)
0	1	-1		B	OB , rubble	25	26	A002	WC-RC-004	Gr	Gst deeply w
1	2	-2		Gr	Gst deeply weathered	26	27	-27		Gy	AF
2	3	-3		Gr	Gst deeply weathered	27	28	-28		Gy	AF
3	4	-4		Gr	Gst deeply weathered	28	29	-29		Gr	Gst deeply w
4	5	-5		Gr	Gst mod weathered	29	30	A006	WC-RC-004	Gr	Gst deeply w
5	6	-6		Gr	Gst mod weathered	30	31	-31		Gr	Gst deeply w
6	7	-7		Gr	Gst mod weathered	31	32	-32		Gr	Gst Fresh H2O
7	8	-8		Gr	Gst mod weathered	32	33	-33		Gr	Gst Fresh H2O
8	9	-9		Gr	Gst mod weathered	33	34	-34		Gr	Gst Fresh H2O
9	10	-10		Gr	Gst mod weathered	34	35	-35		Gr	Gst Fresh H2O
10	11	-11		Gr	Gst mod weathered	35	36	-36		Gr	Gst Fresh H2O

11	12	-12		Gr	Gst mod weathered	36	37	-37		Gr	Gst Fresh H2O
12	13	-13		Gr	Gst mod weathered	37	38	-38		Gr	Gst Fresh H2O
13	14	-14		Gr	Gst mod weathered	38	39	-39		Gr	Gst Fresh H2O
14	15	-15		Gr	Gst mod weathered	39	40	-40		Gr	Gst Fresh H2O
15	16	-16		Gr	Gst mod weathered	40	41	-41		Gr	Gst Fresh H2O
16	17	-17		Gr	Gst mod weathered	41	42	-42		Gr	Gst Fresh H2O
17	18	-18		Gr	Gst mod weathered	42	43	-43		Gr	Gst Fresh H2O
18	19	-19		Gr	Gst mod weathered	43	44	-44		Gr	Gst Fresh H2O
19	20	-20		Gr	Gst mod weathered	44	45	-45		Gr	Gst Fresh H2O
20	21	-21		Gr	Gst mod weathered	45	46	-46		Gr	Gst Fresh H2O
21	22	-22		Gr	Gst mod weathered	46	47	-47		Gr	Gst Fresh H2O

22	23	-23		Gr	Gst mod weathered	47	48	-48		Gr	Gst Fresh H2O
23	24	-24		Gr	Gst mod weathered	48	49	-49		Gr	Gst Fresh H2O
24	25	A001	WC-RC-004	Gr	Gst mod weathered	49	50	-50		Gr	Gst Fresh H2O

BIKITA MINERALS (PVT) LIMITED **DRILL LOG & SAMPLING FORM** Page 2 of 2 pages

		NO. LAB			V.M/
DATE:	11/7/2017	**SAMPLES:**	15	**SAMPLER:**	A.G
		NO. GEO			
SECTOR:	WEST	**SAMPLES:**	15	**GEO:**	J.P.A
HOLE NO.:	WC-RC-004				
TYPE*	RC	**DATUM:**	WGS 84		
EOH:	90M	**X:**	336476		
Inclination:	-90	**Y:**	7793924		
Azimuth:	0	**Z:**			

*Type: * PD; RC; DD (core)*

Coluor: *** Brown (B); Red (R); Grey (Gy); Green (Gr); Pink (Pk); Purple (Pl); White (W)

Black (Bk); Yellow (Y).

Geology**							
OB	Overburden/rubble	**A**	Amblygonite	**L**	Lepidolite	**Hect**	Hectorite
W	Weathered	**SQI**	Spodumene	**Be**	Beryl	**D**	Dolerite
F	Fresh	**Pt**	Petalite	**Ta**	Tantalite	**AF**	Albite Feldspar
Q	Quartz	**Pol**	Pollucite	**C**	Cassiterite	**MF**	Microcline Feldspar
BM	Biotite Mica	**MM**	Muscovite Mica	**Gst**	Greenstone	**Eucr**	Eucryptite

From (m)	To (m)	Lab Spl. No	Geo sample (X)	colour***	Geology** (E.g. Q + F)	From (m)	To (m)	Lab Spl. No	Geo sample (X)	colour***	Geology** (E.g. Q + F)
50	51	-51		Gr	Gst Fresh H2O	75	76	-76		Gr	Gst Fresh H2O
51	52	-52		Gr	Gst Fresh H2O	76	77	-77		Gr	Gst Fresh H2O
52	53	-53		Gr	Gst Fresh H2O	77	78	-78		Gr	Gst Fresh H2O
53	54	-54		Gr	Gst Fresh H2O	78	79	-79		Gr	Gst Fresh H2O
54	55	-55		Gr	Gst Fresh H2O	79	80	-80		Gr	Gst Fresh H2O

55	56	-56		Gr	Gst Fresh H2O	80	81	-81		Gr	Gst Fresh H2O
56	57	-57		Gr	Gst Fresh H2O	81	82	-82		Gr	Gst Fresh H2O
57	58	-58		Gr	Gst Fresh H2O	82	83	-83		Gr	Gst Fresh H2O
58	59	A007 - 59	WC-RC-004	Gr	Gst Fresh H2O	83	84	-84		Gr	Gst Fresh H2O
59	60	-60		Gr	Gst, MM, AF ,Q, L	84	85	-85		Gr	Gst Fresh H2O
60	61	-61		Gy	Q, L ,AF, MM	85	86	-86		Gr	Gst Fresh H2O
61	62	-62		Gy	Q , AF, L, MM	86	87	-87		Gr	Gst Fresh H2O
62	63	-63		Gy	AF, Q , MM ,C	87	88	-88		Gr	Gst Fresh H2O
63	64	-64		Gy	AF, Gst, C	88	89	-89		Gr	Gst Fresh H2O
64	65	-65		Gy	Gst Fresh	89	90	-90		Gr	Gst Fresh H2O
65	66	-66		Gr	Gst Fresh H2O	90	91	-91		Gr	Gst Fresh H2O

66	67	A015 - 67	WC-RC-004	Gr	Gst Fresh H2O	91	92	-92			
67	68	-68		Gr	Gst Fresh H2O	92	93	-93			
68	69	-69		Gr	Gst Fresh H2O	93	94	-94			
69	70	-70		Gr	Gst Fresh H2O	94	95	-95			
70	71	-71		Gr	Gst Fresh H2O	95	96	-96			
71	72	-72		Gr	Gst Fresh H2O	96	97	-97			
72	73	-73		Gr	Gst Fresh H2O	97	98	-98			
73	74	-74		Gr	Gst Fresh H2O	98	99	-99			
74	75	-75		Gr	Gst Fresh H2O	99	100	-100			

Appendix 1d: Diamond drilling log sheets

BIKITA MINERALS DIAMOND DRILLING LOG SHEET

LOCATION: AL HAYAT DUTUM: WGS 84

HOLE I.D: AHH-DDH-002 COORDS: 336721/7793249

DATE: E.O.H.D: 89.58m

DIP: -90 AZIMUTH: 0

LOGGED BY: ARTHUR GOGODO ELEVATION: 1161.423

DEPTH (m)		**GEOLOGY**
From	To	(lithology, structure, description)
0	26.24	Deeply weathered sheared and decomposed Gst. Possible dump material.
26.24	28	Highly fractured ,oxidised Gst getting more solid and competent .Sharp Gst-Peg contact at 28m
28	29.4	Spotted dog albite
29.4	30.05	Massive petalite with minor muscovite inclusions
30.05	31.21	Microcline feldspar intermixed with muscovite
31.21	31.81	Massive petalite.
31.81	32.62	Mixed microcline and albite
32.62	33.59	Massive petalite
33.59	35.73	Fine grained spotted dog albite
35.73	42.18	Fine grained spotted dog albite mixed with microcline and blocky petalite
42.18	50.6	Mixed zone dominated by microcline and blocky petalite with muscovite inclusions
50.6	55.09	Massive petalite with a microcline and muscovite matrix.
55.09	56.35	Massive microcline
56.35	57.5	Massive petalite
57.5	61.76	Massive microcline intermixed with muscovite and quartz as well as blocky petalite
61.76	66.55	Massive petalite within a microcline and muscovite matrix
66.55	69.5	Microcline mixed with muscovite and blocky petalite
69.5	75.01	Spotted dog albite
75.01	75.5	Massive petalite
75.5	84.57	Spotted albite intermixed with microcline and blocky petalite. Gradational

		contact with development of epidote towards the contact at 84.57m.
84.57	89.58	Massive Gst with epidote alteration.

BIKITA MINERALS DIAMOND DRILLING LOG SHEET

LOCATION: NIGELS DUTUM: WGS 84

HOLE I.D: NIG-DDH-002 COORDS: 336717/7793516

DATE: E.O.H.D: 41.03

DIP: -90 AZIMUTH: 0

LOGGED BY: ARTHUR GOGODO ELEVATION: 1171.538

DEPTH (m)		**GEOLOGY**
From	To	(lithology, structure, description)
0	3	Overburden of Est dump
3	6.46	Spotted dog Albite
6.46	7.3	Massive microcline
7.3	8.02	Med weathered petalite intermixed with muscovite
8.02	9	with a small lepidolite lens
9	16.4	Massive petalite intermixed with muscovite
16.4	17.6	Spotted dog albite with blocky petalite
17.6	19.8	Fluidised petalite intermixed with spotted dog albite. Traces of eucryptite
19.8	21	Eucryptite being altered to Bikitaite within a spotted dog albite
21	21.82	Spotted dog albite with patches of fluidised SQI
21.82	31	Mixed zone with petalite eucryptite being altered to Bikitaite, SQI within a spotted dog albite matrix
31	37.48	Spotted dog albite within minor patches of fluidised petalite and lepidolite. Sharp peg/gst contact at 37.48m
37.48	41.03	Massive Gst with a 20cm Qtz vein at 38.96m

BIKITA MINERALS DIAMOND DRILLING LOG SHEET

LOCATION: LEDINGHAM DUTUM: WGS 84

HOLE I.D: SQI-DDH-12 COORDS: 336087.7/7793006

DATE: E.O.H.D: 73.44

DIP: -60 AZIMUTH: 130

LOGGED BY: ARTHUR GOGODO ELEVATION: 1177.472

DEPTH (m)		**GEOLOGY**
From	To	(lithology, structure, description)
0	3	Deeply weathered/oxidised and decomposed Gst sharp Gst/Peg contact at 3.00m
3	6.9	Microcline-spotted dog albite-Qtz matrix with minor green lithian muscovite .Mod weathered from the contact to 4m
6.9	7.6	Massive coarse grained pink SQI
7.6	9.3	Microcline intermixed with muscovite
9.3	9.6	Coarse grained pink SQI embedded in microcline
9.6	10	Microcline intermixed with muscovite
10	11.21	Massive med-grained pink SQI embedded in microcline
11.21	12	Qtz-microcline matrix
12	12.6	Med-grained pink SQI embedded in microcline-Qtz matrix
12.6	13.14	Microcline-spotted dog albite-Qtz matrix with Qtz brecciation
13.14	18.15	Med grained pink SQI embedded in a microcline -Qtz muscovite matrix with minor black Fe/Fe veinlets
18.15	21.5	Microcline-Qtz-muscovite with minor SQI traces and black Fe/Mn veinlets
21.5	29	Coarse grained pink SQI embedded in spotted dog albite-microcline matrix with abundant black Fe/Mn veinlets
29	32.15	Microcline-spotted dog albite matrix with disseminated SQI traces. Possible alteration of hectorite after SQI
32.15	46.67	Disseminated-massive coarse grained pink SQI embedded in albite

		and microcline with minor traces of epidote and abundant black Fe/ Mn veinlets to lenses
46.67	47.5	Albite with black Fe/Mn veinlets lenses and minor traces of SQI
47.5	48.2	Coarse-grained pink SQI embedded in Albite
48.2	49.2	Altered albite being replaced with epidote and maroon tint colouration, minor traces of SQI black Fe/Mn lenses
49.2	53.3	Massive med-coarse grained pink SQI with maroon tint colouration embedded within a spotted dog albite
53.3	56.23	Spotted albite with disseminated black Fe/Mn veinlets at minor traces of SQI
56.23	57.2	Med-grained pink SQI embedded in spotted dog albite-microcline matrix with disseminated black Fe/Mn veinlets
57.2	57.65	Spotted dog albite with minor traces of SQI
57.65	58	Med-grained pink SQI embedded in spotted dog albite
58	64.65	Spotted dog albite with minor black Fe/Mn lenses and epidote alteration from 62.9m to the Peg/Gst contact at 64.65m.
64.65	73.44	Massive throughout and fractured close to the contact for

BIKITA MINERALS DIAMOND DRILLING LOG SHEET

LOCATION: LEDINGHAM DUTUM: WGS 84

HOLE I.D: SQI-DDH-44 COORDS: 336206/7793286

DATE: E.O.H.D: 102.58m

DIP: -90 AZIMUTH: 0

LOGGED BY: ARTHUR GOGODO ELEVATION: 1159.414

DEPTH (m)		**GEOLOGY**
From	To	(lithology, structure, description)
0	1	Gst rubble
1	6	Deeply weathered and decomposed Gst
6	7.36	Coarse grained albite intermixed with green mica
7.36	9	Coarse grained albite intermixed with grey muscovite and blocky coarse grained pink SQI

9	9.7	Massive white microcline feldspar with minor muscovite inclusions as well as blocky coarse grained lepidolite
9.7	10.1	Quartz vein
10.1	11.35	Mixed zone with bladed prismatic lepidolite and weathered blocky SQI within a quartz albite-muscovite matrix.
11.35	13	Microcline intermixed with muscovite and quartz breccia
13	15.61	Spotted dog albite with a sharp contact within the Gst at 15.61m
15.61	19.47	Massive Gst with several cm size late stage quartz vein
19.47	41.15	Massive Gst
41.15	41.4	Friable amphibole
41.4	47.08	Massive Gst
47.08	47.52	Albite -quartz -muscovite vein
47.52	53.02	Massive Gst
53.02	53.73	Friable albite with gradational minor epidote alteration
53.73	56.5	Albite with epidote alteration
56.5	56.95	Albite with minor epidote alteration and possible Ta inclusions
56.95	62.27	Albite-microcline-muscovite zone with blocky petalite
62.27	64.31	Massive petalite with minor microcline lenses
64.31	65.3	Microcline intermixed with muscovite ,blocky petalite and quartz
65.3	65.7	Massive microcline
65.7	66.18	Massive quartz
66.18	67.26	Massive microcline mixed with quartz
67.26	76.57	Mixed zone dominated by brecciated -blocky petalite within an albite matrix
76.57	80.15	Spotted dog albite with blocky petalite
80.15	92.34	Mixed zone with blocky petalite within a spotted dog albite and microcline matrix
92.34	97.5	Albite with high epidote alteration and brecciation developing a gradational contact with the Gst at 97.50m
97.5	102.58	Massive Gst with mm size carbonate veinlets

BIKITA MINERALS DIAMOND DRILLING LOG SHEET

LOCATION: VICTORS DUTUM: WGS 84

HOLE I.D: VB-DDH-001 COORDS: 336841/7793513

DATE: E.O.H.D: 97.83

DIP: -61 AZIMUTH: 180

LOGGED BY: ARTHUR GOGODO ELEVATION: 1170.634

DEPTH (m)		**GEOLOGY**
From	To	(lithology, structure, description)
0	13.6	Massive Gst with mm-size carbonate veinlets.
13.6	19.5	Fractured-altered Gst .
19.5	22	Cleavelandite mixed with bladed prismatic lepidolite and quartz.
22	23.3	Spotted dog albite Sharp peg /Gst contact at 23.30.
23.3	42	Altered Gst.
42	45.12	Spotted dog albite with minor fluidised SQI inclusions.
45.12	47.3	Mixed zone with blocky petalite and fluidised SQI within a spotted dog albite matrix.
47.3	49.27	Massive petalite with patchy spotted dog lenses.
49.27	50.4	Spotted dog albite.
50.4	57.47	Mixed zone with blocky petalite, disseminated lepidolite ,fluidised SQI within a spotted dog matrix.
57.47	69.38	Massive petalite with minor lepidolite inclusions.
69.38	70.3	Microcline zone with disseminated lepidolite.
70.3	72.68	Massive petalite with muscovite and quartz inclusions.
72.68	76.62	Spotted dog albite.
76.62	77.34	Gst xenolith with a gradational contact with the pegmatite
77.34	88.16	Spotted dog albite with blocky coarse grained lepidolite
88.16	89.41	Massive fluidised pink med-grained SQI within a spotted dog matrix and hectorite alteration
89.41	93.66	Spotted dog albite with minor fluidised fine grained SQI inclusions.
93.66	93.83	Sheared and altered Gst showing minor silicification on some portions.

BIKITA MINERALS DIAMOND DRILLING LOG SHEET

LOCATION: VICTORS DUTUM: WGS 84

HOLE I.D: VB-DDH-008 COORDS: 336939/7793458

DATE: E.O.H.D: 37.03

DIP: -90 AZIMUTH: 0

LOGGED BY: ARTHUR GOGODO ELEVATION: 1134.293

DEPTH (m)		**GEOLOGY**
From	To	(lithology, structure, description)
0	6.32	Altered oxidised ,sheared ,box-worked Gst with high-mod weathering sharp Gst-peg contact at 6.32m
6.32	7.05	Spotted dog albite
7.05	8.81	Mixed zone composed dominantly of fluidised petalite ,qtz, muscovite, albite, lepidolite and beryl.
8.81	13.72	Spotted dog albite zone with minor lepidolite inclusions.
13.72	14.71	Massive med-grained pink SQI intermixed with disseminated lepidolite and minor inclusions of quartz and albite.
14.71	16.3	Disseminated lepidolite with a matrix of albite ,qtz and SQI.
16.3	17.36	Massive petalite with minor lepidolite inclusions.
17.36	17.72	Mixed zone with disseminated med-grained lepidolite within an albite and SQI matrix.
17.72	18.06	Massive petalite with minor muscovite inclusions.
18.06	21.17	Mixed zone with disseminated med-grained lepidolite and blocky hectorite alteration within a spotted dog matrix .
21.17	21.52	Massive pink coarse grained SQI mixed with minor lepidolite.
21.52	23.1	Massive qrtz with minor lepidolite inclusions.
23.1	29	Bladed prismatic lepidolite zone within a qrtz and albite matrix.
29	31.6	Spotted albite .Sharp peg-Gst contract at 31.60m.
31.6	37.03	Massive carbonated Gst with minor epidote inclusions.

Appendix 2a: Channel Chip XRF Results

Sample ID	Ta (ppm)	Fe (ppm)	Sn (ppm)	Nb (ppm)	Rb (ppm)	Sr (ppm)
MK-001	*1642*	*0*	*0*	*315*	*0*	*360*
MK-002	*2059*	*0*	*385*	*366*	*22669*	*317*
MK-003	*770*	*0*	*192*	*116*	*16806*	*162*
MK-004	*3708*	*0*	*514*	*620*	*36700*	*373*
MK-005	*1092*	*3608*	*0*	*332*	*34424*	*540*
MK-006	*660*	*2105*	*458*	*122*	*24892*	*274*
BS-001	*493*	*0*	*503*	*130*	0	0
BS-002	*610*	*0*	*460*	*158*	0	0
BS-003	*204*	*10490*	*158*	*0*	0	0
BS-004	*759*	*0*	*384*	*212*	0	0
BS-005	*397*	*967*	*176*	0	0	0
BS-006	*703*	*0*	*369*	0	0	0
BS-007	*671*	*247*	*292*	0	0	0
BS-008	*694*	*0*	*384*	*91*	*33801*	*328*
BS-009	*693*	*0*	*406*	*82*	*32126*	*370*
BS-010	*365*	*0*	*457*	*0*	*191629*	*119*
BS-011	*698*	*0*	*394*	*63*	*36273*	*339*
BS-012	*94*	*1044*	*0*	*0*	*475*	*10*
BS-013	*145*	*866*	*84*	*0*	*1024*	*24*
BS-014	*2699*	*0*	*377*	*424*	*36564*	*349*
BS-015	*211*	*687*	*359*	*0*	*5936*	*129*
BS-016	*420*	*28587*	*207*	*55*	*161*	*0*
BS-017	*2958*	*2639*	*573*	*633*	*2308*	*159*
BN-001	*2467*	*1225*	*755*	*462*	*564*	*40*
BN-002	*273*	*524*	*119*	*63*	*6370*	*128*
BN-003	*433*	*0*	*245*	*116*	*17697*	*183*
BN-004	*298*	*0*	*251*	*103*	*22234*	*231*
BN-005	*18860*	*1271*	*9701*	*2623*	*7263*	*257*
BN-006	*1008*	*1901*	*129*	*162*	*629*	*33*
BN-007	*1751*	*456*	*533*	*290*	*1274*	*82*
BN-008	*782*	*0*	*347*	*87*	*20870*	*219*
AH-001	*941*	*750*	*383*	*168*	*405*	*25*
AH-002	*1151*	*902*	*664*	*193*	*258*	*16*
AH-003	*569*	*927*	*217*	*93*	*1285*	*92*

AH-004	*2211*	*1034*	*1029*	*415*	*1348*	*0*
AH-005	*176*	*941*	*72*	*32*	*443*	*25*
AH-006	*435*	*774*	*243*	*56*	*12*	*0*
AH-007	*163*	*606*	*85*	*0*	*166*	*17*
AH-008	*142*	*793*	*72*	*168*	*340*	*103*
AH-009	*176*	*3091*	*0*	*870*	*0*	*0*
AH-010	*181*	*758*	*0*	*0*	*0*	*0*
AH-011	*83*	*932*	*0*	*0*	*110*	*0*
AH-012	*158*	*832*	*90*	*32*	*188*	*6*
AH-013	*192*	*1531*	*70*	*0*	*146*	*0*
AH-014	*242*	*1578*	*94*	*79*	*1518*	*32*
AH-015	*740*	*976*	*311*	*73*	*3824*	*393*
AH-016	*693*	*0*	*395*	*77*	*2979*	*308*
VP-001	*581*	*0*	*290*	*211*	*24990*	*141*
VP-002	*397*	*0*	*304*	*64*	*27272*	*273*
VP-003	*1108*	*0*	*390*	*120*	*32350*	*336*
NG-001	*384*	*0*	*205*	*43*	*21159*	*217*
NG-002	*140*	*1537*	*90*	*0*	*1053*	*15*
NG-003	*140*	*1600*	*0*	*0*	*413*	*11*
NG-004	*252*	*0*	*177*	*48*	*18762*	*177*
NG-005	*140*	*1528*	*0*	*0*	*641*	*7*
DS-001	*2086*	*0*	*1336*	*330*	*44283*	*517*
DS-002	*258*	*2220*	*179*	*37*	*709*	*29*
DS-003	*348*	*1259*	*120*	*42*	*654*	*24*
DS-004	*832*	*472*	*347*	*137*	*121*	*236*
DS-005	*1273*	*464*	*1272*	*173*	*8904*	*121*
DS-006	*161*	*1270*	*99*	*0*	*1108*	*16*
DS-007	*437*	*456*	*131*	*49*	*162*	*331*
DS-008	*591*	*0*	*121*	*111*	*12964*	*144*
DS-009	*472*	*353*	*0*	*35*	*121*	*222*

Appendix 2b: Percussion Drilling XRF Results

BH.ID	Sample ID	From	To	Ta (ppm)	Fe (ppm)	Sn (ppm)	Nb (ppm)	Rb (ppm)	Sr (ppm)
MC-LP-PD-009	A001	0	1	198	1603	0	47	2890	63
MC-LP-PD-009	A002	1	2	268	2117	0	49	2068	44
MC-LP-PD-009	A003	2	3	213	1795	192	75	6485	44
MC-LP-PD-009	A004	3	4	180	0	160	79	5579	24
MC-LP-PD-009	A005	4	5	383	385	138	0	2921	26
MC-LP-PD-009	A006	5	6	258	1076	202	41	1425	78
MC-LP-PD-009	A007	6	7	307	0	129	41	6181	101
MC-LP-PD-009	A008	7	8	380	935	181	58	5076	79
MC-LP-PD-009	A009	8	9	143	3590	88	0	3394	33
MC-LP-PD-009	A010	9	10	145	3158	110	50	3026	36
MC-LP-PD-009	A011	10	11	2777	4323	421	0	2241	40
MC-LP-PD-009	A012	11	12	3482	3605	524	67	1751	40
MC-LP-PD-009	A013	12	13	1475	5209	245	82	7832	105
MC-LP-PD-009	A014	13	14	1157	8325	1924	384	8008	140
MC-LP-PD-009	A015	14	15	510	2986	216	79	8563	100
MC-LP-PD-009	A016	15	16	413	3872	224	74	1303	129

MC-LP-PD-009	A017	16	17	215	4847	188	109	8077	110
MC-LP-PD-009	A018	17	18	108	86942	91	28	4726	87
MC-LP-PD-009	A019	18	19	118	11639	95	51	5729	101
MC-LP-PD-009	A020	19	20	109	90201	0	31	5630	88
MC-LP-PD-009	A021	20	21	112	79390	0	0	1523	40
MC-LP-PD-014	A001	0	1	323	11682	231	90	5117	79
MC-LP-PD-014	A002	1	2	535	5188	327	170	4311	65
MC-LP-PD-014	A003	2	3	227	1102	171	50	1067	28
MC-LP-PD-014	A004	3	4	335	2759	168	18	679	32
MC-LP-PD-014	A005	4	5	329	1139	92	38	1860	80
MC-LP-PD-014	A006	5	6	265	2117	79	59	1410	67
MC-LP-PD-014	A007	6	7	339	3189	80	48	1111	66
MC-LP-PD-014	A008	7	8	520	769	114	140	2128	221
MC-LP-PD-014	A009	8	9	422	529	219	90	4850	289
MC-LP-PD-014	A010	9	10	459	510	276	80	5115	311
MC-LP-PD-014	A011	10	11	463	774	228	118	10421	218
MC-LP-PD-014	A012	11	12	418	657	119	97	10613	206
MC-LP-PD-014	A013	12	13	255	1026	170	49	11198	157
MC-LP-PD-014	A014	13	14	221	953	138	47	12845	147

MC-LP-PD-014	A015	14	15	325	0	91	130	16416	173
MC-LP-PD-014	A016	15	16	251	1325	218	77	8672	116
MC-LP-PD-014	A017	16	17	230	1820	181	121	3247	47
MC-LP-PD-014	A018	17	18	228	4552	225	182	6309	67
MC-LP-PD-014	A019	18	19	238	2657	165	151	5764	73
MC-LP-PD-014	A020	19	20	223	1565	136	140	3555	51
MC-LP-PD-014	A021	20	21	221	1224	111	187	2169	36
MC-LP-PD-014	A022	21	22	186	1079	0	98	1840	49
MC-LP-PD-014	A023	22	23	210	1479	137	127	2655	30
MC-LP-PD-014	A024	23	24	164	1729	0	82	2243	60

Appendix 2c: Reverse Circulation Chip XRF Results

BH.ID	Sample ID	From	To	Ta (ppm)	Fe (ppm)	Sn (ppm)	Nb (ppm)	Rb (ppm)	Sr (ppm)
BE-RC-PET-001	A001	34	35	*312*	*40979*	*379*	*316*	*12941*	*160*
BE-RC-PET-001	A002	35	36	*84*	*1944*	*0*	*77*	*13001*	*160*
BE-RC-PET-001	A003	36	37	*76*	*705*	*115*	*63*	*9664*	*134*
BE-RC-PET-001	A004	37	38	*84*	*1583*	*96*	*47*	*8340*	*154*
BE-RC-PET-001	A005	38	39	*0*	*425*	*0*	*0*	*13765*	*169*
BE-RC-PET-001	A006	39	40	*137*	*1251*	*96*	*80*	*16218*	*184*
BE-RC-PET-001	A007	40	41	*0*	*482*	*0*	*40*	*12367*	*144*
BE-RC-PET-001	A008	41	42	*67*	*1231*	*0*	*0*	*25*	*0*
BE-RC-PET-001	A009	42	43	*58*	*637*	*0*	*0*	*27*	*0*
BE-RC-PET-001	A010	43	44	*54*	*1242*	*0*	*0*	*0*	*0*
BE-RC-PET-001	A011	44	45	*62*	*929*	*0*	*0*	*20*	*0*
BE-RC-PET-001	A012	45	46	*70*	*2172*	*0*	*0*	*9*	*0*
BE-RC-PET-001	A013	46	47	*51*	*2301*	*0*	*0*	*0*	*0*

BE-RC-PET-001	A014	47	48	*47*	*1792*	*0*	*0*	*11*	*0*
BE-RC-PET-001	A015	48	49	*47*	*1532*	*0*	*0*	*20*	*0*
BE-RC-PET-001	A016	49	50	*55*	*601*	*0*	*0*	*8*	*0*
BE-RC-PET-001	A017	50	51	*49*	*1157*	*79*	*0*	*9*	*0*
BE-RC-PET-001	A018	51	52	*65*	*1241*	*0*	*0*	*3559*	*0*
BE-RC-PET-001	A019	52	53	*191*	*666*	*0*	*41*	*5522*	*0*
BE-RC-PET-001	A020	53	54	*77*	*1179*	*0*	*0*	*2011*	*0*
BE-RC-PET-001	A021	54	55	*180*	*966*	*0*	*0*	*1321*	*0*
BE-RC-PET-001	A022	55	56	*273*	*909*	*81*	*0*	*3587*	*196*
BE-RC-PET-001	A023	56	57	*402*	*465*	*189*	*35*	*5536*	*170*
BE-RC-PET-001	A024	57	58	*324*	*277*	*305*	*52*	*7844*	*179*
BE-RC-PET-001	A025	58	59	*126*	*1842*	*0*	*0*	*1243*	*103*
BE-RC-PET-001	A026	59	60	*170*	*923*	*94*	*0*	*2485*	*53*
BE-RC-PET-001	A027	60	61	*205*	*692*	*123*	*0*	*10944*	*83*
BE-RC-PET-001	A028	61	62	*334*	*666*	*265*	*0*	*15596*	*175*
BE-RC-PET-001	A029	62	63	*355*	*409*	*179*	*65*	*9464*	*146*
BE-RC-PET-001	A030	63	64	*298*	*409*	*120*	*0*	*5569*	*187*
BE-RC-PET-001	A031	64	65	*153*	*1500*	*120*	*0*	*2101*	*113*
BE-RC-PET-001	A032	65	66	*260*	*341*	*163*	*41*	*4369*	*90*
BE-RC-PET-001	A033	66	67	*479*	*255*	*270*	*120*	*7459*	*90*
BE-RC-PET-001	A034	67	68	*456*	*0*	*153*	*82*	*8590*	*104*
BE-RC-PET-001	A035	68	69	*393*	*350*	*92*	*73*	*0*	*5*
BE-RC-PET-001	A036	69	70	*383*	*0*	*131*	*54*	*7099*	*93*
BE-RC-PET-001	A037	70	71	*421*	*0*	*134*	*74*	*11735*	*120*
BE-RC-PET-001	A038	71	72	*274*	*0*	*166*	*71*	*18391*	*186*
BE-RC-PET-001	A039	72	73	*474*	*0*	*323*	*71*	*18920*	*194*
BE-RC-PET-001	A040	73	74	*187*	*2169*	*92*	*0*	*5516*	*69*
BE-RC-PET-001	A041	74	75	*222*	*722*	*129*	*46*	*8187*	*86*
BE-RC-PET-001	A042	75	76	*240*	*266*	*132*	*0*	*9290*	*122*
BE-RC-PET-001	A043	76	77	*284*	*219*	*139*	*0*	*9617*	*109*
BE-RC-PET-001	A044	77	78	*190*	*216*	*132*	*0*	*9368*	*116*
BE-RC-PET-001	A045	78	79	*223*	*188*	*144*	*0*	*8077*	*177*
BE-RC-PET-001	A046	79	80	*195*	*188*	*133*	*0*	*9282*	*194*
BE-RC-PET-001	A047	80	81	*286*	*220*	*0*	*44*	*8019*	*108*
BE-RC-PET-001	A048	81	82	*265*	*194*	*0*	*0*	*9384*	*114*
BE-RC-PET-001	A049	82	83	*200*	*207*	*170*	*0*	*9546*	*117*
AH-RC-PET-009	A001	17	18	*178*	*915*	*104*	*52*	*4090*	*56*

AH-RC-PET-009	A002	18	19	*215*	*4847*	*188*	*109*	*8077*	*110*
AH-RC-PET-009	A003	19	20	*108*	*86942*	*91*	*28*	*4726*	*87*
AH-RC-PET-009	A004	20	21	*118*	*11639*	*95*	*51*	*5729*	*101*
AH-RC-PET-009	A005	21	22	*109*	*90201*	*0*	*31*	*5630*	*88*
AH-RC-PET-009	A006	22	23	*112*	*79390*	*0*	*0*	*1523*	*40*
AH-RC-PET-009	A007	23	24	*92*	*3389*	*88*	*28*	*2667*	*67*
AH-RC-PET-009	A008	24	25	*64*	*836*	*0*	*39*	*8171*	*82*
AH-RC-PET-009	A009	25	26	*63*	*676*	*90*	*0*	*8105*	*70*
AH-RC-PET-009	A010	26	27	*147*	*958*	*0*	*0*	*12593*	*146*
AH-RC-PET-009	A011	27	28	*184*	*0*	*0*	*0*	*16836*	*178*
AH-RC-PET-009	A012	28	29	*105*	*1648*	*0*	*0*	*7203*	*81*
AH-RC-PET-009	A013	29	30	*123*	*1265*	*92*	*50*	*3084*	*41*
AH-RC-PET-009	A014	30	31	*208*	*2980*	*150*	*57*	*6545*	*82*
AH-RC-PET-009	A015	31	32	*100*	*1176*	*91*	*0*	*9696*	*106*
AH-RC-PET-009	A016	32	33	*133*	*1175*	*0*	*43*	*3081*	*61*
AH-RC-PET-009	A017	33	34	*121*	*1220*	*0*	*46*	*4876*	*67*
AH-RC-PET-009	A018	34	35	*244*	*2393*	*0*	*96*	*4105*	*55*
AH-RC-PET-009	A019	35	36	*262*	*2740*	*155*	*69*	*6248*	*73*
AH-RC-PET-009	A020	36	37	*191*	*1049*	*106*	*42*	*1512*	*32*
AH-RC-PET-009	A021	37	38	*162*	*1883*	*0*	*0*	*3556*	*37*
AH-RC-PET-009	A033	49	50	*111*	*1671*	*110*	*0*	*4311*	*61*
AH-RC-PET-009	A034	50	51	*129*	*6728*	*276*	*140*	*6979*	*78*
AH-RC-PET-009	A035	51	52	*89*	*1510*	*89*	*34*	*4681*	*74*
AH-RC-PET-009	A036	52	53	*128*	*1477*	*0*	*48*	*6265*	*84*
AH-RC-PET-009	A037	53	54	*182*	*4663*	*179*	*90*	*6237*	*84*
AH-RC-PET-009	A038	54	55	*108*	*4681*	*90*	*99*	*3165*	*60*
AH-RC-PET-009	A039	55	56	*147*	*3739*	*122*	*71*	*5887*	*92*
AH-RC-PET-009	A040	56	57	*105*	*3222*	*80*	*49*	*5081*	*70*
AH-RC-PET-009	A041	57	58	*181*	*7534*	*240*	*123*	*5992*	*75*
AH-RC-PET-009	A042	58	59	*164*	*5033*	*180*	*82*	*5130*	*59*
AH-RC-PET-009	A043	59	60	*171*	*3980*	*121*	*113*	*7275*	*81*
AH-RC-PET-009	A044	60	61	*179*	*3161*	*0*	*80*	*1893*	*26*
AH-RC-PET-009	A045	61	62	*99*	*78441*	*378*	*0*	*979*	*57*
AH-RC-PET-009	A046	62	63	*176*	*6147*	*456*	*78*	*3265*	*51*
AH-RC-PET-009	A047	63	64	*126*	*24373*	*1043*	*59*	*2312*	*32*
AH-RC-PET-009	A048	64	65	*133*	*74408*	*0*	*0*	*617*	*16*

AHS-RC-PET-001	A025	56	57	*95*	*489*	*0*	*0*	*9802*	*115*
AHS-RC-PET-001	A026	57	58	*138*	*974*	*0*	*0*	*7081*	*90*
AHS-RC-PET-001	A027	58	59	*105*	*1282*	*0*	*0*	*548*	*8*
AHS-RC-PET-001	A028	59	60	*103*	*443*	*90*	*0*	*3286*	*52*
AHS-RC-PET-001	A029	60	61	*129*	*1163*	*0*	*0*	*1423*	*172*
AHS-RC-PET-001	A030	61	62	*169*	*795*	*0*	*0*	*4522*	*493*
AHS-RC-PET-001	A031	62	63	*110*	*822*	*0*	*0*	*3074*	*110*
AHS-RC-PET-001	A032	63	64	*143*	*834*	*0*	*0*	*8479*	*56*
AHS-RC-PET-001	A033	64	65	*120*	*643*	*0*	*54*	*7540*	*138*
AHS-RC-PET-001	A034	65	66	*139*	*1001*	*85*	*51*	*8713*	*58*
AHS-RC-PET-001	A035	66	67	*93*	*1525*	*0*	*41*	*1619*	*46*
AHS-RC-PET-001	A036	67	68	*198*	*889*	*58*	*0*	*3086*	*50*
AHS-RC-PET-001	A037	68	69	*147*	*753*	*96*	*0*	*1843*	*92*
AHS-RC-PET-001	A038	69	70	*149*	*503*	*80*	*60*	*3009*	*110*
AHS-RC-PET-001	A039	70	71	*176*	*823*	*93*	*49*	*4180*	*39*
AHS-RC-PET-001	A040	71	72	*107*	*782*	*0*	*0*	*9302*	*46*
AHS-RC-PET-001	A041	72	73	121	929	123	62	7592	49
V-RC-PET-028	A001	17	18	*143*	*73269*	*0*	*0*	*78*	*47*
V-RC-PET-028	A002	18	19	*104*	*76618*	*0*	*0*	*78*	*50*
V-RC-PET-028	A003	19	20	*761*	*29213*	*215*	*152*	*3322*	*67*
V-RC-PET-028	A004	21	22	*258*	*2186*	*148*	*121*	*11761*	*51*

V-RC-PET-028	A005	22	23	*246*	*2373*	*189*	*159*	*5406*	*67*
V-RC-PET-028	A006	23	24	*113*	*9206*	*148*	*86*	*4189*	*52*
V-RC-PET-028	A007	24	25	*83*	*64645*	*0*	*0*	*99*	*70*
V-RC-PET-028	A008	41	42	*117*	*63404*	*0*	*0*	*99*	*70*
V-RC-PET-028	A009	42	43	*18*	*81824*	*0*	*0*	*112*	*52*
V-RC-PET-028	A010	43	44	*87*	*74626*	*0*	*0*	*113*	*66*
V-RC-PET-028	A011	44	45	*136*	*42005*	*0*	*0*	*2129*	*69*
V-RC-PET-028	A012	56	57	*231*	*3948*	*0*	*95*	*7833*	*51*
V-RC-PET-028	A013	59	60	*0*	*4074*	*0*	*60*	*4960*	*57*
V-RC-PET-028	A015	60	61	*80*	*3833*	*0*	*45*	*1608*	*21*
V-RC-PET-028	A016	61	62	*114*	*3742*	*0*	*40*	*9136*	*80*
V-RC-PET-028	A017	62	63	*2119*	*8575*	*125*	*119*	*13526*	*132*
V-RC-PET-028	A018	63	64	*136*	*5825*	*137*	*76*	*7528*	*77*
V-RC-PET-028	A019	64	65	*187*	*8117*	*114*	*80*	*8308*	*82*
V-RC-PET-028	A020	65	66	*104*	*3125*	*0*	*0*	*1154*	*27*
V-RC-PET-028	A021	66	67	*96*	*3964*	*0*	*0*	*417*	*51*
V-RC-PET-028	A022	67	68	*76*	*3877*	*0*	*0*	*1745*	*0*
V-RC-PET-028	A023	68	69	*120*	*3496*	*0*	*0*	*3418*	*34*
V-RC-PET-028	A024	69	70	*177*	*1737*	*73*	*0*	*10444*	*37*
V-RC-PET-028	A025	20	21	*158*	*4086*	*0*	*43*	*3374*	*39*
V-RC-PET-028	A026	45	46	*128*	*2432*	*0*	*0*	*3774*	*36*
V-RC-PET-028	A027	46	47	*249*	*2582*	*0*	*0*	*3832*	*40*
V-RC-PET-028	A028	48	49	*228*	*2271*	*0*	*0*	*1987*	*26*
V-RC-PET-028	A029	49	50	*190*	*3869*	*160*	*63*	*5426*	*51*
V-RC-PET-028	A030	58	59	*220*	*3885*	*120*	*60*	*5338*	*53*
V-RC-PET-028	A031	47	48	*249*	*5618*	*166*	*66*	*6490*	*62*
V-RC-PET-028	A032	50	51	*144*	*4677*	*105*	*89*	*5712*	*57*
V-RC-PET-028	A033	51	52	*146*	*3528*	*105*	*0*	*6236*	*58*
V-RC-PET-028	A034	57	58	*140*	*3480*	*0*	*38*	*6263*	*62*
V-RC-PET-028	A035	53	54	*148*	*3480*	*0*	*0*	*837*	*33*
V-RC-PET-028	A036	55	56	*180*	*5416*	*0*	*47*	*4850*	*60*
V-RC-PET-028	A037	52	53	*108*	*6602*	*0*	*0*	*839*	*51*
SH-RC- PET-001	A001	0	1	*3047*	*5740*	*342*	*841*	*1648*	*74*
SH-RC- PET-001	A002	1	2	*560*	*2468*	*0*	*182*	*2976*	*43*
SH-RC- PET-001	A003	2	3	*242*	*2683*	*0*	*37*	*530*	*29*
SH-RC- PET-001	A004	42	43	*291*	*4428*	*83*	*87*	*2266*	*25*
SH-RC- PET-001	A005	43	44	*329*	*2791*	*75*	*93*	*2878*	*39*

SH-RC- PET-001	A006	44	45	*322*	*2009*	*105*	*116*	*2857*	*36*
SH-RC- PET-001	A007	45	46	*282*	*1819*	*153*	*80*	*4125*	*47*
SH-RC- PET-001	A008	46	47	*283*	*1644*	*0*	*62*	*3522*	*65*
SH-RC- PET-001	A009	47	48	*281*	*2225*	*0*	*134*	*4225*	*88*
SH-RC- PET-001	A010	48	49	*174*	*1540*	*84*	*81*	*1470*	*52*
SH-RC- PET-001	A011	49	50	*122*	*975*	*0*	*82*	*2843*	*62*
SH-RC- PET-001	A012	50	51	*171*	*1029*	*78*	*0*	*3634*	*65*
SH-RC- PET-001	A013	51	52	*151*	*1083*	*76*	*0*	*2525*	*51*
SH-RC- PET-001	A014	52	53	*133*	*1259*	*0*	*44*	*1093*	*36*
SH-RC- PET-001	A015	53	54	*207*	*640*	*0*	*83*	*8551*	*100*
SH-RC- PET-001	A016	54	55	*109*	*1473*	*0*	*463*	*459*	*23*
SH-RC- PET-001	A017	55	56	*89*	*579*	*0*	*0*	*1023*	*88*
SH-RC- PET-001	A018	56	57	*111*	*1433*	*0*	*0*	*8103*	*80*
SH-RC- PET-001	A019	57	58	*131*	*0*	*0*	*0*	*17692*	*152*
SH-RC- PET-001	A020	58	59	*77*	*1353*	*0*	*0*	*2518*	*46*
SH-RC- PET-001	A021	59	60	*117*	*1378*	*0*	*0*	*4677*	*58*
SH-RC- PET-001	A022	60	61	*140*	*1776*	*0*	*25*	*742*	*14*
SH-RC- PET-001	A023	61	62	*207*	*1606*	*80*	*56*	*2815*	*57*
SH-RC- PET-001	A024	62	63	*121*	*1666*	*0*	*71*	*1021*	*31*
SH-RC- PET-001	A025	63	64	*110*	*1386*	*0*	*37*	*509*	*50*
SH-RC- PET-001	A026	64	65	*150*	*1062*	*0*	*39*	*4920*	*80*
SH-RC- PET-001	A027	65	66	*138*	*1578*	*99*	*0*	*1138*	*38*
SH-RC- PET-001	A028	66	67	*171*	*2193*	*88*	*81*	*1795*	*29*
SH-RC-PET-020	A001	10	11	*275*	*4369*	*232*	*0*	*7130*	*77*
SH-RC-PET-020	A002	11	12	*173*	*3200*	*126*	*0*	*7640*	*123*
SH-RC-PET-020	A003	12	13	*177*	*1815*	*0*	*0*	*9638*	*102*
SH-RC-PET-020	A004	13	14	*151*	*1497*	*137*	*0*	*8406*	*114*
SH-RC-PET-020	A005	14	15	*181*	*2230*	*100*	*0*	*3822*	*73*
SH-RC-PET-020	A006	15	16	*153*	*1109*	*126*	*0*	*5077*	*79*
SH-RC-PET-020	A007	16	17	*170*	*1834*	*0*	*35*	*2089*	*38*
SH-RC-PET-020	A008	17	18	101	1714	0	40	5902	110
SH-RC-PET-020	A009	18	19	*130*	*2379*	*91*	*57*	*2114*	*44*
SH-RC-PET-020	A010	65	66	*133*	*3646*	*107*	*48*	*2268*	*67*
SH-RC-PET-020	A011	66	67	*158*	*1492*	*0*	*0*	*4284*	*66*
SH-RC-PET-020	A012	67	68	*162*	*1267*	*127*	*47*	*3877*	*64*
SH-RC-PET-020	A013	68	69	*210*	*1457*	*223*	*0*	*7833*	*89*

SH-RC-PET-020	A014	69	70	*137*	*1723*	*115*	*0*	*5608*	*122*
SH-RC-PET-020	A015	70	71	*243*	*2037*	*1390*	*110*	*7571*	*126*
SH-RC-PET-020	A016	71	72	125	2078	154	0	1359	46
SH-RC-PET-020	A017	72	73	*197*	*1067*	*110*	*87*	*2320*	*38*
SH-RC-PET-020	A018	73	74	*132*	*957*	*108*	*82*	*1220*	*23*
SH-RC-PET-020	A019	74	75	*160*	*1759*	*120*	*70*	*7470*	*39*
SH-RC-PET-020	A020	75	76	*222*	*1337*	*59*	*53*	*6489*	*25*
SH-RC-PET-020	A021	76	77	*317*	*1493*	*249*	*32*	*4148*	*36*
SH-RC-PET-020	A022	77	78	*251*	*774*	*177*	*61*	*2840*	*49*
SH-RC-PET-020	A023	78	79	*201*	*1136*	*133*	*39*	*5048*	*42*
SH-RC-PET-020	A024	79	80	*148*	*580*	*328*	*46*	*4104*	*41*
SH-RC-PET-020	A025	80	81	*195*	*638*	*320*	*89*	*3603*	*103*
SH-RC-PET-020	A026	81	82	*98*	*535*	*248*	*0*	*8208*	*80*
SH-RC-PET-020	A027	82	83	*220*	*935*	*307*	*56*	*5658*	*82*
SH-RC-PET-020	A028	83	84	*319*	*1083*	*407*	*117*	*2150*	*60*
SH-RC-PET-020	A029	84	85	*206*	*1368*	*510*	*0*	*2607*	*71*
SH-RC-PET-020	A030	85	86	*249*	*932*	*469*	*91*	*5407*	*54*
SH-RC-PET-020	A031	86	87	177	1810	288	40	4602	48
SH-RC-PET-034	A001	4	5	*174*	*2396*	*453*	*79*	*4546*	*55*
SH-RC-PET-034	A002	5	6	*192*	*1935*	*329*	*55*	*4319*	*65*
SH-RC-PET-034	A003	6	7	*148*	*66527*	*116*	*0*	*438*	*51*
SH-RC-PET-034	A004	11	12	*227*	*15343*	*324*	*96*	*7064*	*84*
SH-RC-PET-034	A005	43	44	*132*	*51568*	*0*	*50*	*2921*	*41*
SH-RC-PET-034	A006	44	45	*221*	*1978*	*0*	*0*	*2886*	*35*
SH-RC-PET-034	A007	45	46	*236*	*1733*	*91*	*76*	*3983*	*51*
SH-RC-PET-034	A008	46	47	209	1405	0	92	5299	74
SH-RC-PET-034	A009	47	48	*142*	*2624*	*0*	*36*	*2561*	*62*
SH-RC-PET-034	A010	48	49	*115*	*2445*	*0*	*0*	*1177*	*26*
SH-RC-PET-034	A011	49	50	*129*	*1730*	*0*	*66*	*13738*	*135*
SH-RC-PET-034	A012	50	51	*129*	*1259*	*0*	*41*	*13027*	*146*
SH-RC-PET-034	A013	51	52	*92*	*2733*	*0*	*63*	*5586*	*54*
SH-RC-PET-034	A014	52	53	*85*	*887*	*0*	*0*	*18592*	*165*
SH-RC-PET-034	A015	53	54	*41*	*557*	*0*	*33*	*17991*	*152*
SH-RC-PET-034	A016	54	55	90	544	0	28	17992	141

SH-RC-PET-034	A017	55	56	*214*	*1741*	*0*	*93*	*2507*	*24*
SH-RC-PET-034	A018	56	57	*222*	*1630*	*0*	*95*	*2515*	*23*
SH-RC-PET-034	A019	57	58	*243*	*3164*	*127*	*198*	*2293*	*42*
SH-RC-PET-034	A020	58	59	*90*	*1869*	*81*	*52*	*1504*	*18*
SH-RC-PET-034	A021	59	60	*95*	*1928*	*0*	*0*	*1542*	*18*
SH-RC-PET-034	A022	60	61	*81*	*3114*	*0*	*0*	*1830*	*28*
SH-RC-PET-034	A023	61	62	*119*	*3030*	*72*	*29*	*930*	*11*
SH-RC-PET-034	A024	62	63	169	2075	0	66	3979	38
SH-RC-PET-034	A025	63	64	*268*	*3808*	*140*	*217*	*5429*	*59*
SH-RC-PET-034	A026	64	65	*250*	*2804*	*81*	*121*	*4331*	*48*
SH-RC-PET-034	A027	65	66	*139*	*2655*	*93*	*39*	*4620*	*44*
SH-RC-PET-034	A028	66	67	*173*	*2600*	*0*	*96*	*5031*	*48*
SH-RC-PET-034	A029	67	68	*127*	*2464*	*88*	*69*	*2954*	*29*
SH-RC-PET-034	A030	68	69	*147*	*1892*	*0*	*0*	*6348*	*71*
SH-RC-PET-034	A031	69	70	*142*	*2523*	*76*	*65*	*3751*	*43*
SH-RC-PET-034	A032	70	71	135	1769	94	0	2558	30
SH-RC-PET-034	A033	71	72	*201*	*3750*	*83*	*82*	*4818*	*42*
SH-RC-PET-034	A034	72	73	*140*	*2467*	*88*	*85*	*4202*	*37*
SH-RC-PET-034	A035	73	74	*230*	*2576*	*125*	*121*	*3615*	*40*
SH-RC-PET-034	A036	74	75	*190*	*4057*	*137*	*67*	*4940*	*49*
SH-RC-PET-034	A037	75	76	*193*	*2484*	*126*	*42*	*7044*	*86*
SH-RC-PET-034	A038	76	77	*148*	*1791*	*0*	*0*	*3929*	*42*
SH-RC-PET-034	A039	77	78	*136*	*2289*	*0*	*47*	*1914*	*30*
SH-RC-PET-034	A040	78	79	228	3127	92	119	3009	31
SH-RC-PET-034	A041	79	80	*140*	*2428*	*87*	*36*	*4248*	*61*
SH-RC-PET-034	A042	80	81	*117*	*1470*	*0*	*0*	*4201*	*64*
SH-RC-PET-034	A043	81	82	*113*	*1820*	*0*	*0*	*828*	*32*
SH-RC-PET-034	A044	82	83	*100*	*1837*	*0*	*31*	*6177*	*125*
SH-RC-PET-034	A045	83	84	*197*	*1935*	*0*	*65*	*1553*	*36*
SH-RC-PET-034	A046	84	85	*118*	*2859*	*0*	*0*	*1963*	*32*
SH-RC-PET-034	A047	85	86	*197*	*2264*	*82*	*29*	*1973*	*43*
LN -RC -PET 004	A001	24	25	*178*	*3983*	*3077*	*51*	*2577*	*35*
LN -RC -PET 004	A002	25	26	*175*	*2299*	*84*	*48*	*2048*	*26*
LN -RC -PET 004	A003	26	27	*200*	*2019*	*65*	*43*	*1988*	*24*

LN -RC -PET 004	A004	27	28	*187*	*2528*	*0*	*43*	*2312*	*27*
LN -RC -PET 004	A005	28	29	*202*	*2616*	*69*	*56*	*2163*	*34*
LN -RC -PET 004	A006	29	30	*266*	*3006*	*65*	*44*	*2060*	*25*
LN -RC -PET 004	A007	30	31	*231*	*2224*	*52*	*53*	*2117*	*42*
LN -RC -PET 004	A008	31	32	*204*	*1591*	*144*	*136*	*3632*	*39*
LN -RC -PET 004	A009	32	33	*227*	*986*	*141*	*76*	*938*	*13*
LN -RC -PET 004	A010	33	34	*235*	*2459*	*83*	*120*	*4668*	*58*
LN -RC -PET 004	A011	34	35	*138*	*878*	*0*	*95*	*4949*	*58*
LN -RC -PET 004	A012	35	36	*187*	*1695*	*0*	*123*	*3867*	*38*
LN -RC -PET 004	A013	36	37	*238*	*1942*	*88*	*307*	*2944*	*41*
LN -RC -PET 004	A014	37	38	*153*	*2196*	*105*	*29*	*2523*	*28*
LN -RC -PET 004	A015	38	39	*142*	*2057*	*99*	*32*	*1171*	*15*
LN -RC -PET 004	A016	39	40	*180*	*1166*	*102*	*0*	*3361*	*35*
LN -RC -PET 004	A017	40	41	*234*	*1729*	*99*	*41*	*5129*	*58*
LN -RC -PET 004	A018	41	42	*205*	*1043*	*91*	*0*	*5932*	*97*
LN -RC -PET 004	A019	42	43	*148*	*1459*	*84*	*0*	*3319*	*20*
LN -RC -PET 004	A020	43	44	*179*	*1741*	*117*	*50*	*2222*	*60*
LN -RC -PET 004	A021	44	45	*238*	*2208*	*86*	*71*	*4614*	*20*
LN -RC -PET 004	A022	45	46	206	1399	98	0	1884	36
LN -RC -PET 004	A023	46	47	*148*	*0*	*121*	*59*	*1106*	*33*
LN -RC -PET 004	A024	47	48	*127*	*1330*	*110*	*40*	*2395*	*45*
LN -RC -PET 004	A025	48	49	*219*	*2296*	*100*	*35*	*5799*	*41*
LN -RC -PET 004	A026	49	50	*180*	*3099*	*99*	*0*	*4022*	*57*
LN -RC -PET 004	A027	50	51	*109*	*1988*	*89*	*49*	*7288*	*15*
LN -RC -PET 004	A028	51	52	*106*	*892*	*72*	*55*	*7179*	*72*
LN -RC -PET 004	A029	52	53	*155*	*4267*	*0*	*40*	*4449*	*80*
LN -RC -PET 004	A030	53	54	253	7225	157	0	2802	30
LN -RC -PET 004	A031	54	55	*155*	*2600*	*339*	*40*	*1019*	*41*
LN -RC -PET 004	A032	55	56	*127*	*2519*	*180*	*59*	*1858*	*33*
LN -RC -PET 004	A033	56	57	*213*	*3749*	*196*	*83*	*3002*	*71*
LN -RC -PET 004	A034	57	58	*207*	*991*	*157*	*73*	*4662*	*57*
LN -RC -PET 004	A035	58	59	*117*	*7096*	*177*	*0*	*2314*	*49*
LN -RC -PET 004	A036	59	60	*151*	*4339*	*106*	*0*	*3261*	*21*
LN -RC -PET 004	A037	60	61	*131*	*2066*	*102*	*93*	*2579*	*28*
WC-RC-003	A001	0	1	*178*	*928*	*104*	*48*	*1855*	*24*
WC-RC-003	A002	1	2	*215*	*4847*	*188*	*47*	*3852*	*49*
WC-RC-003	A003	2	3	*108*	*87536*	*91*	*0*	*921*	*16*

WC-RC-003	A004	3	4	*118*	*11652*	*95*	*0*	*95*	*27*
WC-RC-003	A005	59	60	*112*	*89335*	*0*	*0*	*0*	*83*
WC-RC-003	A006	60	61	*110*	*79353*	*0*	*0*	*249*	*75*
WC-RC-003	A007	61	62	*88*	*3424*	*84*	*58*	*946*	*66*
WC-RC-003	A008	62	63	*189*	*4335*	*85*	*39*	*2660*	*49*
WC-RC-003	A009	63	64	*101*	*3726*	*0*	*26*	*692*	*55*
WC-RC-003	A010	64	65	*131*	*3394*	*87*	*36*	*9775*	*116*
WC-RC-003	A011	65	66	*137*	*7027*	*114*	*38*	*2967*	*48*
WC-RC-003	A012	66	67	*128*	*5416*	*263*	*45*	*4564*	*55*
WC-RC-003	A013	67	68	*155*	*5188*	*151*	*43*	*6053*	*74*
WC-RC-003	A014	68	69	*144*	*88*	*88*	*58*	*8834*	*93*
WC-RC-003	A015	69	70	*147*	*3912*	*75*	*62*	*2846*	*32*
WC-RC-003	A016	70	71	*185*	*3365*	*81*	*67*	*1523*	*22*
WC-RC-003	A017	71	72	*196*	*6834*	*0*	*95*	*2377*	*28*
WC-RC-003	A018	72	73	*155*	*6305*	*97*	*43*	*3482*	*46*
WC-RC-003	A019	73	74	*235*	*3797*	*0*	*38*	*1583*	*22*
WC-RC-003	A020	74	75	*126*	*8026*	*115*	*40*	*5456*	*63*
WC-RC-003	A021	75	76	*181*	*14656*	*117*	*67*	*8834*	*36*
WC-RC-003	A022	76	77	*85*	*77726*	*0*	*0*	*327*	*68*
WC-RC-003	A023	77	78	*93*	*13425*	*0*	*0*	*322*	*41*
WC-RC-004	A001	25	26	*286*	*85240*	*124*	*42*	*117*	*95*
WC-RC-004	A002	24	25	*99*	*81066*	*153*	*0*	*176*	*77*
WC-RC-004	A003	26	27	*130*	*47611*	*113*	*35*	*894*	*31*
WC-RC-004	A004	27	28	*186*	*13168*	*0*	*58*	*306*	*31*
WC-RC-004	A005	28	29	*93*	*85179*	*83*	*0*	*554*	*54*
WC-RC-004	A006	29	30	*109*	*95839*	*0*	*34*	*409*	*67*
WC-RC-004	A007	58	59	*147*	*115633*	*0*	*0*	*189*	*97*
WC-RC-004	A008	59	60	*194*	*74730*	*251*	*67*	*2257*	*104*
WC-RC-004	A009	60	61	*282*	*13814*	*368*	*184*	*6438*	*82*
WC-RC-004	A010	61	62	*151*	*6701*	*0*	*48*	*6070*	*77*
WC-RC-004	A011	62	63	*338*	*12725*	*2616*	*181*	*11731*	*143*
WC-RC-004	A012	63	64	*1575*	*5843*	*28291*	*856*	*1523*	*29*
WC-RC-004	A013	64	65	*238*	*39402*	*2227*	*101*	*3604*	*57*
WC-RC-004	A014	65	66	*218*	*7833*	*150*	*110*	*4647*	*43*
MKS-RC-PET-003	A001	19	20	*191*	*87800*	*406*	*33*	*2063*	*110*

MKS-RC-PET-003	A002	20	21	*174*	*3460*	*262*	*89*	*2776*	*33*
MKS-RC-PET-003	A003	21	22	*232*	*2426*	*122*	*137*	*2487*	*31*
MKS-RC-PET-003	A004	22	23	*211*	*1525*	*97*	*57*	*660*	*15*
MKS-RC-PET-003	A005	23	24	*252*	*2959*	*114*	*168*	*5009*	*54*
MKS-RC-PET-003	A006	24	25	*205*	*2315*	*135*	*143*	*5080*	*58*
MKS-RC-PET-003	A007	25	26	*208*	*1372*	*93*	*104*	*2903*	*31*
MKS-RC-PET-003	A008	26	27	*196*	*2201*	*78*	*69*	*1100*	*25*
MKS-RC-PET-003	A009	27	28	*186*	*13305*	*1117*	*84*	*1452*	*26*
MKS-RC-PET-003	A010	28	29	*108*	*103234*	*0*	*0*	*1118*	*20*

Appendix 3a: Channel Chip AAS Results

SAMPLE NAME	**%Li_2O**	**%K_2O**	**%Na_2O**	**%Al_2O_3**	**%Fe_2O_3**	**%Cs_2O**	**%Rb_2O**
AH-001	4.14	0.09	0.24	16.39	0.038	0.79	0.92
AH-002	5.69	0.10	0.16	17.27	0.040	0.86	0.79
AH-003	2.35	0.44	1.07	15.66	0.061	0.95	0.68
AH-004	4.32	0.25	0.40	16.48	0.071	0.37	0.14
AH-005	3.79	0.20	1.81	16.23	0.070	0.59	0.26
AH-006	5.40	0.12	0.44	16.11	0.063	0.16	0.06
AH-007	5.66	0.03	0.74	16.98	0.045	0.19	0.03
AH-008	4.27	0.07	0.84	16.53	0.047	0.33	0.30
AH-009	4.47	0.07	0.50	16.68	0.043	0.23	0.09
AH-010	4.28	0.11	1.01	16.60	0.067	0.49	0.32
AH-011	4.80	0.02	1.16	16.70	0.063	0.19	0.04
AH-012	4.48	0.02	0.16	16.54	0.053	0.32	0.16
AH-013	4.80	0.02	0.24	16.67	0.091	0.17	0.22
AH-014	4.16	0.31	0.85	16.32	0.110	0.24	1.80
AH-015	3.43	7.97	0.31	16.89	0.037	0.32	4.82
AH-016	2.46	9.51	0.45	15.92	0.035	0.38	5.30

BN-001	2.08	5.11	1.18	15.80	0.065	0.10	3.48
BN-002	4.29	0.30	0.52	16.65	0.119	0.20	0.06
BN-003	2.32	4.94	3.70	15.10	0.075	0.34	2.96
BN-004	0.79	2.57	7.59	15.55	0.070	0.47	0.93
BN-005	1.16	2.08	6.54	15.82	0.162	0.29	0.94
BN-006	4.47	0.28	0.47	16.64	0.017	0.37	0.01
BN-007	4.80	0.36	0.59	16.07	0.115	0.33	0.01
BN-008	2.37	6.00	1.21	15.82	0.050	0.19	3.57
BS-001	2.32	7.62	0.57	16.32	0.042	0.36	4.42
BS-002	7.28	0.15	0.11	16.33	0.015	0.42	0.37
BS-003	3.43	0.43	1.08	15.96	0.058	0.52	0.38
BS-004	3.89	7.78	0.54	15.99	0.010	0.28	5.60
BS-005	3.75	0.24	1.56	15.87	0.049	0.93	0.67
BS-006	2.81	6.52	1.68	15.62	0.032	0.79	4.63
BS-007	2.45	5.28	1.66	15.29	0.018	0.12	3.55
BS-008	2.92	6.03	0.73	15.91	0.014	0.34	4.55
BS-009	2.97	7.32	0.59	15.97	0.015	0.78	5.38
BS-010	1.16	3.26	2.06	14.88	0.016	20.97	2.66
BS-011	3.09	7.87	0.84	15.89	0.021	0.15	5.55
BS-012	3.08	0.18	0.11	15.79	0.045	0.71	0.26
BS-013	4.33	0.18	0.17	16.32	0.047	0.94	1.09
BS-014	2.99	7.29	1.06	15.88	0.033	0.68	5.70
BS-015	1.28	3.50	2.44	14.87	0.039	12.27	2.04
BS-016	0.56	4.46	5.30	12.66	0.216	0.67	2.21
BS-017	0.49	1.19	8.50	12.19	0.109	0.60	1.06
DS-001	3.86	7.72	0.58	15.93	0.099	0.42	5.13
DS-002	3.12	0.22	1.93	15.83	0.089	0.54	0.20
DS-003	3.69	0.20	1.55	15.89	0.063	0.38	0.23
DS-004	8.63	0.05	0.09	17.19	0.016	0.11	0.14
DS-005	0.75	6.78	2.61	17.9	0.114	22.02	1.7
DS-006	0.76	0.11	0.91	15.49	0.053	0.28	0.26
DS-007	7.77	0.02	0.04	17.12	0.014	0.10	0.16
DS-008	8.36	0.99	0.04	16.70	0.098	0.92	0.16
DS-009	0.65	3.6	2.03	18.6	0.074	23.1	2.11
MK-001	3.63	7.46	1.40	16.02	0.115	0.76	3.84
MK-002	2.67	5.69	0.61	15.70	0.138	0.88	3.89
MK-003	2.57	6.38	3.22	15.67	0.095	0.59	6.23

MK-004	3.10	7.68	0.79	15.88	0.185	0.62	4.62
MK-005	3.30	7.28	3.67	15.93	0.192	0.82	6.19
MK-006	2.25	4..96	0.91	15.62	0.172	0.49	2.72
NG-001	2.39	4.96	0.85	15.62	0.029	0.63	3.11
NG-002	4.47	0.19	0.34	16.64	0.097	0.19	0.08
NG-003	5.44	0.06	0.29	16.93	0.09	0.16	0.07
NG-004	2.54	4.95	0.90	15.70	0.067	0.39	2.86
NG-005	4.23	0.13	1.34	16.38	0.092	0.23	0.2
NG-POL-001	0.45	2.21	2.22	17.36	0.120	19.63	2.35
NG-POL-002	0.43	3.12	2.20	17.55	0.114	20.24	3.63
NG-POL-003	0.46	2.78	2.28	17.63	0.119	17.73	3.29
NG-POL-004	0.69	2.95	2.36	17.48	0.138	16.90	3.01
VP-001	1.33	7.79	0.52	15.49	0.032	0.71	4.24
VP-002	2.56	6.54	0.54	15.70	0.051	0.68	3.68
VP-003	2.03	8.69	0.66	15.58	0.003	0.66	5.28
V-POL-001	0.46	1.42	2.32	17.76	0.035	26.78	0.91
V-POL-002	0.33	1.26	2.50	17.85	0.025	26.15	0.88

Appendix 3b: Percussion Drilling AAS Results

Sample_Name	From	To	Li_2O_pct	K_2O_pct	Na_2O_pct	Al_2O_3_pct	Fe_2O_3_pct	Cs_2O_pct	Rb_2O_pct	Easting	Northing	Elevation
C-PD-PET-006A001	9	10	0.16	0.36	2.84	14.26	0.166	0.33	0.32	336063	7793622	1124
C-PD-PET-006A002	10	11	1.09	0.73	2.67	15.3	0.159	0.23	0.47	336063	7793622	1123
C-PD-PET-006A003	11	12	1.33	2.3	1.35	15.46	0.162	0.25	0.95	336063	7793622	1122
C-PD-PET-006A004	12	13	3.07	0.29	0.57	16.05	0.18	0.31	0.21	336063	7793622	1121
C-PD-PET-006A005	13	14	0.98	1.45	3.09	15	0.171	0.37	0.5	336063	7793622	1120
C-PD-PET-006A006	14	15	0.76	1.71	5.77	14.8	0.196	0.31	0.77	336063	7793622	1119
C-PD-PET-006A007	15	16	0.27	2.34	8.3	14.32	0.184	0.36	0.77	336063	7793622	1118
C-PD-PET-006A008	16	17	0.2	0.5	2.06	14.28	0.165	0.34	0.25	336063	7793622	1117
C-PD-PET-016A001	21	22	0.23	0.22	2.32	13.33	0.406	0.31	0.1	336182	7793667	1109
C-PD-PET-016A002	22	23	0.13	0.54	3.55	13.13	0.398	0.46	0.12	336182	7793667	1108
C-PD-PET-016A003	23	24	0.21	3.17	3.67	13.21	0.298	0.46	0.15	336182	7793667	1107
C-PD-PET-016A004	24	25	2.58	2.69	0.94	15.58	0.26	0.68	0.16	336182	7793667	1106
C-PD-PET-016A005	25	26	1.2	2.39	2.39	14.2	0.205	0.21	0.3	336182	7793667	1105
C-PD-PET-016A006	26	27	3.49	6.38	1.01	16.49	0.34	0.53	0.4	336182	7793667	1104
C-PD-PET-016A007	27	28	3.28	0.24	1.14	16.28	0.287	0.71	0.51	336182	7793667	1103
C-PD-PET-016A008	28	29	3.23	0.28	1.4	16.23	0.241	0.34	0.19	336182	7793667	1102
C-PD-PET-016A009	29	30	3.35	0.2	1.47	16.35	0.244	0.7	0.3	336182	7793667	1101
BS-PD-SQI-008A001	1	2	0.41	1.03	5.9	13.3	0.387	0.15	0.32	336241	7792319	1179

BS-PD-SQI-008A002	2	3	0.23	0.9	5.31	14.9	0.196	0.17	0.21	336241	7792319	1178
BS-PD-SQI-008A003	3	4	3.02	0.16	0.39	16	0.132	0.08	0.04	336241	7792319	1177
BS-PD-SQI-008A004	4	5	4.2	0.04	0.6	16.75	0.12	0.12	0.18	336241	7792319	1176
BS-PD-SQI-008A005	5	6	5.17	0.07	0.16	16.85	0.087	0.05	0.02	336241	7792319	1175
BS-PD-SQI-008A006	6	7	4.51	0.05	0.13	16.79	0.131	0.09	0.01	336241	7792319	1174
BS-PD-SQI-008A007	7	8	3.04	0.18	1.87	15.26	0.072	0.19	0.18	336241	7792319	1173
BS-PD-SQI-008A008	8	9	2.26	0.41	1.83	15.26	0.072	0.19	0.18	336241	7792319	1172
BS-PD-SQI-008A009	9	10	1.41	0.85	4.24	14.85	0.066	0.12	0.39	336241	7792319	1171
BS-PD-SQI-008A010	10	11	0.84	0.92	7.46	13.92	0.07	0.14	1.04	336241	7792319	1170
BS-PD-SQI-008A011	11	12	1.52	1.62	4.17	15.7	0.064	0.14	0.5	336241	7792319	1169
BS-PD-SQI-008A012	12	13	1.4	1.17	3.5	15.8	0.09	0.17	0.64	336241	7792319	1168

BS-PD-SQI-008A013	13	14	2.04	4.17	3.68	15.21	0.071	0.31	1.19	336241	7792319	1167
BS-PD-SQI-008A014	14	15	1.29	2.61	2.86	15.21	0.071	0.31	1.19	336241	7792319	1166
BS-PD-SQI-008A015	15	16	0.85	1.92	5.09	14.86	0.132	0.41	0.73	336241	7792319	1165
BS-PD-SQI-008A016	16	17	0.34	1.02	6.64	14.38	0.126	0.29	0.26	336241	7792319	1164
BS-PD-SQI-008A017	17	18	0.45	1.56	5.7	14.5	0.012	0.32	0.41	336241	7792319	1163
BS-PD-SQI-008A018	18	19	0.39	0.93	2.38	14.41	0.156	0.5	0.21	336241	7792319	1162
BS-PD-SQI-008A019	19	20	0.62	1.26	6.74	14.58	0.156	0.61	0.42	336241	7792319	1161
BS-PD-SQI-008A020	20	21	0.28	0.94	5.13	14.11	0.132	0.48	0.26	336241	7792319	1160
BS-PD-POL-041A001	0	1	0.12	0.28	0.09	14.64	0.202	0.8	0.02	336313	7792353	1174
BS-PD-POL-041A002	1	2	0.14	0.29	0.04	15.74	0.149	0.05	0.01	336327	7792349	1173
BS-PD-POL-041A003	2	3	0.15	0.02	0.06	16.28	0.139	0.25	0.02	336327	7792349	1172

BS-PD-POL-041A004	3	4	0.13	0.01	0.05	15.34	0.187	0.47	0.01	336327	7792349	1171
BS-PD-POL-041A005	4	5	0.22	0.03	0.05	15.48	0.157	0.54	0.01	336327	7792349	1170
BS-PD-POL-041A006	5	6	0.27	0.01	5.98	15.55	0.074	0.25	0.01	336327	7792349	1169
BS-PD-POL-041A007	6	7	1.84	0.63	1.14	14.72	0.116	0.55	0.2	336327	7792349	1168
BS-PD-POL-041A008	7	8	0.93	0.17	0.69	14.64	0.069	0.54	0.97	336327	7792349	1167
BS-PD-POL-041A009	8	9	0.82	2.17	1.75	15.25	0.06	0.51	0.93	336327	7792349	1166
BS-PD-POL-041A010	9	10	0.86	1.86	4.35	15.67	0.051	0.23	0.93	336327	7792349	1165
BS-PD-POL-041A011	10	11	0.23	1.97	6.1	13.92	0.046	0.25	0.29	336327	7792349	1164
BS-PD-POL-041A012	11	12	0.05	1.03	7.46	14.89	0.044	0.25	0.12	336327	7792349	1163
BS-PD-POL-041A013	12	13	0.18	0.51	6.46	14.8	0.067	0.55	0.22	336327	7792349	1162
BS-PD-POL-041A014	13	14	0.42	0.74	7.15	14.73	0.045	0.54	0.42	336327	7792349	1161

BS-PD-POL-041A015	14	15	1.91	1.14	2.6	15.65	0.042	0.24	1.29	336327	7792349	1160
BS-PD-POL-041A016	15	16	0.82	3.09	4.58	15.58	0.091	0.54	0.31	336327	7792349	1159
BS-PD-POL-041A017	16	17	0.28	1.3	3.4	15.64	0.051	0.54	0.57	336327	7792349	1158
BS-PD-POL-041A018	17	18	0.73	2.29	2.95	14.49	0.078	0.05	1.23	336327	7792349	1157
BS-PD-POL-041A019	18	19	1.49	5.6	3.96	14.7	0.086	0.54	2.36	336327	7792349	1156
BS-PD-POL-041A020	19	20	1.69	4.71	4.46	15.6	0.056	0.24	2.37	336327	7792349	1155
BS-PD-POL-041A021	20	21	0.98	1.74	6.28	13.98	0.151	0.26	0.79	336327	7792349	1154
BS-PD-POL-041A022	21	22	0.9	0.98	5.98	13.9	0.154	0.01	0.49	336327	7792349	1153
BS-PD-POL-041A023	22	23	0.72	0.95	7.33	13.72	0.157	0.31	0.15	336327	7792349	1152
BS-PD-POL-041A024	23	24	1.37	1.83	5.08	13.37	0.16	0.37	1.05	336327	7792349	1151
BS-PD-POL-041A025	24	25	1.55	2.52	4.61	14.55	0.157	0.38	1.33	336327	7792349	1150

BS-PD-POL-041A026	25	26	1.83	3.39	3.62	14.83	0.153	0.39	1.72	336327	7792349	1149
BS-PD-POL-041A027	26	27	1.58	3.22	2.57	14.58	0.154	0.39	1.64	336327	7792349	1148
BS-PD-POL-041A028	27	28	1.47	3.21	2.73	14.47	0.161	0.36	1.65	336327	7792349	1147
BS-PD-POL-041A029	28	29	1.15	2.36	2.48	14.15	0.152	0.39	1.12	336327	7792349	1146
BS-PD-POL-041A030	29	30	1.42	3.41	2.99	14.42	0.149	0.39	1.52	336327	7792349	1145
BN-PD-SQI-009A001	0	1	1.65	2.57	4.45	16.22	0.35	0.39	1.14	336362	7792505	1173
BN-PD-SQI-009A002	1	2	2.44	5.3	4.15	16.28	0.37	0.4	2.52	336362	7792505	1172
BN-PD-SQI-009A003	2	3	2.06	2.82	6.2	15.4	0.34	0.61	1.03	336362	7792505	1171
BN-PD-SQI-009A004	3	4	3.4	0.26	3.13	15.86	0.36	0.69	0.05	336362	7792505	1170
BN-PD-SQI-009A005	4	5	2.21	1.4	2.17	15.99	0.366	0.68	0.46	336362	7792505	1169
BN-PD-SQI-009A006	5	6	2.44	0.88	3.99	15.98	0.37	0.65	0.27	336362	7792505	1168

BN-PD-SQI-009A007	6	7	3.42	0.42	1.56	15.72	0.133	0.67	0.09	336362	7792505	1167
BN-PD-SQI-009A008	7	8	2.83	0.1	0.44	15.86	0.094	0.67	0.01	336362	7792505	1166
BN-PD-SQI-009A009	8	9	2.34	0.13	1.83	15.6	0.101	0.67	0.02	336362	7792505	1165
BN-PD-SQI-009A010	9	10	3.77	0.07	0.68	16.59	0.34	0.65	0.01	336362	7792505	1164
BN-PD-SQI-009A011	10	11	4.6	0.05	0.48	16.66	0.103	0.66	0.01	336362	7792505	1163
BN-PD-SQI-009A012	11	12	3.72	0.06	0.38	16.5	0.097	0.63	0.03	336362	7792505	1162
BN-PD-SQI-009A013	12	13	4.44	0.05	0.55	16.68	0.355	0.64	0.01	336362	7792505	1161
BN-PD-SQI-009A014	13	14	4.56	0.04	0.62	16.69	0.34	0.06	0.01	336362	7792505	1160
BN-PD-SQI-009A015	14	15	4.69	0.02	0.33	16.71	0.36	0.63	0.01	336362	7792505	1159
BN-PD-SQI-009A016	15	16	2.67	1.64	2.04	14.01	0.16	0.68	0.48	336362	7792505	1158
BN-PD-SQI-009A017	16	17	0.66	1.88	7.4	14.88	0.15	0.55	0.43	336362	7792505	1157

BN-PD-SQI-009A018	17	18	1.03	1.92	6.63	14.97	0.095	0.17	0.68	336362	7792505	1156
BN-PD-SQI-009A019	18	19	1.68	3.66	4.39	14.52	0.134	0	1.39	336362	7792505	1155
BN-PD-SQI-009A020	19	20	1.12	3.29	4.02	15.14	0.22	0.18	0.8	336362	7792505	1154
BN-PD-SQI-009A021	20	21	0.84	1.93	2.96	15.11	0.2	0.36	0.63	336362	7792505	1153
BN-PD-SQI-009A022	21	22	0.8	1.55	1.76	16.22	0.14	0.4	0.49	336362	7792505	1152
BN-PD-SQI-009A023	22	23	1.31	3.04	2.65	16.17	0.128	0.45	1.12	336362	7792505	1151
BN-PD-SQI-009A024	23	24	1.32	3.23	4.65	15.18	0.141	0.42	1.13	336362	7792505	1150
BN-PD-SQI-009A025	24	25	1.21	2.5	6.13	15.19	0.15	0.51	0.91	336362	7792505	1149
BN-PD-SQI-009A026	25	26	1.7	4.22	6.1	16.2	0.18	0.46	1.62	336362	7792505	1148
BN-PD-SQI-009A027	26	27	0.54	1.26	8.1	16.25	0.16	0.59	0.38	336362	7792505	1147
BN-PD-SQI-009A028	27	28	0.37	0.88	7.24	17.71	0.17	0.61	0.23	336362	7792505	1146

BN-PD-SQI-009A029	28	29	0.97	2.76	6	17.8	0.181	0.6	0.75	336362	7792505	1145
BN-PD-SQI-009A030	29	30	0.47	1.01	7.49	16.19	0.14	0.62	0.27	336362	7792505	1144
BN-PD-SQI-009A031	30	31	0.26	0.41	8.05	14.2	0.18	0.65	0.12	336362	7792505	1143
BN-PD-SQI-009A032	31	32	0.23	0.5	2.63	15.34	0.157	0.64	0.08	336362	7792505	1142
BN-PD-SQI-009A033	32	33	0.1	0.19	2.16	15.48	0.18	0.63	0.02	336362	7792505	1141

Appendix 3c: Reverse Circulation AAS Results

Sample_Name	From	To	Li_2O_pct	K_2O_pct	Na_2O_pct	Al_2O_3_pct	Fe_2O_3_pct	Cs_2O_pct	Rb_2O_pct	Easting	Northing	Elevation
AH-RC-PET-009A001	17	18	0.13	0.26	2.72	14.72	0.5	0.27	0.01	336702	7793154	1122
AH-RC-PET-009A002	18	19	0.12	0.1	1.94	14.19	0.46	0.26	0.04	336702	7793154	1121
AH-RC-PET-009A003	19	20	0.41	3.19	4.6	14.58	0.46	0.32	0.7	336702	7793154	1120
AH-RC-PET-009A004	20	21	0.73	9.32	2.69	14.27	0.46	0.32	3.1	336702	7793154	1119
AH-RC-PET-009A005	21	22	0.6	8.57	3.72	14.55	0.114	0.36	2.13	336702	7793154	1118
AH-RC-PET-009A006	22	23	3.37	0.47	2.13	16.13	0.153	0.4	0.08	336702	7793154	1117
AH-RC-PET-009A007	23	24	4.39	0.18	0.58	16.66	0.138	0.41	0.04	336702	7793154	1116

AH-RC-PET-009A008	24	25	4.56	0.1	0.33	16.69	0.132	0.43	0.03	336702	7793154	1115
AH-RC-PET-009A009	25	26	4.55	0.16	0.38	16.7	0.136	0.47	0.03	336702	7793154	1114
AH-RC-PET-009A010	26	27	3.53	1.18	2	16	0.122	0.48	0.19	336702	7793154	1113
AH-RC-PET-009A011	27	28	1.99	4.87	3.49	15.87	0.112	0.52	1.03	336702	7793154	1112
AH-RC-PET-009A012	28	29	3.57	0.6	0.93	16.4	0.131	0.53	0.11	336702	7793154	1111
AH-RC-PET-009A013	29	30	4.38	0.2	0.53	16.69	0.131	0.55	0.06	336702	7793154	1110
AH-RC-PET-009A014	30	31	2.52	5.83	1.92	15.99	0.127	0.6	1.17	336702	7793154	1109
AH-RC-PET-009A015	31	32	0.87	7.83	2.69	14.65	0.093	0.64	1.96	336702	7793154	1108
AH-RC-PET-009A016	32	33	0.3	10.56	3.44	14.79	0.46	0.69	3.11	336702	7793154	1107
AH-RC-PET-009A017	33	34	1.07	8.16	4.16	14.6	0.109	0.75	2.27	336702	7793154	1106
AH-RC-PET-009A018	34	35	1.16	4.94	2.21	14.82	0.46	0.74	1.83	336702	7793154	1105
AH-RC-PET-009A019	35	36	0.69	9.32	2.96	14.18	0.46	0.79	3.14	336702	7793154	1104
AH-RC-PET-009A020	36	37	0.01	0.01	0.08	14.28	0.003	0.74	0.03	336702	7793154	1103
AH-RC-PET-009A021	37	38	1.43	4.56	3.21	14.52	0.37	0.05	1.35	336702	7793154	1102
AH-RC-PET-009A022	38	39	4.26	0.28	0.69	16.68	0.145	0.08	0.03	336702	7793154	1101
AH-RC-PET-009A023	39	40	4.22	0.3	0.78	16.61	0.145	0.04	0.05	336702	7793154	1100
AH-RC-PET-009A024	40	41	4.26	0.33	0.82	16.57	0.146	0.07	0.07	336702	7793154	1099
AH-RC-PET-009A025	41	42	3.52	0.66	1.27	16.11	0.143	0.08	0.18	336702	7793154	1098
AH-RC-PET-009A026	42	43	1.48	1.84	2.6	14.6	0.366	0.03	0.64	336702	7793154	1097
AH-RC-PET-009A027	43	44	2.03	3.71	3.06	15.1	0.296	0.03	1.5	336702	7793154	1096
AH-RC-PET-009A028	44	45	2.31	3.13	2.83	15.22	0.385	0.07	0.96	336702	7793154	1095
AH-RC-PET-009A029	45	46	1.95	4.94	2.56	16.56	0.14	0.08	0.94	336702	7793154	1094

AH-RC-PET-009A030	46	47	3.38	0.78	1.96	15.94	0.103	0.09	0.15	336702	7793154	1093
AH-RC-PET-009A031	47	48	2.52	1.17	2.68	15.96	0.139	0.14	0.28	336702	7793154	1092
AH-RC-PET-009A032	48	49	1.58	3.86	3.12	15.55	0.22	0.13	0.86	336702	7793154	1091
AH-RC-PET-009A033	49	50	0.86	1.39	3.65	12.57	0.178	0.84	0.58	336702	7793154	1090
AH-RC-PET-009A034	50	51	0.72	3.27	3.65	16.23	0.2	0.08	1.27	336702	7793154	1089
AH-RC-PET-009A035	51	52	0.77	4.87	5.29	16.91	0.078	0.03	0.87	336702	7793154	1088
AH-RC-PET-009A036	52	53	0.54	5.43	5.46	15.28	0.12	0.01	1.08	336702	7793154	1087
AH-RC-PET-009A037	53	54	1.51	3.6	3.14	15.34	0.22	0.02	1.09	336702	7793154	1086
AH-RC-PET-009A038	54	55	2.28	1.23	3.72	16.38	0.2	0.04	0.42	336702	7793154	1085
AH-RC-PET-009A039	55	56	1.06	4.04	3.74	14.87	0.16	0.07	0.89	336702	7793154	1084
AH-RC-PET-009A040	56	57	2.05	3.78	2.77	16.34	0.128	0.09	0.82	336702	7793154	1083
AH-RC-PET-009A041	57	58	1.47	2.56	3.46	16.06	0.2	0.16	0.86	336702	7793154	1082
AH-RC-PET-009A042	58	59	0.82	2.78	4.97	16.18	0.18	0.19	0.8	336702	7793154	1081
AH-RC-PET-009A043	59	60	0.53	5.69	4.61	16.35	0.183	0.25	1.48	336702	7793154	1080
AH-RC-PET-009A044	60	61	0.2	0.86	7.35	16.34	0.114	0.28	0.31	336702	7793154	1079
AH-RC-PET-009A045	61	62	0.23	0.62	2.78	14.99	2.46	0.39	0.11	336702	7793154	1078
AH-RC-PET-009A046	62	63	0.2	1.95	4.85	15.1	0.2	0.42	0.51	336702	7793154	1077
AH-RC-PET-009A047	63	64	0.17	2.2	5.03	15.94	1.18	0.63	0.39	336702	7793154	1076
AH-RC-PET-009A048	64	65	0.3	0.68	2.72	11.21	2.08	0.56	0.07	336702	7793154	1075
AH-RC-PET-009A049	65	66	0.42	0.22	3.69	12.44	2.18	0.41	0.04	336702	7793154	1074
AHS-RC-PET-001A001	32	33	0.3	1.04	3.37	13.3	0.161	0.77	0.17	336548	7792852	1120

AHS-RC-PET-001A002	33	34	0.3	1.52	4.76	13.3	0.151	0.95	0.19	336548	7792852	1119
AHS-RC-PET-001A003	34	35	0.81	7.93	2.86	13.81	0.161	0.86	0.3	336548	7792852	1118
AHS-RC-PET-001A004	35	36	0.89	10.21	3.47	13.89	0.151	0.15	0.36	336548	7792852	1117
AHS-RC-PET-001A005	36	37	0.17	7.82	4.27	13.17	0.079	0.8	0.41	336548	7792852	1116
AHS-RC-PET-001A006	37	38	0.19	8.19	3.99	13.19	0.113	0.09	0.51	336548	7792852	1115
AHS-RC-PET-001A007	38	39	0.25	7.06	4.82	13.25	0.129	0.83	0.19	336548	7792852	1114
AHS-RC-PET-001A008	39	40	0.16	8.11	5.02	13.16	0.122	0.69	0.33	336548	7792852	1113
AHS-RC-PET-001A009	40	41	0.78	9.64	5.36	13.78	0.048	0.71	0.41	336548	7792852	1112
AHS-RC-PET-001A010	41	42	2.1	2.93	4.72	15.1	0.072	0.61	0.62	336548	7792852	1111
AHS-RC-PET-001A011	42	43	0.9	6.36	4.16	13.9	0.058	0.53	0.51	336548	7792852	1110
AHS-RC-PET-001A012	43	44	0.16	10.56	4.24	13.16	0.069	0.51	0.41	336548	7792852	1109

AHS-RC-PET-001A013	44	45	0.14	10.53	3.67	13.14	0.02	0.61	0.32	336548	7792852	1108
AHS-RC-PET-001A014	45	46	0.14	8.59	2.7	13.14	0.023	0.1	0.33	336548	7792852	1107
AHS-RC-PET-001A015	46	47	2.6	5.41	2.34	15.6	0.049	0.17	0.36	336548	7792852	1106
AHS-RC-PET-001A016	47	48	3.51	3.58	2.5	15.82	0.063	0.22	1.15	336548	7792852	1105
AHS-RC-PET-001A017	48	49	0.34	10.99	3.57	17.59	0.043	0.16	5.6	336548	7792852	1104
AHS-RC-PET-001A018	49	50	3.68	3.94	1.67	16.06	0.085	0.2	0.51	336548	7792852	1103
AHS-RC-PET-001A019	50	51	4.1	0.64	3.58	16.3	0.062	0.21	1.18	336548	7792852	1102
AHS-RC-PET-001A020	51	52	0.45	7.93	2.5	14.2	0.025	0.16	3.4	336548	7792852	1101
AHS-RC-PET-001A021	52	53	0.25	10.2	3.64	17.15	0.087	0.25	4.93	336548	7792852	1100
AHS-RC-PET-001A022	53	54	0.57	7.07	6.34	14.5	0.105	0.31	3.09	336548	7792852	1099
AHS-RC-PET-001A023	54	55	0.78	9.96	5.99	14.81	0.1	0.37	3.92	336548	7792852	1098

AHS-RC-PET-001A024	55	56	1.22	4.93	4.87	15.61	0.125	0.43	3.89	336548	7792852	1097
AHS-RC-PET-001A025	56	57	1.05	4.14	5.13	15.5	0.163	0.55	3.74	336548	7792852	1096
AHS-RC-PET-001A026	57	58	4.06	0.23	2	16.29	0.214	0.55	0.29	336548	7792852	1095
AHS-RC-PET-001A027	58	59	4	1.61	2.32	16.25	0.191	0.7	1.34	336548	7792852	1094
AHS-RC-PET-001A028	59	60	3.22	1.56	2.66	15.91	0.142	0.81	0.86	336548	7792852	1093
AHS-RC-PET-001A029	60	61	1.41	1.43	4.76	15.6	0.091	0.86	0.59	336548	7792852	1092
AHS-RC-PET-001A030	61	62	1.39	1.41	4.79	15.58	0.108	0.99	1.87	336548	7792852	1091
AHS-RC-PET-001A031	62	63	2.33	3.63	3.66	15.91	0.073	0.55	1.07	336548	7792852	1090
AHS-RC-PET-001A032	63	64	0.66	2.54	4.2	14.53	0.26	0.12	1.06	336548	7792852	1089
AHS-RC-PET-001A033	64	65	0.06	6.89	2.97	14.42	0.094	0.26	2.46	336548	7792852	1088
AHS-RC-PET-001A034	65	66	0.14	9.56	3.98	16.98	0.148	0.28	3.54	336548	7792852	1087

AHS-RC-PET-001A035	66	67	0.32	3.23	7.17	14.15	0.02	0.37	1.14	336548	7792852	1086
AHS-RC-PET-001A036	67	68	0.42	2.96	5.65	14.6	0.24	0.1	0.88	336548	7792852	1085
AHS-RC-PET-001A037	68	69	0.52	7.48	3.03	14.31	0.26	0.09	2.78	336548	7792852	1084
AHS-RC-PET-001A038	69	70	0.31	1.07	5.33	14.44	0.145	0.02	0.67	336548	7792852	1083
AHS-RC-PET-001A039	70	71	0.6	3.13	5.29	14.35	0.14	0.05	1.46	336548	7792852	1082
AHS-RC-PET-001A040	71	72	0.19	0.91	7.48	14.6	0.153	0.01	0.43	336548	7792852	1081
AHS-RC-PET-001A041	72	73	0.18	0.48	1.56	14.53	0.4	0.06	0.23	336548	7792852	1080
BE-RC-PET-001A001	34	35	0.74	4.31	2.1	14.12	0.24	0.24	1.55	336443	7792480	1157
BE-RC-PET-001A002	35	36	0.37	9.27	3.53	13.6	0.16	0.23	2.27	336443	7792480	1156
BE-RC-PET-001A003	36	37	0.35	8.02	3.91	13.29	0.09	0.22	2.13	336443	7792480	1155
BE-RC-PET-001A004	37	38	0.37	7.97	3.98	13.51	0.089	0.34	1.97	336443	7792480	1154
BE-RC-PET-001A005	38	39	0.31	5.6	5.34	13.38	0.144	0.13	1.13	336443	7792480	1153
BE-RC-PET-001A006	39	40	0.28	5.57	5.4	13.22	0.128	0.16	1.12	336443	7792480	1152
BE-RC-PET-001A007	40	41	0.25	5.07	4.95	13.41	0.111	0.09	0.95	336443	7792480	1151
BE-RC-PET-001A008	41	42	0.23	4.84	4.87	13.32	0.102	0.1	0.89	336443	7792480	1150

BE-RC-PET-001A009	42	43	0.05	10.97	2.59	13.06	0.07	0.02	2.74	336443	7792480	1149
BE-RC-PET-001A010	43	44	0.04	11.88	2.54	13.07	0.067	0.04	2.65	336443	7792480	1148
BE-RC-PET-001A011	44	45	0.26	11.41	2.85	13.43	0.09	0.11	2.67	336443	7792480	1147
BE-RC-PET-001A012	45	46	0.28	10.42	2.99	13.46	0.093	0.03	2.91	336443	7792480	1146
BE-RC-PET-001A013	46	47	0.34	9.22	3.55	13.45	0.188	0.05	2.1	336443	7792480	1145
BE-RC-PET-001A014	47	48	0.32	9.13	3.42	13.4	0.195	0.18	2.07	336443	7792480	1144
BE-RC-PET-001A015	48	49	0.34	7.75	3.81	13.47	0.112	0.17	1.64	336443	7792480	1143
BE-RC-PET-001A016	49	50	0.33	7.72	3.55	15.32	0.091	0.37	1.66	336443	7792480	1142
BE-RC-PET-001A017	50	51	0.25	4.91	5.19	13.62	0.127	0.1	1.53	336443	7792480	1141
BE-RC-PET-001A018	51	52	0.24	3.16	3.93	13.59	0.091	0.06	0.9	336443	7792480	1140
BE-RC-PET-001A019	52	53	1.29	5.07	5.64	14.84	0.073	0.27	1.22	336443	7792480	1139
BE-RC-PET-001A020	53	54	0.31	1.36	5.49	13.27	0.163	0.31	0.33	336443	7792480	1138
BE-RC-PET-001A021	54	55	1.46	1.02	5.15	14.91	0.141	0.3	0.2	336443	7792480	1137
BE-RC-PET-001A022	55	56	0.63	1.71	5.38	13.31	0.054	0.3	0.6	336443	7792480	1136
BE-RC-PET-001A023	56	57	0.72	1.34	7.61	13.27	0.076	0.29	0.89	336443	7792480	1135
BE-RC-PET-001A024	57	58	1.13	1.94	5.72	14.86	0.046	0.33	1.22	336443	7792480	1134
BE-RC-PET-001A025	58	59	0.43	0.48	6.33	13.33	0.159	0.42	0.39	336443	7792480	1133
BE-RC-PET-001A026	59	60	0.65	0.91	6.3	13.42	0.074	0.32	0.49	336443	7792480	1132
BE-RC-PET-001A027	60	61	1.35	3.33	3.88	14.79	0.081	0.28	1.66	336443	7792480	1131
BE-RC-PET-001A028	61	62	1.42	6.11	4.25	14.87	0.083	0.15	2.97	336443	7792480	1130
BE-RC-PET-001A029	62	63	1.15	3.5	7.04	14.95	0.079	0.26	1.63	336443	7792480	1129
BE-RC-PET-001A030	63	64	0.91	1.65	5.45	14.17	0.075	0.24	0.82	336443	7792480	1128

BE-RC-PET-001A031	64	65	0.64	0.91	6.33	14.24	0.164	0.4	0.43	336443	7792480	1127
BE-RC-PET-001A032	65	66	0.71	1.06	7.1	14.31	0.058	0.58	0.61	336443	7792480	1126
BE-RC-PET-001A033	66	67	1.06	1.61	6.64	14.74	0.063	0.13	1.13	336443	7792480	1125
BE-RC-PET-001A034	67	68	1.08	1.71	6.29	14.25	0.061	0.2	1.16	336443	7792480	1124
BE-RC-PET-001A035	68	69	0.69	1.17	7.27	13.71	0.058	0.15	0.84	336443	7792480	1123
BE-RC-PET-001A036	69	70	1.14	1.5	7.02	14.9	0.054	0.23	1.08	336443	7792480	1122
BE-RC-PET-001A037	70	71	1.43	2.54	5.16	14.99	0.06	0.37	1.51	336443	7792480	1121
BE-RC-PET-001A038	71	72	2.07	4.2	4.39	15.43	0.042	0.16	2.29	336443	7792480	1120
BE-RC-PET-001A039	72	73	2.02	5.01	3.89	14.02	0.049	0.6	3.06	336443	7792480	1119
BE-RC-PET-001A040	73	74	0.8	1.66	2.79	13.8	0.126	0.87	0.88	336443	7792480	1118
BE-RC-PET-001A041	74	75	0.9	2.2	5.48	13.9	0.092	0.1	1.23	336443	7792480	1117
BE-RC-PET-001A042	75	76	1.17	2.94	6.44	14.17	0.055	0.05	1.67	336443	7792480	1116
BE-RC-PET-001A043	76	77	1.61	5.74	5.34	14.61	0.161	0.92	2.98	336443	7792480	1115
BE-RC-PET-001A044	77	78	0.46	1.52	8.5	13.46	0.13	0.06	0.65	336443	7792480	1114
BE-RC-PET-001A045	78	79	2.07	6.07	4.61	15.7	0.21	0.22	2.83	336443	7792480	1113
BE-RC-PET-001A046	79	80	0.55	2.2	6.79	13.55	0.211	0.65	0.66	336443	7792480	1112
BE-RC-PET-001A047	80	81	0.53	1.88	1.88	6.81	0.215	0.62	0.45	336443	7792480	1111
BE-RC-PET-001A048	81	82	0.05	0.29	2.1	13.1	0.15	0.42	0.08	336443	7792480	1110
BE-RC-PET-001A049	82	83	0.07	0.68	8.12	13.07	0.21	0.33	0.11	336443	7792480	1109
GE-RC-PET-001A001	2	3	1.75	4.26	3.68	13.26	0.132	0.81	1.15	336028	7793323	1141
GE-RC-PET-001A002	3	4	2.9	1.41	2.12	13.96	0.219	0.69	0.39	336028	7793323	1140
GE-RC-PET-001A003	4	5	1.85	0.41	2.97	14.41	0.222	0.85	0.2	336028	7793323	1139

GE-RC-PET-001A004	5	6	1.66	2.6	2.27	15.61	0.142	0.77	0.74	336028	7793323	1138
GE-RC-PET-001A005	6	7	0.38	1.56	4.15	16.21	0.482	0.6	0.48	336028	7793323	1137
GE-RC-PET-001A006	7	8	3.01	1.25	2.12	14.71	0.143	0.63	0.42	336028	7793323	1136
GE-RC-PET-001A007	8	9	4.89	0.1	0.38	14.89	0.089	0.56	0.14	336028	7793323	1135
GE-RC-PET-001A008	9	10	1.1	1.89	4.43	14.21	0.131	0.8	0.55	336028	7793323	1134
GE-RC-PET-001A009	10	11	1.9	1.18	4.21	14.39	0.135	0.78	0.4	336028	7793323	1133
GE-RC-PET-001A010	11	12	0.81	5.91	4.05	14.41	0.103	0.08	1.9	336028	7793323	1132
GE-RC-PET-001A011	12	13	4.74	2.98	1.2	14.27	0.095	0.02	0.86	336028	7793323	1131
GE-RC-PET-001A012	13	14	1.88	1.92	4.27	14.3	0.128	0.04	0.42	336028	7793323	1130
GE-RC-PET-001A013	14	15	0.35	0.93	2.92	14.27	0.59	0.97	0.26	336028	7793323	1129
GE-RC-PET-001A014	15	16	0.67	4	2.3	14.32	0.112	0.86	1.07	336028	7793323	1128
GE-RC-PET-001A015	16	17	2.45	1.96	1.99	15.68	0.148	0.23	0.48	336028	7793323	1127
GE-RC-PET-001A016	17	18	1.76	3.53	3.11	15.02	0.111	0.24	0.83	336028	7793323	1126
GE-RC-PET-001A017	18	19	0.97	5.88	2.99	14.12	0.151	0.42	1.6	336028	7793323	1125
GE-RC-PET-001A018	19	20	3.18	1.73	0.82	15.97	0.219	0.28	0.52	336028	7793323	1124
GE-RC-PET-001A019	20	21	0.44	4.31	3.59	14.03	0.262	0.19	1.03	336028	7793323	1123
GE-RC-PET-001A020	21	22	3.18	0.33	0.91	15.95	0.157	0.26	0.13	336028	7793323	1122
GE-RC-PET-001A021	22	23	2.2	1.04	2.6	15.71	0.123	0.03	0.21	336028	7793323	1121
GE-RC-PET-001A022	23	24	1.5	0.82	3.22	15.43	0.115	0.27	0.18	336028	7793323	1120
GE-RC-PET-001A023	24	25	2.17	1.54	2.35	15.69	0.171	0.09	0.44	336028	7793323	1119
GE-RC-PET-001A024	25	26	1.86	1.19	3.3	15.75	0.19	0.2	0.42	336028	7793323	1118
GE-RC-PET-001A025	26	27	1.13	0.71	4.02	15.48	0.153	0.17	0.21	336028	7793323	1117

GE-RC-PET-001A026	27	28	0.18	0.07	0.51	14.12	0.162	0.13	0.06	336028	7793323	1116
GE-RC-PET-001A027	28	29	0.7	0.83	1.82	14.17	0.205	0.17	0.2	336028	7793323	1115
GE-RC-PET-001A028	29	30	1.3	2.93	4.13	15.38	0.213	0.34	0.65	336028	7793323	1114
GE-RC-PET-001A029	30	31	1.59	1.75	3.97	15.39	0.116	0.25	0.4	336028	7793323	1113
GE-RC-PET-001A030	31	32	1	1.8	3.47	15.28	0.144	0.27	0.42	336028	7793323	1112
GE-RC-PET-001A031	32	33	1.04	4.88	2.92	15.32	0.196	0.29	1.11	336028	7793323	1111
GE-RC-PET-001A032	33	34	0.35	3.26	4.88	14.07	0.321	0.24	0.75	336028	7793323	1110
GE-RC-PET-001A033	34	35	0.57	1.29	2.76	14.13	0.31	0.35	0.29	336028	7793323	1109
GE-RC-PET-001A034	45	46	0.35	1.68	3.84	13.89	0.282	0.14	0.37	336028	7793323	1098
GE-RC-PET-001A035	46	47	0.89	2.43	4.01	13.89	0.191	0.79	0.16	336028	7793323	1097
GE-RC-PET-001A036	47	48	0.41	0.52	3.45	13.41	0.163	0.19	0.66	336028	7793323	1096
LN-RC-PET-004A001	24	25	0.89	1.7	3.16	13.89	0.21	0.56	0.19	336080	7793111	1132
LN-RC-PET-004A002	25	26	0.13	1.64	5.3	13.13	0.211	0.43	0.21	336080	7793111	1131
LN-RC-PET-004A003	26	27	1.37	0.9	4.44	14.37	0.19	0.94	1.6	336080	7793111	1130
LN-RC-PET-004A004	27	28	3.35	0.17	1.53	16.35	0.12	0.72	2.1	336080	7793111	1129
LN-RC-PET-004A005	28	29	4.51	0.1	0.57	16.51	0.16	0.07	1.86	336080	7793111	1128
LN-RC-PET-004A006	29	30	3.54	0.18	1.79	16.54	0.117	0.72	1.96	336080	7793111	1127
LN-RC-PET-004A007	30	31	3.54	0.18	1.79	16.54	0.117	0.72	1.96	336080	7793111	1126
LN-RC-PET-004A008	31	32	0.39	0.39	6.77	13.39	0.096	0.88	1.31	336080	7793111	1125
LN-RC-PET-004A009	32	33	0.1	0.23	8.1	13.1	0.077	0.66	0.46	336080	7793111	1124
LN-RC-PET-004A010	33	34	0.25	0.43	6.83	13.25	0.123	0.37	0.71	336080	7793111	1123
LN-RC-PET-004A011	34	35	0.29	0.53	6.89	13.29	0.126	0.07	0.89	336080	7793111	1122

LN-RC-PET-004A012	35	36	0.43	2.21	6.44	13.43	0.089	0.19	0.39	336080	7793111	1121
LN-RC-PET-004A013	36	37	0.73	1.59	5.71	13.23	0.141	0.17	0.4	336080	7793111	1120
LN-RC-PET-004A014	37	38	1.8	0.94	2.85	14.8	0.131	0.72	0.55	336080	7793111	1119
LN-RC-PET-004A015	38	39	3.28	0.29	1.63	16.28	0.161	0.55	0.71	336080	7793111	1118
LN-RC-PET-004A016	39	40	1.75	1.92	3.51	14.75	0.131	0.59	0.82	336080	7793111	1117
LN-RC-PET-004A017	40	41	1.32	2.86	3.67	14.32	0.172	0.52	0.31	336080	7793111	1116
LN-RC-PET-004A018	41	42	1.08	2.81	4.03	14.08	0.12	0.22	0.96	336080	7793111	1115
LN-RC-PET-004A019	42	43	2	3.52	2.17	15	0.11	0.49	0.17	336080	7793111	1114
LN-RC-PET-004A020	43	44	2.5	1.29	2.18	15.5	0.152	0.61	0.32	336080	7793111	1113
LN-RC-PET-004A021	44	45	2.19	0.59	2.75	15.91	0.161	0.79	0.21	336080	7793111	1112
LN-RC-PET-004A022	45	46	2.02	1.3	3.92	15.16	0.172	0.64	0.11	336080	7793111	1111
LN-RC-PET-004A023	46	47	1.16	1.71	4.79	16.16	0.179	0.58	0.44	336080	7793111	1110
LN-RC-PET-004A024	47	48	2.07	2.35	3.26	15.07	0.156	0.57	0.68	336080	7793111	1109
LN-RC-PET-004A025	48	49	2.13	3.84	2.2	15.13	0.149	0.47	0.04	336080	7793111	1108
LN-RC-PET-004A026	49	50	1.72	3.02	3.59	14.72	0.172	0.28	0.28	336080	7793111	1107
LN-RC-PET-004A027	50	51	3.04	0.91	1.17	16.04	0.151	0.19	0.15	336080	7793111	1106
LN-RC-PET-004A028	51	52	2	1.97	3.03	15	0.162	0.37	0.33	336080	7793111	1105
LN-RC-PET-004A029	52	53	0.84	2.24	4.81	13.84	0.158	0.61	0.54	336080	7793111	1104
LN-RC-PET-004A030	53	54	1.7	1.62	3.58	14.7	0.19	0.22	0.67	336080	7793111	1103
LN-RC-PET-004A031	54	55	1.55	2.59	3.04	14.55	0.195	0.84	0.44	336080	7793111	1102
LN-RC-PET-004A032	55	56	0.53	1.47	6.22	13.53	0.21	0.95	0.39	336080	7793111	1101
LN-RC-PET-004A033	56	57	0.78	1.98	5.95	13.78	0.197	0.66	0.29	336080	7793111	1100

LN-RC-PET-004A034	57	58	0.84	5.61	3.43	13.04	0.188	0.74	0.31	336080	7793111	1099
LN-RC-PET-004A035	58	59	1.43	1.1	2.78	14.43	0.153	0.38	0.81	336080	7793111	1098
LN-RC-PET-004A036	59	60	2.46	0.25	3.1	15.46	0.21	0.72	0.36	336080	7793111	1097
LN-RC-PET-004A037	60	61	2.47	0.75	2.75	15.47	0.166	0.63	0.41	336080	7793111	1096
LN-RC-PET-004A038	61	62	2.31	2.17	1.76	15.31	0.168	0.92	0.52	336080	7793111	1095
LN-RC-PET-004A039	62	63	1.82	2.48	3.56	15.63	0.009	0.28	0.41	336080	7793111	1094
LN-RC-PET-004A040	63	64	2.31	1.54	3.06	16.81	0.01	0.17	0.29	336080	7793111	1093
LN-RC-PET-004A041	64	65	0.67	2.31	4.77	14.65	0.004	0.5	0.52	336080	7793111	1092
LN-RC-PET-004A042	65	66	0.15	2.62	5.87	14.23	0.009	0.4	0.51	336080	7793111	1091
LN-RC-PET-004A043	66	67	0.31	1.74	3.43	14.86	0.012	0.25	0.23	336080	7793111	1090
SH-RC-PET-020A001	10	11	0.02	0.22	0.91	13.27	0.061	0.1	0.37	336247	7793369	1150
SH-RC-PET-020A002	11	12	0.14	7.62	3.61	13.44	0.36	0.08	1.95	336247	7793369	1149
SH-RC-PET-020A003	12	13	0.53	6.78	3.11	15.6	0.18	0.91	1.62	336247	7793369	1148
SH-RC-PET-020A004	13	14	0.62	1.35	4.34	15.55	0.16	0.84	0.02	336247	7793369	1147
SH-RC-PET-020A005	14	15	1.7	1.31	3.46	15.66	0.153	0.76	0.39	336247	7793369	1146
SH-RC-PET-020A006	15	16	0.18	9.46	2.82	13.33	0.096	0.68	2.66	336247	7793369	1145
SH-RC-PET-020A007	16	17	2	2.14	2.77	13.58	0.04	0.15	0.32	336247	7793369	1144
SH-RC-PET-020A008	17	18	1.08	1.59	5.23	13.67	0.06	0.18	0.28	336247	7793369	1143
SH-RC-PET-020A009	18	19	0.05	0.65	8.19	14.95	0.113	0.2	0.05	336247	7793369	1142
SH-RC-PET-020A010	65	66	0.41	3.22	4.31	15.67	0.073	0.1	0.72	336247	7793369	1095
SH-RC-PET-020A011	66	67	0.61	0.72	6.97	13.02	0.127	0.16	0.09	336247	7793369	1094
SH-RC-PET-020A012	67	68	3.61	0.36	1.23	16.04	0.11	0.15	0.03	336247	7793369	1093

SH-RC-PET-020A013	68	69	2.32	0.99	2.58	15.89	0.121	0.13	0.15	336247	7793369	1092
SH-RC-PET-020A014	69	70	3.99	0.32	1.17	16.07	0.137	0.08	0.04	336247	7793369	1091
SH-RC-PET-020A015	70	71	3.46	0.35	2.34	15.99	0.109	0.07	0.03	336247	7793369	1090
SH-RC-PET-020A016	71	72	4.02	0.33	1.23	16.1	0.078	0.01	0.01	336247	7793369	1089
SH-RC-PET-020A017	72	73	3.45	0.5	2.27	15.87	0.06	0.01	0.02	336247	7793369	1088
SH-RC-PET-020A018	73	74	4.12	0.77	1.06	16.44	0.129	0.09	0.05	336247	7793369	1087
SH-RC-PET-020A019	74	75	1.94	2.63	3.23	16.79	0.114	0.13	0.6	336247	7793369	1086
SH-RC-PET-020A020	75	76	1.6	2.67	2.56	14.84	0.134	0.14	0.32	336247	7793369	1085
SH-RC-PET-020A021	76	77	3.07	1.47	2.18	15.06	0.116	0.16	0.06	336247	7793369	1084
SH-RC-PET-020A022	77	78	0.75	1.32	5.94	12.09	0.113	0.19	0.06	336247	7793369	1083
SH-RC-PET-020A023	78	79	0.92	7.21	3.1	14.64	0.095	0.22	1.86	336247	7793369	1082
SH-RC-PET-020A024	79	80	1.97	4.94	2.59	13.49	0.121	0.28	0.87	336247	7793369	1081
SH-RC-PET-020A025	80	81	2.41	1.04	3.76	14.66	0.151	0.33	0.08	336247	7793369	1080
SH-RC-PET-020A026	81	82	2.64	0.96	3.65	15.79	0.155	0.33	0.1	336247	7793369	1079
SH-RC-PET-020A027	82	83	3.15	0.74	1.64	15.83	0.125	0.38	0.12	336247	7793369	1078
SH-RC-PET-020A028	83	84	2.73	0.84	2.79	14.79	0.01	0.43	0.09	336247	7793369	1077
SH-RC-PET-020A029	84	85	2.19	3.16	1.88	13.66	0.152	0.46	0.36	336247	7793369	1076
SH-RC-PET-020A030	85	86	0.46	1.16	3.74	12.21	0.151	0.52	0.09	336247	7793369	1075
SH-RC-PET-020A031	86	87	0.74	1.69	4.43	12.63	0.129	0.55	0.21	336247	7793369	1074
SH-RC-PET-020A032	87	88	2.6	0.65	2.21	10.67	0.106	0.6	0.07	336247	7793369	1073
SH-RC-PET-020A033	88	89	1.64	0.88	3.62	14.99	0.118	0.61	0.09	336247	7793369	1072
SH-RC-PET-020A034	89	90	2.38	1.19	4.31	15.63	0.131	0.62	0.26	336247	7793369	1071

SH-RC-PET-020A035	90	91	3.19	1.59	1.56	15.84	0.13	0.72	0.1	336247	7793369	1070
SH-RC-PET-020A036	91	92	2.48	2.37	2.48	14.99	0.112	0.76	0.34	336247	7793369	1069
SH-RC-PET-020A037	92	93	0.91	4.12	3.92	10.33	0.12	0.79	0.84	336247	7793369	1068
SH-RC-PET-020A038	93	94	1.13	6.77	2.88	14.66	0.118	0.76	1.91	336247	7793369	1067
SH-RC-PET-020A039	94	95	2.15	1.8	3.33	15.72	0.122	0.89	0.21	336247	7793369	1066
SH-RC-PET-020A040	95	96	1.3	3.77	4.45	14.44	0.12	0.99	0.61	336247	7793369	1065
SH-RC-PET-020A041	96	97	0.1	2.81	3.66	15.49	0.074	0.29	0.97	336247	7793369	1064
SH-RC-PET-020A042	97	98	0.8	1.05	3.4	15.8	0.096	0.04	0.05	336247	7793369	1063
SH-RC-PET-020A043	98	99	0.1	1.41	4.66	15.61	0.115	0.07	0.08	336247	7793369	1062
SH-RC-PET-001A001	0	1	0.2	0.46	2.8	15.4	0.219	0.08	0.02	336201	7793259	1159
SH-RC-PET-001A002	1	2	0.11	1.9	5.96	15.39	0.131	0.12	0.25	336201	7793259	1158
SH-RC-PET-001A003	2	3	0.08	0.25	3.76	15.67	0.494	0.16	0.03	336201	7793259	1157
SH-RC-PET-001A004	42	43	0.06	1.07	3.93	15.28	0.211	0.21	0.08	336201	7793259	1117
SH-RC-PET-001A005	43	44	0.08	2.75	5.49	13.08	0.159	0.62	0.26	336201	7793259	1116
SH-RC-PET-001A006	44	45	0.07	4.27	5.24	13.07	0.129	0.74	0.08	336201	7793259	1115
SH-RC-PET-001A007	45	46	0.16	5.16	3.32	13.16	0.143	0.76	0.09	336201	7793259	1114
SH-RC-PET-001A008	46	47	0.15	2.74	8.1	13.15	0.161	0.11	0.82	336201	7793259	1113
SH-RC-PET-001A009	47	48	0.3	0.54	4.78	13.3	0.148	0.13	0.26	336201	7793259	1112
SH-RC-PET-001A010	48	49	1.76	2.06	2.03	14.76	0.102	0.22	0.1	336201	7793259	1111
SH-RC-PET-001A011	49	50	1.27	3.19	2.17	14.27	0.08	0.35	0.15	336201	7793259	1110
SH-RC-PET-001A012	50	51	2.34	2.6	1.61	15.34	0.169	0.49	0.41	336201	7793259	1109
SH-RC-PET-001A013	51	52	1.22	0.55	6.48	14.22	0.098	0.63	0.31	336201	7793259	1108

SH-RC-PET-001A014	52	53	1.33	5.82	4.17	14.33	0.086	0.66	0.03	336201	7793259	1107
SH-RC-PET-001A015	53	54	0.31	0.2	4.55	13.31	0.083	0.77	1.41	336201	7793259	1106
SH-RC-PET-001A016	54	55	2.98	6.77	1.36	14.98	0.095	0.84	0.52	336201	7793259	1105
SH-RC-PET-001A017	55	56	1.55	5.4	1.79	14.55	0.074	0.1	2.23	336201	7793259	1104
SH-RC-PET-001A018	56	57	1.37	8.6	1.21	14.37	0.094	0.17	1.5	336201	7793259	1103
SH-RC-PET-001A019	57	58	0.09	1.95	1.95	13.09	0.075	0.3	4.29	336201	7793259	1102
SH-RC-PET-001A020	58	59	3.57	3.78	1.33	16.57	0.095	0.23	0.77	336201	7793259	1101
SH-RC-PET-001A021	59	60	2.5	0.3	1.55	15.5	0.088	0.34	0.2	336201	7793259	1100
SH-RC-PET-001A022	60	61	4.3	2.04	0.89	16.32	0.124	0.42	0.27	336201	7793259	1099
SH-RC-PET-001A023	61	62	2.51	0.4	3.4	15.51	0.109	0.16	0.11	336201	7793259	1098
SH-RC-PET-001A024	62	63	3.05	0.15	2.25	16.05	0.107	0.29	0.09	336201	7793259	1097
SH-RC-PET-001A025	63	64	3.39	3.79	2.42	16.39	0.085	0.38	0.74	336201	7793259	1096
SH-RC-PET-001A026	64	65	2.18	0.58	2.78	15.18	0.083	0.53	0.09	336201	7793259	1095
SH-RC-PET-001A027	65	66	2.82	0.25	4.01	15.82	0.111	0.57	0.1	336201	7793259	1094
SH-RC-PET-001A028	66	67	0.92	2.53	1.89	13.92	0.019	0.52	0.49	336201	7793259	1093
SH-RC-PET-001A029	67	68	0.83	0.95	3.45	13.85	0.065	0.6	0.41	336201	7793259	1092
SH-RC-PET-001A030	68	69	0.62	2.24	4.85	13.62	0.021	0.88	0.58	336201	7793259	1091
SH-RC-PET-001A031	69	70	1.1	0.59	4.04	14.1	0.065	0.6	0.96	336201	7793259	1090
SH-RC-PET-001A032	70	71	1.91	0.8	4.14	14.91	0.159	0.87	0.34	336201	7793259	1089
SH-RC-PET-001A033	71	72	0.75	2.07	2.31	13.84	0.101	0.12	0.67	336201	7793259	1088
SH-RC-PET-001A034	72	73	1.5	0.8	1.46	16.09	0.104	0.06	0.64	336201	7793259	1087
SH-RC-PET-001A035	73	74	1.94	0.77	1.3	13.8	0.1	0.03	0.63	336201	7793259	1086

SH-RC-PET-001A036	74	75	0.92	0.52	3.21	14.62	0.089	0.02	0.78	336201	7793259	1085
SH-RC-PET-001A037	75	76	1.65	0.92	2.31	14.23	0.096	0.1	0.65	336201	7793259	1084
SH-RC-PET-001A038	76	77	2.2	0.44	1.61	15.3	0.075	0.08	0.55	336201	7793259	1083
SH-RC-PET-001A039	77	78	3.98	1.31	1.81	15.28	0.09	0.15	0.75	336201	7793259	1082
SH-RC-PET-001A040	78	79	3.01	0.23	1.34	15.91	0.087	0.1	0.65	336201	7793259	1081
SH-RC-PET-001A041	79	80	3.37	0.27	1.77	14.32	0.087	0.28	0.68	336201	7793259	1080
SH-RC-PET-001A042	80	81	2.13	5.02	1.34	15.33	0.077	0.29	1.77	336201	7793259	1079
SH-RC-PET-001A043	81	82	2.83	3.34	1.6	15.81	0.1	0.49	1.41	336201	7793259	1078
SH-RC-PET-001A044	82	83	1.04	3.3	5.62	16.3		0.101	0.67	336201	7793259	1077
SH-RC-PET-001A045	83	84	0.44	3.91	9.2	16.24	0.16	0.67	1.35	336201	7793259	1076
SH-RC-PET-001A046	84	85	0.07	2.73	6.86	15.45	0.09	0.86	1.28	336201	7793259	1075
SH-RC-PET-001A047	85	86	0.2	0.33	2.42	15.82	0.159	0.81	0.72	336201	7793259	1074
SH-RC-PET-001A048	86	87	0.21	0.36	2.49	13.62	0.112	0.77	0.28	336201	7793259	1073
SH-RC-PET-034A001	4	5	0.86	1.55	2.78	13.86	0.155	0.33	1.03	336309	7793326	1162
SH-RC-PET-034A002	5	6	0.49	1.75	4.65	13.49	0.161	0.54	0.73	336309	7793326	1161
SH-RC-PET-034A003	6	7	0.34	0.15	5.61	13.44	0.171	0.79	0.67	336309	7793326	1160
SH-RC-PET-034A004	11	12	0.44	2.41	1.82	13.44	0.192	0.62	0.88	336309	7793326	1155
SH-RC-PET-034A005	43	44	0.27	0.58	1.31	13.41	0.723	0.13	0.24	336309	7793326	1123
SH-RC-PET-034A006	44	45	0.08	1.68	4	13.56	0.253	0.02	0.4	336309	7793326	1122
SH-RC-PET-034A007	45	46	0.04	1.97	4.26	13.39	0.199	0.08	0.43	336309	7793326	1121
SH-RC-PET-034A008	46	47	0.16	3	3.87	13.42	0.152	0.17	0.65	336309	7793326	1120
SH-RC-PET-034A009	47	48	2.04	0.32	1.29	14.29	0.257	0.09	0.17	336309	7793326	1119

SH-RC-PET-034A010	48	49	0.07	0.85	4.96	14.41	0.201	0.25	0.22	336309	7793326	1118
SH-RC-PET-034A011	49	50	0.1	8.09	2.25	14.29	0.129	0.16	2.2	336309	7793326	1117
SH-RC-PET-034A012	50	51	0.11	5.81	1.77	13.29	0.246	0.23	1.23	336309	7793326	1116
SH-RC-PET-034A013	51	52	2.24	0.17	3.08	13.71	0.152	0.11	0.11	336309	7793326	1115
SH-RC-PET-034A014	52	53	0.01	8.3	1.83	13.29	0.108	0.04	2.51	336309	7793326	1114
SH-RC-PET-034A015	53	54	0.02	1.03	3.12	13.41	0.142	0.14	5.25	336309	7793326	1113
SH-RC-PET-034A016	54	55	0.65	0.85	2.71	13.79	0.168	0.21	3.91	336309	7793326	1112
SH-RC-PET-034A017	55	56	0.95	7.5	1.99	13.81	0.193	0.25	2.24	336309	7793326	1111
SH-RC-PET-034A018	56	57	2.17	2.58	1.78	13.71	0.215	0.21	0.55	336309	7793326	1110
SH-RC-PET-034A019	57	58	1.99	0.52	3.21	14.6	0.023	0.32	0.14	336309	7793326	1109
SH-RC-PET-034A020	58	59	2.34	0.31	3.85	13.4	0.111	0.35	0.04	336309	7793326	1108
SH-RC-PET-034A021	59	60	2.95	0.17	1.34	14.9	0.13	0.41	0.01	336309	7793326	1107
SH-RC-PET-034A022	60	61	3.53	0.42	1.55	15.6	0.44	0.52	0.1	336309	7793326	1106
SH-RC-PET-034A023	61	62	3.79	0.2	1.64	14.52	0.145	0.55	0.39	336309	7793326	1105
SH-RC-PET-034A024	62	63	1.95	1.89	4.01	13.46	0.145	0.55	0.39	336309	7793326	1104
SH-RC-PET-034A025	63	64	0.53	1.19	6.58	14.7	0.444	0.64	0.24	336309	7793326	1103
SH-RC-PET-034A026	64	65	0.09	1.11	8.15	14.15	0.142	0.77	0.2	336309	7793326	1102
SH-RC-PET-034A027	65	66	1.85	2.26	3.81	15.49	0.4	0.71	0.47	336309	7793326	1101
SH-RC-PET-034A028	66	67	1.18	2.94	4.58	13.6	0.157	0.97	0.67	336309	7793326	1100
SH-RC-PET-034A029	67	68	1.92	0.72	4.82	14.89	0.4	0.12	0.71	336309	7793326	1099
SH-RC-PET-034A030	68	69	0.99	3.32	6.02	13.4	0.34	0.12	0.71	336309	7793326	1098
SH-RC-PET-034A031	69	70	1.58	1.51	5.5	15.39	0.36	0.1	0.29	336309	7793326	1097

SH-RC-PET-034A032	70	71	1.88	0.97	4.18	15.44	0.26	0.16	0.2	336309	7793326	1096
SH-RC-PET-034A033	71	72	0.59	0.86	7.19	13.55	0.3	0.26	0.22	336309	7793326	1095
SH-RC-PET-034A034	72	73	0.46	1.46	6.71	13.66	0.116	0.38	0.25	336309	7793326	1094
SH-RC-PET-034A035	73	74	0.24	1.05	7.08	13.74	0.108	0.46	0.23	336309	7793326	1093
SH-RC-PET-034A036	74	75	0.2	1.01	7.17	13.39	0.32	0.39	0.27	336309	7793326	1092
SH-RC-PET-034A037	75	76	0.44	5.28	4.55	13.44	0.155	0.21	0.71	336309	7793326	1091
SH-RC-PET-034A038	76	77	1.62	3.3	3.49	14.62	0.126	0.21	0.51	336309	7793326	1090
SH-RC-PET-034A039	77	78	2.1	0.72	3.54	15.1	0.161	0.15	1.52	336309	7793326	1089
SH-RC-PET-034A040	78	79	0.52	1.23	5.34	13.52	0.21	0.16	0.69	336309	7793326	1088
SH-RC-PET-034A041	79	80	1.21	2.18	4.18	14.21	0.156	0.15	1.1	336309	7793326	1087
SH-RC-PET-034A042	80	81	2.33	0.62	3.59	15.33	0.211	0.11	0.71	336309	7793326	1086
SH-RC-PET-034A043	81	82	0.22	5.97	4.71	13.22	0.169	0.19	0.54	336309	7793326	1085
SH-RC-PET-034A044	82	83	0.11	1.07	6.19	13.11	0.171	0.14	0.69	336309	7793326	1084
SH-RC-PET-034A045	83	84	0.23	1.48	4.7	13.22	0.159	0.17	0.82	336309	7793326	1083
SH-RC-PET-034A046	84	85	0.11	1.16	4.17	13.15	0.211	0.22	0.33	336309	7793326	1082
SH-RC-PET-034A047	85	86	1.69	4.09	6.53	14.69	0.169	0.98	0.41	336309	7793326	1081
V-RC-PET-028A001	17	18	0.11	0.12	1.89	13.09	0.38	0.21	0.05	336854	7793544	1157
V-RC-PET-028A002	18	19	0.07	0.1	2.32	13.39	0.26	0.24	0.13	336854	7793544	1156
V-RC-PET-028A003	19	20	0.28	1.63	2.74	15.61	0.54	0.38	0.32	336854	7793544	1155
V-RC-PET-028A004	20	21	1.62	2.87	3.04	15.09	0.36	0.72	1.19	336854	7793544	1154
V-RC-PET-028A005	21	22	0.84	1.41	5.82	14.6	0.33	0.56	0.64	336854	7793544	1153
V-RC-PET-028A006	22	23	0.84	3.12	6.11	13.41	0.56	0.62	0.74	336854	7793544	1152

V-RC-PET-028A007	23	24	0.12	0.23	1.47	13.07	0.28	0.66	0.06	336854	7793544	1151
V-RC-PET-028A008	24	25	0.04	0.16	0.83	13.04	0.46	0.74	0.07	336854	7793544	1150
V-RC-PET-028A009	41	42	0.14	0.15	1.58	13.02	0.34	0.81	0.07	336854	7793544	1133
V-RC-PET-028A010	42	43	0.13	0.18	2.44	13.06	0.56	0.92	0.05	336854	7793544	1132
V-RC-PET-028A011	43	44	0.38	1.1	4.63	14.29	0.54	1.04	0.05	336854	7793544	1131
V-RC-PET-028A012	44	45	0.48	3.69	5.09	15.09	0.48	0.14	0.75	336854	7793544	1130
V-RC-PET-028A013	45	46	1.28	1.98	4.47	15.69	0.38	0.22	0.58	336854	7793544	1129
V-RC-PET-028A014	46	47	1.5	3.15	4.47	15.68	0.36	0.12	0.69	336854	7793544	1128
V-RC-PET-028A015	47	48	2.66	0.58	1.96	15.44	0.36	0.16	0.69	336854	7793544	1127
V-RC-PET-028A016	48	49	1.01	5.73	2.04	15.41	0.36	0.09	0.22	336854	7793544	1126
V-RC-PET-028A017	49	50	1.37	6.5	1.39	15.62	0.54	0.07	1.12	336854	7793544	1125
V-RC-PET-028A018	50	51	2.47	2.5	1.02	15.81	0.48	0.06	2.03	336854	7793544	1124
V-RC-PET-028A019	51	52	2.55	2.51	0.39	17.29	0.38	0.05	0.86	336854	7793544	1123
V-RC-PET-028A020	52	53	5.4	0.29	0.65	16.82	0.54	0.08	0.98	336854	7793544	1122
V-RC-PET-028A021	53	54	3.03	0.3	0.32	16.81	0.48	0.1	0.22	336854	7793544	1121
V-RC-PET-028A022	54	55	5.2	0.64	1.75	17.09	0.52	0.06	0.2	336854	7793544	1120
V-RC-PET-028A023	55	56	4.61	2.08	2.3	16.9	0.36	0.1	0.24	336854	7793544	1119
V-RC-PET-028A024	56	57	0.04	6.55	6.07	10.09	0.42	0.22	1.53	336854	7793544	1118
V-RC-PET-028A025	57	58	2.4	0.75	2.67	15.6	0.56	0.17	0.32	336854	7793544	1117
V-RC-PET-028A026	58	59	1.76	1.1	3.88	15.81	0.48	0.13	0.01	336854	7793544	1116
V-RC-PET-028A027	59	60	0.55	0.92	5.71	15.33	0.48	0.06	0.05	336854	7793544	1115
V-RC-PET-028A028	60	61	0.28	0.53	7.71	14.29	0.5	0.26	0.12	336854	7793544	1114

V-RC-PET-028A029	61	62	0.41	1.77	5.51	14.4	0.66	0.69	0.52	336854	7793544	1113
V-RC-PET-028A030	62	63	0.41	2.01	5.42	14.4	0.6	0.68	0.54	336854	7793544	1112
V-RC-PET-028A031	63	64	0.58	2.16	3.15	14.47	0.68	0.65	0.52	336854	7793544	1111
V-RC-PET-028A032	64	65	0.98	2.22	3.33	14.77	0.68	0.52	0.54	336854	7793544	1110
V-RC-PET-028A033	65	66	0.45	3.35	4.14	14.39	0.5	0.62	0.78	336854	7793544	1109
V-RC-PET-028A034	66	67	0.36	3.38	5.37	14.33	0.48	0.64	0.73	336854	7793544	1108
V-RC-PET-028A035	67	68	0.34	0.44	1.63	14.39	0.46	0.54	0.03	336854	7793544	1107
V-RC-PET-028A036	68	69	0.18	2.9	5.31	14.09	0.48	0.67	0.49	336854	7793544	1106
V-RC-PET-028A037	69	70	0.38	0.53	1.69	14.48	0.46	0.18	0.01	336854	7793544	1105
WC-RC-003A001	0	1	0.08	0.69	7.24	10.01	0.522	0.5	0.16	336369	7793761	1127
WC-RC-003A002	1	2	0.11	1.88	5.7	12.27	0.688	0.2	0.44	336369	7793761	1126
WC-RC-003A003	2	3	0.09	0.1	0.52	12.18	0.88	0.1	0.08	336369	7793761	1125
WC-RC-003A004	3	4	0.16	0.39	0.3	12.09	0.87	0.11	0.14	336369	7793761	1124
WC-RC-003A005	59	60	0.18	0.4	1.38	16.85	0.872	0.98	0.14	336369	7793761	1068
WC-RC-003A006	60	61	0.15	0.45	1.36	16.8	0.869	0.89	0.16	336369	7793761	1067
WC-RC-003A007	61	62	0.28	1.37	6.61	12.39	0.476	0.1	0.64	336369	7793761	1066
WC-RC-003A008	62	63	2.71	0.36	1.78	15.7	0.522	0.1	0.44	336369	7793761	1065
WC-RC-003A009	63	64	3.01	0.2	0.82	15.89	0.565	0.11	0.36	336369	7793761	1064
WC-RC-003A010	64	65	0.71	6.25	3.07	15.07	0.5	0.08	2.15	336369	7793761	1063
WC-RC-003A011	65	66	2.66	0.95	1.43	15.89	0.619	0.06	0.39	336369	7793761	1062
WC-RC-003A012	66	67	2.39	2.82	1.37	15.62	0.56	0.08	0.91	336369	7793761	1061
WC-RC-003A013	67	68	1.72	3.54	2.69	15.9	0.504	0.11	1.02	336369	7793761	1060

WC-RC-003A014	68	69	1.13	6.69	2.69	15.72	0.451	0.12	1.96	336369	7793761	1059
WC-RC-003A015	69	70	2.16	1.13	2.22	15.8	0.08	0.13	0.47	336369	7793761	1058
WC-RC-003A016	70	71	1.59	0.81	4.82	15.81	0.65	0.09	0.35	336369	7793761	1057
WC-RC-003A017	71	72	0.42	1.2	6.33	14.39	0.589	0.12	0.48	336369	7793761	1056
WC-RC-003A018	72	73	0.43	2.18	4.36	14.51	0.842	0.14	0.74	336369	7793761	1055
WC-RC-003A019	73	74	0.15	0.96	6.42	14.01	0.84	0.12	0.84	336369	7793761	1054
WC-RC-003A020	74	75	0.11	3.4	5.24	13	0.546	0.23	1.19	336369	7793761	1053
WC-RC-003A021	75	76	0.3	2.65	5.91	15.01	0.19	0.3	0.66	336369	7793761	1052
WC-RC-003A022	76	77	0.82	0.52	4.51	14.55	0.191	0.3	0.04	336369	7793761	1051
WC-RC-003A023	77	78	0.64	0.85	6.88	14.58	0.2	0.25	0.08	336369	7793761	1050
WC-RC-004A002	25	26	0.14	0.55	3.31	16.98	0.196	1.03	0	336530	7793664	1117
WC-RC-004A001	24	25	0.08	0.27	2.37	16.59	0.203	0.98	0.02	336530	7793664	1118
WC-RC-004A003	26	27	0.22	2.85	5.23	15.56	0.198	0.3	0.22	336530	7793664	1116
WC-RC-004A004	27	28	0.09	0.44	0.86	15.66	0.19	0.2	0.03	336530	7793664	1115
WC-RC-004A005	28	29	0.1	0.39	2.12	16.68	0.192	0.95	0.01	336530	7793664	1114
WC-RC-004A006	29	30	0.08	0.53	4.05	14.48	0.21	0.31	0.04	336530	7793664	1113
WC-RC-004A007	58	59	0.21	1.93	3.63	14.5	0.222	0.34	0.08	336530	7793664	1084
WC-RC-004A008	59	60	0.22	1.64	3.32	14.66	0.221	0.22	0.28	336530	7793664	1083
WC-RC-004A009	60	61	0.44	2.11	3.07	14.68	0.23	0.25	0.1	336530	7793664	1082
WC-RC-004A010	61	62	0.42	0.36	1.1	14.69	0.195	0.28	0.22	336530	7793664	1081
WC-RC-004A011	62	63	0.75	0.98	1.74	16.94	0.192	1.06	0.7	336530	7793664	1080
WC-RC-004A012	63	64	1.75	4.5	5.52	14.59	0.191	0.3	0.36	336530	7793664	1079

WC-RC-004A013	64	65	0.16	1.11	0.86	14.6	0.192	0.26	0.39	336530	7793664	1078
WC-RC-004A014	65	66	0.16	0.1	3.09	15.6	0.193	0.22	0.3	336530	7793664	1077
WC-RC-004A015	66	67	0.36	1.81	5.87	15.55	0.095	0.28	0.38	336530	7793664	1076
MKS-RC-PET-003A001	19	20	0.11	2.07	2.07	15.7	0.084	0.02	0.22	336805	7794550	1081
MKS-RC-PET-003A002	20	21	0.1	1.27	6	14.72	0.086	0.1	0.41	336805	7794550	1080
MKS-RC-PET-003A003	21	22	0.15	1.02	7.46	14.22	0.138	0.1	0.3	336805	7794550	1079
MKS-RC-PET-003A004	22	23	0.06	0.26	8.26	14.01	0.072	0.12	0.1	336805	7794550	1078
MKS-RC-PET-003A005	23	24	0.46	1.96	5.65	14.3	0.152	0.16	0.52	336805	7794550	1077
MKS-RC-PET-003A006	24	25	0.46	1.61	5.68	14.3	0.137	0.17	0.46	336805	7794550	1076
MKS-RC-PET-003A007	25	26	0.2	0.55	5.31	14.28	0.091	0.15	0.15	336805	7794550	1075
MKS-RC-PET-003A008	26	27	0.18	0.66	8.3	14.26	0.09	0.18	0.16	336805	7794550	1074
MKS-RC-PET-003A009	27	28	0.18	1.8	6.27	14.26	0.198	0.22	0.21	336805	7794550	1073
MKS-RC-PET-003A010	28	29	0.28	2.34	2.95	14.2	0.206	0.27	0.13	336805	7794550	1072

Appendix 3d: DDH AAS Results

Sample_Name	From	To	Li_2O_pct	K_2O_pct	Na_2O_pct	Al_2O_3_pct	Fe_2O_3_pct	Cs_2O_pct	Rb_2O_pct	Easting	Northing	Elevation
SQI_DDH_12A002	2.5	3	0.37							336089	7793005	1175
SQI_DDH_12A003	3	3.5	0.31							336089	7793005	1175
SQI_DDH_12A004	3.5	4	0.2							336089	7793004	1174
SQI_DDH_12A005	4	4.5	0.14							336089	7793004	1174
SQI_DDH_12A006	4.5	5	0.21							336090	7793004	1173
SQI_DDH_12A007	5	5.5	0.18							336090	7793004	1173
SQI_DDH_12A008	5.5	6	1.22							336090	7793004	1172
SQI_DDH_12A009	6	6.5	0.36							336090	7793004	1172
SQI_DDH_12A010	6.5	7	1.87							336090	7793003	1172
SQI_DDH_12A011	7	7.5	3.05							336090	7793003	1171
SQI_DDH_12A012	7.5	8	0.67							336091	7793003	1171
SQI_DDH_12A013	8	8.5	0.1							336091	7793003	1170
SQI_DDH_12A014	8.5	9	0.27							336091	7793003	1170
SQI_DDH_12A015	9	9.5	1.32							336091	7793003	1169
SQI_DDH_12A016	9.5	10	0.08							336091	7793002	1169
SQI_DDH_12A017	10	10.5	2.28							336092	7793002	1169
SQI_DDH_12A018	10.5	11	3.15							336092	7793002	1168
SQI_DDH_12A019	11	11.5	1.6							336092	7793002	1168

SQI_DDH_12A020	11.5	12	2.63							336092	7793002	1167
SQI_DDH_12A021	12	12.5	2.65							336092	7793002	1167
SQI_DDH_12A022	12.5	13	0.61							336093	7793001	1166
SQI_DDH_12A023	13	13.5	2.51							336093	7793001	1166
SQI_DDH_12A024	13.5	14	3.07							336093	7793001	1166
SQI_DDH_12A025	14	14.5	5.47							336093	7793001	1165
SQI_DDH_12A026	14.5	15	2.92							336093	7793001	1165
SQI_DDH_12A027	15	15.5	1.35							336094	7793001	1164
SQI_DDH_12A028	15.5	16	1.61							336094	7793001	1164
SQI_DDH_12A029	16	16.5	0.75							336094	7793000	1163
SQI_DDH_12A030	16.5	17	2.35							336094	7793000	1163
SQI_DDH_12A031	17	17.5	0.57							336094	7793000	1163
SQI_DDH_12A032	17.5	18	0.89							336094	7793000	1162
SQI_DDH_12A033	18	18.5	0.39							336095	7793000	1162
SQI_DDH_12A034	18.5	19	0.28							336095	7793000	1161
SQI_DDH_12A035	19	19.5	0.8							336095	7792999	1161
SQI_DDH_12A036	19.5	20	0.18							336095	7792999	1160
SQI_DDH_12A037	20	20.5	2.78							336095	7792999	1160
SQI_DDH_12A038	20.5	21	1.38							336096	7792999	1160
SQI_DDH_12A039	21	21.5	2.02							336096	7792999	1159
SQI_DDH_12A040	21.5	22	3.9							336096	7792999	1159
SQI_DDH_12A041	22	22.5	1.65							336096	7792998	1158

SQI_DDH_12A042	22.5	23	3.14							336096	7792998	1158
SQI_DDH_12A043	23	23.5	1.66							336097	7792998	1157
SQI_DDH_12A044	23.5	24	1.66							336097	7792998	1157
SQI_DDH_12A045	24	24.5	1.14							336097	7792998	1156
SQI_DDH_12A046	24.5	25	1.91							336097	7792998	1156
SQI_DDH_12A047	25	25.5	1.56							336097	7792997	1156
SQI_DDH_12A048	25.5	26	1.93							336098	7792997	1155
SQI_DDH_12A049	26	26.5	1.83							336098	7792997	1155
SQI_DDH_12A050	26.5	27	0.33							336098	7792997	1154
SQI_DDH_12A051	27	27.5	1.55							336098	7792997	1154
SQI_DDH_12A052	27.5	28	1.09							336098	7792997	1153
SQI_DDH_12A053	28	28.5	2.42							336099	7792996	1153
SQI_DDH_12A054	28.5	29	1.84							336099	7792996	1153
SQI_DDH_12A055	29	29.5	0.33							336099	7792996	1152
SQI_DDH_12A056	29.5	30	1.31							336099	7792996	1152
SQI_DDH_12A057	30	30.5	0.76							336099	7792996	1151
SQI_DDH_12A058	30.5	31	1.32							336099	7792996	1151
SQI_DDH_12A059	31	31.5	1.53							336100	7792996	1150
SQI_DDH_12A060	31.5	32	1.43							336100	7792995	1150
SQI_DDH_12A061	32	32.5	1.8							336100	7792995	1150
SQI_DDH_12A062	32.5	33	3.01							336100	7792995	1149
SQI_DDH_12A063	33	33.5	2.45							336100	7792995	1149

SQI_DDH_12A064	33.5	34	2.22							336101	7792995	1148
SQI_DDH_12A065	34	34.5	1.77							336101	7792995	1148
SQI_DDH_12A066	34.5	35	0.31							336101	7792994	1147
SQI_DDH_12A067	35	35.5	2.34							336101	7792994	1147
SQI_DDH_12A068	35.5	36	3.47							336101	7792994	1147
SQI_DDH_12A069	36	36.5	2.12							336102	7792994	1146
SQI_DDH_12A070	36.5	37	1.49							336102	7792994	1146
SQI_DDH_12A071	37	37.5	1.81							336102	7792994	1145
SQI_DDH_12A072	37.5	38	1.44							336102	7792993	1145
SQI_DDH_12A073	38	38.5	1.8							336102	7792993	1144
SQI_DDH_12A074	38.5	39	1.46							336103	7792993	1144
SQI_DDH_12A075	39	39.5	1.21							336103	7792993	1143
SQI_DDH_12A076	39.5	40	2.07							336103	7792993	1143
SQI_DDH_12A077	40	40.5	1.89							336103	7792993	1143
SQI_DDH_12A078	40.5	41	3.05							336103	7792992	1142
SQI_DDH_12A079	41	41.5	1.29							336103	7792992	1142
SQI_DDH_12A080	41.5	42	0.78							336104	7792992	1141
SQI_DDH_12A081	42	42.5	1.13							336104	7792992	1141
SQI_DDH_12A082	42.5	43	3.24							336104	7792992	1140
SQI_DDH_12A083	43	43.5	2.06							336104	7792992	1140
SQI_DDH_12A084	43.5	44	0.79							336104	7792992	1140
SQI_DDH_12A085	44	44.5	2.07							336105	7792991	1139

SQI_DDH_12A086	44.5	45	1.03							336105	7792991	1139
SQI_DDH_12A087	45	45.5	0.6							336105	7792991	1138
SQI_DDH_12A088	45.5	46	1.52							336105	7792991	1138
SQI_DDH_12A089	46	46.5	1.92							336105	7792991	1137
SQI_DDH_12A090	46.5	47	0.65							336106	7792991	1137
SQI_DDH_12A091	47	47.5	0.54							336106	7792990	1137
SQI_DDH_12A092	47.5	48	3.4							336106	7792990	1136
SQI_DDH_12A093	48	48.5	2.01							336106	7792990	1136
SQI_DDH_12A094	48.5	49	0.48							336106	7792990	1135
SQI_DDH_12A095	49	49.5	1.65							336107	7792990	1135
SQI_DDH_12A096	49.5	50	1.72							336107	7792990	1134
SQI_DDH_12A097	50	50.5	1.81							336107	7792989	1134
SQI_DDH_12A098	50.5	51	3.4							336107	7792989	1134
SQI_DDH_12A099	51	51.5	3.18							336107	7792989	1133
SQI_DDH_12A100	51.5	52	2.06							336108	7792989	1133
SQI_DDH_12A101	52	52.5	4.7							336108	7792989	1132
SQI_DDH_12A102	52.5	53	3.34							336108	7792989	1132
SQI_DDH_12A103	53	53.5	1.11							336108	7792988	1131
SQI_DDH_12A104	53.5	54	0.52							336108	7792988	1131
SQI_DDH_12A105	54	54.5	0.57							336108	7792988	1130
SQI_DDH_12A106	54.5	55	0.29							336109	7792988	1130
SQI_DDH_12A107	55	55.5	0.17							336109	7792988	1130

SQI_DDH_12A108	55.5	56	0.74							336109	7792988	1129
SQI_DDH_12A109	56	56.5	1.2							336109	7792987	1129
SQI_DDH_12A110	56.5	57	2.5							336109	7792987	1128
SQI_DDH_12A111	57	57.5	1.11							336110	7792987	1128
SQI_DDH_12A112	57.5	58	2.21							336110	7792987	1127
SQI_DDH_12A113	58	58.5	0.44							336110	7792987	1127
SQI_DDH_12A114	58.5	59	0.44							336110	7792987	1127
SQI_DDH_12A115	59	59.5	0.28							336110	7792987	1126
SQI_DDH_12A116	59.5	60	0.31							336111	7792986	1126
SQI_DDH_12A117	60	60.5	0.27							336111	7792986	1125
SQI_DDH_12A118	60.5	61	0.28							336111	7792986	1125
SQI_DDH_12A119	61	61.5	0.26							336111	7792986	1124
SQI_DDH_12A120	61.5	62	0.43							336111	7792986	1124
SQI_DDH_12A121	62	62.5	0.18							336112	7792986	1124
SQI_DDH_12A122	62.5	63	0.36							336112	7792985	1123
SQI_DDH_12A123	63	63.5	0.58							336112	7792985	1123
SQI_DDH_12A124	63.5	64	0.24							336112	7792985	1122
SQI_DDH_12A125	64	64.5	0.13							336112	7792985	1122
SQI_DDH_12A126	64.5	65	0.22							336112	7792985	1121
SQI_DDH_12A127	65	65.5	0.18							336113	7792985	1121
SQI_DDH_12A128	65.5	65.9	0.1							336113	7792984	1121
SQI_DDH_44A002	5.5	6	0.12	1.51	0.17	14.09	0.11	0	0	336207	7793286	1154

SQI_DDH_44A003	6	6.5	0.11	1.81	7.41	17.8	0.144	0	0.31	336207	7793286	1153
SQI_DDH_44A004	6.5	7	0.08	0.99	7.59	17.73	0.147	0	0	336207	7793286	1153
SQI_DDH_44A005	7	7.5	0.1	1.66	4.33	16.54	0.14	0	0.28	336207	7793286	1152
SQI_DDH_44A006	7.5	8	0.2	1.94	3.77	15.6	0.147	0	0	336207	7793286	1152
SQI_DDH_44A007	8	8.5	0.05	0.87	5.56	15.9	0.111	0	0.13	336207	7793286	1151
SQI_DDH_44A008	8.5	9	0.37	2.26	2.59	15.28	0.109	0	0.86	336207	7793286	1151
SQI_DDH_44A009	9	9.5	0.08	7.08	0.43	14.12	0.044	0	0.1	336207	7793286	1150
SQI_DDH_44A010	9.5	10	0.49	1.87	3.85	16.64	0.045	0	0	336207	7793286	1150
SQI_DDH_44A011	10	10.5	0.36	2.07	2.16	15.48	0.127	0	0	336207	7793286	1149
SQI_DDH_44A012	10.5	11	0.26	1.43	1.31	14.33	0.126	0	0	336207	7793286	1149
SQI_DDH_44A013	11	11.5	0.12	0.8	6.03	16.7	0.12	0	1.01	336207	7793286	1148
SQI_DDH_44A014	11.5	12	0.01	1.1	5.39	16.98	0.125	0	0.57	336207	7793286	1148
SQI_DDH_44A015	12	12.5	0.59	3.85	4.69	16.42	0.123	0	0.43	336207	7793286	1147
SQI_DDH_44A016	12.5	13	0.1	4.64	2.77	15.16	0.042	0	0	336207	7793286	1147
SQI_DDH_44A017	13	13.5	0.07	1.08	6.26	17.1	0.062	0	0	336207	7793286	1146
SQI_DDH_44A018	13.5	14	0.06	1.02	6.96	17.19	0.069	0	1.41	336207	7793286	1146
SQI_DDH_44A019	14	14.5	0.09	0.57	7.86	17.34	0.088	0	1.06	336207	7793286	1145
SQI_DDH_44A020	14.5	15	0.13	0.04	7.56	17.28	0.103	0	1.76	336207	7793286	1145
SQI_DDH_44A021	15	15.5	0.11	0.62	4.73	16.4	0.163	0	1.35	336207	7793286	1144
SQI_DDH_44A022	15.5	16	0.02	1.02	1.45	14.29	0.179	0	1.42	336207	7793286	1144
SQI_DDH_44A023	16	16.5	0.11	0.37	1.05	14.17	0.164	0	2.35	336207	7793286	1143
SQI_DDH_44A024	16.5	17	0.06	0.23	1.17	14.15	0.178	0	1.98	336207	7793286	1143

SQI_DDH_44A025	46.5	47	0.14	0.48	2.1	15.34	0.166	0	0	336207	7793286	1113
SQI_DDH_44A026	47	47.5	0.1	1.29	4.5	16.22	0.173	0	0	336207	7793286	1112
SQI_DDH_44A027	47.5	48	0.08	0.45	2.2	15.19	0.177	0	0	336207	7793286	1112
SQI_DDH_44A028	52	52.5	0.08	0.44	1.58	14.6	0.166	0	0	336207	7793286	1107
SQI_DDH_44A029	52.5	53	0.42	0.67	1.72	14.27	0.174	0	0	336207	7793286	1107
SQI_DDH_44A030	53	53.5	0.05	2.19	3.71	15.38	0.165	0	0	336207	7793286	1106
SQI_DDH_44A031	53.5	54	0.05	0.57	5.11	17.35	0.122	0	0.14	336207	7793286	1106
SQI_DDH_44A032	54	54.5	0.06	1.71	5.15	15.29	0.148	0	0.36	336207	7793286	1105
SQI_DDH_44A033	54.5	55	0.05	2.26	5.21	17.31	0.135	0	0.56	336207	7793286	1105
SQI_DDH_44A034	55	55.5	0.03	2.31	5.36	17.28	0.159	0	0.84	336207	7793286	1104
SQI_DDH_44A035	55.5	56	0.06	1.98	5.2	17.1	0.158	0	0.25	336207	7793286	1104
SQI_DDH_44A036	56	56.5	0.1	1.31	5.32	16.39	0.151	0	0.13	336207	7793286	1103
SQI_DDH_44A037	56.5	57	0.82	1.36	3.69	15.39	0.161	0	0.12	336207	7793286	1103
SQI_DDH_44A038	57	57.5	1.99	2.27	1.97	15.3	0.1	0	0.33	336207	7793286	1102
SQI_DDH_44A039	57.5	58	1.14	5.84	1.96	16.24	0.052	0	1.34	336207	7793286	1102
SQI_DDH_44A040	58	58.5	0.41	8.47	2.2	16.38	0.054	0	2.9	336207	7793286	1101
SQI_DDH_44A041	58.5	59	0.11	7.38	2.65	15.63	0.118	0	2.32	336207	7793286	1101
SQI_DDH_44A042	59	59.5	2.45	1.29	1.89	16.44	0.078	0	0.35	336207	7793286	1100
SQI_DDH_44A043	59.5	60	0.29	0.43	1.27	15.39	0.024	0	0.79	336207	7793286	1100
SQI_DDH_44A044	60	60.5	0.52	1.37	3.18	16.4	0.065	0	1	336207	7793286	1099
SQI_DDH_44A045	60.5	61	1.62	0.3	4.69	16.4	0.09	0	1.24	336207	7793286	1099
SQI_DDH_44A046	61	61.5	2.34	0.78	2.97	16.39	0.096	0	2.4	336207	7793286	1098

SQI_DDH_44A047	61.5	62	0.22	5.57	3.16	16.28	0.112	0	1.61	336207	7793286	1098
SQI_DDH_44A048	62	62.5	2.11	3.41	1.49	16.31	0.092	0	0.89	336207	7793286	1097
SQI_DDH_44A049	62.5	63	3.71	0.7	0.38	16.34	0.093	0	0.02	336207	7793286	1097
SQI_DDH_44A050	63	63.5	4.46	0.24	0.45	16.4	0.085	0	0.12	336207	7793286	1096
SQI_DDH_44A051	63.5	64	4.25	0.14	1.03	16.28	0.119	0	0.1	336207	7793286	1096
SQI_DDH_44A052	64	64.5	3.39	0.94	0.42	16.31	0.119	0	0.43	336207	7793286	1095
SQI_DDH_44A053	64.5	65	4.03	0.16	0.91	15.38	0.134	0	0.86	336207	7793286	1095
SQI_DDH_44A054	65	65.5	1.81	3.86	1.2	17.39	0.114	0	0.91	336207	7793286	1094
SQI_DDH_44A055	65.5	66	0.46	4.75	1.22	17.4	0.148	0	0.43	336207	7793286	1094
SQI_DDH_44A056	66	66.5	0.26	6.06	1.25	16.44	0.148	0	0.86	336207	7793286	1093
SQI_DDH_44A057	66.5	67	3.1	6.63	1.25	15.44	0.095	0	0.91	336207	7793286	1093
SQI_DDH_44A058	67	67.5	2.76	0.08	0.19	16.24	0.138	0	0.41	336207	7793286	1092
SQI_DDH_44A059	67.5	68	4.44	0.22	0.43	16.34	0.14	0	0.06	336207	7793286	1092
SQI_DDH_44A060	68	68.5	3.84	0.42	0.68	16.3	0.129	0	0.14	336207	7793286	1091
SQI_DDH_44A061	68.5	69	1.9	4.07	1.64	16.39	0.129	0	0.16	336207	7793286	1091
SQI_DDH_44A062	69	69.5	2.15	2.81	2.36	15.82	0.014	0.02	0.61	336207	7793286	1090
SQI_DDH_44A063	69.5	70	1.13	4.56	3.68	15.61	0.127	0.03	0.95	336207	7793286	1090
SQI_DDH_44A064	70	70.5	2.09	4.27	2.26	15.66	0.117	0.09	1.08	336207	7793286	1089
SQI_DDH_44A065	70.5	71	2.6	1.05	1.09	15.81	0.014	0.07	0.04	336207	7793286	1089
SQI_DDH_44A066	71	71.5	1.65	1.66	4.99	15.94	0.151	0.05	0.39	336207	7793286	1088
SQI_DDH_44A067	71.5	72	2.49	1.5	4.09	15.78	0.101	0.01	0.25	336207	7793286	1088
SQI_DDH_44A068	72	72.5	2.77	2.2	2.39	15.65	0.243	0.03	0.42	336207	7793286	1087

SQI_DDH_44A069	72.5	73	2.88	1.99	2.93	15.73	0.112	0.01	0.25	336207	7793286	1087
SQI_DDH_44A070	73	73.5	2.82	1.47	2.51	15.68	0.143	0.05	0.71	336207	7793286	1086
SQI_DDH_44A071	73.5	74	2.5	2.93	2.35	15.98	0.136	0.06	0.89	336207	7793286	1086
SQI_DDH_44A072	74	74.5	2.99	4.16	1.44	15.45	0.121	0.04	0.24	336207	7793286	1085
SQI_DDH_44A073	74.5	75	4.26	1	0.67	16.94	0.124	0.06	0.24	336207	7793286	1085
SQI_DDH_44A074	75	75.5	0.24	2.08	3.39	15.8	2.14	0.09	0.43	336207	7793286	1084
SQI_DDH_44A075	75.5	76	3.28	1.47	1.78	16	0.152	0.02	0.35	336207	7793286	1084
SQI_DDH_44A076	76	76.5	2.3	1.92	3.96	15.63	0.146	0.05	0.32	336207	7793286	1083
SQI_DDH_44A077	76.5	77	1.44	2.58	4.47	15.41	0.23	0.07	0.76	336207	7793286	1083
SQI_DDH_44A078	77	77.5	0.73	0.81	6.15	13.5	0.107	0.02	0.03	336207	7793286	1082
SQI_DDH_44A079	77.5	78	1.77	0.93	5.58	16.51	0.139	0.04	0	336207	7793286	1082
SQI_DDH_44A080	78	78.5	1.9	4.25	2.79	16.84	0.116	0.06	0	336207	7793286	1081
SQI_DDH_44A081	78.5	79	0.57	1.33	0.37	12.23	0.119	0.08	0	336207	7793286	1081
SQI_DDH_44A082	79	79.5	0.57	0.54	1.65	13.23	0.126	0.02	0.36	336207	7793286	1080
SQI_DDH_44A083	79.5	80	1.47	1.16	6.07	16.51	0.106	0.03	0.7	336207	7793286	1080
SQI_DDH_44A084	80	80.5	1.68	1.64	4.95	16.57	0.123	0.04	0.67	336207	7793286	1079
SQI_DDH_44A085	80.5	81	2.97	0.9	4.41	17.8	0.098	0.05	0.41	336207	7793286	1079
SQI_DDH_44A086	81	81.5	0.3	0.11	4.25	13.3	0.147	0.06	0.93	336207	7793286	1078
SQI_DDH_44A087	81.5	82	0.34	0.82	0.61	13.34	0.106	0.01	0.3	336207	7793286	1078
SQI_DDH_44A088	82	82.5	1.07	4.27	2.04	16.55	0.092	0.09	1.75	336207	7793286	1077
SQI_DDH_44A089	82.5	83	0.95	3.18	4.63	15.7	0.065	0.04	1.54	336207	7793286	1077
SQI_DDH_44A090	83	83.5	3.23	6.83	2.89	17.6	0.088	0.05	3	336207	7793286	1076

SQI_DDH_44A091	83.5	84	4.01	0.3	0.75	16.57	0.163	0.02	0	336207	7793286	1076
SQI_DDH_44A092	84	84.5	4.07	1.75	0.28	16.7	0.159	0.01	0	336207	7793286	1075
SQI_DDH_44A093	84.5	85	2.68	9.64	1.76	16.7	0.148	0.02	0	336207	7793286	1075
SQI_DDH_44A094	85	85.5	3.2	3.17	5.19	16.9	0.148	0.06	0	336207	7793286	1074
SQI_DDH_44A095	85.5	86	3	0.58	7.9	17.16	0.112	0.04	0	336207	7793286	1074
SQI_DDH_44A096	86	86.5	3.99	0.02	1.52	17.5	0.153	0.08	0	336207	7793286	1073
SQI_DDH_44A097	86.5	87	2.22	0.76	5.06	16.7	0.063	0.09	0	336207	7793286	1073
SQI_DDH_44A098	87	87.5	1.36	0.61	4.86	14.5	0.064	0.1	0	336207	7793286	1072
SQI_DDH_44A099	87.5	88	0.39	0.3	7.52	13.6	0.076	0.05	0	336207	7793286	1072
SQI_DDH_44A100	88	88.5	0.45	0.53	7.6	16.55	0.053	4	0	336207	7793286	1071
SQI_DDH_44A101	88.5	89	2.55	1.36	1.51	17.9	0.114	0.06	0.18	336207	7793286	1071
SQI_DDH_44A102	89	89.5	3.69	0.61	1.37	17.87	0.138	0.03	0.17	336207	7793286	1070
SQI_DDH_44A103	89.5	90	3.66	0.82	1.83	16.7	0.149	0.05	0.36	336207	7793286	1070
SQI_DDH_44A104	90	90.5	2.5	1.83	3.03	16.57	0.165	0.07	0.94	336207	7793286	1069
SQI_DDH_44A105	90.5	91	1.28	2.05	5.18	16.59	0.147	9	1.34	336207	7793286	1069
SQI_DDH_44A106	91	91.5	1.37	0.88	5.63	14.36	0.144	0.11	1.09	336207	7793286	1068
SQI_DDH_44A107	91.5	92	0.77	1.44	5.88	16.7	0.122	0.02	1.27	336207	7793286	1068
SQI_DDH_44A108	92	92.5	1.62	0.96	5.17	17.7	0.11	0.01	1.39	336207	7793286	1067
SQI_DDH_44A109	92.5	93	3.19	1	2.41	17.6	0.086	0.02	2.42	336207	7793286	1067
SQI_DDH_44A110	93	93.5	3.6	1.3	0.74	13.5	0.063	0.01	2.85	336207	7793286	1066
SQI_DDH_44A111	93.5	94	0.35	4.81	4.44	13.4	0.055	0.02	0.09	336207	7793286	1066
SQI_DDH_44A112	94	94.5	0.25	7.69	4.08	13.49	0.118	0.03	1.64	336207	7793286	1065

SQI_DDH_44A113	94.5	95	1.22	2.02	2.22	16.59	0.104	0.04	1.85	336207	7793286	1065
SQI_DDH_44A114	95	95.5	2.09	1.24	2.8	13.26	0.146	0.01	2.2	336207	7793286	1064
SQI_DDH_44A115	95.5	96	0.48	1.99	4.62	14.5	0.139	0.02	1.6	336207	7793286	1064
SQI_DDH_44A116	96	96.5	0.79	2.34	3.1	14.5	0.163	0.03	2.16	336207	7793286	1063
SQI_DDH_44A117	96.5	97	0.63	2.43	2.96	14.7	0.138	0.01	2.49	336207	7793286	1063
SQI_DDH_44A118	97	97.5	0.65	2.42	3.89	14.55	0.082	0.02	2.12	336207	7793286	1062
SQI_DDH_44A119	97.5	98	0.34	3.22	5.21	15.26	0.164	0.05	2.23	336207	7793286	1062
SQI_DDH_44A120	98	98.5	0.36	1.44	4.93	14.53	0.17	0.06	2.23	336207	7793286	1061
SQI_DDH_44A121	98.5	99	0.46	1.39	1.04	12.06	0.176	0.01	1.69	336207	7793286	1061
SQI_DDH_44A001	5	5.5	0.06	1.09	0.52	14.1	0.159	0	0	336207	7793286	1154
NIG-DDH-002A001	3	6	0.77	3.68	6.23	13.17	0.1	0.5	1.87	336717	7793516	1167
NIG-DDH-002A002	6.46	7	0.18	0.17	2.5	13.51	0.115	0.51	0.4	336717	7793516	1165
NIG-DDH-002A003	7	7.5	2.19	5.6	1.81	16.2	0.026	0.33	2.07	336717	7793516	1164
NIG-DDH-002A004	7.5	8	3.52	0.65	0.71	16.88	0.034	0.35	0.29	336717	7793516	1164
NIG-DDH-002A005	8	8.5	1.45	1.21	5.94	15.24	0.031	0.54	0.79	336717	7793516	1163
NIG-DDH-002A006	8.5	9	1.29	3.21	3.95	15.99	0.035	0.29	2.14	336717	7793516	1163
NIG-DDH-002A007	9	9.5	3.6	0.15	0.23	17.08	0.031	0.31	0.21	336717	7793516	1162
NIG-DDH-002A008	9.5	10	4.99	0.03	0.09	17.46	0.1	0.38	0.12	336717	7793516	1162
NIG-DDH-002A009	10	10.5	4.78	0.01	0.08	17.38	0.06	0.41	0.12	336717	7793516	1161
NIG-DDH-002A010	10.5	11	4.79	0.02	0.1	17.41	0.01	0.22	0.07	336717	7793516	1161
NIG-DDH-002A011	11	11.5	4.71	0.02	0.11	17.23	0.008	0.11	0.12	336717	7793516	1160
NIG-DDH-002A012	11.5	12	4.5	0.42	0.2	17.49	0.06	0.68	0.19	336717	7793516	1160

NIG-DDH-002A013	12	12.5	3.43	0.19	2.85	17.02	0.027	0.12	0.2	336717	7793516	1159
NIG-DDH-002A014	12.5	13	3.94	0.19	0.88	16.16	0.02	0.4	0.22	336717	7793516	1159
NIG-DDH-002A015	13	13.5	4.03	0.58	1.52	16.3	0.048	0.58	0.3	336717	7793516	1158
NIG-DDH-002A016	13.5	14	3.7	0.46	2.19	15.7	0.033	0.86	0.39	336717	7793516	1158
NIG-DDH-002A017	14	14.5	2.35	0.48	4.61	14.33	0.022	0.16	0.89	336717	7793516	1157
NIG-DDH-002A018	14.5	15	3.77	0.25	0.48	15.9	0.013	0.35	0.66	336717	7793516	1157
NIG-DDH-002A019	15	15.5	4.25	0.22	0.59	16.36	0.011	0.67	1.3	336717	7793516	1156
NIG-DDH-002A020	15.5	16	4.27	0.12	0.71	16.49	0.008	0.25	1.49	336717	7793516	1156
NIG-DDH-002A021	16	16.5	3.26	0.48	2.38	15.62	0.017	0.54	0.54	336717	7793516	1155
NIG-DDH-002A022	16.5	17	1.97	2.5	2.97	14.52	0.07	0.73	0.22	336717	7793516	1155
NIG-DDH-002A023	17	17.5	0.83	2.21	6.53	14.21	0.078	0.9	0.06	336717	7793516	1154
NIG-DDH-002A024	17.5	18	2.93	0.79	2.62	14.7	0.084	0.25	0.26	336717	7793516	1154
NIG-DDH-002A025	18	18.5	3.9	0.26	0.86	15.69	0.032	0.53	0.33	336717	7793516	1153
NIG-DDH-002A026	18.5	19	3.61	0.5	1.63	15.5	0.087	0.69	0.04	336717	7793516	1153
NIG-DDH-002A027	19	19.5	3.15	1.49	1.76	15.4	0.104	0.98	0.07	336717	7793516	1152
NIG-DDH-002A028	19.5	20	2.12	0.3	1.05	14.3	0.028	0.23	0.3	336717	7793516	1152
NIG-DDH-002A029	20	20.5	3.24	1.26	1.18	14.62	0.066	0.15	1.3	336717	7793516	1151
NIG-DDH-002A030	20.5	21	4.25	0.05	0.49	16	0.006	0.46	1.33	336717	7793516	1151
NIG-DDH-002A031	21	21.5	1.56	3.27	2.46	17.2	0.23	0.61	1.44	336717	7793516	1150
NIG-DDH-002A032	21.5	22	3.01	1.28	1.18	15.28	0.151	0.88	0.1	336717	7793516	1150
NIG-DDH-002A033	22	22.5	2.3	4.03	1.89	17.1	0.009	0.05	0.12	336717	7793516	1149
NIG-DDH-002A034	22.5	23	3.87	0.41	1.78	15.87	0.026	0.29	1.78	336717	7793516	1149

NIG-DDH-002A035	23	23.5	2.51	1.86	2.06	14.86	0.028	0.46	2.3	336717	7793516	1148
NIG-DDH-002A036	23.5	24	1.36	1.06	3.52	14.6	0.066	0.76	4.64	336717	7793516	1148
NIG-DDH-002A037	24	24.5	2.35	1	3.43	13.53	0.07	0.91	3.2	336717	7793516	1147
NIG-DDH-002A038	24.5	25	1.37	0.96	5.56	12.96	0.084	0.07	1.7	336717	7793516	1147
NIG-DDH-002A039	25	25.5	2.32	0.57	3.75	14.28	0.065	0.05	0.06	336717	7793516	1146
NIG-DDH-002A040	25.5	26	1.99	0.28	4.21	14.41	0.026	0.37	0.27	336717	7793516	1146
NIG-DDH-002A041	26	26.5	1.66	1.54	6.44	13.34	0.106	0.71	0.12	336717	7793516	1145
NIG-DDH-002A042	26.5	27	3.66	1.01	0.68	15.88	0.081	0.86	0.34	336717	7793516	1145
NIG-DDH-002A043	27	27.5	3.02	1.12	1.59	15.6	0.078	0.84	1.69	336717	7793516	1144
NIG-DDH-002A044	27.5	28	2.79	1.5	1.78	14.5	0.106	0.09	1.24	336717	7793516	1144
NIG-DDH-002A045	28	28.5	0.67	5.8	5.01	17.3	0.056	0.25	0.8	336717	7793516	1143
NIG-DDH-002A046	28.5	29	1.06	1.29	3.18	14.29	0.012	0.33	0.27	336717	7793516	1143
NIG-DDH-002A047	29	29.5	1.69	2.86	3.99	15.86	0.041	0.41	0.39	336717	7793516	1142
NIG-DDH-002A048	29.5	30	2.2	1.11	4.02	15.62	0.079	0.17	0.12	336717	7793516	1142
NIG-DDH-002A049	30	30.5	3.07	0.6	2.23	15.66	0.079	0.29	0.08	336717	7793516	1141
NIG-DDH-002A050	30.5	31	2.65	2.81	3.13	15.1	0.076	0.45	0.73	336717	7793516	1141
NIG-DDH-002A051	31	31.5	2.07	0.56	4.32	15.03	0.045	0.5	0.15	336717	7793516	1140
NIG-DDH-002A052	31.5	32	1.96	1.48	4.55	14.71	0.049	0.65	0.17	336717	7793516	1140
NIG-DDH-002A053	32	32.5	1.03	2.18	4.94	14.6	0.054	0.76	0.85	336717	7793516	1139
NIG-DDH-002A054	32.5	33	1.36	1.61	4.41	14.88	0.056	0.8	0.69	336717	7793516	1139
NIG-DDH-002A055	33	33.5	0.31	4.01	4.83	14.01	0.094	0.93	0.47	336717	7793516	1138
NIG-DDH-002A056	33.5	34	0.98	1.3	5.99	14.16	0.103	0.96	0.61	336717	7793516	1138

NIG-DDH-002A057	34	34.5	0.47	1.72	7.77	14.22	0.154	0.19	0.8	336717	7793516	1137
NIG-DDH-002A058	34.5	35	0.17	9.17	7.09	14.11	0.121	0.29	4.01	336717	7793516	1137
NIG-DDH-002A059	35	35.5	1.19	6.04	3.41	14.88	0.035	0.39	2.19	336717	7793516	1136
NIG-DDH-002A060	35.5	36	1.76	2.36	1.98	14.91	0.081	0.5	1.05	336717	7793516	1136
NIG-DDH-002A061	36	36.5	0.22	0.87	4.15	14.2	0.274	0.56	0.21	336717	7793516	1135
NIG-DDH-002A062	36.5	37	0.34	1.18	6.09	14.01	0.091	0.54	0.47	336717	7793516	1135
NIG-DDH-002A063	37	37.5	0.3	1.41	3.02	14.03	0.093	0.77	0.53	336717	7793516	1134
VB-DDH-PET-001A001	19.5	20	0.38	1.27	3.61	13.41	0.058	0.02	0.56	336841	7793504	1153
VB-DDH-PET-001A002	20	20.5	0.54	4.37	7.77	14.54	0.044	0.13	2.51	336841	7793504	1153
VB-DDH-PET-001A003	20.5	21	2.41	6.62	0.57	14.39	0.064	0.08	4.88	336841	7793503	1152
VB-DDH-PET-001A004	21	21.5	0.85	2.58	7.86	13.16	0.05	0.1	1.04	336841	7793503	1152
VB-DDH-PET-001A005	21.5	22	0.34	1.07	7.82	13.28	0.058	0.12	0.39	336841	7793503	1152
VB-DDH-PET-001A006	22	22.5	0.15	1.95	6	13.94	0.044	0.09	0.34	336841	7793503	1151
VB-DDH-PET-001A007	22.5	23.3	0.29	2.15	6.03	13.76	0.087	0.2	0.56	336841	7793502	1151

VB-DDH-PET-001A008	42	42.5	0.6	2.87	5.02	13.21	0.18	0.14	0.93	336841	7793493	1134
VB-DDH-PET-001A009	42.5	43	0.24	2.05	7.5	13.27	0.061	0.04	0.52	336841	7793493	1133
VB-DDH-PET-001A010	43	43.5	0.28	0.83	8.58	14.02	0.037	0.02	0.31	336841	7793492	1133
VB-DDH-PET-001A011	43.5	44	0.43	4.58	6.89	14.3	0.039	0.08	1.11	336841	7793492	1132
VB-DDH-PET-001A012	44	44.5	0.26	1.31	3.62	13.99	0.035	0.11	0.35	336841	7793492	1132
VB-DDH-PET-001A013	44.5	45	0.84	1	8.23	14.08	0.041	0.15	0.26	336841	7793492	1131
VB-DDH-PET-001A014	45	45.5	1.76	0.92	3.08	14.34	0.069	0.12	0.33	336841	7793491	1131
VB-DDH-PET-001A015	45.5	46	0.55	4.99	6.77	14.5	0.048	0.1	1.32	336841	7793491	1131
VB-DDH-PET-001A016	46	46.5	1.29	1.31	4.96	14.97	0.093	0.17	0.39	336841	7793491	1130
VB-DDH-PET-001A017	46.5	47	1.9	0.98	4.91	14.88	0.054	0.01	0.33	336841	7793491	1130
VB-DDH-PET-001A018	47	47.5	1.68	0.8	4.1	15.2	0.04	0.19	0.27	336841	7793490	1129

VB-DDH-PET-001A019	47.5	48	1.4	0.12	1.73	13.4	0.033	0.73	0.43	336841	7793490	1129
VB-DDH-PET-001A020	48	48.5	3.05	0.56	2.07	16.01	0.022	0.07	0.2	336841	7793490	1128
VB-DDH-PET-001A021	48.5	49	2.01	0.61	2.1	15.95	0.056	0.22	0.19	336841	7793490	1128
VB-DDH-PET-001A022	49	49.5	2.34	1.3	2.12	15.38	0.064	0.13	0.5	336841	7793490	1128
VB-DDH-PET-001A023	49.5	50	0.62	1.49	7.39	13.04	0.048	0.21	0.46	336841	7793489	1127
VB-DDH-PET-001A024	50	50.5	1.5	2.92	2.45	14.51	0.081	0.18	1.11	336841	7793489	1127
VB-DDH-PET-001A025	50.5	51	2.69	2.03	0.5	15.13	0.08	0.2	1.01	336841	7793489	1126
VB-DDH-PET-001A026	51	51.5	3.43	1.01	0.34	16.19	0.074	0.14	0.4	336841	7793489	1126
VB-DDH-PET-001A027	51.5	52	2.87	1.66	0.64	16.21	0.096	0.09	0.62	336841	7793488	1125
VB-DDH-PET-001A028	52	52.5	1.28	5.24	0.62	15.48	0.042	0.12	2.45	336841	7793488	1125
VB-DDH-PET-001A029	52.5	53	1.16	2.74	5.32	15.3	0.032	0.28	1.05	336841	7793488	1124

VB-DDH-PET-001A030	53	53.5	1	2.89	5.15	15.23	0.056	0.16	1.15	336841	7793488	1124
VB-DDH-PET-001A031	53.5	54	0.98	2.38	5.14	13.33	0.076	0.15	0.85	336841	7793487	1124
VB-DDH-PET-001A032	54	54.5	1.49	3.71	2.16	13.49	0.114	0.9	1.92	336841	7793487	1123
VB-DDH-PET-001A033	54.5	55	2.38	1.1	1.68	15.38	0.052	0.58	0.53	336841	7793487	1123
VB-DDH-PET-001A034	55	55.5	2.55	2.77	1.47	15.55	0.078	0.77	1.4	336841	7793487	1122
VB-DDH-PET-001A035	55.5	56	3.13	1.03	1.47	16.13	0.059	0.92	0.67	336841	7793486	1122
VB-DDH-PET-001A036	56	56.5	2.27	1.98	1.93	14.27	0.047	0.42	1.16	336841	7793486	1121
VB-DDH-PET-001A037	56.5	57	2.53	2.03	1.87	14.53	0.044	0.63	1.15	336841	7793486	1121
VB-DDH-PET-001A038	57	57.5	0.04	0.01	0.08	13.04	0.084	0.84	0.33	336841	7793486	1121
VB-DDH-PET-001A039	57.5	58	3.47	0.8	1.08	16.47	0.035	0.05	0.65	336841	7793485	1120
VB-DDH-PET-001A041	58.5	59	4.32	0.26	0.59	16.02	0.109	0.57	0.5	336841	7793485	1119

VB-DDH-PET-001A042	59	59.5	4.3	0.21	0.61	16.4	0.034	0.77	0.46	336841	7793485	1119
VB-DDH-PET-001A043	59.5	60	3.11	1.821	1.16	15.11	0.06	0.93	1.11	336841	7793484	1118
VB-DDH-PET-001A044	60	60.5	3.13	0.31	1.87	15.13	0.029	0.42	0.52	336841	7793484	1118
VB-DDH-PET-001A045	60.5	61	3.55	0.32	1.11	15.55	0.032	0.72	0.45	336841	7793484	1118
VB-DDH-PET-001A046	61	61.5	2.96	1.06	1.8	14.96	0.049	0.96	0.76	336841	7793484	1117
VB-DDH-PET-001A047	61.5	62	2.76	0.99	1.64	14.76	0.116	0.64	0.7	336841	7793483	1117
VB-DDH-PET-001A048	62	62.5	3.14	0.29	1.68	15.14	0.037	0.86	0.53	336841	7793483	1116
VB-DDH-PET-001A049	62.5	63	5.69	0.45	0.31	16.69	0.05	0.2	0.1	336841	7793483	1116
VB-DDH-PET-001A050	63	63.5	3.26	0.38	1.73	15.26	0.043	0.97	0.44	336841	7793483	1115
VB-DDH-PET-001A051	63.5	64	3.28	0.32	1.56	15.28	0.089	0.31	0.55	336841	7793482	1115
VB-DDH-PET-001A052	64	64.5	4.56	0.03	0.27	16.56	0.039	0.48	0.06	336841	7793482	1114

VB-DDH-PET-001A053	64.5	65	4.53	0.14	0.36	16.53	0.034	0.76	0.34	336841	7793482	1114
VB-DDH-PET-001A054	65	65.5	3.79	0.56	0.85	15.79	0.019	0.23	0.5	336841	7793482	1114
VB-DDH-PET-001A056	66	66.5	4.56	0.14	0.15	16.23	0.018	0.14	0.13	336841	7793481	1113
VB-DDH-PET-001A057	66.5	67	4.08	0.22	0.59	16.14	0.006	0.8	0.08	336841	7793481	1112
VB-DDH-PET-001A058	67	67.5	4.06	0.18	0.89	16.38	0.02	0.13	0.05	336841	7793481	1112
VB-DDH-PET-001A059	67.5	68	3.94	0.52	1.52	16.02	0.021	0.09	0.12	336841	7793481	1111
VB-DDH-PET-001A060	68	68.5	4.31	0.07	0.09	16.91	0.005	0.17	0.13	336841	7793480	1111
VB-DDH-PET-001A061	68.5	69	4.1	19	1.54	16.73	0.006	0.1	0.08	336841	7793480	1111
VB-DDH-PET-001A062	69	69.5	2.23	4.95	1.07	15.48	0.036	0.07	1.67	336841	7793480	1110
VB-DDH-PET-001A063	69.5	70	0.98	5.77	4.13	13.21	0.015	0.17	1.4	336841	7793480	1110
VB-DDH-PET-001A064	70	70.5	4.29	0.13	0.34	16.3	0.015	0.15	0.06	336841	7793479	1109

VB-DDH-PET-001A065	70.5	71	4.44	0.08	0.15	16.88	0.008	0.2	0.09	336841	7793479	1109
VB-DDH-PET-001A066	71	71.5	3.37	1.44	0.16	15.84	0.05	0.09	0.55	336841	7793479	1108
VB-DDH-PET-001A067	71.5	72	3.12	0.76	0.33	15.93	0.057	0.1	0.14	336841	7793479	1108
VB-DDH-PET-001A068	72	72.5	2.17	0.8	0.57	16.64	0.064	0.12	0.15	336841	7793478	1107
VB-DDH-PET-001A069	72.5	73	2.19	0.17	0.83	15.69	0.048	0.03	0.02	336841	7793478	1107
VB-DDH-PET-001A070	73	73.5	1.52	5.59	0.38	14.04	0.14	0.17	2.02	336841	7793478	1107
VB-DDH-PET-001A071	73.5	74	1.03	1.66	1.94	14.33	0.14	0.16	1.64	336841	7793478	1106
VB-DDH-PET-001A072	74	74.5	0.46	2.04	1.91	13.71	0.147	0.21	0.49	336841	7793477	1106
VB-DDH-PET-001A073	74.5	75	0.78	1.68	6.06	13.42	0.085	0.23	0.65	336841	7793477	1105
VB-DDH-PET-001A074	75	75.5	0.43	1.89	8.21	13.44	0.081	0.18	0.46	336841	7793477	1105
VB-DDH-PET-001A075	75.5	76	0.38	0.73	5.3	13.17	0.117	0.22	0.52	336841	7793477	1104

VB-DDH-PET-001A076	76	76.62	0.25	1.38	7.96	13.29	0.065	0.16	0.09	336841	7793476	1104
VB-DDH-PET-001A077	77.5	78	0.11	0.73	5.43	13.75	0.145	0.11	0.32	336841	7793476	1103
VB-DDH-PET-001A078	78	78.5	0.1	1.36	7.34	13.56	0.082	0.13	0.11	336841	7793475	1102
VB-DDH-PET-001A079	78.5	79	0.15	1.48	4.09	13.5	0.103	0.25	0.3	336841	7793475	1102
VB-DDH-PET-001A080	79	79.5	0.39	1.73	2.1	13.44	0.151	0.29	0.42	336841	7793475	1101
VB-DDH-PET-001A081	79.5	80	0.56	4.15	2.69	13.37	0.135	0.15	0.57	336841	7793475	1101
VB-DDH-PET-001A082	80	80.5	1.12	4.17	1.05	14.28	0.14	0.08	1.08	336841	7793474	1100
VB-DDH-PET-001A083	80.5	81	1.36	1.22	3.07	14.32	0.16	0.26	1.81	336841	7793474	1100
VB-DDH-PET-001A084	81	81.5	0.26	1.91	5.02	13.69	0.102	0.31	0.14	336841	7793474	1100
VB-DDH-PET-001A085	81.5	82	0.61	4.66	2.46	13.48	0.16	0.09	0.43	336841	7793474	1099
VB-DDH-PET-001A086	82	82.5	1.14	4.73	0.78	14.57	0.148	0.19	2.07	336841	7793474	1099

VB-DDH-PET-001A087	82.5	83	1.48	6.58	0.62	14.53	0.18	0.47	1.08	336841	7793473	1098
VB-DDH-PET-001A088	83	83.5	2.29	4.11	0.41	15.25	0.173	0.04	2.51	336841	7793473	1098
VB-DDH-PET-001A089	83.5	84	1.22	4.31	0.37	14.22	0.169	0.09	0.1	336841	7793473	1097
VB-DDH-PET-001A090	84	84.5	0.97	2.7	0.92	13.97	0.151	0.03	0.07	336841	7793473	1097
VB-DDH-PET-001A091	84.5	85	0.57	1.58	4.93	13.57	0.117	0.04	0.11	336841	7793472	1097
VB-DDH-PET-001A092	85	85.5	0.54	1.18	4.41	13.54	0.12	0.12	0.12	336841	7793472	1096
VB-DDH-PET-001A093	85.5	86	0.48	1.16	2.15	13.48	0.121	0.26	0.1	336841	7793472	1096
VB-DDH-PET-001A094	86	86.5	0.6	2.53	0.94	13.6	0.12	0.41	0.15	336841	7793472	1095
VB-DDH-PET-001A095	86.5	87	0.8	2.16	0.38	13.8	0.119	0.58	0.19	336841	7793471	1095
VB-DDH-PET-001A096	87	87.5	0.66	1.43	0.14	13.66	0.119	0.78	0.16	336841	7793471	1094
VB-DDH-PET-001A097	87.5	88	0.99	1.92	0.83	13.99	0.123	0.98	0.19	336841	7793471	1094

VB-DDH-PET-001A098	88	88.5	2.12	1.01	0.71	15.12	0.109	1.24	0.25	336841	7793471	1093
VB-DDH-PET-001A099	88.5	89	2.28	0.4	2.36	15.28	0.136	1.43	0.27	336841	7793470	1093
VB-DDH-PET-001A100	89	89.5	1.32	0.63	4.82	14.32	0.045	1.7	0.36	336841	7793470	1093
VB-DDH-PET-001A101	89.5	90	0.53	1.25	3.13	13.53	0.113	1.95	0.53	336841	7793470	1092
VB-DDH-PET-001A102	90	90.5	1.41	3.68	2.04	14.41	0.169	2.26	0.41	336841	7793470	1092
VB-DDH-PET-001A103	90.5	91	0.47	0.88	6.4	13.47	0.064	2.48	0.47	336841	7793469	1091
VB-DDH-PET-001A104	91	91.5	0.61	1.09	6.38	13.61	0.044	2.71	0.25	336841	7793469	1091
VB-DDH-PET-001A105	91.5	92	0.36	1.1	6.86	13.36	0.073	3.06	0.5	336841	7793469	1090
VB-DDH-PET-001A106	92	92.5	0.38	1.07	5.37	13.38	0.084	3.37	0.17	336841	7793469	1090
VB-DDH-PET-001A107	92.5	93	0.36	1.02	5.71	13.36	0.087	3.61	0.19	336841	7793468	1090
VB-DDH-PET-001A108	93	93.65	0.18	0.67	7.54	13.18	0.083	3.75	0.3	336841	7793468	1089

VB-DDH-PET-001A040	58	58.5	4.22	0.26	0.59	16.02	0.109	0.23	0.65	336841	7793485	1120
VB-DDH-PET-008A001	6.32	7	0.59	2.42	2.36	15.82	0.34	0.57	1.02	336939	7793458	1128
VB-DDH-PET-008A002	7	7.5	2.24	2.43	0.91	15.99	0.338	0.73	1.48	336939	7793458	1127
VB-DDH-PET-008A003	7.5	8	0.67	0.93	0.26	15.7	0.155	0.74	0.98	336939	7793458	1127
VB-DDH-PET-008A004	8	8.5	2.84	1.49	2.07	15.33	0.039	0.12	0.09	336939	7793458	1126
VB-DDH-PET-008A005	8.5	9	4.02	6.1	2.05	15.92	0.073	0.36	3.82	336939	7793458	1126
VB-DDH-PET-008A006	9	9.5	0.78	2.63	9.4	15.82	0.057	0.24	1.43	336939	7793458	1125
VB-DDH-PET-008A007	9.5	10	1.55	5.38	8.09	16.25	0.118	0.46	3.02	336939	7793458	1125
VB-DDH-PET-008A008	10	10.5	1.14	3.79	3.95	16.14	0.152	0.54	1.66	336939	7793458	1124
VB-DDH-PET-008A009	10.5	11	1.62	5.05	0.4	15.29	0.348	0.8	3.51	336939	7793458	1124
VB-DDH-PET-008A010	11	11.5	0.93	4.04	5.29	15.82	0.152	2.68	1.61	336939	7793458	1123

VB-DDH-PET-008A011	11.5	12	0.69	2.57	5.67	15.74	0.074	0.84	1.05	336939	7793458	1123
VB-DDH-PET-008A012	12	12.5	0.8	3.35	6.93	15.4	0.127	0.94	1.15	336939	7793458	1122
VB-DDH-PET-008A013	12.5	13	0.47	1.81	6.62	15.6	0.083	0.43	0.22	336939	7793458	1122
VB-DDH-PET-008A014	13	13.5	0.49	2.02	6.64	15.72	0.051	0.54	0.42	336939	7793458	1121
VB-DDH-PET-008A015	13.5	14	1.37	3.47	4.15	16.15	0.031	0.59	0.6	336939	7793458	1121
VB-DDH-PET-008A016	14	14.5	3.97	0.79	0.53	16.42	0.027	0.12	0.55	336939	7793458	1120
VB-DDH-PET-008A017	14.5	15	3.52	3.05	0.84	16.38	0.021	0.42	0.86	336939	7793458	1120
VB-DDH-PET-008A018	15	15.5	1.13	3.37	6.15	15.9	0.016	0.09	0.05	336939	7793458	1119
VB-DDH-PET-008A019	15.5	16	1.41	3.98	3.47	15.85	0.024	0.62	0.83	336939	7793458	1119
VB-DDH-PET-008A020	16	16.5	2.11	1.76	4.46	15.91	0.029	0.66	0.02	336939	7793458	1118
VB-DDH-PET-008A021	16.5	17	3.94	0.22	1.18	16.16	0.031	0.2	0.24	336939	7793458	1118

VB-DDH-PET-008A022	17	17.5	2.04	0.79	2.28	15.79	0.015	0.33	0.29	336939	7793458	1117
VB-DDH-PET-008A023	17.5	18	1.77	1.32	4.81	14.32	0.038	0.59	0.81	336939	7793458	1117
VB-DDH-PET-008A024	18	18.5	2.03	2.44	3.28	15.44	0.032	0.83	1.24	336939	7793458	1116
VB-DDH-PET-008A025	18.5	19	0.45	4.64	7.7	16.64	0.01	0.02	1.5	336939	7793458	1116
VB-DDH-PET-008A026	19	19.5	0.46	1.66	7.78	14.66	0.013	0.24	0.73	336939	7793458	1115
VB-DDH-PET-008A027	19.5	20	0.85	2.05	5.95	14.5	0.014	0.49	0.82	336939	7793458	1115
VB-DDH-PET-008A028	20	20.5	1.61	4.19	3.06	15.49	0.073	0.68	2.66	336939	7793458	1114
VB-DDH-PET-008A029	20.5	21	1.77	3.86	3.4	15.86	0.027	0.28	2.32	336939	7793458	1114
VB-DDH-PET-008A030	21	21.5	2.5	1.22	3	14.22	0.032	0.28	0.6	336939	7793458	1113
VB-DDH-PET-008A031	21.5	22	1.39	0.96	0.51	13.96	0.028	0.83	0.23	336939	7793458	1113
VB-DDH-PET-008A032	22	22.5	0.12	0.12	0.47	13.12	0.02	0.47	0.12	336939	7793458	1112

VB-DDH-PET-008A033	22.5	23	0.24	0.77	0.78	12.77	0.029	0.69	0.05	336939	7793458	1112
VB-DDH-PET-008A034	23	23.5	0.27	0.58	5.72	13.58	0.018	0.04	0.29	336939	7793458	1111
VB-DDH-PET-008A035	23.5	24	1.4	3.46	2.13	15.46	0.037	0.22	1.52	336939	7793458	1111
VB-DDH-PET-008A036	24	24.5	1.36	4.25	2.02	16.25	0.092	0.32	2.08	336939	7793458	1110
VB-DDH-PET-008A037	24.5	25	1.01	3.15	2.34	16.51	0.18	0.58	0.6	336939	7793458	1110
VB-DDH-PET-008A038	25	25.5	1.3	3.95	0.34	15.95	0.132	0.78	2.12	336939	7793458	1109
VB-DDH-PET-008A039	25.5	26	1.87	4.92	1.03	16.3	0.097	0.91	2.3	336939	7793458	1109
VB-DDH-PET-008A040	26	26.5	1.57	4.57	0.84	16.16	0.116	0.04	2.09	336939	7793458	1108
VB-DDH-PET-008A041	26.5	27	3.03	7.42	1.44	17.8	0.135	0.91	5.6	336939	7793458	1108
VB-DDH-PET-008A042	27	27.5	1.35	7.82	7.5	17.59	0.28	0.32	3.81	336939	7793458	1107
VB-DDH-PET-008A043	27.5	28	3.69	8.75	2.75	17.9	0.299	0.65	5.5	336939	7793458	1107

VB-DDH-PET-008A044	28	28.5	3.31	8.26	3.93	17.88	0.1	0.68	5.55	336939	7793458	1106
VB-DDH-PET-008A045	28.5	29	2.29	6.89	2.61	16.75	0.22	0.74	5.08	336939	7793458	1106
VB-DDH-PET-008A046	29	29.5	1.88	6.96	1.71	16.7	0.249	0.09	4.23	336939	7793458	1105
VB-DDH-PET-008A047	29.5	30	1.64	5.6	6.24	16.56	0.283	0.92	3.31	336939	7793458	1105
VB-DDH-PET-008A048	30	30.5	0.87	4.44	8.5	16.44	0.247	0.86	2.3	336939	7793458	1104
VB-DDH-PET-008A049	30.5	31	0.83	3.34	8.69	16.43	0.266	0.91	1.53	336939	7793458	1104
VB-DDH-PET-008A050	31	31.6	0.38	2.06	9.2	15.6	0.096	0.04	0.53	336939	7793458	1103
AHH-DDH-002A001	28.5	29	0.31	2.36	1.09	13.31	0.161	0.61	0.58	336721	7793249	1133
AHH-DDH-002A002	29	29.5	0.25	4.3	3.94	13.25	0.072	0.72	0.78	336721	7793249	1132
AHH-DDH-002A003	29.5	30	3.73	1.03	1.17	16.73	0.067	0.67	0.25	336721	7793249	1132
AHH-DDH-002A004	30	30.5	1.4	4.38	4.41	15.4	0.036	0.36	0.87	336721	7793249	1131
AHH-DDH-002A005	30.5	31	0.53	8.76	3.64	13.53	0.019	0.19	2.64	336721	7793249	1131
AHH-DDH-002A006	31	31.5	2.03	4.18	3.52	14.03	0.037	0.38	0.87	336721	7793249	1130
AHH-DDH-002A007	31.5	32	2.65	1.85	3.28	15.65	0.044	0.44	0.45	336721	7793249	1130
AHH-DDH-002A008	32	32.5	1.23	5.84	3.49	14.23	0.049	0.49	1.4	336721	7793249	1129

AHH-DDH-002A009	32.5	33	3.15	1.1	0.93	16.15	0.044	0.48	0.18	336721	7793249	1129
AHH-DDH-002A010	33	33.5	4.22	0.31	0.64	16.02	0.056	0.26	0.13	336721	7793249	1128
AHH-DDH-002A011	33.5	34	1.48	2.2	1.99	14.48	0.159	0.22	0.74	336721	7793249	1128
AHH-DDH-002A012	34	34.5	0.23	0.67	7.31	13.23	0.094	0.22	0.35	336721	7793249	1127
AHH-DDH-002A013	34.5	35	0.18	0.79	7.98	13.19	0.067	0.36	0.35	336721	7793249	1127
AHH-DDH-002A014	35	35.5	1.49	3.66	2.63	14.49	0.128	0.31	0.81	336721	7793249	1126
AHH-DDH-002A015	35.5	36	2.83	0.53	2.99	15.83	0.063	0.52	0.36	336721	7793249	1126
AHH-DDH-002A016	36	36.5	1.38	1.42	5.77	14.38	0.079	0.57	0.3	336721	7793249	1125
AHH-DDH-002A017	36.5	37	2.19	2.4	3.96	15.19	0.054	0.72	0.58	336721	7793249	1125
AHH-DDH-002A018	37	37.5	2.25	0.69	3.16	15.25	0.04	0.82	0.29	336721	7793249	1124
AHH-DDH-002A019	37.5	38	1.96	0.84	4.54	15.23	0.042	0.08	0.06	336721	7793249	1124
AHH-DDH-002A020	38	38.5	0.25	10.86	3.16	15.34	0.029	0.13	3.76	336721	7793249	1123
AHH-DDH-002A021	38.5	39	0.47	6.22	2.59	15.22	0.08	0.2	1.38	336721	7793249	1123
AHH-DDH-002A022	39	39.5	2.52	1.32	2.58	15.69	0.128	0.17	0.11	336721	7793249	1122
AHH-DDH-002A023	39.5	40	1.27	1.68	1.45	15.48	0.104	0.22	0.01	336721	7793249	1122
AHH-DDH-002A024	40	40.5	2.46	2.17	2.03	15.71	0.36	0.36	0.46	336721	7793249	1121
AHH-DDH-002A025	40.5	41	2.83	1.06	1.36	14.84	0.131	0.33	0.17	336721	7793249	1121
AHH-DDH-002A026	41	41.5	2.48	1.18	0.72	15.68	0.126	0.39	0.17	336721	7793249	1120
AHH-DDH-002A027	41.5	42	2.63	2.33	0.72	15.99	0.37	0.47	0.05	336721	7793249	1120
AHH-DDH-002A028	42	42.5	1.77	5.85	2.45	14.94	0.073	0.53	0.95	336721	7793249	1119
AHH-DDH-002A029	42.5	43	1.76	5.98	1.7	14.73	0.116	0.68	1.3	336721	7793249	1119
AHH-DDH-002A030	43	43.5	4.08	0.25	0.83	16.66	0.022	0.67	0.21	336721	7793249	1118

AHH-DDH-002A031	43.5	44	3.34	0.6	2.35	16.15	0.056	0.75	0.04	336721	7793249	1118
AHH-DDH-002A032	44	44.5	0.44	0.35	3.22	15.45	0.076	0.92	3.55	336721	7793249	1117
AHH-DDH-002A033	44.5	45	0.19	4.02	4.21	15.32	0.051	0.96	4.95	336721	7793249	1117
AHH-DDH-002A034	45	45.5	0.52	13.18	3.32	15.7	0.013	0.08	6.28	336721	7793249	1116
AHH-DDH-002A035	45.5	46	4.06	11.22	0.97	16.64	0.069	0.18	0.19	336721	7793249	1116
AHH-DDH-002A036	46	46.5	2.99	2.95	0.69	15.82	0.016	0.3	0.21	336721	7793249	1115
AHH-DDH-002A037	46.5	47	2.2	2.88	3.3	15.4	0.04	0.42	3.73	336721	7793249	1115
AHH-DDH-002A038	47	47.5	0.85	11.18	2.29	13.99	0.024	0.48	0.81	336721	7793249	1114
AHH-DDH-002A039	47.5	48	3.33	5.58	0.21	16.4	0.077	0.63	0.2	336721	7793249	1114
AHH-DDH-002A040	48	48.5	1.54	0.22	2.2	14.88	0.019	0.73	0.89	336721	7793249	1113
AHH-DDH-002A041	48.5	49	2.28	5.7	2.67	15.75	0.028	0.91	1.58	336721	7793249	1113
AHH-DDH-002A042	49	49.5	2.89	7.2	0.96	15.9	0.058	0.1	0.06	336721	7793249	1112
AHH-DDH-002A043	49.5	50	3.02	2.56	1	16.25	0.059	0.24	0.31	336721	7793249	1112
AHH-DDH-002A044	50	50.5	1.25	2.75	2.1	14.72	0.144	0.51	1.32	336721	7793249	1111
AHH-DDH-002A045	50.5	51	3.36	5.84	1.18	16.38	0.073	0.66	0.5	336721	7793249	1111
AHH-DDH-002A046	51	51.5	1.36	6.39	2.16	14.8	0.156	0.82	1.67	336721	7793249	1110
AHH-DDH-002A047	51.5	52	4.55	0.08	0.23	16.57	0.011	0.04	0.05	336721	7793249	1110
AHH-DDH-002A048	52	52.5	4.54	0.08	0.19	16.34	0.012	0.09	0.11	336721	7793249	1109
AHH-DDH-002A049	52.5	53	4.08	0.26	0.58	16.88	0.018	0.1	0.16	336721	7793249	1109
AHH-DDH-002A050	53	53.5	3.17	2.33	0.68	15.2	0.104	0.12	0.46	336721	7793249	1108
AHH-DDH-002A051	53.5	54	3.33	0.93	0.36	14.99	0.104	0.07	0.23	336721	7793249	1108
AHH-DDH-002A052	54	54.5	4.57	0.06	0.14	16.21	0.069	0.08	0.13	336721	7793249	1107

AHH-DDH-002A053	54.5	55	4.26	0.13	0.2	16.61	0.091	0.1	0.14	336721	7793249	1107
AHH-DDH-002A054	55	55.5	1.93	0.16	1.66	15.7	0.081	0.13	1.55	336721	7793249	1106
AHH-DDH-002A055	55.5	56	0.21	6.84	2.59	15.73	0.042	0.17	3.58	336721	7793249	1106
AHH-DDH-002A056	56	56.5	3.04	5.14	0.91	15.68	0.072	0.16	0.77	336721	7793249	1105
AHH-DDH-002A057	56.5	57	4.82	0.59	0.07	16.8	0.08	0.2	0.11	336721	7793249	1105
AHH-DDH-002A058	57	57.5	4.59	0.03	0.04	16.72	0.087	0.17	0.14	336721	7793249	1104
AHH-DDH-002A059	57.5	58	1.56	4.02	2.1	15.31	0.08	0.13	1.63	336721	7793249	1104
AHH-DDH-002A060	58	58.5	0.23	6.49	3.25	15.38	0.06	0.14	2.53	336721	7793249	1103
AHH-DDH-002A061	58.5	59	0.28	8.98	1.59	15.23	0.138	0.12	2.06	336721	7793249	1103
AHH-DDH-002A062	59	59.5	2.26	7.87	1.04	15.78	0.13	0.08	0.84	336721	7793249	1102
AHH-DDH-002A063	59.5	60	1.22	4.48	1.76	15.04	0.123	0.09	1.78	336721	7793249	1102
AHH-DDH-002A064	60	60.5	2.38	7.33	0.5	15.17	0.1	0.13	0.41	336721	7793249	1101
AHH-DDH-002A065	60.5	61	1.01	1.37	2.07	15.15	0.131	0.14	1.85	336721	7793249	1101
AHH-DDH-002A066	61	61.5	1.02	7.73	1.34	15.32	0.22	0.06	1.17	336721	7793249	1100
AHH-DDH-002A067	61.5	62	2.49	5.39	1.49	15.81	0.16	0.15	0.65	336721	7793249	1100
AHH-DDH-002A068	62	62.5	3.29	3.38	1.3	15.93	0.099	0.17	0.46	336721	7793249	1099
AHH-DDH-002A069	62.5	63	3.64	2.37	0.9	15.98	0.111	0.11	0.44	336721	7793249	1099
AHH-DDH-002A070	63	63.5	4.2	1.94	0.45	16.44	0.13	0.18	0.18	336721	7793249	1098
AHH-DDH-002A071	63.5	64	4.5	0.52	0.27	16.48	0.11	0.09	0.18	336721	7793249	1098
AHH-DDH-002A072	64	64.5	2.92	0.13	1.03	15.09	0.125	0.13	0.73	336721	7793249	1097
AHH-DDH-002A073	64.5	65	3.6	3.59	0.9	15.14	0.122	0.12	0.43	336721	7793249	1097
AHH-DDH-002A074	65	65.5	2.46	2.11	1.44	15.28	0.085	0.07	1.21	336721	7793249	1096

AHH-DDH-002A075	65.5	66	1.96	5.84	1.56	17.2	0.044	0.24	0.13	336721	7793249	1096
AHH-DDH-002A076	66	66.5	4.36	0.09	0.14	16.59	0.046	0.29	0.8	336721	7793249	1095
AHH-DDH-002A077	66.5	67	1.82	6.61	1.57	17.39	0.112	0.36	1.01	336721	7793249	1095
AHH-DDH-002A078	67	67.5	2.31	5.81	1.31	16.81	0.131	0.31	0.13	336721	7793249	1094
AHH-DDH-002A079	67.5	68	3.22	2.4	1.04	16.16	0.134	0.26	0.57	336721	7793249	1094
AHH-DDH-002A080	68	68.5	3.31	1.23	0.63	16.1	0.269	0.36	0.04	336721	7793249	1093
AHH-DDH-002A081	68.5	69	1.44	5.46	1.65	16.46	0.136	0.22	0.94	336721	7793249	1093
AHH-DDH-002A082	69	69.5	2.2	3.05	1.66	15.89	0.022	0.54	0.3	336721	7793249	1092
AHH-DDH-002A083	69.5	70	1.36	4.56	1.73	17.3	0.054	0.89	0.44	336721	7793249	1092
AHH-DDH-002A084	70	70.5	0.79	2.79	3.51	14.79	0.022	0.1	0.78	336721	7793249	1091
AHH-DDH-002A085	70.5	71	0.27	1.36	6.32	15.36	0.233	0.24	0.59	336721	7793249	1091
AHH-DDH-002A086	71	71.5	0.37	1.81	5.89	14.81	0.247	0.21	1.39	336721	7793249	1090
AHH-DDH-002A087	71.5	72	0.37	1.09	6.43	14.68	0.129	0.23	0.3	336721	7793249	1090
AHH-DDH-002A088	72	72.5	0.29	0.73	7	14.72	0.075	0.49	0.15	336721	7793249	1089
AHH-DDH-002A089	72.5	73	0.3	2.22	7.46	14.59	0.08	0.52	0.36	336721	7793249	1089
AHH-DDH-002A090	73	73.5	0.84	5.72	3.91	14.28	0.081	0.66	1.34	336721	7793249	1088
AHH-DDH-002A091	73.5	74	0.7	4.85	3.99	14.6	0.136	0.82	1.14	336721	7793249	1088
AHH-DDH-002A092	74	74.5	0.36	5.83	4.93	14.82	0.077	0.94	1.33	336721	7793249	1087
AHH-DDH-002A093	74.5	75	1.3	3.61	3.72	16	0.077	0.6	0.63	336721	7793249	1087
AHH-DDH-002A094	75	75.5	3.71	1	0.33	16.45	0.02	0.22	0.11	336721	7793249	1086
AHH-DDH-002A095	75.5	76	0.96	4.9	3.58	14.88	0.139	0.39	1.13	336721	7793249	1086
AHH-DDH-002A096	76	76.5	0.24	5.73	5.72	14.64	0.057	0.46	1.19	336721	7793249	1085

AHH-DDH-002A097	76.5	77	0.28	5.73	4.82	14.9	0.081	0.59	1.19	336721	7793249	1085
AHH-DDH-002A098	77	77.5	0.25	5.79	5.39	14.55	0.071	0.61	1.24	336721	7793249	1084
AHH-DDH-002A099	77.5	78	1	3.96	3.74	16.1	0.36	0.77	0.98	336721	7793249	1084
AHH-DDH-002A100	78	78.5	1.9	3.38	2.61	16.15	0.351	0.9	0.74	336721	7793249	1083
AHH-DDH-002A101	78.5	79	0.76	5.69	3.21	14.62	0.149	0.94	1.48	336721	7793249	1083
AHH-DDH-002A102	79	79.5	1.57	3.89	3.53	15.98	0.088	0.07	0.81	336721	7793249	1082
AHH-DDH-002A103	79.5	80	1.96	4.66	2.13	15.89	0.053	0.17	0.86	336721	7793249	1082
AHH-DDH-002A104	80	80.5	1.6	3.07	3.86	15.77	0.087	0.25	0.61	336721	7793249	1081
AHH-DDH-002A105	80.5	81	3.04	1.36	2	16.5	0.061	0.4	0.24	336721	7793249	1081
AHH-DDH-002A106	81	81.5	1.87	2.69	3.04	15.28	0.045	0.34	0.44	336721	7793249	1080
AHH-DDH-002A107	81.5	82	1.57	2.87	3.47	15.75	0.106	0.52	0.68	336721	7793249	1080
AHH-DDH-002A108	82	82.5	1.3	1.832	2.35	15.4	0.35	0.62	0.53	336721	7793249	1079
AHH-DDH-002A109	82.5	83	1.37	2.91	4.65	15.32	0.054	0.75	0.5	336721	7793249	1079
AHH-DDH-002A110	83	83.5	2.15	1.99	3.61	16.25	0.073	0.84	0.34	336721	7793249	1078
AHH-DDH-002A111	83.5	84	1.25	2.04	4.36	16.05	0.087	0.9	0.36	336721	7793249	1078
AHH-DDH-002A112	84	84.5	0.1	0.7	9.4	14.81	0.082	0.01	0.1	336721	7793249	1077

Appendix 4: Diamond Drill Hole Lithostratigraphic profiles

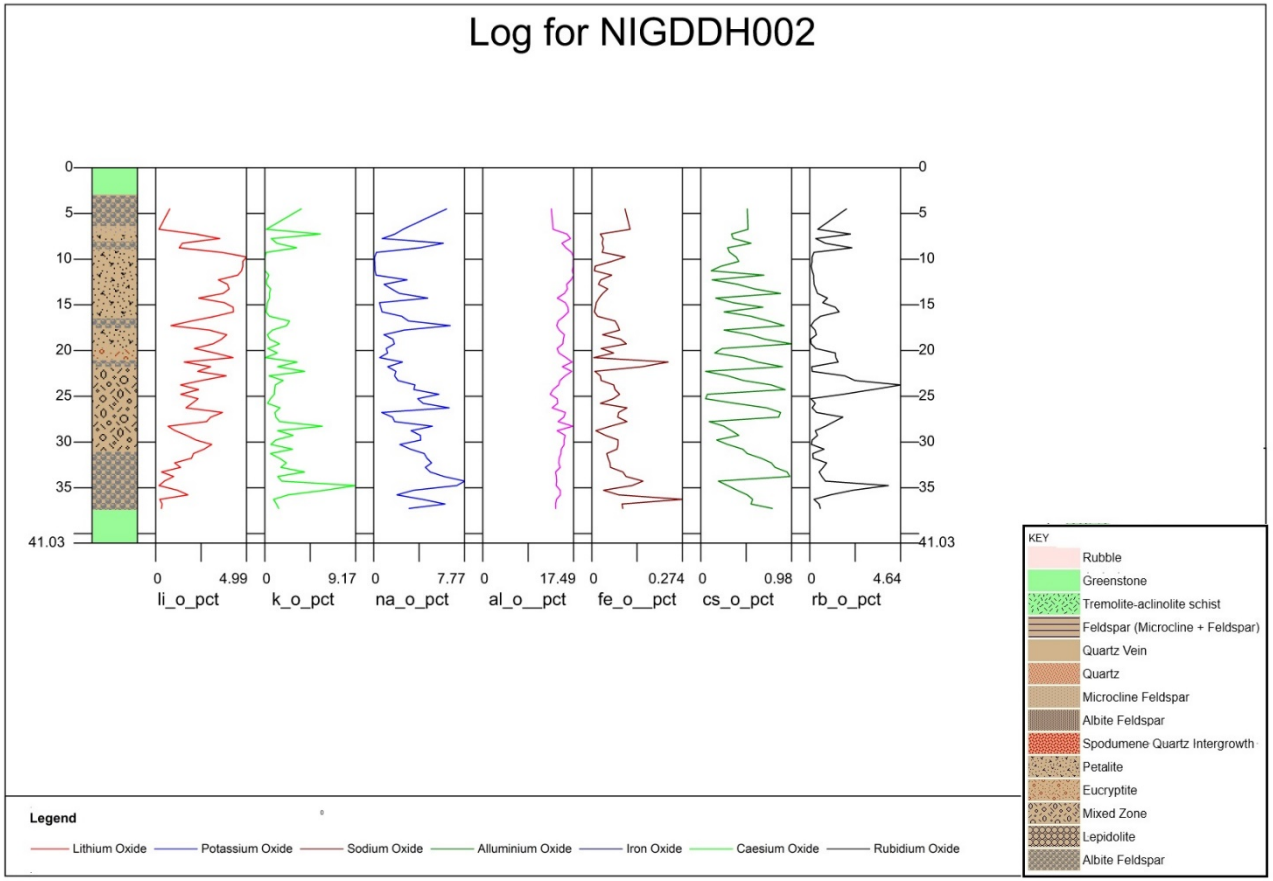
Log for NIGDDH002
0
5
10
15
20
25
30
35
41.03
0 4.99 li_o_pct
0 9.17 k_o_pct
0 7.77 na_o_pct
0 17.49 al_o__pct
0 0.274 fe_o__pct
0 0.98 cs_o_pct
0 4.64 rb_o_pct
Legend
Lithium Oxide
Potassium Oxide
Sodium Oxide
Alluminium Oxide
Iron Oxide
Caesium Oxide
Rubidium Oxide
KEY
Rubble
Greenstone
Tremolite-aclinolite schist
Feldspar (Microcline + Feldspar)
Quartz Vein
Quartz
Microcline Feldspar
Albite Feldspar
Spodumene Quartz Intergrowth
Petalite
Eucryptite
Mixed Zone
Lepidolite
Albite Feldspar

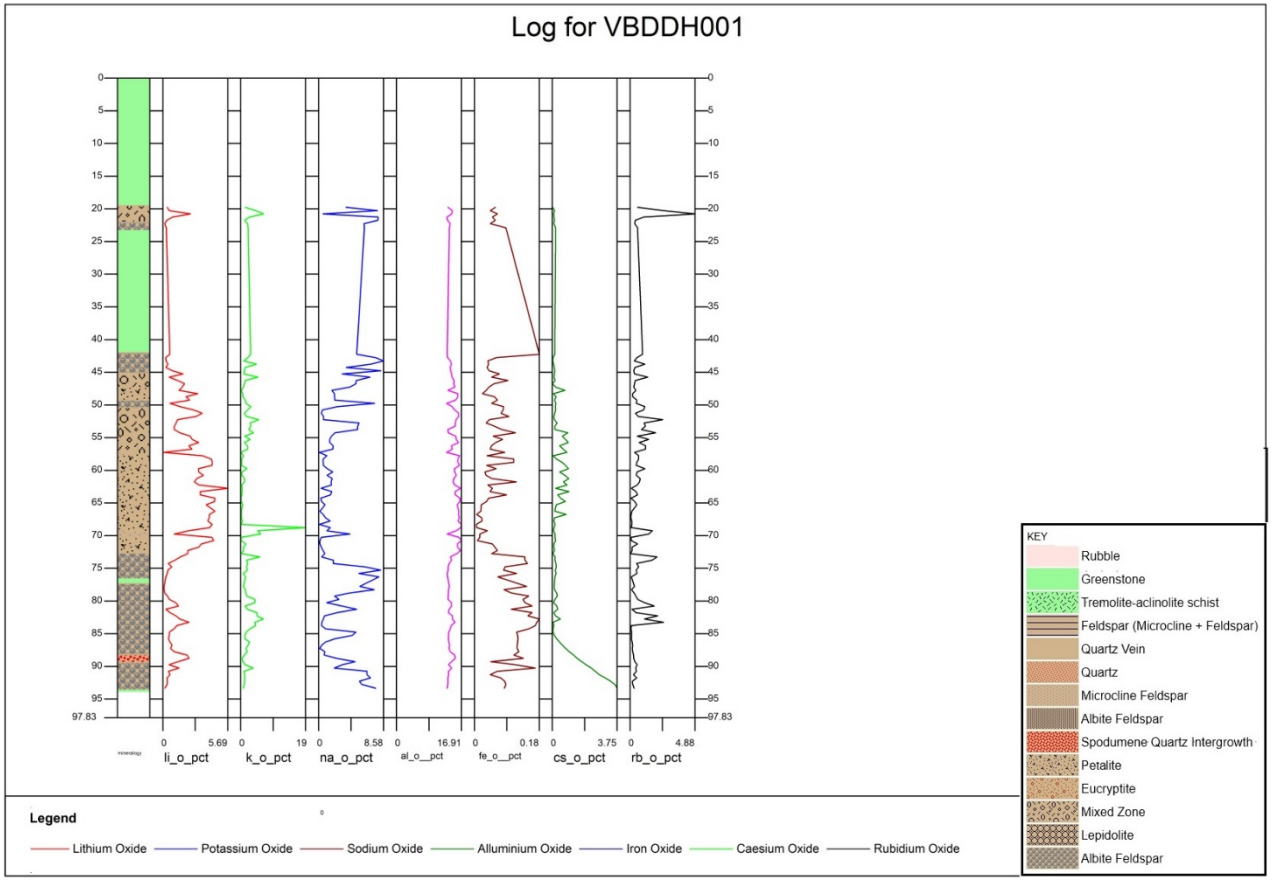
Log for VBDDH001
li_o_pct
k_o_pct
na_o_pct
al_o__pct
fe_o__pct
cs_o_pct
rb_o_pct
Legend
Lithium Oxide
Potassium Oxide
Sodium Oxide
Alluminium Oxide
Iron Oxide
Caesium Oxide
Rubidium Oxide
KEY
Rubble
Greenstone
Tremolite-aclinolite schist
Feldspar (Microcline + Feldspar)
Quartz Vein
Quartz
Microcline Feldspar
Albite Feldspar
Spodumene Quartz Intergrowth
Petalite
Eucryptite
Mixed Zone
Lepidolite
Albite Feldspar

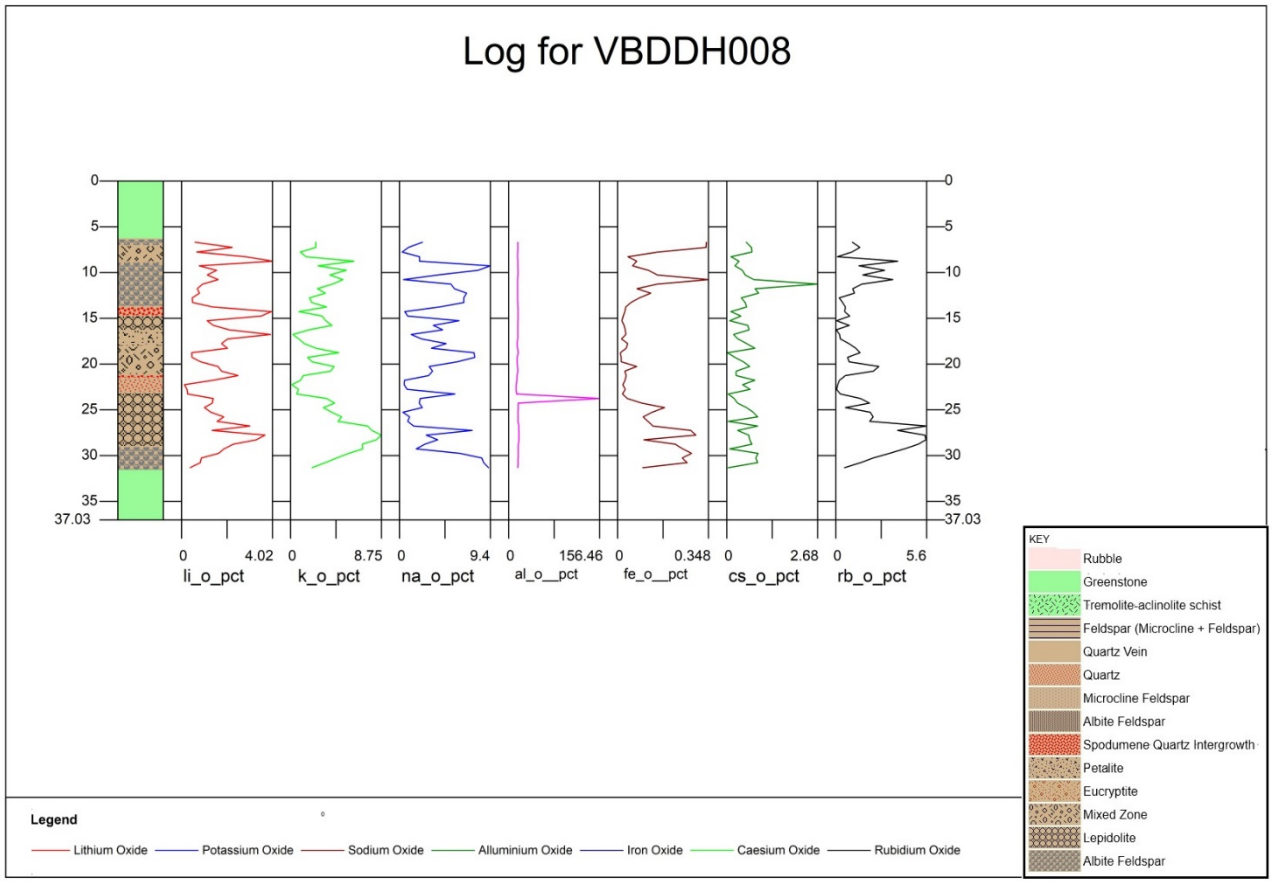
Log for VBDDH008
0
5
10
15
20
25
30
35
37.03
0 4.02 li_o_pct
0 8.75 k_o_pct
0 9.4 na_o_pct
0 156.46 al_o__pct
0 0.348 fe_o__pct
0 2.68 cs_o_pct
0 5.6 rb_o_pct
Legend
Lithium Oxide
Potassium Oxide
Sodium Oxide
Alluminium Oxide
Iron Oxide
Caesium Oxide
Rubidium Oxide
KEY
Rubble
Greenstone
Tremolite-aclinolite schist
Feldspar (Microcline + Feldspar)
Quartz Vein
Quartz
Microcline Feldspar
Albite Feldspar
Spodumene Quartz Intergrowth
Petalite
Eucryptite
Mixed Zone
Lepidolite
Albite Feldspar

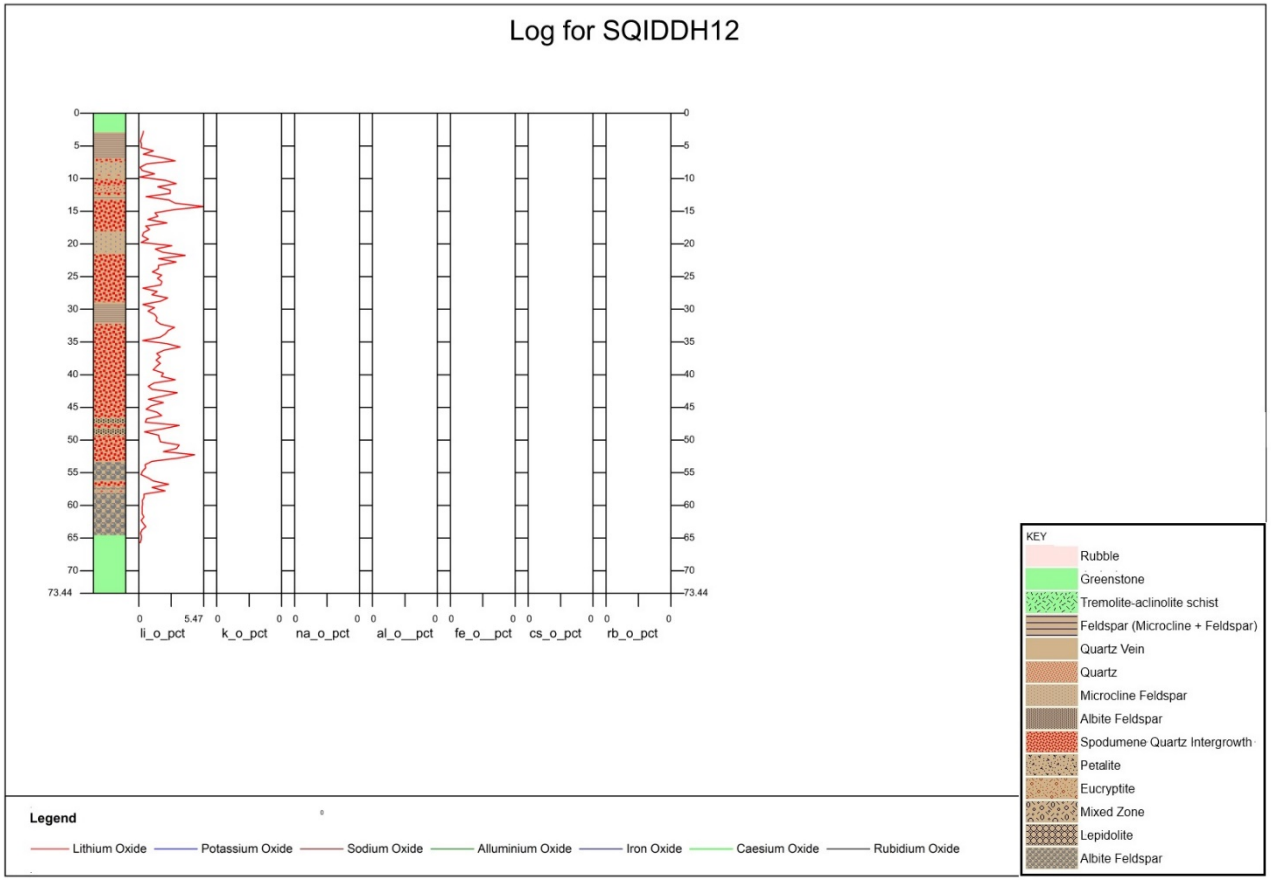
Log for SQIDDH12
li_o_pct
k_o_pct
na_o_pct
al_o__pct
fe_o__pct
cs_o_pct
rb_o_pct
73.44
5.47
Legend
Lithium Oxide
Potassium Oxide
Sodium Oxide
Alluminium Oxide
Iron Oxide
Caesium Oxide
Rubidium Oxide
KEY
Rubble
Greenstone
Tremolite-aclinolite schist
Feldspar (Microcline + Feldspar)
Quartz Vein
Quartz
Microcline Feldspar
Albite Feldspar
Spodumene Quartz Intergrowth
Petalite
Eucryptite
Mixed Zone
Lepidolite
Albite Feldspar

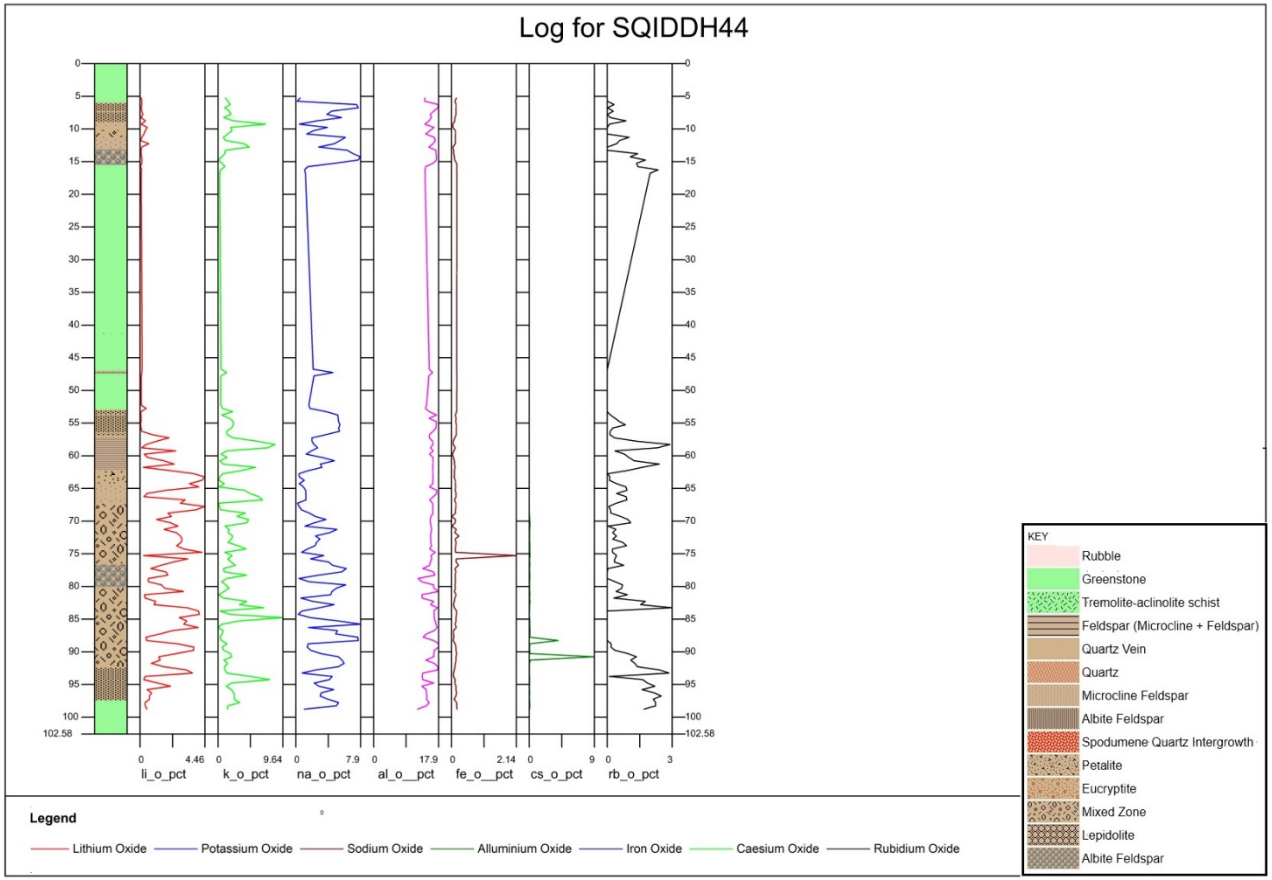
Log for SQIDDH44
li_o_pct
k_o_pct
na_o_pct
al_o__pct
fe_o__pct
cs_o_pct
rb_o_pct
Legend
Lithium Oxide
Potassium Oxide
Sodium Oxide
Alluminium Oxide
Iron Oxide
Caesium Oxide
Rubidium Oxide
KEY
Rubble
Greenstone
Tremolite-aclinolite schist
Feldspar (Microcline + Feldspar)
Quartz Vein
Quartz
Microcline Feldspar
Albite Feldspar
Spodumene Quartz Intergrowth
Petalite
Eucryptite
Mixed Zone
Lepidolite
Albite Feldspar

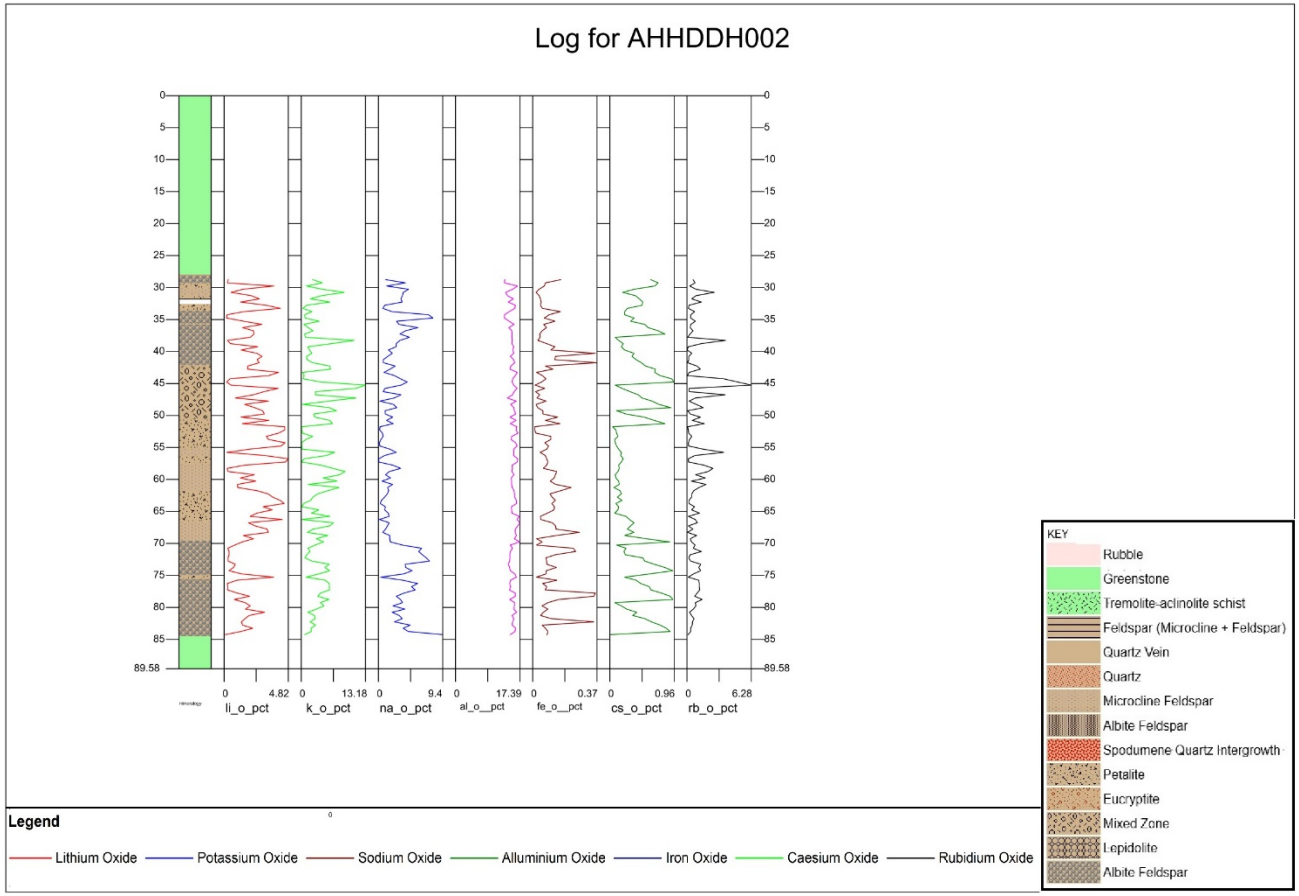
Log for AHHDDH002
li_o_pct
k_o_pct
na_o_pct
al_o__pct
fe_o__pct
cs_o_pct
rb_o_pct
Legend
Lithium Oxide
Potassium Oxide
Sodium Oxide
Alluminium Oxide
Iron Oxide
Caesium Oxide
Rubidium Oxide
KEY
Rubble
Greenstone
Tremolite-aclinolite schist
Feldspar (Microcline + Feldspar)
Quartz Vein
Quartz
Microcline Feldspar
Albite Feldspar
Spodumene Quartz Intergrowth
Petalite
Eucryptite
Mixed Zone
Lepidolite
Albite Feldspar

Appendix 5: Structural field measurements

Structure ID	Structure Type	Strike	Dip	Dip Direction	Easting	Nothing	Elevation
S1	Fault	284°	54°	North magnetic	336397	7792660	1167
S2	Micro fracture	200°	18°	East magnetic	336352	7792316	1175
S3	Fault filled with tourmaline	211°	20°	SE magnetic	336354	7792252	1186
S4	Fault	260°	30°	S magnetic	336334	7792191	1199
S5	Fault	186°	20°	E magnetic	336413	7792482	1168
S6	Shear Zone	225°	74°	N magnetic	336372	7792305	1189
S8	Shear Zone	206°	20°	W magnetic	336289	7792576	1194
S9	Shear Zone	081°	68°	NE magnetic	336404	7792498	1186
S10	Fault	197°	30°	SE magnetic	336656	7792955	1120
S11	Fault	226°	30°	SE magnetic	336428	7792514	1183
S12	Shear Zone	229°	20°	SE magnetic	336716	7793036	1136
S13	Shear Zone	290°	80°	S magnetic	336671	7793218	1145
S14	Shear Zone	232°	50°	S magnetic	336798	7795581	1077
S15	Shear Zone	264°	85°	S magnetic	336649	7793177	1151

S16	Shear Zone	238°	74°	N magnetic	336951	7793295	1140
S17	Shear Zone	267°	78°	SE magnetic	336972	7793374	1140
S18	Shear Zone	239°	76°	SE magnetic	336987	7793471	1150
S19	Shear Zone	260°	80°	SE magnetic	336783	7793578	1161
S20	Shear Zone	244°	70°	NW magnetic	336796	7793379	1147
S21	Fault	284°	8°	NE magnetic	336250	7791995	1196
S22	Fault	106°	64°	S magnetic	336309	7792204	1200
S23	Fault	185°	45°	E magnetic	336437	7792472	1188
S24	Fault	092°	50°	S magnetic	336337	7792645	1189
S25	Shear Zone	091°	78°	S magnetic	336695	7793222	1144
S26	Shear Zone	108°	76°	S magnetic	336709	7793196	1138
S27	Shear Zone	049°	82°	S magnetic	336727	7793161	1143
S28	Shear Zone	254°	70°	NW magnetic	336899	7793352	1147

Appendix 6a: RC Lithologic contacts summary

Hole ID	From	To	Lithology
V-RC-PET-028	0	1	Rubble
	1	13	Gst (Mod weathered)
	13	19	Gst (Fresh)
	19	22.5	AF (Spotted dog)
	22.5	43.5	Gst
	43.5	47	AF (Spotted dog)
	47	48	Pt
	48	49	MF
	49	50	M
	50	52	AF (Spotted dog)
	52	54	Pt
	54	56	Eucr
	56	57	MF
	57	58	L
	58	68	AF (Spotted dog)
	68	73	Gst
WC-RC-003	0	2	AF (Spotted dog)
	2	60	Gst
	60	73	MZ (AF, Pt, L, Be, Q)
	73	74.5	AF (Spotted dog)
	74.5	85	Gst
WC-RC-004	0	1	Rubble
	1	26	Gst
	26	28	AF
	28	59.5	Gst
	59.5	63.5	MZ (AF, C, L, M, Q)
	63.5	90	Gst
SH-RC-PET-001	0	2.5	AF
	2.5	42	Gst
	42	43	SQI
	43	50	AF
	50	63	MZ (AF, Eucr, MF, SQI)
	63	64	Eucr

	64	66	MZ (AF, Pt, Eury)
	66	73	AF
	73	74	Eucr
	74	79	MZ (AF, Eucr, Pt)
	79	83	Pt
	83	86.5	AF (Spotted dog)
	86.5	88	Gst
SH-RC-PET-020	0	10	Gst
	10	11	AF (Spotted dog)
	11	13	MF
	13	14	M
	14	15	AF
	15	16	MF
	16	19	AF (Spotted dog)
	19	64.5	Gst
	64.5	67	AF (Spotted dog)
	67	74	Pt
	74	91	MZ (AF, MF, M, Pt, Q, Eucr)
	91	98.5	AF (Spotted dog)
	98.5	100	Gst
SH-RC-PET-034	0	2	Rubble
	2	4	Gst
	4	6.5	AF (Spotted dog)
	6.5	11	Gst
	11	12	M
	12	43.5	Gst
	43.5	49	AF
	49	50	Pt
	50	57	MF
	57	61	AF
	61	62	Pt
	62	67	AF
	67	68	Pt
	68	70	AF
	70	71	Pt
	71	86	AF
	86	87	Gst

LN-RC-PET-004	0	24.5	Gst
	24.5	26	AF (Spotted dog)
	26	31	Pt
	31	37	AF
	37	39	Pt
	39	65	MZ (AF, Pt, SQI, Q, M, MF, Eury)
	65	66.5	AF (Spotted dog)
	66.5	69	Gst
GE-RC-PET-001	0	2	Rub
	2	3	AF (Spotted dog)
	3	6	MZ (AF,Q, Pt, MF)
	6	9	Pt
	9	16	AF
	16	18	Pt
	18	19	MF
	19	20	Pt
	20	21	AF
	21	22	SQI
	22	24	Eucr
	24	26	MF
	26	27.5	AF (Spotted dog)
	27.5	34	AF
	34	45.5	Gst
	45.5	47.5	MF
	47.5	60	Gst
AHS-RC-PET-001	0	33	Gst
	33	35	AF (Spotted dog)
	35	47	MF
	47	48	Pt
	48	49	MF
	49	51	Pt
	51	57	MF
	57	60	Pt
	60	62	L
	62	63	Pt
	63	64	M

	64	66	MF
	66	69	M
	69	72	AF
	72	73	Gst
AH-RC-PET-009	0	19.5	Gst
	19.5	20	M
	20	23	MZ (M, Pt, L ,MF, Q)
	23	27	Pt
	27	28	AF
	28	29	Q
	29	30	MF
	30	31	Q
	31	34	MF
	34	37	M
	37	42	Pt
	42	45	MF
	45	50	Pt
	50	55	M
	55	56	MF
	56	57	Pt
	57	59	M
	59	63.5	AF (Spotted dog)
	63.5	69	Gst
BE-RC-PET-001	0	34.5	Gst
	34.5	41	MF
	41	52	Q
	52	53	MF
	53	54	Q
	54	60	FL
	60	64	L
	64	71	FL
	71	73	L
	73	75	Q
	75	76	L
	76	83	AF (Spotted dog)
	83	84	Gst

Appendix 6b: PD Lithologic contacts summary

Hole ID	From	To	Lithology
V-PD-PET-301	0	7	Gst (Massive)
	7	9	AF, L, Q matrix
	9	10	AF
	10	18.5	Gst (Massive)
	18.5	21.5	AF
	21.5	37.5	Gst (Massive)
	37.5	39	AF,M matrix
	39	40	MF
V-PD-PET-302	0	12	Gst (Massive)
	12	13.5	AF
	13.5	19.5	Gst
	19.5	20	M, AF matrix
	20	22	AF
	22	39	Gst
	39	40	AF,M
V-PD-PET-303	0	2	Gst (weathered/oxidised)
	2	16	Gst (Massive)
	16	17	AF,M matrix
	17	18	L
	18	19	FL
	19	22	AF
	22	38.5	Gst (Massive)
	38.5	40	AF,M
V-PD-PET-272	0	1	OB (MF)
	1	4	MF
	4	7	Q, MF matrix
	7	8	MF
	8	10	Q, MF matrix
	10	11	M, Q matrix
	11	14	AF
	14	15	L (Coarse flakes)
	15	17	MQ matrix

	17	18	AF, Q matrix
	18	19	QM matrix
	19	22.5	Gst (Massive)
	22.5	23	AF,Q matrix
	23	34.5	Gst (Massive)
	34.5	35	AF, M matrix
	35	40	AF,Q matrix
V-PD-PET-273	0	2	OB (Weathered dump)
	2	5	Q
	5	11	MF
	11	12	Q,M matrix
	12	13	MF
	13	14	M
	14	16	MF,Q matrix
	16	19	QL
	19	21	AF,Q, M matrix
	21	22.5	AF
	22.5	24	SQI
	24	37	Gst
	37	39	M,MF matrix
	39	40	MF
V-PD-PET-274	0	3	OB (Oxidised dump)
	3	6	MF
	6	8	L (Dark med-grained)
	8	11	AF (Spotted dog)
	11	12	M,Q matrix
	12	13	Q
	13	14	AF
	14	17	Q,L matrix
	17	21	M
	21	22	AF
	22	23	Pt
	23	25	AF
	25	39	Gst
	39	40	Pt
V-PD-PET-275	0	1	OB (M,Q)
	1	2	OB (Oxidised dump)

	2	6	Gst (Deeply weathered/decomposed
	6	15	Gst (Massive)
	15	17	Q, L matrix
	17	19	Q
	19	21	AF
	21	22	FL
	22	23	AF
	23	40	Gst (Massive)
V-PD-PET-220	0	2	OB (Q,F)
	2	7	MF
	7	8	M,Q matrix
	8	17.5	MF
	17.5	19	AF
	19	24	MF
	24	37	AF (Spotted dog)
V-PD-PET-221	0	2	Q
	2	3	MF
	3	4	Q
	4	6	MF
	6	7.5	Q,M matrix
	7.5	10.5	MF
	10.5	12	AF
	12	13.5	Eucr
	13.5	15	AF
	15	16	MQ matrix
	16	18	MF,M,Q matrix
	18	27	AF,M,Q matrix
	27	28	Q
	28	30	MF
	30	31	Q,M matrix
	31	33	AF,M matrix
	33	34	Pet
	34	40	MF,M matrix
V-PD-PET-222	0	2	OB (Q)
	2	10	Q,M, AF matrix
	10	11	L

	11	14	AF,Q matrix
	14	14.5	Q,M
	14.5	22.5	Gst (Massive)
	22.5	25	AF
	25	26	M
	26	29	MF
	29	30	Q
	30	33	MF
	33	34	Pt
	34	37	AF
	37	40	Pt
V-PD-PET-223	0	3	OB (Q,F)
	3	5	F,M matrix
	5	7	Pt (Weathered)
	7	17	Q,F,M Matrix
	17	30.5	Gst (Massive)
	30.5	32	M,F matrix
	32	38	Q,L matrix
	38	39	Feldspathic L
	39	40	L (Coarse flakes)
MC-LP-PD-009	0	6	L
	6	8	AF
	8	11	L
	11	13	AF
	13	20	AF (Spotted dog)
	20	22	Gst
MC-LP-PD-014	0	1	Rub
	1	2	M
	2	4	Q
	4	6	MF
	6	7	Q
	7	9	AF
	9	13	FL
	13	15	L
	15	17	AF (Spotted dog)
	17	21	M
	21	24	AF (Spotted dog)

	24	25	Gst
BN-PD-SQI-009	0	4	FL
	4	6	Pt
	6	7	AF
	7	8	Pt
	8	10	SQI
	10	17	Pt
	17	23	MZ (MF,AF, L, Q)
	23	27	FL
	27	32.5	AF (Spotted dog)
	32.5	40	Gst
BS-PD-POL-041	0	7	Q
	7	27	L
	27	30	AF (Spotted dog)
C-PD-PET-006	0	2	Rub
	2	10	Gst
	10	13	MZ (AF, Q, M, Pt, Be)
	13	16	AF (Spotted dog)
	16	22	Gst
C-PD-PET-016	0	22.5	Gst
	22.5	23.5	AF
	23.5	28	Pt
	28	30	AF (Spotted dog)
BS-PD-SQI-008	0	1	Rub
	1	5	SQI
	5	7	Pt
	7	12	FL
	12	15	L
	15	20.5	AF (Spotted dog)
	20.5	22	Gst

Appendix 6c: DDH Lithologic contacts summary

Hole ID	From	To	Mineralogy
SQI-DDH-12	0	3	Gst
	3	6.9	F
	6.9	7.6	SQI

	7.6	9.3	MF
	9.3	9.6	SQI
	9.6	10	MF
	10	11.21	SQI
	11.21	12	Q
	12	12.6	SQI
	12.6	13.14	F
	13.14	18.15	SQI
	18.15	21.5	MF
	21.5	29	SQI
	29	32.15	F
	32.15	46.67	SQI
	46.67	47.5	AF
	47.5	48.2	SQI
	48.2	49.2	AF
	49.2	53.3	SQI
	53.3	56.23	AF (Spotted dog)
	56.23	57.2	SQI
	57.2	57.65	AF (Spotted dog)
	57.65	58	SQI
	58	64.65	AF (Spotted dog)
	64.65	73.44	Gst
SQI-DDH-44	0	1	Gst
	1	6	Gst
	6	7.36	AF
	7.36	9	AF
	9	9.7	MF
	9.7	10.1	QV
	10.1	11.35	MZ
	11.35	13	MF
	13	15.61	AF (Spotted dog)
	15.61	19.47	Gst
	19.47	41.15	Gst

	41.15	41.4	Amphibole
	41.4	47.08	Gst
	47.08	47.52	AF (Spotted dog)
	47.52	53.02	Gst
	53.02	53.73	AF
	53.73	56.5	AF
	56.5	56.95	AF
	56.95	62.27	F
	62.27	64.31	Pt
	64.31	65.3	MF
	65.3	65.7	MF
	65.7	66.18	MF
	66.18	67.26	MF
	67.26	76.57	MZ
	76.57	80.15	AF (Spotted dog)
	80.15	92.34	MZ
	92.34	97.5	AF
	97.5	102.58	Gst
NIG-DDH-002	0	3	Gst
	3	6.46	AF (Spotted dog)
	6.46	7.3	MF
	7.3	8.02	Pt
	8.02	9	AF (Spotted dog)
	9	16.4	Pt
	16.4	17.6	AF (Spotted dog)
	17.6	19.8	Pt
	19.8	21	Eucr
	21	21.82	AF (Spotted dog)
	21.82	31	MZ

	31	37.48	AF (Spotted dog)
	37.48	41.03	Gst
VB-DDH-001	0	13.6	Gst
	13.6	19.5	Gst
	19.5	22	MZ
	22	23.3	AF (Spotted dog)
	23.3	42	Gst
	42	45.12	AF (Spotted dog)
	45.12	47.3	MZ
	47.3	49.27	Pt
	49.27	50.4	AF (Spotted dog)
	50.4	57.47	MZ
	57.47	69.38	Pt
	69.38	70.3	MF
	70.3	72.68	Pt
	72.68	76.62	AF (Spotted dog)
	76.62	77.34	Gst
	77.34	88.16	AF (Spotted dog)
	88.16	89.41	SQI
	89.41	93.66	AF (Spotted dog)
	93.66	93.83	Gst
VB-DDH-008	0	6.32	Gst
	6.32	7.05	AF (Spotted dog)
	7.05	8.81	MZ
	8.81	13.72	AF (Spotted dog)
	13.72	14.71	SQI
	14.71	16.3	L
	16.3	17.36	Pt

	17.36	17.72	MZ
	17.72	18.06	Pt
	18.06	21.17	MZ
	21.17	21.52	SQI
	21.52	23.1	Q
	23.1	29	L
	29	31.6	AF (Spotted dog)
	31.6	37.03	Gst
AHH-DDH-002	0	26.24	Gst
	26.24	28	Gst
	28	29.4	AF (Spotted dog)
	29.4	30.05	Pt
	30.05	31.21	MF
	31.21	31.81	Pt
	31.81	32.62	F
	32.62	33.59	Pt
	33.59	35.73	AF (Spotted dog)
	35.73	42.18	AF (Spotted dog)
	42.18	50.6	MZ
	50.6	55.09	Pt
	55.09	56.35	MF
	56.35	57.5	Pt
	57.5	61.76	MF
	61.76	66.55	Pt
	66.55	69.5	MF
	69.5	75.01	AF (Spotted dog)
	75.01	75.5	Pt
	75.5	84.57	AF (Spotted dog)
	84.57	89.58	Gst

Appendix 8: Sample Preparation

The samples are crushed in order to acquire homogeneous whole-rock for qualitative and quantitative geochemical analysis using XRF and AAS analytical methods. The wet/damp samples are then taken to the ovens for drying in order to remove the moisture within the samples. The recommended drying temperature is between 105-120° and the duration of the samples in the ovens is dependent on the sample moisture content. The samples are crushed to reduce the nugget factor and to facilitate faster grinding /pulverisation. The sizes of the laboratory jaw crushers are -150 mm,-50 mm, -28 mm and a Boyd crusher which produces an output crushed from -10 mm to 5 mm. (Figure 8.1).



Figure 8.1: Laboratory crushing equipment. (a) Photograph of the -28mm jaw crusher (b) Photograph of the -150mm jaw crusher (c) Photograph of the Boyd Crusher

Those samples which are less than -5 mm undergo pulverisation with a ball and swing mill to create homogeneity within the sample. This also increases surface area to volume ratio hence there is faster digestion required in analysis using AAS. For every step in crushing and pulverising the samples are first rolled in Rexene cloth to create homogeneity in the sample. The grinding equipment used is a six-pot chromium Tema mill (Figure 8.2) and it grinds the sample to -53 microns.

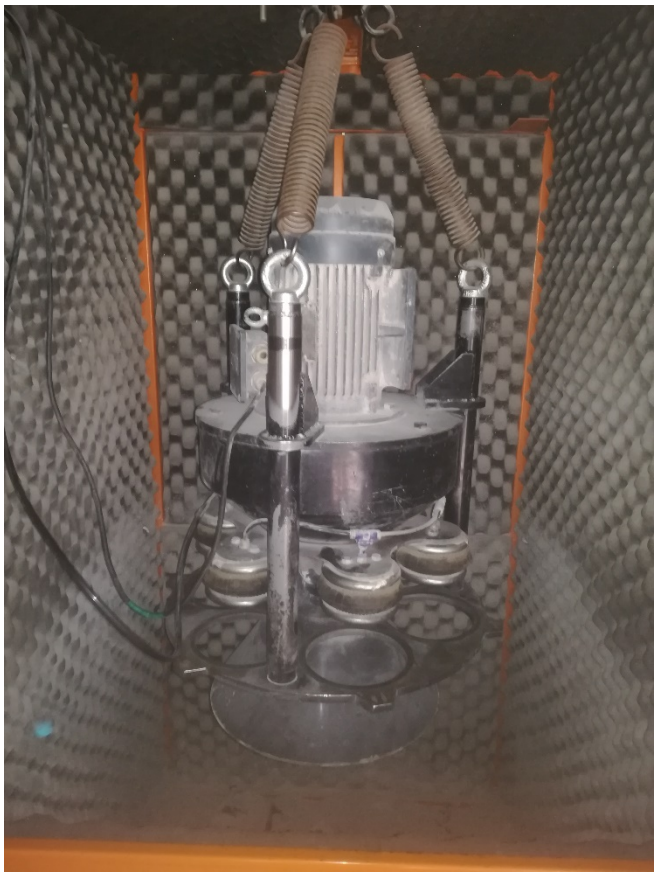

Figure 8.2: Laboratory six pot Tema mill

After pulverising, the samples are thoroughly cone and quartered to obtain a representative portion of about an average of about 20-30 g of powder which is then used for AAS using a Pinnacle 900 machine (Figure 8.3)

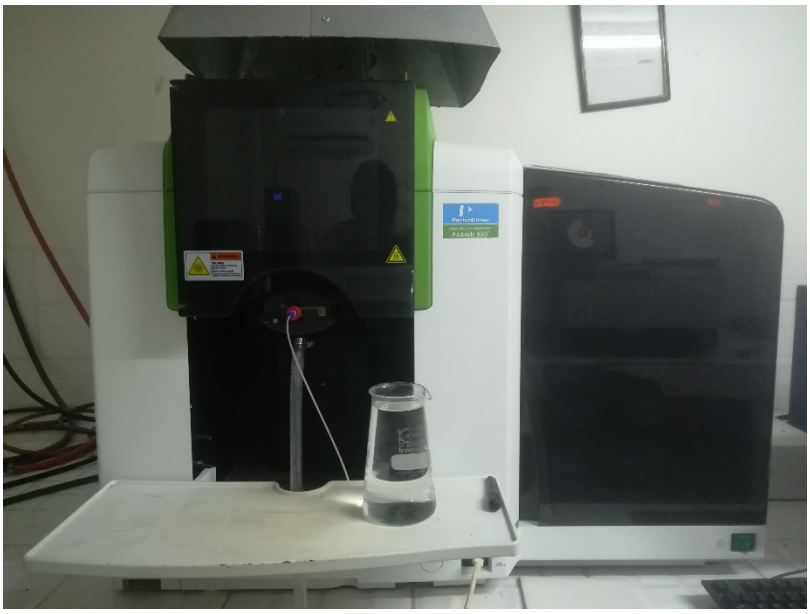

Figure 8.3: Laboratory Pinnacle 900 AAS machine

The remaining pulp goes for zapping using a handheld Innov XRF gun (Figure 8.4) which is calibrated to either soil or mining mode.



Figure 8.4: Portable Innov-X hand-held XRF gun

Appendix 8: Major element detection limits

Elements	% Limit
Li_2O	0.01
Cs_2O	0.01
Rb_2O	0.01
Fe_2O_3	0.001
Al_2O_3	0.1
Na_2O	0.01
K_2O	0.01